

# DISSERTATION

submitted to the  
Combined Faculty of Natural Sciences and Mathematics  
of the Ruperto Carola University Heidelberg, Germany  
for the degree of  
Doctor of Natural Sciences

Presented by  
**M.Sc. Monika Jankowska-Döllken**  
born in Gniezno, Poland

Oral examination: 31.07.2019



Functional studies on  
the chloroquine resistance transporter (PfCRT)  
and the HECT E3 ubiquitin-protein ligase (PfUT)  
in *Plasmodium falciparum*

**Referees:**

Prof. Dr. Michael Lanzer

Prof. Dr. Christine Clayton



Ich erkläre hiermit, dass ich die vorliegende Doktorarbeit selbstständig unter Anleitung verfasst und keine anderen als die angegebenen Quellen und Hilfsmittel benutzt habe.

Ich erkläre hiermit, dass ich an keiner anderen Stelle ein Prüfungsverfahren beantragt bzw. die Dissertation in dieser oder anderer Form bereits anderweitig als Prüfungsarbeit verwendet oder einer anderen Fakultät als Dissertation vorgelegt habe.

Die vorliegende Arbeit wurde am Department für Infektiologie, Abteilung Parasitologie des Universitätsklinikum Heidelberg in der Zeit von Oktober 2014 bis Mai 2019 unter der Leitung von Prof. Dr. Michael Lanzer ausgeführt.

.....

Datum

.....

Monika Jankowska-Döllken



# Table of content

|   |     |
|---|-----|
| Acknowledgments .....   | I   |
| Summary .....   | III |
| Zusammenfassung .....   | V   |
| List of abbreviations .....   | VII |
| 1. Introduction .....   | 1   |
| 1.1. The biology of <i>Plasmodium</i> .....                         | 1   |
| 1.1.1. The life cycle of <i>P. falciparum</i> .....                 | 1   |
| 1.1.2. The blood stage development .....                            | 3   |
| 1.2. Antimalarial drugs .....                                       | 4   |
| 1.2.1. Mode of action .....   | 5   |
| 1.2.2. Resistance .....   | 5   |
| 1.2.3. The first to treat malaria: quinine and chloroquine .....    | 9   |
| 1.3. Posttranslational modifications (PTMs) .....                   | 10  |
| 1.3.1. Role of PTMs in drug resistance .....                        | 11  |
| 1.3.2. Phosphorylation and its role in the activity of PfCRT .....  | 12  |
| 1.3.3. The ubiquitin pathway and PfUT-mediated ubiquitination ..... | 13  |
| 1.4. Genetic manipulation of <i>P. falciparum</i> genome .....      | 17  |
| 1.4.1. Genome editing tools .....                                   | 17  |
| 1.4.2. Conditional gene downregulation methods .....                | 20  |
| 1.5. Aim of the study .....   | 21  |
| 2. Materials and Methods .....                                      | 23  |
| 2.1. Materials .....  | 23  |
| 2.1.1. Equipments .....   | 23  |
| 2.1.2. Consumables .....  | 24  |
| 2.1.3. Chemicals .....  | 25  |
| 2.1.4. KITs .....   | 26  |
| 2.1.5. Biological material .....                                    | 26  |
| 2.1.5.1. Antibodies .....   | 26  |
| 2.1.5.2. Enzymes .....  | 27  |
| 2.1.5.3. Fluorescent dyes .....                                     | 27  |
| 2.1.5.4. Size markers and loading dyes .....                        | 27  |

|           |   |    |
|-----------|---|----|
| 2.1.5.5.  | Plasmids.....   | 28 |
| 2.1.5.6.  | Oligonucleotides.....   | 28 |
| 2.1.5.7.  | <i>E. coli</i> strains.....                                     | 30 |
| 2.1.5.8.  | <i>P. falciparum</i> strains.....                               | 30 |
| 2.1.6.    | Buffers, media and solutions.....                               | 30 |
| 2.1.7.    | Computer software and databases.....                            | 33 |
| 2.2.      | Methods.....  | 33 |
| 2.2.1.    | Parasitology.....   | 33 |
| 2.2.1.1.  | <i>In vitro</i> cultivation of <i>P. falciparum</i> .....       | 33 |
| 2.2.1.2.  | Parasites freezing and thawing.....                             | 33 |
| 2.2.1.3.  | Parasites synchronization.....                                  | 34 |
| 2.2.1.4.  | Magnetic purification of late stage parasites.....              | 35 |
| 2.2.1.5.  | Transfection of <i>P. falciparum</i> .....                      | 35 |
| 2.2.1.6.  | Cloning by limiting dilution.....                               | 36 |
| 2.2.1.7.  | Growth inhibition assay and IC <sub>50</sub> determination..... | 37 |
| 2.2.2.    | Microbiology and molecular biology.....                         | 38 |
| 2.2.2.1.  | Preparation of electrocompetent <i>E. coli</i> .....            | 38 |
| 2.2.2.2.  | Transformation of <i>E. coli</i> .....                          | 38 |
| 2.2.2.3.  | Genomic DNA isolation from <i>P. falciparum</i> .....           | 39 |
| 2.2.2.4.  | Polymerase Chain Reaction (PCR).....                            | 39 |
| 2.2.2.5.  | Agarose gel electrophoresis.....                                | 40 |
| 2.2.2.6.  | DNA extraction from agarose gel.....                            | 41 |
| 2.2.2.7.  | Determination of nucleic acid concentration and purity.....     | 41 |
| 2.2.2.8.  | Restriction enzymes digestion.....                              | 41 |
| 2.2.2.9.  | Dephosphorylation of DNA ends.....                              | 42 |
| 2.2.2.10. | Ligation of DNA fragments.....                                  | 42 |
| 2.2.2.11. | Plasmid DNA isolation.....                                      | 43 |
| 2.2.2.12. | DNA sequencing.....   | 44 |
| 2.2.2.13. | Total RNA extraction from <i>P. falciparum</i> .....            | 44 |
| 2.2.2.14. | DNase treatment.....  | 45 |
| 2.2.2.15. | Reverse transcription.....                                      | 45 |
| 2.2.2.16. | Quantitative real-time PCR.....                                 | 45 |
| 2.2.3.    | Biochemistry and cell biology.....                              | 46 |
| 2.2.3.1.  | Preparation <i>P. falciparum</i> protein extracts.....          | 46 |



|            |   |    |
|------------|---|----|
| 2.2.3.2.   | SDS-PAGE electrophoresis .....  | 46 |
| 2.2.3.3.   | Coomassie staining .....  | 47 |
| 2.2.3.4.   | Western blot.....   | 47 |
| 2.2.3.5.   | Western blot membrane stripping .....   | 48 |
| 2.2.3.6.   | Immunofluorescence assay (IFA) .....  | 48 |
| 2.2.3.7.   | Transmission electron microscopy (TEM) .....  | 49 |
| 2.2.3.8.   | Flow cytometry based analysis.....  | 50 |
| 2.2.3.8.1. | Determination of parasitemia and multiple-infections .....  | 50 |
| 2.2.3.8.2. | Quantification of parasite multiplication rates (PMR).....  | 51 |
| 2.2.3.8.3. | Determination of merozoites number .....  | 52 |
| 2.2.3.8.4. | Determination of asexual life cycle duration.....   | 52 |
| 2.2.3.8.5. | Egress and invasion assay .....   | 52 |
| 2.2.3.8.6. | Merozoites attachment assay.....  | 53 |
| 2.2.4.     | <i>In vitro</i> development of resistance to quinine .....  | 53 |
| 2.2.5.     | Data analysis.....  | 54 |
| 3.         | Results .....   | 55 |
| 3.1.       | Analysis of the role of PfCRT phosphorylation at S33 in resistance to chloroquine and quinine ..... | 55 |
| 3.1.1.     | The kinase inhibitor ML-7 reduces chloroquine and quinine resistance .....                          | 55 |
| 3.1.2.     | Phosphorylation of PfCRT's serine 33 modulates chloroquine and quinine responsiveness .....         | 57 |
| 3.1.3.     | Multiplication rate variation in the PfCRT S33 mutants.....   | 59 |
| 3.1.4.     | Fitness advantage of PfCRT S33 mutants results from an increased numbers of merozoites.....         | 61 |
| 3.2.       | Functional characterization of PfUT in the parasite's asexual life cycle .....                      | 65 |
| 3.2.1.     | Conditional knockdown of PfUT using glmS ribozyme system .....                                      | 65 |
| 3.2.1.1.   | Generation of PfUT-HA-glmS parasite line .....  | 65 |
| 3.2.1.2.   | Determination of optimal glucosamine concentrations .....   | 66 |
| 3.2.1.3.   | PfUT is overexpressed in the HA-glmS mutant line.....   | 67 |
| 3.2.1.4.   | PfUT-HA localizes to the ER/Golgi complex.....  | 70 |
| 3.2.1.5.   | PfUT-HA-glmS line displays a reduced growth phenotype.....  | 74 |
| 3.2.1.6.   | The impaired growth of the PfUT-HA-glmS line results from an extended cell cycle duration .....     | 75 |
| 3.2.1.7.   | Analysis of the ubiquitination patterns.....  | 78 |
| 3.2.1.8.   | Investigating PfCRT as a substrate of PfUT.....   | 79 |

|          |  |     |
|----------|--|-----|
| 3.2.1.9. | PfUT-HA-glmS parasites are more susceptible to quinine and quinidine .....                                   | 80  |
| 3.2.2.   | Inactivation of PfUT's HECT catalytic domain .....   | 82  |
| 3.2.3.   | PfUT disruption using SLI-TGD system .....   | 83  |
| 4.       | Discussion and Outlook .....   | 85  |
| 4.1.     | Unravelling the role of PfCRT phosphorylation at position S33 in resistance to chloroquine and quinine ..... | 85  |
| 4.1.1.   | Phosphorylation of PfCRT's serine 33 modulates chloroquine and quinine responsiveness .....                  | 85  |
| 4.1.2.   | Fitness advantage of PfCRT S33 mutants results from the increased numbers of merozoites.....                 | 88  |
| 4.2.     | Functional characterization of PfUT in the parasite's asexual life cycle .....                               | 96  |
| 4.2.1.   | Overexpression of PfUT results in cell cycle lengthening of PfUT-HA-glmS parasites ..                        | 96  |
| 4.2.2.   | Investigating the biological substrates of PfUT .....  | 100 |
| 4.2.3.   | PfUT is likely essential for <i>P. falciparum</i> blood stages .....   | 105 |
| 4.2.4.   | Association of PfUT with resistance to quinine and quinidine.....  | 108 |
| 5.       | Conclusion .....   | 111 |
| 6.       | References.....  | 112 |
|          | Appendix I: Supplementary figures .....  | 139 |
|          | Appendix II: Plasmid maps .....  | 144 |
|          | Appendix III: DNA sequences .....  | 147 |

# Acknowledgments

I would like to thank my supervisor, Prof. Michael Lanzer, for the opportunity to work on this really exciting project, as well as for help and guidance along the way. Moreover, I would like to express my deepest gratitude for his support and understanding during the period of my sickness.

I am deeply grateful to the other members of my thesis advisory committee, Prof. Christine Clayton, Prof. Frauke Melchior and Prof. Marcel Deponte, for their time, guidance and motivating discussions.

I would like to express my sincere gratitude and appreciation to Dr. Silvia Portugal and PD Dr. Jude Przyborski for their “OK, let’s do it!” and a heartfelt smile, despite the last minute request to join my examination committee.

I would like to give my very special thanks to Dr. Ryan Henrici for priceless advices regarding the Western Blot analysis, leading to a breakthrough in my project, when I already lost hope that my Western Blots could ever work.

I would also like to thank all scientific and non-scientific members of our department, working at all the positions you can think of, for their honest smile, for “how are you doing?”, for small talks and bigger talks, just for the friendly environment in my daily work. I am very thankful to our secretaries, Miriam Griesheimer and Sandra Niebel, who always magically could solve the mystery of how to deal with the paperwork and administrative issues, and who were always friendly, empathic, supportive and patient. Special thanks to Dr. Markus Ganter and Dr. Jude Przyborski for numerous motivating discussions, technical guidance and reagents. Many thanks to Jessica Kehrer and Dr. Julia Sattler for the microscopy guidance and patience to press the right button each time, when I panicked that I can’t see my image ;) Thanks to Sonja Engels and Mathias Diehl for scientific and non-scientific discussions, about everything and nothing, and for almost spontaneous cocktails whenever we needed them :D I also thank Klára Obrová, for being my sport-, party- and German course-mate!

I would like to express my sincere thanks to all the present and previous AG Lanzer lab members, who accompanied me during recent years, through good and bad times. Particular thanks to my “lab family”, Dr. Maëlle Duffey, Dr. Christine “Tina” Lansche, Dr. Sonia Moliner Cubel, Dr. Hani Kartini Agustar and Dr. Sirikamol “Nick” Srismith, for all the great and stressful times we went through together, for patience when I asked stupid questions, for brainstorming, for cooking evenings, parties, dinners, cocktails, karaoke, amusement parks, game nights, swimming pool relax, travelling, gossips, hugs, coffee, tea or hot water ;) Thank you for being good friends! Additional enormous thank you to Nick for all the nights together in the lab and making sure I did not oversleep for next time point of my time course! Thanks to Dr. Sebastiano “Seba” Bellanca for knowing exactly when it was time to go to Uni-Shop or Botanic! Lovely thanks to Dr. Britta Nyboer for being always soooo

friendly, empathic, supportive and helpful, always there for you with a smile – even if her day was so busy that she barely had time to eat! Thanks to Marina Müller and Stefan Prior for their valuable technical support and for almost being patient, and not screaming too much, when I had questions or did something wrong :P Absolutely heartfelt thanks to my new amazing, positive and clever lab mates, Marianne Papagrigorakes, Romina “Romi” Celada and Fiona Berger, for sincere kindness, support, motivation and optimism, for taking a wonderful care of my emotional balance in the recent months and for being there for me before I even asked for it ☺ Thanks to Sophia Frangos for countless questions, which not only shaped my patience (or at least improved it a bit :D), but also forced me to think about alternative solutions. Thanks to Atdhe “Adi” Kernaja for maybe sometimes overdosed, but ALWAYS a positive spirit, even when nobody else could anymore ;)

Huge thanks to my Polish gang, Dr. Marta Bogacz, Dr. Marek Cyrklaff and Kamil Wolanin – for fabulous Polish lunches (if we were lucky even with “pierogi”!), for discussions about important and silly things, for a little bit of high quality Polishness abroad :D

Pragnę podziękować moim najlepszym przyjaciołom, Magdalenie Nowaczyk i Michałowi Lachowi, za wszystkie winne i nie-winne Skype’y i za rozmowy na wszelakie tematy! Dziękuję Wam za wymianę doświadczeń naukowych i życiowych. Dziękuję Wam za uświadomienie mi, że wszyscy jedziemy na tym samym wózku :D, ale jak Polak chce, to Polak potrafi i jakoś dobrać do obranego celu ;)

Serdeczne podziękowania kieruję ku mojej rodzinie, za bezgraniczną wiarę w moje możliwości i bezcenne wsparcie odkąd tylko sięgam pamięcią. Szczególnie pragnę podziękować mojej mamie, Małgorzacie Jankowskiej, bez której, dosłownie, nie byłoby mnie tu teraz. Mamuś, dziękuję Ci za trud edukacji, za wspieranie wszystkich moich decyzji jakiekolwiek by nie były, za stawianie mnie do pionu, gdy byłam w rozsypce. Przeogromnie dziękuję mojej najlepszej Siorce EVER, Karolinie Jankowskiej, która zawsze wspiera i motywuje, która jednym słowem potrafi cofnąć mój najpaskudniejszy nastrój i która jak nikt inny rozumie ambicję Jankowskich ;) Dziękuję moim kochanym dziadkom, Monice i Olkowi Kujda, za serdeczne słowa, motywację i wiarę we mnie bez względu na wszystko, i za przypominanie mi o wyjściu na świeże powietrze i jedzeniu owoców, zwłaszcza w trakcie pisanie pracy doktorskiej ;) Kocham Was wszystkich bardzo!

And most importantly, I would like to thank my one and only husband, Markus Döllken. Thank you for ALL the discussions and for teaching me how to look at things from another perspective. Thank you for trying to always be up to date with my project, even if you may have had no idea what I was talking about ;) Thank you for your patience and understanding when work was dominating the private life. Thank you for being there for me through all the happy and tough times. Thank you for making me feel at home, despite my roots being far away. Thank you for your love, enormous support, motivation and believing in me when I didn’t believe in myself.

# Summary

Posttranslational modifications (PTMs) affect fundamental cellular functions of the human malaria parasite *Plasmodium falciparum*, including regulation of protein stability, metabolism, proliferation, apoptosis and signal transduction. This study investigates the importance of phosphorylation and ubiquitination in modulating the parasite intraerythrocytic development, as well as their implication in antimalarial drug resistance.

The chloroquine resistance transporter PfCRT is a drug-metabolite carrier annotated as a prominent determinant of parasite's reduced susceptibility to quinoline drugs. PfCRT is posttranslationally modified by phosphorylation and palmitoylation. However, the role of these PTMs in regulation of PfCRT function is not fully resolved. Chemical and genetic approaches employed in the current study revealed the relevance of PfCRT phosphorylation at serine 33 in regulating the drug resistance-mediating function of this transporter and *in vitro* fitness of the parasite. The PfCRT allelic exchange mutants, in which serine 33 was replaced by alanine showed increased sensitivity to chloroquine and quinine. Moreover, PfCRT serine 33 substitution by phospho-mimicking amino acids, glutamic and aspartic acid, could respectively partially and fully, restore the resistance phenotype. The fitness variation between the PfCRT mutants was linked to differences in merozoite numbers and their invasion efficiencies, with alanine mutants displaying a significant advantage in this regard. Identification of a kinase implicated in this phenomenon is desired, as its inhibition in combination with chloroquine could reduce or prevent the further spread of resistance.

A HECT E3 ubiquitin ligase, termed ubiquitin transferase PfUT, is a novel candidate gene for multifactorial resistance to quinine. PfUT was shown to localize to the parasite's ER/Golgi complex, but its role in reduced susceptibility to quinine and its physiological function remain unclear. Characterization of PfUT was attempted by a glmS ribozyme-based conditional knockdown of encoding it gene, generated using the CRISPR-Cas9 genome editing technology. Unexpectedly, integration of the glmS sequence resulted in a 2-fold increase in PfUT transcripts correlated with protein levels. PfUT overexpression, in turn, led to S phase-associated lengthening of parasite's cycle, reflected in impaired growth. Glucosamine-induced incomplete downregulation partially restored the wild type phenotype. Moreover, the transgenic parasites exhibited an enhanced susceptibility to quinine and quinidine. An alternative disruption of the *pfut* locus via a selection-linked integration (SLI-TGD) strategy was unsuccessful, despite multiple attempts. These results underline the importance of PfUT in parasite proliferation and survival. However, a direct proof of PfUT's association with quinine resistance and identification of its biological substrates await further investigation.



# Zusammenfassung

Die posttranslationalen Modifikationen (PTMs) wirken sich signifikant auf die grundlegenden zellulären Funktionen des humanen Malaria-Parasiten *Plasmodium falciparum* aus, einschließlich der Regulierung von Proteinstabilität, Stoffwechsel, Proliferation, Apoptose und Signaltransduktion. Diese Studie untersuchte die Bedeutung von Phosphorylierung und Ubiquitinierung bei der Modulation der intraerythrozytären Entwicklung des Parasiten sowie deren Auswirkungen auf die Resistenz gegen Malariamedikamente.

Der Chloroquin-Resistenz-Transporter PfCRT ist ein Wirkstoff-Metabolit-Transporter, der als prominente Determinante der reduzierten Anfälligkeit des Parasiten für Chinolin-Medikamente beschrieben ist. PfCRT wird posttranslational durch Phosphorylierung und Acetylierung modifiziert. Die Rolle dieser PTMs bei der Regulierung der PfCRT-Funktion ist jedoch noch nicht vollständig geklärt. Chemische und genetische Ansätze, die in der aktuellen Studie eingesetzt wurden, zeigten die Relevanz der PfCRT-Phosphorylierung des Serin 33 in der Regulierung der resistenzassoziierten Funktion dieses Transporters und der *in vitro* Fitness des Parasiten. Die PfCRT-Allel-Austauschmutanten, in denen Serin 33 durch Alanin ersetzt wurde, zeigten eine erhöhte Empfindlichkeit gegenüber Chloroquin und Chinin. Darüber hinaus konnte die Substitution von PfCRT Serin 33 durch phospho-ähnliche Aminosäuren, Glutamin und Asparaginsäure, jeweils teilweise und vollständig, den Resistenzphänotyp wiederherstellen. Die Fitnessvariation zwischen den PfCRT-Mutanten war mit Unterschieden in der Merozoitenzahl und deren invasiver Effizienz verbunden, wobei Alanin-Mutanten in dieser Hinsicht einen signifikanten Vorteil aufwiesen. Die Identifizierung einer an diesem Phänomen beteiligten Kinase wäre wünschenswert, da durch ihre Hemmung in Kombination mit Chloroquin eine weitere Ausbreitung von Resistenzen reduziert oder verhindert werden könnte.

Eine HECT E3 Ubiquitin-Ligase, die so genannte Ubiquitin-Transferase PfUT, ist ein neuartiges Kandidatengen für die multifaktorielle Resistenz gegen Chinin. Es wurde gezeigt, dass PfUT im ER/Golgi-Komplex des Parasiten lokalisiert ist, aber seine Rolle bei der reduzierten Anfälligkeit für Chinin und seine physiologische Funktion bleibt unklar. Die Charakterisierung von PfUT wurde durch einen glmS ribozym-basierten, konditionellen Knockdown des kodierenden Gens untersucht, der mit der CRISPR-Cas9 Genombearbeitungstechnologie erzeugt wurde. Unerwartet führte die Integration der glmS-Sequenz zu einem 2-fachen Anstieg des PfUT-Transkripts, das mit dem Proteingehalt korreliert. Die Überexpression von PfUT wiederum führte zu einer Verlängerung der S-Phase des Zyklus des Parasiten, die sich auch im beeinträchtigten Wachstum widerspiegelt. Die durch

Glukosamin induzierte unvollständige Herunterregulierung stellte den Phänotyp des Wildtyps teilweise wieder her. Darüber hinaus zeigten die transgenen Parasiten eine erhöhte Anfälligkeit für Chinin und Chinidin. Eine alternative Unterbrechung des pfut-Locus durch eine Selection-Linked Integration (SLI-TGD)-Strategie blieb trotz mehrfacher Versuche erfolglos. Diese Ergebnisse unterstreichen die Bedeutung von PfUT für die Proliferation und das Überleben des Parasiten. Ein direkter Beweis für die Assoziation von PfUT mit der Chininresistenz und der Identifizierung seiner biologischen Substrate steht jedoch noch aus.



# List of abbreviations

|                    |   |
|--------------------|---|
| A                  | Absorbance OR alanine OR adenine                          |
| ABC                | ATP-binding cassette (transporter family)                 |
| ACT                | Artemisinin-based combination therapy                     |
| Amp                | Ampicillin  |
| AmpR               | Ampicillin resistance                                     |
| APEX2              | Ascorbate peroxidase                                      |
| APS                | Ammonium persulphate                                      |
| ART                | Artemisinin   |
| ATP                | Adenosine triphosphate                                    |
| BirA               | Biotin ligase   |
| bp                 | Base pairs  |
| BSA                | Bovine serum albumin                                      |
| C                  | Cysteine OR cytosine                                      |
| Cas9               | CRISPR associated protein 9                               |
| cDNA               | Complementary DNA   |
| CQ                 | Chloroquine   |
| CRISPR             | Clustered regularly interspaced short palindromic repeats |
| CRT                | Chloroquine resistance transporter                        |
| C-terminus         | Carboxyl-terminus   |
| Cyt.D              | Cytochalasin D  |
| ddH <sub>2</sub> O | Double distilled water                                    |
| DHFR               | Dihydrofolate reductase                                   |
| DHODH              | Dihydroorotate dehydrogenase                              |
| di-Gly             | Glycine-glycine (remnants)                                |
| DMSO               | Dimethyl sulfoxide  |
| DNA                | Desoxyribonucleic acid                                    |
| DNase              | Deoxyribonuclease   |
| dNTP               | Desoxyribonucleoside triphosphate                         |
| DSB                | Double-strand break                                       |
| DSBR               | Double-strand break repair                                |
| dsDNA              | Double stranded DNA                                       |
| DUB                | Deubiquitinating enzyme                                   |
| DV                 | Digestive vacuole   |
| <i>E. coli</i>     | <i>Escherichia coli</i>                                   |
| EDTA               | Ethylenediaminetetraacetate                               |
| ER                 | Endoplasmic reticulum                                     |
| et al.             | Et alia (and others)                                      |
| EtBr               | Ethidium Bromide  |
| FA                 | Fatty Acid  |
| FACS               | Fluorescence activated cell sorting                       |
| For                | Forward   |
| FSC                | Forward scatter   |

|                  |  |
|------------------|--|
| GA               | Glutaraldehyde                                       |
| gDNA             | Genomic DNA  |
| GFP              | Green Fluorescent Protein                            |
| GlcN             | Glucosamine  |
| glmS             | Glucosamine-6-phosphate activated ribozyme           |
| gRNA             | Guide RNA  |
| HA               | Hemagglutinin  |
| HECT             | Homologous to E6-associated protein C-Terminus       |
| HEPES            | 4-(2-hydroxyethyl)-1-piperazineethanesulfonic acid   |
| HR               | Homology region                                      |
| IC <sub>50</sub> | Half of maximal inhibitory concentration             |
| IFA              | Indirect fluorescence assay                          |
| IgG              | Immunoglobulin G                                     |
| IP3              | Inositol triphosphates                               |
| iRBC             | Infected red blood cell                              |
| K                | Lysine   |
| K13              | Kelch 13 protein                                     |
| kb               | Kilobase pair  |
| KD               | Knockdown  |
| kDa              | Kilodalton   |
| KO               | Knockout   |
| kV               | Kilovolts  |
| LB               | Luria Bertani  |
| LPL              | Lysophospholipids                                    |
| LPLA             | Lysophospholipase A                                  |
| Mb               | Megabasepair   |
| MDR1             | Multidrug resistance protein 1                       |
| mRNA             | Messenger RNA  |
| NCBI             | National Center for Biotechnology Information        |
| NEB              | New England Biolabs                                  |
| Neo              | Neomycin   |
| NHEJ             | Non-homologous end joining                           |
| NLS              | Nuclear localization signal                          |
| N-terminus       | Amino-terminus                                       |
| OD               | Optical density                                      |
| ON               | Overnight  |
| <i>P.</i>        | <i>Plasmodium</i>                                    |
| p.i.             | Post-invasion  |
| PAGE             | Polyacrylamide gel electrophoresis                   |
| PAM              | Protospacer adjacent motif                           |
| <i>Pb</i>        | <i>Plasmodium berghei</i>                            |
| PBS              | Phosphate-buffered saline                            |
| PBST             | Phosphate buffered saline supplemented with Tween-20 |
| PC               | Phosphatidylcholine                                  |
| PCR              | Polymerase chain reaction                            |

|           |  |
|-----------|--|
| <i>Pf</i> | <i>Plasmodium falciparum</i>   |
| PFA       | Paraformaldehyde   |
| PfCRT     | <i>P. falciparum</i> chloroquine resistance transporter              |
| PfUT      | <i>P. falciparum</i> ubiquitin transferase                           |
| PLA       | Phospholipase A  |
| PlasmoDB  | <i>Plasmodium</i> database   |
| PLC       | Phospholipase C  |
| PMR       | Parasite Multiplication Rate   |
| POD       | Peroxidase   |
| PTM       | Posttranslational modification                                       |
| PV        | Parasitophorous vacuole  |
| PVDF      | Polyvinylidene fluoride  |
| PVM       | Parasitophorous vacuolar membrane                                    |
| PYR       | Pyrimethamine  |
| QN        | Quinine  |
| QD        | Quinidine  |
| qPCR      | Quantitative PCR   |
| RAMA      | Rhoptry associated membrane antigen                                  |
| RBC       | Red blood cell   |
| Rev       | Reverse  |
| RIPA      | Radioimmunoprecipitation assay buffer                                |
| RNA       | Ribonucleic acid   |
| RNase     | Ribonuclease   |
| rpm       | Revolutions per minute   |
| RPMI      | Rosewell Park Memorial Institute                                     |
| RT        | Room temperature OR reverse transcriptase                            |
| S         | Serine   |
| S33       | Serine at position 33  |
| S33A      | Substitution of serine at position 33 to alanine                     |
| SB        | Super broth  |
| SD        | Standard deviation   |
| SDS       | Sodium dodecyl sulfate   |
| SEM       | Standard error of the mean   |
| sgRNA     | Single-guide RNA   |
| SLI       | Selection-linked integration   |
| SNP       | Single nucleotide polymorphism                                       |
| SOB       | Super optimal broth  |
| SOC       | Super optimal broth with catabolite repression                       |
| SSC       | Side scatter   |
| STRING    | Search Tool for the Retrieval of Interacting Genes/Proteins database |
| T         | Threonine  |
| T2A       | Skip peptide   |
| Taq       | <i>Thermus aquaticus</i>   |
| TEM       | Transmission electron microscopy                                     |
| TEMED     | Tetramethylethylenediamine   |

|       |                                      |
|-------|--------------------------------------|
| TGD   | Targeted gene disruption             |
| TM    | Transmembrane domain                 |
| TSAP  | Thermosensitive Alkaline Phosphatase |
| TUBEs | Tandem ubiquitin-binding entities    |
| Y     | Tyrosine                             |
| Y2H   | Yeast-2-Hybrid                       |
| U     | Unit                                 |
| USA   | United States of America             |
| UBD   | Ubiquitin-binding domain             |
| UT    | Ubiquitin transferase                |
| UTR   | Untranslated region                  |
| UV    | Ultra violet                         |
| v/v   | Volume to volume                     |
| w/v   | Weight to volume                     |
| WHO   | World Health Organization            |
| WT    | Wild type                            |

# 1. Introduction

## 1.1. The biology of *Plasmodium*

*Plasmodium* species, the causative agents of malaria are unicellular protozoan parasites belonging to the phylum Apicomplexa. Apicomplexan parasites are characterized by a presence of apical organelles found at certain stages of their life cycles. These organelles are especially important for host cell invasion. Vertebrate host vulnerable to *Plasmodium* infection include mammals, reptiles and birds (Aravind et al., 2003). Amongst the 200 *Plasmodium* species, only five routinely infect humans, comprising *Plasmodium falciparum*, *Plasmodium vivax*, *Plasmodium malariae*, *Plasmodium ovale* and *Plasmodium knowlesi*. Of the five species, *P. falciparum* is the most virulent and responsible for the vast majority of fatal cases, whereas *P. vivax* is the most geographically widespread (WHO, 2017). In recent years, the global malaria burden has promisingly begun to decline, mainly due to the distribution of insecticide-treated bed nets and administration of antimalarial drug-based combination therapies (Tizifa et al., 2018). Nevertheless, malaria remains one of the most life-threatening infectious diseases, with over 200 million cases and 400 000 deaths reported annually, mainly in the sub-Saharan Africa (WHO, 2018b).

### 1.1.1. The life cycle of *P. falciparum*

The life cycle of *P. falciparum* is divided between the insect vector and the human host. The parasites are transmitted in the digestive system of the mosquito from the genus *Anopheles*. During a blood meal of *Plasmodium*-infected mosquito, parasites are injected from the salivary gland of the vector into the host's skin, further migrating via the bloodstream to the liver, where they infect hepatocytes (Fig. 1.1) (Aravind et al., 2003). After extensive proliferation, infected liver cells release merozoites, initially contained inside host cell-derived vesicles called merosomes, into the blood vessels. Liberated merozoites subsequently invade red blood cells, where again they undergo multiple rounds of asexual replication (Baer et al., 2007; Miller et al., 2013). The first symptoms of the disease occur with a rupture of mature parasitized erythrocytes, releasing millions of invasive merozoites into the bloodstream. Clinical manifestations of uncomplicated *P. falciparum*-infection include fever, chills, headache, fatigue and nausea, whereas severe malaria is associated with acute anemia, pulmonary oedema, jaundice or coma (Church et al., 1997; White et al., 2014). While the majority of the released merozoites will continuously repeat the intraerythrocytic developmental cycle, a small proportion differentiates into gametocytes. Gametocytes, as the malaria transmission-forms are ingested by a mosquito during a blood meal, initiating the sexual development inside the vector. In a

process called sporogony, male and female gametes fuse, in the end giving rise to thousands of motile sporozoites. The new cycle begins with the mosquito bite inoculating saliva containing the invasive sporozoites to another human host (Aravind et al., 2003).

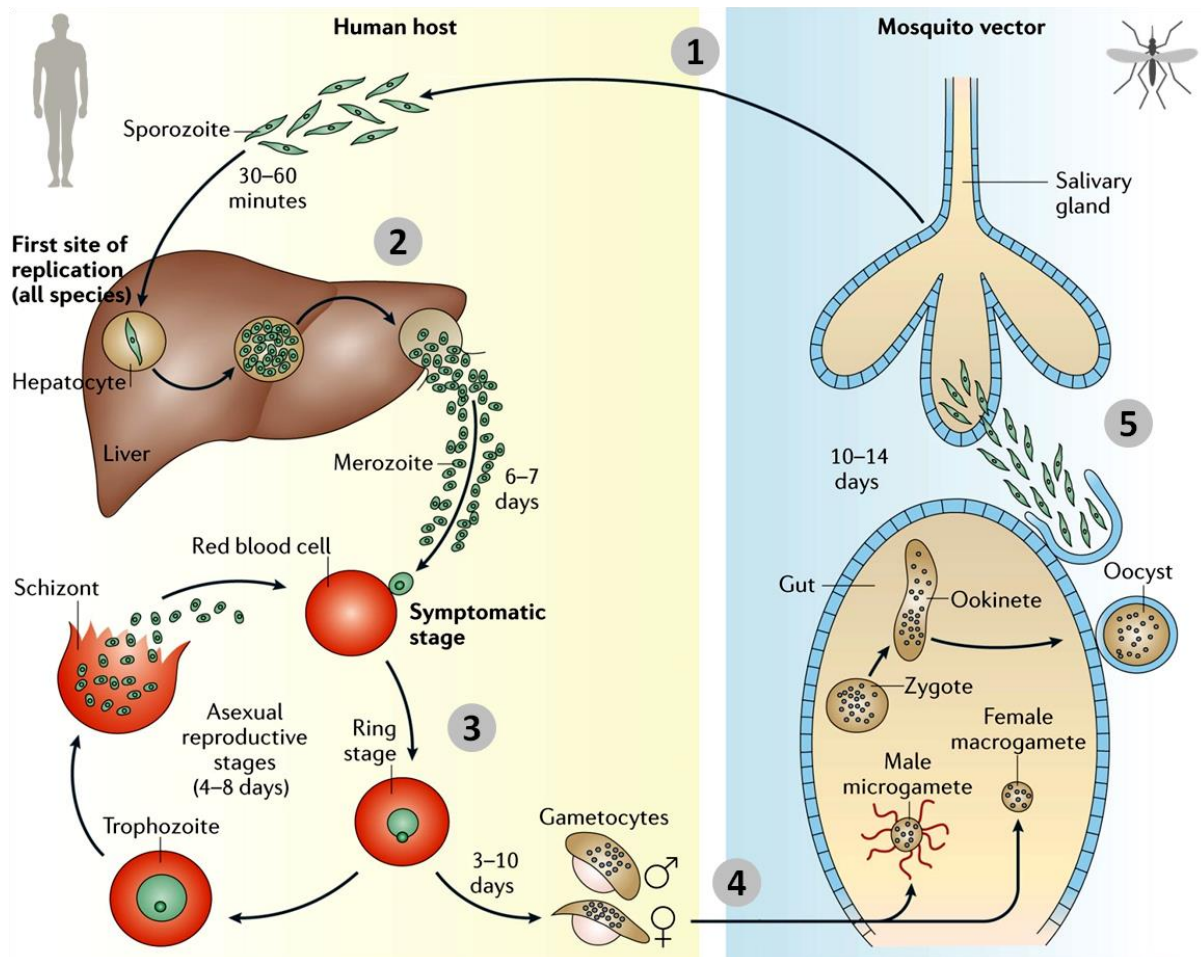


**Figure 1.1. The life cycle of human malaria parasite *P. falciparum*.** The infection begins with a bite of a female *Anopheles* mosquito inoculating sporozoites into the human host (1). Within 30–60 min sporozoites reach the **liver**, where they multiply and re-differentiate generating thousands of merozoites (2). Merozoites released into the bloodstream invade host's erythrocytes, initiating the **blood stage** of the infection (3). Parasite develops inside the red blood cell (RBC) through the stages of ring, trophozoite and schizont. A mature schizont eventually burst releasing daughter merozoites, which further invade new erythrocytes. At the same time, some of the merozoites will differentiate into gametocytes. Gametocytes will be further transmitted to the mosquito vector after being ingested during a blood meal (4). Inside the **mosquito** gut, gametocytes mature into gametes. Fertilized female gametes develop into ookinetes, which further forms oocysts. Multiple mitotic nuclear divisions inside the oocyst result in the generation of numerous invasive sporozoites. Upon oocyst rupture, sporozoites find their way to the salivary gland (5). The new malaria cycle starts again once a mosquito carrying the parasites bites another human host. Adapted from Phillips et al. (2017).

## 1.1.2. The blood stage development

The most thoroughly studied amongst the three *P. falciparum* life stages is the intraerythrocytic developmental cycle, primarily due to its ease to be maintained in the *in vitro* culture and as the majority of available antimalarials target this stage of infection (Wilson et al., 2013). During each cycle taking approximately 48 h, growth of a single merozoite inside the red blood cell proceeds through the subsequent cellular stages of ring, trophozoite and schizont (Fig. 1.2.A and B). In order to grow and proliferate, *P. falciparum* degrades the host's haemoglobin in the digestive vacuole (food vacuole). While converting the toxic heme into a hemozoin crystal, the parasite generates amino acids, which can be subsequently used for its reproduction (Fong & Wright, 2013). In a process called schizogony, a single nucleated parasite replicates forming between 8 and 24 daughter merozoites in a mature parasitized erythrocyte. Apart of sporozoites and ookinetes, merozoites are amongst the parasite forms possessing the apical organelles, required for *P. falciparum* host cell invasion (Fig. 1.2.C). The two main secretory organelles localizing to the merozoite's apical end, rhoptries and exonemes, are filled with proteins involved in invasion and egress, respectively (Counihan et al., 2013; Janse & Waters, 2007).

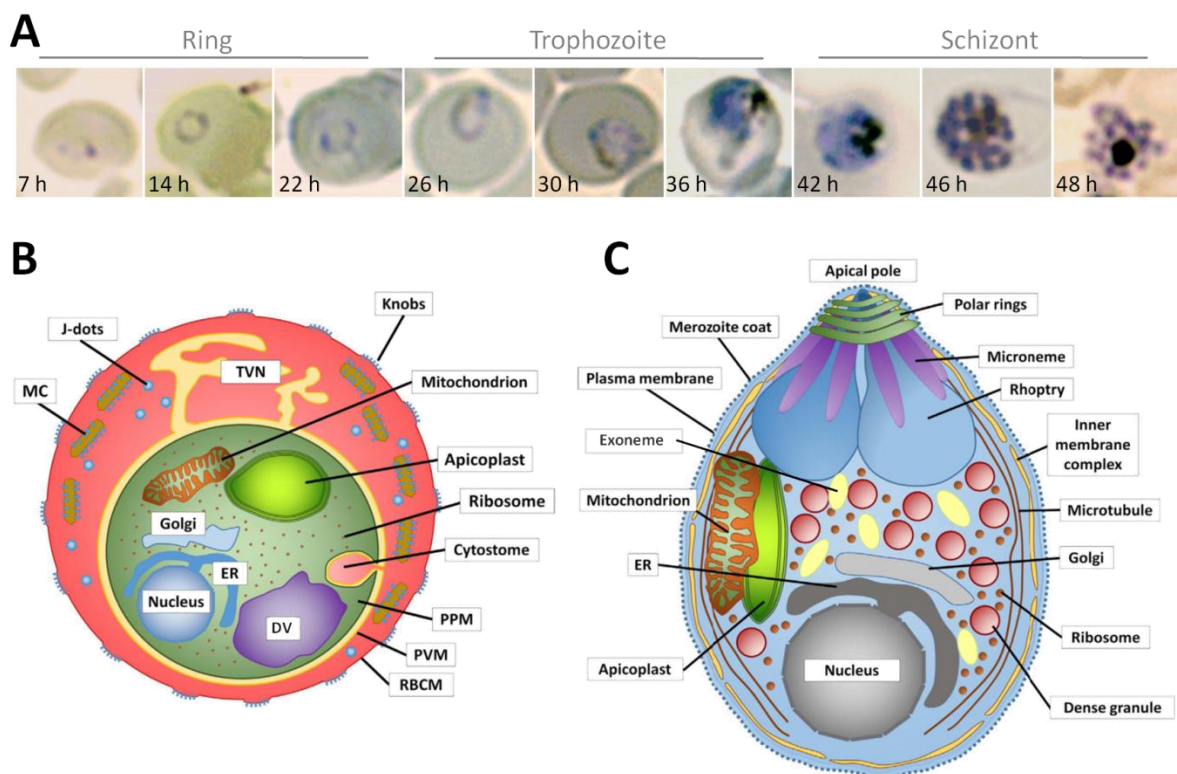


**Figure 1.2. The *P. falciparum* intraerythrocytic development.** **A.** The different stages of the parasite blood stage development including ring (0-24 h), trophozoite (24-36 h) and schizont stages (40-48 h), depicted in Giemsa-stained thin blood smears. **B.** Cellular architecture of the trophozoite-infected erythrocyte. **C.** Structure of the invasive merozoite. ER - endoplasmic reticulum; DV - digestive

vacuole; IMC - inner membrane complex; MC -Maurer's cleft; PPM - parasite plasma membrane; PVM - parasitophorous vacuole membrane; RBCM - red blood cell membrane; TVN - tubovesicular network. Adapted from Flammersfeld et al. (2018).

The intraerythrocytic cycle ends with an event known as parasite egress, in which mature schizonts burst releasing the daughter merozoites. Within a minute, free merozoites bind and actively invade new red blood cells (Fig. 1.3) (Lehmann et al., 2018; Miller et al., 2013).

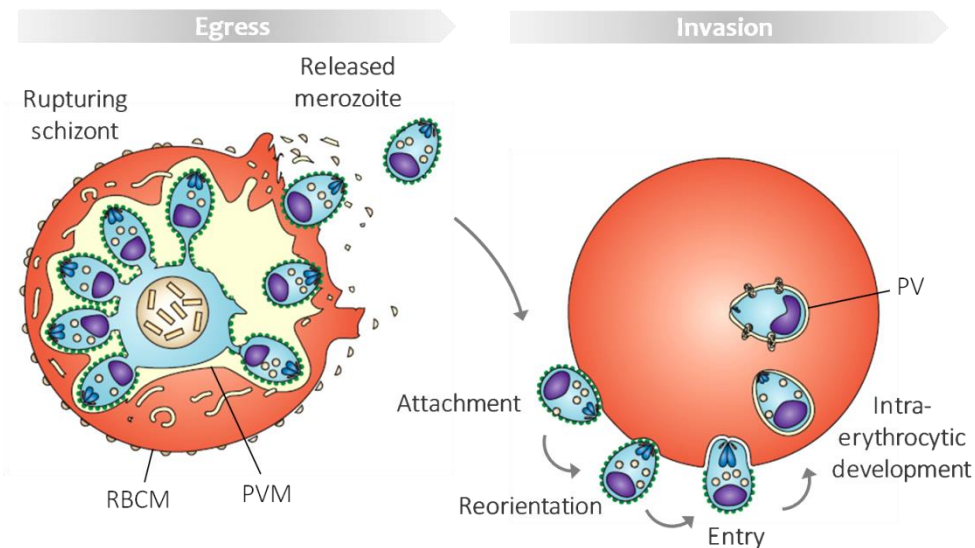


**Figure 1.3. Merozoites egress and invasion into new red blood cells.** The release of merozoites from a mature schizont, known as egress, is preceded by degradation of the parasitophorous vacuole membrane (PVM) and the red blood cell membrane (RBCM). Invasion of a new erythrocyte by a released merozoite takes less than a minute. It involves the recognition of the receptors on the RBCM, attachment to the RBCM, reorientation of merozoite apical end towards the RBCM and finally the active entry, during which the parasitophorous vacuole (PV) is formed. Afterwards parasite grows and replicates within the PV, isolated from the red blood cell cytosol. Adapted from Maier et al. (2009).

## 1.2. Antimalarial drugs

A variety of drugs, belonging to the different families and inhibiting distinct stages of parasite's development, is available for prevention and treatment of malaria. With regard to their chemical structure and mode of action, current antimalarials can be classified into quinoline derivatives (quinine, quinidine, chloroquine, amodiaquine, mefloquine, halofantrine, lumefantrine, primaquine, piperaquine), antifolates (sulphonamides, pyrimethamine, proguanil), hydroxynaphthaquinones (atovaquone), antimicrobials (tetracycline, doxycycline, clindamycin), and artemisinin derivatives (artemisinin, dihydroartemisinin, artemether, arteether, artesunate) (Müller & Hyde, 2010; Travassos & Laufer, 2016). The prophylaxis and malaria treatment have become challenging due to the development of drug resistance. In response to the parasites acquiring resistance to antimalarials



used as a monotherapy, various combination strategies have been introduced, with an artemisinin-based combination therapy (ACT) recommended as a first line treatment of uncomplicated *P. falciparum* malaria (WHO, 2018a). ACT consists of two antimalarials differing in the mechanism of action, a fast acting artemisinin-based compound and a partner drug displaying a long half-life (WHO, 2018a). Despite the significant improvements made towards vaccine development in recent years, with candidate RTS,S/AS01 reaching phase III clinical trial, an efficient vaccine providing long-term protection especially against severe malaria, is not yet available (Neafsey et al., 2015; Olotu et al., 2016).

### 1.2.1. Mode of action

Depending on the stage of action, specific drugs can be used to prevent or cure the symptoms of the disease. Antimalarials can be categorized depending on their activity into the liver and blood schizonticides, gametocytocides and sporontocides (Bruce-Chwatt, 1962). **Quinolines** exhibit activity mainly against the asexual erythrocytic stages of malaria infection. These drugs accumulate in the parasite's digestive vacuole, where they interfere with the conversion of toxic heme into hemozoin, by inhibiting the heme polymerase activity. In spite of its blood stage activity, primaquine also eliminates hepatic schizonts, dormant liver forms (hypnozoites), as well as gametocytes (Arrow et al., 2004; Travassos & Laufer, 2016). **Antifolates** are blood schizonticides, blocking the enzymes of the parasite's folate biosynthesis pathway, dihydrofolate reductase (DHFR) and dihydropteroate synthase (DHPS). **Atovaquone**, administered as a partner drug of the antifolate proguanil, binds to the mitochondrial cytochrome bc<sub>1</sub> complex, thus interfering with electron transport and disrupting the membrane potential (Antony & Parija, 2016; Müller & Hyde, 2010). While **antimicrobials** display antiparasitic activity by targeting parasite's apicoplast, they act relatively slow. Thereby, their use is recommended in combination with fast acting antimalarials, such as quinine (Arrow et al., 2004; Okombo & Chibale, 2018). **Artemisinin compounds** are the fastest acting amongst the available antimalarial drugs, killing blood stage parasite forms and suppressing gametocyte transmission (Okombo & Chibale, 2018; Travassos & Laufer, 2016). The mechanism of action of artemisinins is associated with a peroxide bridge within their chemical structure. Upon binding of iron, the peroxide bridge breaks, releasing free radicals that damage membrane proteins, ultimately leading to the parasite death (Saifi, 2014; Travassos & Laufer, 2016).

### 1.2.2. Resistance

The efficacies of antimalarial medicines in the treatment of the disease are limited by a widespread of resistance. *Plasmodium* parasites have developed resistance to all antimalarials in current use,

becoming a global concern, as it affects the vast majority of the malaria endemic countries (Fig. 1.4) (WHO, 2018b).

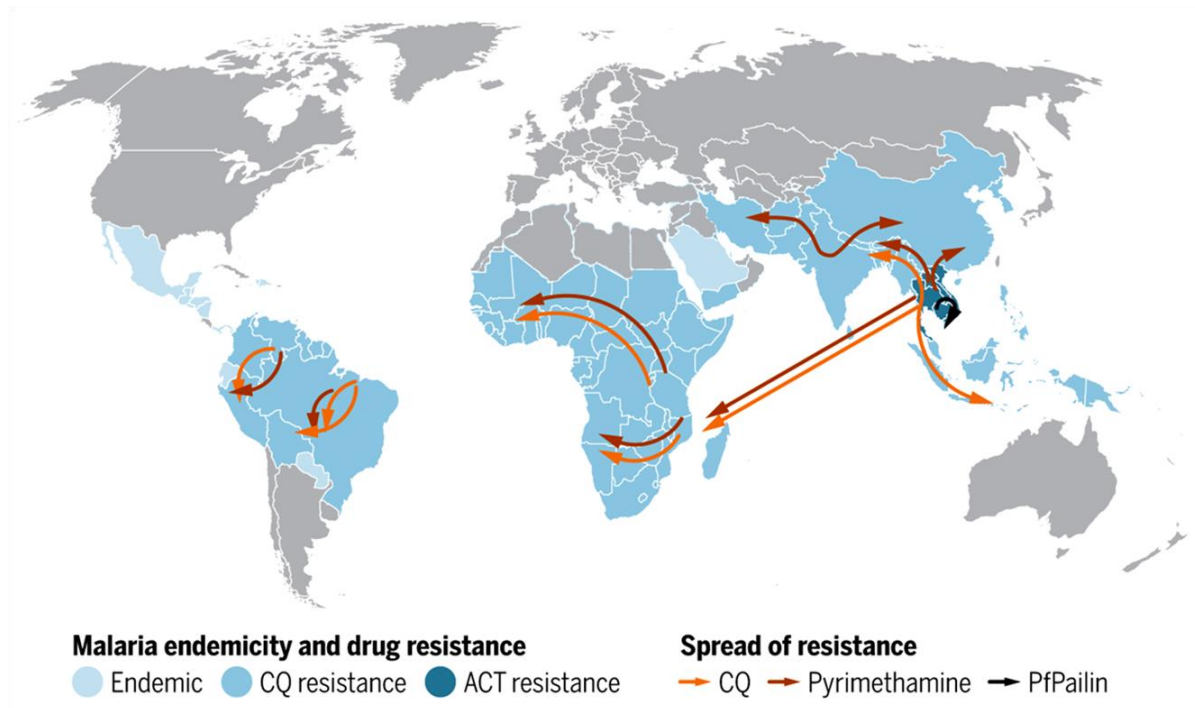


**Figure 1.4. Geographic distribution of *P. falciparum* occurrence and antimalarial drug resistance.** Blue colour highlights the countries in which malaria is endemic. Darker blue points to the worldwide spread of resistance to chloroquine (CQ), whereas navy blue indicates the resistance to artemisinin-based combination therapies (ACTs) in the South-East Asia. Orange and red arrows display the widespread resistance to CQ and pyrimethamine. Black arrow shows the expansion of a new multidrug-resistant malaria parasite lineage *PfPailin*, resistant to artemisinin and its partner drug piperazine. Adapted from Carlton (2018).

The resistance appears to occur through spontaneous *de novo* mutations or gene duplications. Under selective drug pressure, the resistant parasites exhibit a survival advantage over the sensitive strains. However, conferring resistance might be associated with a fitness cost. Thus, in the absence of a drug, the susceptible parasites might overgrow the resistant mutants (Bloland, 2001; Arrow et al., 2004; White, 2004).

The emergence and spread of resistance depends on several factors, including the parasite mutation rate, the number of parasites exposed to the drug, the fitness cost of acquired resistance, the concentration of the administered antimalarial and the treatment in the presence or absence of a partner drug, to which the parasite is sensitive (Arrow et al., 2004; White, 2004).

Resistance to the majority of antimalarials has developed either through alteration in predicted parasite transporters or via mutations in components of the pathways critical for parasite survival (Cui et al., 2015). Chloroquine resistance has been acquired by specific mutations in the gene

encoding *P. falciparum* chloroquine resistance transporter PfCRT, located in the parasite's digestive vacuole. A lysine to threonine substitution at PfCRT's position 76 (K76T) has been identified as a primary mediator of the reduced susceptibility (Lakshmanan et al., 2005). The best studied *P. falciparum* ATP-binding cassette (ABC) transporter is the P-glycoprotein homologue 1 (PfPgh-1), another drug carrier localizing to the food vacuole membrane. Polymorphisms in the gene encoding PfPgh-1, namely the multidrug resistance-1 gene (*pfmdr1*), was found to modulate the sensitivity to multiple antimalarials including chloroquine, amodiaquine, lumefantrine, mefloquine and artemisinins (Hayward et al., 2005; Sidhu et al., 2005; Veiga et al., 2016). Moreover, increased copy number of *pfmdr1* has been linked with resistance to mefloquine, quinine, lumefantrine and artemisinin (Chavchich et al., 2010; Duraisingh & Cowman, 2005; Ferreira et al., 2011; Reed et al., 2000). A point mutation in another ABC transporter, the multidrug resistance protein-1 PfMRP1, which localizes to the parasite plasma membrane, is implicated in the reduced susceptibility to chloroquine, mefloquine, lumefantrine and quinine (Gupta et al., 2014; Mok et al., 2014). Reduced quinine efficacy has also been associated with a highly polymorphic sodium–hydrogen exchanger PfNHE, localizing to the parasite plasma membrane like PfMRP1 (Pascual et al., 2013). Parasites have acquired resistance to the treatment with two combined antifolates, pyrimethamine and sulfadoxine via mutations in their target enzymes, dihydrofolate reductase (DHFR) and dihydropteroate synthase (DHPS), respectively (Oguike et al., 2016; Sharma et al., 2016). Decreased susceptibility to atovaquone is conferred by single-point mutations within the cytochrome b gene (*pfcytb*) (Goodman et al., 2016). Amongst the aforementioned antibacterial agents, resistance has been reported for clindamycin, as a result of two point mutations in the apicoplast-encoded 23S rRNA (Dharia et al., 2010). The parasites' unresponsiveness to artemisinin has been related to the mutation in the propeller domain of the *P. falciparum* Kelch 13 PfK13, a substrate adapter of an E3 ubiquitin ligase (Fig. 1.5) (Ariey et al., 2014; Mbengue et al., 2015). Nonetheless, several studies have reported a K13-independent artemisinin resistance, involving mutations in a mu chain of the adaptor protein 2 PfAP2-mu (Henriques et al., 2015), or in an actin-binding coronin PfCoronin (Demas et al., 2018). An enhanced parasite survival to artemisinin treatment raises the concern of developing resistance against partner antimalarial drugs. A spread of a multidrug resistant strain, denoted as *PfPalain* (after the geographic region, where it was first identified), has been recently reported in malaria endemic countries in the South-East Asia (Imwong et al., 2017). *PfPalain* exhibits resistance to both drugs co-administered in ACT, artemisinin and piperaquine (Imwong et al., 2017).

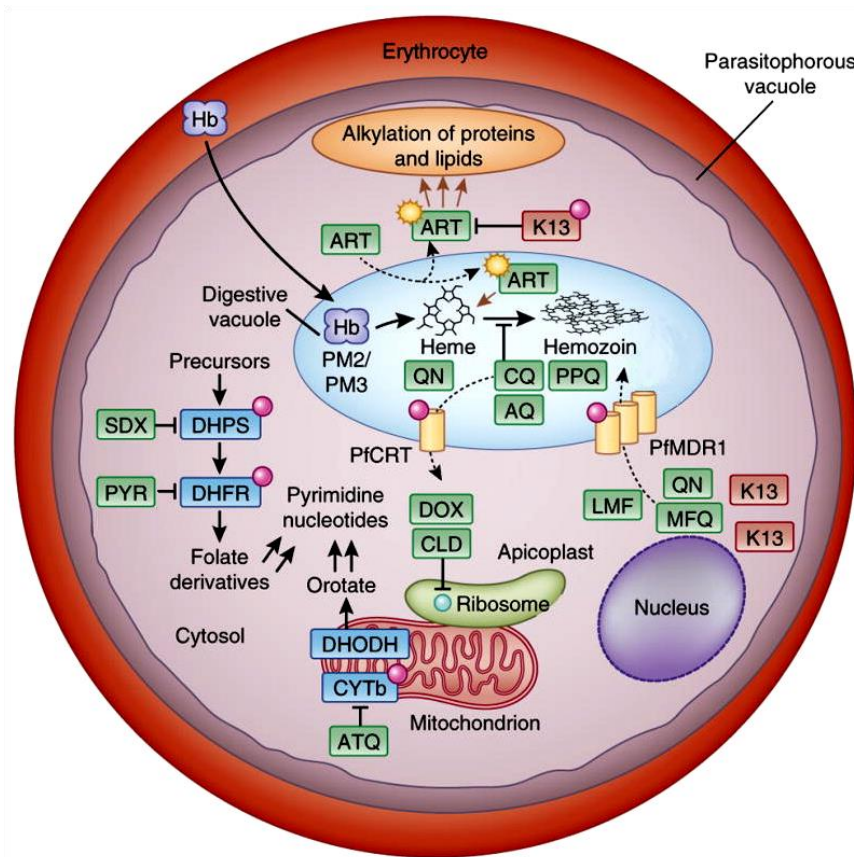


**Figure 1.5. Antimalarial drugs targets and resistance mechanisms.** Parasites have acquired resistance to various antimalarials targeting components of the digestive vacuole (DV), cytosolic folate biosynthesis pathway and mitochondrial respiratory chain. Chloroquine (CQ), quinine (QN), piperaquine (PPQ) and amodiaquine (AQ) accumulate inside the DV, where they block heme detoxification into hemozoin. Iron released during protease-mediated degradation of host haemoglobin (Hb) activates artemisinin compounds (ART) by breaking its endoperoxide bridge (yellow polygonal star symbol). Point mutations (pink dots) in the chloroquine resistance transporter (PfCRT) and the multidrug resistance transporter-1 (PfMDR1) are determinants of resistance to CQ and AQ. Decreased susceptibility to PPQ is linked to the overexpression of the hemoglobins plasmepsin 2 and 3 (PM2/PM3), in the DV, and might be modulated by mutant PfCRT. Increased copy number of *pfmdr1* along with the mutant variants of PfCRT and PfMDR1 alter parasite responsiveness to QN, lumefantrine (LMF) and mefloquine (MFQ), and can regulate ART activity. Polymorphisms in K13-propeller are the primary mediators of ART resistance, observed in the ring stage parasites. Mutations in the dihydropteroate synthase (DHPS) and dihydrofolate reductase (DHFR) confer resistance to antifolates sulfadoxine (SDX) and pyrimethamine (PYR), respectively. Atovaquone (ATQ) disrupts electron transport in the mitochondrion, by binding to the cytochrome b (CYTb), mutations of which enhance the levels of ATQ resistance. Electron transport chain has a critical function in *P. falciparum* blood stages, as it supports *de novo* pyrimidine biosynthesis, by providing electrons for the ubiquinone-dependent dihydroorotate dehydrogenase (DHODH). Antimicrobials such as clindamycin (CLD) and doxycycline (DOX) target protein translation inside the apicoplast. Resistance to CLD has been linked to point mutations in the apicoplast 23S rRNA. Adapted from Blasco et al. (2017).

Resistance has rendered all antimalarials currently in use ineffective for curing malaria. Therefore, to mitigate the further decline of the drug susceptibility, it is desired to sustain the efficacy of available antimalarial medicines, to continuously distribute preventive measures such as bed nets and to develop new antimalarial compounds. Regular monitoring of drug resistance profiles, along with research focused on the diverse contributing factors is crucial for malaria control and elimination.

### 1.2.3. The first to treat malaria: quinine and chloroquine

Two quinoline derivatives, quinine and chloroquine deserve a special attention as they were the first medications used to cure malaria, effective for a long time before the resistance against them has emerged.

**Quinine** is a naturally occurring alkaloid extracted from the bark of Peruvian cinchona tree. The use of this aryl amino alcohol for treating fevers was first documented as early as the 1630s (Achan et al., 2011). Although it is the oldest antimalarial drug, quinine (QN) is still highly appreciated nowadays for treatment of severe malaria cases, and recommended as a drug of choice for woman in the first trimester of pregnancy as well as in case the ACT is not available (WHO, 2017). A diastereoisomer of QN, quinidine, is an anti-arrhythmic agent used as alternative to QN and ACT for treatment of severe *P. falciparum* infections (WHO, 2017). The mechanism by which QN kills the parasite has recently been linked to binding of this quinoline drug to the *P. falciparum* cytosolic purine nucleoside phosphorylase (PfPNP), an enzyme with a critical function for the purine salvage pathway (Dziekan et al., 2019). On the other hand, it has been previously shown that QN accumulates to the parasite's digestive vacuole, where unlike chloroquine it does not lead to the heme build-up (Fitch, 2004). Moreover, phospholipids have also been suggested as a possible molecular target of quinine (Porcar et al., 2003). To enhance the antiparasmodial activity of this short half-life antimalarial, QN is often administered with an antibiotic (clindamycin, doxycycline, or tetracycline), particularly in the areas of emerging QN resistance (WHO, 2017). The reduced susceptibility to QN has evolved slowly and was not reported until 1910 (Peters, 1982). Although the mechanisms underlying the enhanced parasites survival to QN is not fully understood, it seems that it has a complex and multifactorial nature. Resistance to QN has been acquired by mutating the genes encoding several transporter proteins, such as PfCRT, PfMDR1, PfNHE (Cooper et al., 2002, 2007; Ferdig et al., 2004; Nkrumah et al., 2009; Sidhu et al., 2005) and by increasing the copy number of *pfmdr1* (Reed et al., 2000). Nevertheless, a potential involvement of other yet undefined genes in this phenomenon cannot be ruled out. Due to the dose-dependent side-effects associated with a long regimen of QN treatment, it has been later replaced by its synthetic derivative, chloroquine, displaying substantially reduced toxic properties (Achan et al., 2011).

Belonging to the 4-aminoquinolines, **chloroquine** (CQ) was the first antimalarial medication produced on a large scale, and a drug of choice until the introduction of ACT (Fig. 1.6). Due to its efficacy, inexpensiveness and safety, CQ has been the most widely used amongst all antimalarials for chemoprophylaxis and treatment of all types of *Plasmodium* infections (Bloland, 2001; Arrow et al., 2004; WHO, 2017). The mode of CQ's action remains a subject of debate. Being alkaline, CQ accumulates in high concentrations in the acidic food vacuole, where it gets di-protonated, what stops its free diffusion across the vacuolar membranes. Trapped inside the digestive vacuole, CQ binds to a ferriprotoporphyrin IX (FP), also known as ferric heme or hematin, forming a FP-CQ complex, thereby blocking conversion of toxic heme into a malaria pigment (hemozoin). As a consequence, a build-up of reactive free heme leads to membrane disruption and eventually parasite death. It has also been suggested that this antimalarial inhibits DNA and RNA biosynthesis, and as a result protein synthesis (Ridley, 1998; Petersen et al., 2011; Saifi, 2014). Resistance to CQ arose slowly, taking almost 20 years since the introduction of the drug, despite its extensive use for treatment of the disease. This suggests that alteration of several genes was required to confer a resistance phenotype (Saifi, 2014). As mentioned previously, reduced CQ susceptibility has been linked to mutations in genes encoding transporters PfCRT, PfMDR1 and PfMRP1 (Blasco et al., 2017; Travassos & Laufer, 2016).

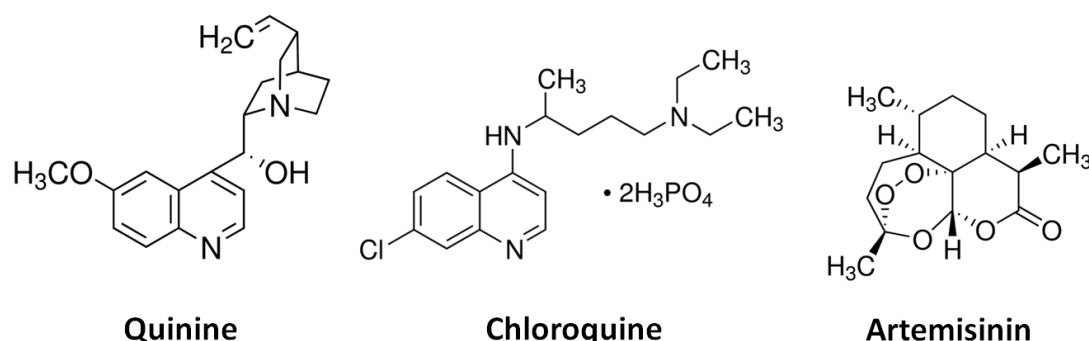


**Figure 1.6.** Chemical structures of the first antimalarial agents, quinine and chloroquine, in comparison to the main component of the ACT, artemisinin.

### 1.3. Posttranslational modifications (PTMs)

Maintaining the cellular homeostasis and control of stress responses is governed by numerous regulatory networks at epigenetic, transcriptional, posttranscriptional and posttranslational level. These mechanisms are important for coordinated gene expression and, hence, *Plasmodium* development. However, the major aspects of life cycle transitions and response to environmental stimuli seem to be modulated posttranslationally (Chung et al., 2009; Doerig et al., 2018).

Posttranslational modification (PTM) refers to a covalent alteration of specific amino acid(s) within a protein, through an enzyme-mediated attachment or removal of a functional group, following protein synthesis. Due to the reversible nature, the PTMs provide a dynamic regulation of protein functions. By changing a protein mass, charge and/or conformation, the PTMs can modulate protein's enzymatic activity and stability, localization and binding affinity (Chung et al., 2009; Doerig et al., 2015). Thereby, they not only generate diversity and complexity of the proteome but also play critical roles in numerous cellular processes and in parasite survival. The most widely described PTMs in *Plasmodium*, include phosphorylation (Solyakov et al., 2011; Pease et al., 2013), acetylation (Filisetti et al., 2013), methylation (Ponts et al., 2013) and lipidation such as prenylation, palmitoylation and GPI-anchoring (Jones et al., 2012; Doerig et al., 2015). Phosphorylation and lipidation have been shown to influence parasite motility, invasion, intraerythrocytic development and egress. Histone methylation and acetylation are believed to regulate expression of *var* genes, encoding the *P. falciparum* erythrocyte membrane proteins PfEMP, in asexual blood stages (Doerig et al., 2015). Among other types of PTMs identified in malaria parasites are ubiquitination, SUMOylation (Issar et al., 2008), glycosylation (Kimura et al., 2000; Macedo et al., 2010), nitrosylation (Wang et al., 2014) and glutathionylation (Kehr et al., 2011). Another form of plasmodial PTMs is proteolytic processing, shown to have critical functions in haemoglobin degradation, as well as during parasite egress and invasion events (Chung et al., 2009). Moreover, some types of PTMs, such as phosphorylation or ubiquitination, have multiple roles, relatively high abundances and broad substrate specificities. On the contrary, other ones such as acetylation exhibit highly specific functions and relatively low abundances, targeting only one or a handful of proteins. Furthermore, the interplay between various PTMs has received a special attention in recent years, as the key to understanding the dynamics and complexity of the PTM regulating the parasite biology (Aggarwal et al., 2017; Yakubu et al., 2018). In *P. falciparum*, a significant crosstalk between the phosphorylation and ubiquitination pathways has been suggested to have an impact on the formation of invasive merozoites (Lasonder et al., 2015).

With the emergence of drug resistance to all antimalarials in clinical use, it is essential to understand the key regulators of *Plasmodium* development, including the PTMs. Due to their crucial function in the control of numerous cellular processes, the mediators of PTMs seem to be attractive targets for antimalarial drug discovery (Chung et al., 2009).

### 1.3.1. Role of PTMs in drug resistance

Distinct PTMs have been implicated in modulation of drug resistance profiles in other systems (Aggarwal et al., 2017; Ahmad & Glazer, 1993; Ardiani et al., 2009; Emery et al., 2018; Germann et al.,

1996). Resistance-conferring mutations can alter a protein's function by either gaining or losing a PTM site. Alternatively, the PTMs may not interact with the drug resistance-mediator directly, but still influence the drug susceptibility of the cells, by upstream regulation of a signalling cascade in which this protein is involved (Aggarwal et al., 2017). For example, a serine substitution by non-phosphorylatable alanine residue was shown to increase drug susceptibility, dependent on phosphorylation of two mammalian ABC transporters (Germann et al., 1996; Xie et al., 2008). A recent study in another protozoan parasite, *Giardia duodenalis*, revealed an association between the drug resistance and protein acetylation (Emery et al., 2018). A potential involvement of palmitoylation in the reduced drug susceptibility of *P. falciparum* has been also considered, as the two main determinants of resistance to quinolines, PfCRT and PfMDR1, are modulated by this modification (Jones et al., 2012).

A thorough understanding of the role of PTMs in altering the parasite signalling pathways may contribute to an improved control or even elimination of drug resistance.

### 1.3.2. Phosphorylation and its role in the activity of PfCRT

Phosphorylation involves kinase-mediated addition of a phosphoryl group, principally to a serine (S), threonine (T) or tyrosine (Y) residue in a substrate protein. This mechanism is antagonized by the activity of phosphatases which remove the modification from the target protein (Chung et al., 2009). Reversible protein phosphorylation is one of the major regulatory mechanisms involved in the control of *Plasmodium* life cycle (Yakubu et al., 2018). This posttranslational modification has been shown as critical for parasite invasion into the host cell (Alam et al., 2015; Vaid et al., 2008), progression inside the red blood cell (Blomqvist et al., 2017; Graeser et al., 1996; Mendenhall et al., 1988; Silva-Neto et al., 2002) and egress of merozoites (Iyer et al., 2018). Moreover, phosphorylation has been implicated in the control of *Plasmodium* sexual differentiation, as well as the host-parasite interactions (Chung et al., 2009).

The role of phosphorylation in mediating the function of a transporter protein has been reported in numerous studies (Foster et al., 2006; Ramamoorthy et al., 2011; Stolarczyk et al., 2011). In *P. falciparum*, the chloroquine resistance transporter PfCRT could be cited as an example of a protein regulated by phosphorylation. PfCRT is a digestive vacuolar membrane protein containing ten putative transmembrane domains and N- and C- terminal lobes facing parasite's cytosol (Fig. 1.7). Apart from being phosphorylated at S33, S411, T416 and S420 (Kuhn et al., 2010; Lasonder et al., 2012; Solyakov et al., 2011), PfCRT is also palmitoylated at cysteine (C) 301 (Jones et al., 2012). While, the T416 phosphorylation has been associated with PfCRT's trafficking from the ER to the food



vacuolar membrane (Kuhn et al., 2010), the relevance of other modifications remains to be resolved. Given that the PTMs were found to modulate the resistance profiles and that PfCRT is a determinant of parasite reduced susceptibility to quinolines, a phosphorylation or palmitoylation of this drug/metabolite carrier could possibly regulate the parasite's responsiveness to antimalarials.

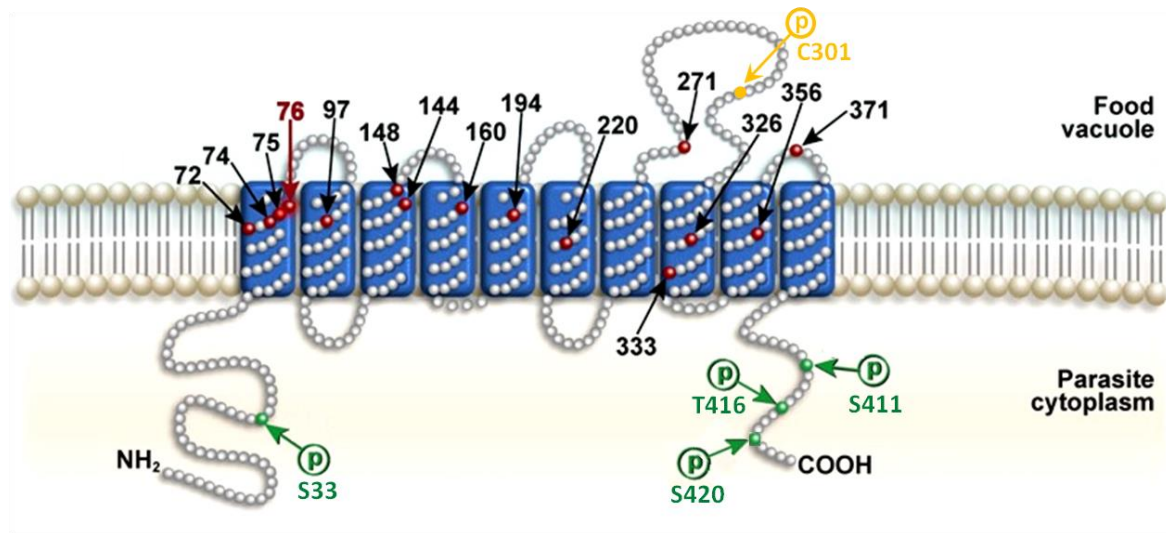


**Figure 1.7. Topology of the chloroquine resistance transporter PfCRT.** *pfCRT* encodes a 424 amino acids protein localizing to the membrane of parasite's digestive vacuole. It contains ten transmembrane domains and N- and C-terminal ends directed towards the parasite cytoplasm. Red dots highlight polymorphic residues. The K76T mutation, a molecular marker of PfCRT-mediated chloroquine resistance is pointed out by a red arrow. PfCRT is posttranslationally modified by phosphorylation at S33, S411, T416 and S420 (green) and palmitoylation at C301 (orange). A green "p" indicates a phosphate group, whereas an orange "p" signifies a palmitoyl group. Adapted from Sanchez et al. (2010).

### 1.3.3. The ubiquitin pathway and PfUT-mediated ubiquitination

Ubiquitination, also known as ubiquitylation or ubiquitynylation, refers to a posttranslational labelling of a substrate protein with a small regulatory protein, namely ubiquitin. It involves formation of an isopeptide bond between the C-terminal glycine of an ubiquitin molecule and a lysine residue on the target protein. Ubiquitination is a three-step process, including ubiquitin activation, conjugation and ligation to the substrate. It is driven by a cascade of enzymes, namely ubiquitin-activating enzymes (E1), ubiquitin-conjugating enzymes (E2) and ubiquitin ligases (E3) (Chung et al., 2009). The latter group comprises of HECT (Homologous to E6-associated protein C-Terminus), RING (Really Interesting New Gene)/U-box and RBR (RING-Between-RING) families, categorized according to the structural organization and mechanism of these E3-type ligases (Lorenz, 2018). Unlike the RING E3-type ubiquitin ligases, the HECT and RBR catalyse the modification of a substrate protein in a two-phase mechanism, involving the formation of a thioester intermediate between an ubiquitin and an E3 catalytic cysteine (Wenzel & Klevit, 2012). Similar to phosphorylation, a covalent attachment of

ubiquitin can be reversed by means of deubiquitinating enzymes (DUBs). *P. falciparum* encodes at least 8 E1 or E1-like proteins, 14 E2 or E2-like proteins, 54 E3 or E3-like proteins and 29 DUBs (Hamilton et al., 2014).

A substrate protein can be modified by a mono-, multi- or polyubiquitination. Depending on the type and length of the ubiquitin chain, the labelled protein can undergo either proteasomal degradation or be regulated in a particular manner (Fig. 1.8.).

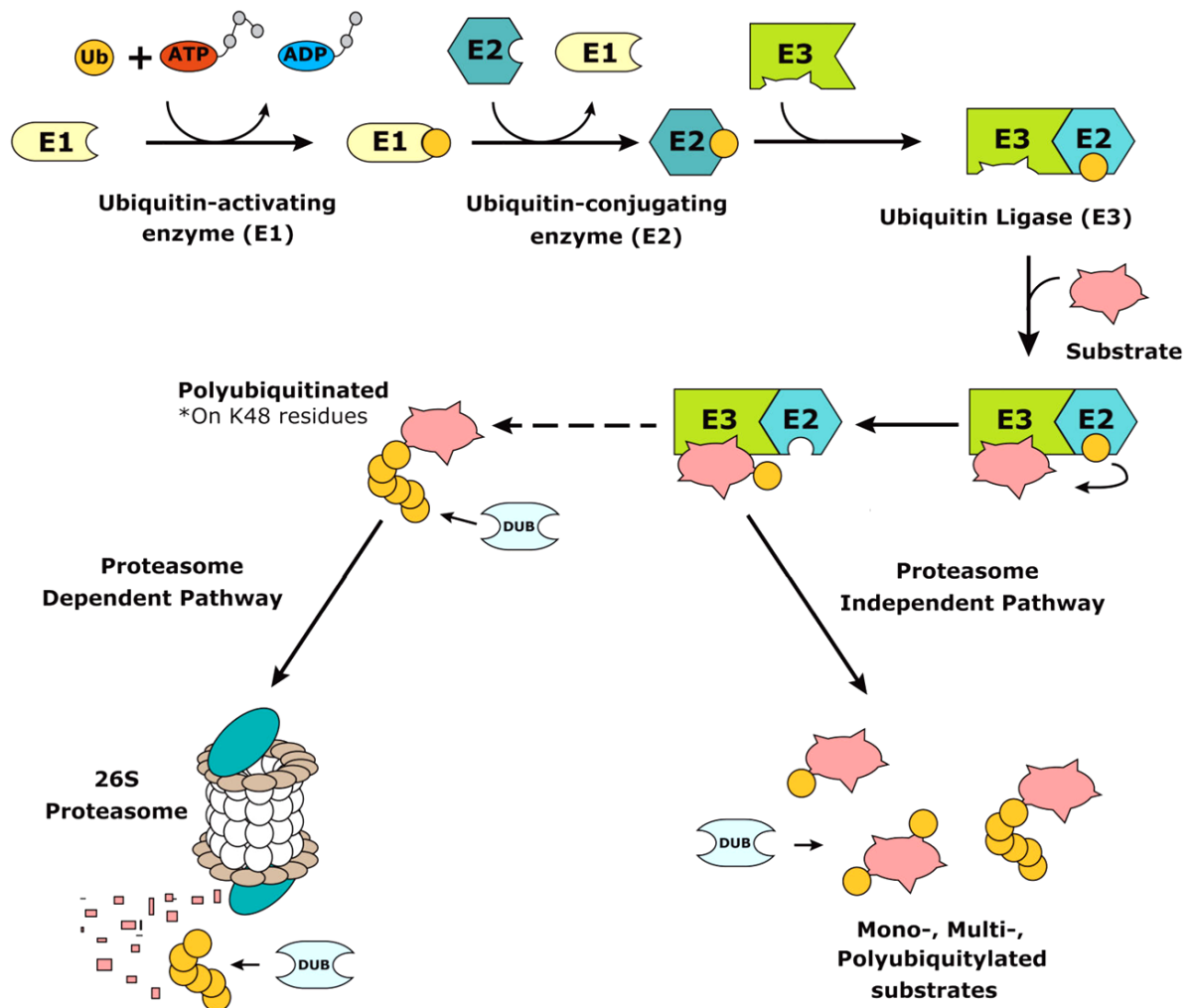


**Figure 1.8. Schematic of the ubiquitin-mediated pathways.** Protein tagging with an ubiquitin moiety consists of three subsequent steps. Initially, ubiquitin (Ub) is activated by the ATP-dependent E1. Ubiquitin is then transferred from E1 to the E2. Ubiquitin-conjugated E2 binds to the E3 ligase. Finally, E3 mediates transfer of ubiquitin from E2 to the substrate protein. In RING and U-box ligases this step occurs directly, whereas the HECT and RBR families form a thioester intermediate. The type and length of the ubiquitin chain defines the pathway, proteasome dependent or independent, which the labelled protein will follow. Ubiquitin can be attached to a substrate as one or several monomers (mono- and multiubiquitination) or polymer (polyubiquitination). K48-linked polyubiquitination directs proteins for proteasomal degradation. Mono- and multiubiquitination mediate among others DNA repair and endocytosis. Similar processes are regulated by K63 polyubiquitin chains, which are additionally implicated in signalling. The role of other modifications

associated with sequential linkage of ubiquitin's internal lysines awaits investigation. Deubiquitinating enzyme (DUB) can remove an ubiquitin mono- or poly-tag from the substrate protein. Thereby, DUBs replenish the pool of free ubiquitin molecules required for ubiquitination process. Adapted from Hamilton et al. (2014).

As ubiquitin molecule contains seven lysine (K) residues at positions 6, 11, 27, 29, 33, 48 and 63, poly-ubiquitin chains of different topology and complexity can be formed. Specific chain types are then captured by ubiquitin-binding domain (UBD)-containing proteins, which target the labelled protein to the respective signalling pathway (Suryadinata et al., 2014). Mono- and multiubiquitination have been shown to modulate DNA repair, gene expression, protein transport and endocytosis (Perrett et al., 2011; Sadowski & Sarcevic, 2010). Ubiquitin conjugated as polymer through lysines at position 48 (K48) predominantly targets proteins for degradation on the proteasome. Similarly, K11-mediated polyubiquitination can also result in proteasomal destruction. In contrast, a protein modified via K63 follows a non-degradative pathway, associated with DNA damage tolerance, ribosomal protein synthesis, endocytosis, signal transduction or activation of protein kinases (Bange et al., 2007; Chung et al., 2009; Wang et al., 2012). The relevance of other polyubiquitin-chain types needs to be resolved. Considering the importance of ubiquitin-mediated protein modification in control of multiple cellular processes, the ubiquitin-proteasome system appears to be an attractive target for novel malaria intervention strategies (Ng et al., 2017).

Apart from ubiquitin, several ubiquitin-like modifiers (UBLs) have been identified in *Plasmodium*. These include SUMO (small-ubiquitin-related modifier), NEDD8 (neural precursor cell expressed developmentally downregulated 8), HUB1 (homologous to ubiquitin 1), URM1 (ubiquitin-related modifier 1) and ATG8 (autophagy 8) proteins (Issar et al., 2008; Ponts et al., 2008; Artavanis-Tsakonas et al., 2010; Reiter et al., 2013). Similarly to ubiquitin, the UBLs regulate substrate proteins via E1-E2-E3 cascade, although they display distinct enzyme specificities (Ponts et al., 2008).

Numerous studies have reported an association between the ubiquitin pathway and the antimalarial drug resistance. For instance, mutations in two E3 ubiquitin ligases, belonging to the HECT and RING families, have been linked with reduced susceptibility of *P. falciparum* to pyrimethamine (Park et al., 2012) and artemisinin (Takala-Harrison et al., 2013), respectively. Moreover, polymorphisms in genes encoding different deubiquitinating enzymes were found to alter the parasite's responsiveness to artesunate and chloroquine (Hunt et al., 2007), as well as to artemisinin (Henriques et al., 2014). Furthermore, resistance to the frontline antimalarial, artemisinin, has been shown to arise from mutations in Kelch 13, an adaptor protein recruiting substrates for a RING E3 ubiquitin ligase (Ariey et al., 2014). Another component of the ubiquitin-proteasome system, the *P. falciparum* ubiquitin

transferase PfUT has been suggested to affect parasites sensitivity to quinine and quinidine (Sanchez et al., 2014).

The ubiquitin transferase is one of the four *P. falciparum*-encoded HECT ubiquitin ligases. *pfut* encodes the 460 kDa membrane protein localizing to the ER/Golgi complex. It contains four predicted transmembrane domains and N- and C-terminal ends, presumably directing the parasite's cytoplasm. PfUT's carboxyl end is characterized by a presence of a HECT catalytic domain, governing the ubiquitination (Fig. 1.9). This domain has been proven catalytically active *in vitro* (Sanchez et al., 2014). Moreover, PfUT is posttranslationally modified by phosphorylation at Y347, T372, S411 and S1873 (Pease et al., 2013) as well as by acetylation at K2929 (Cobbold et al., 2016). As many of the HECT E3 ligases do not possess obvious substrate-binding motifs or domains, the prediction of a target-protein recognition site may be challenging (Beaudenon et al., 2005). PfUT's substrate binding region, however, seems to be localized close to its N-terminus, what could be assumed based on the presence of two long stretches of armadillo (ARM) repeats, typically implicated in protein-protein interactions (PlasmoDB). ARM repeat-containing proteins have been shown to play versatile cellular roles (Tewari et al., 2010). Nevertheless, the physiological function of PfUT in the *Plasmodium* life cycle remains to be established.

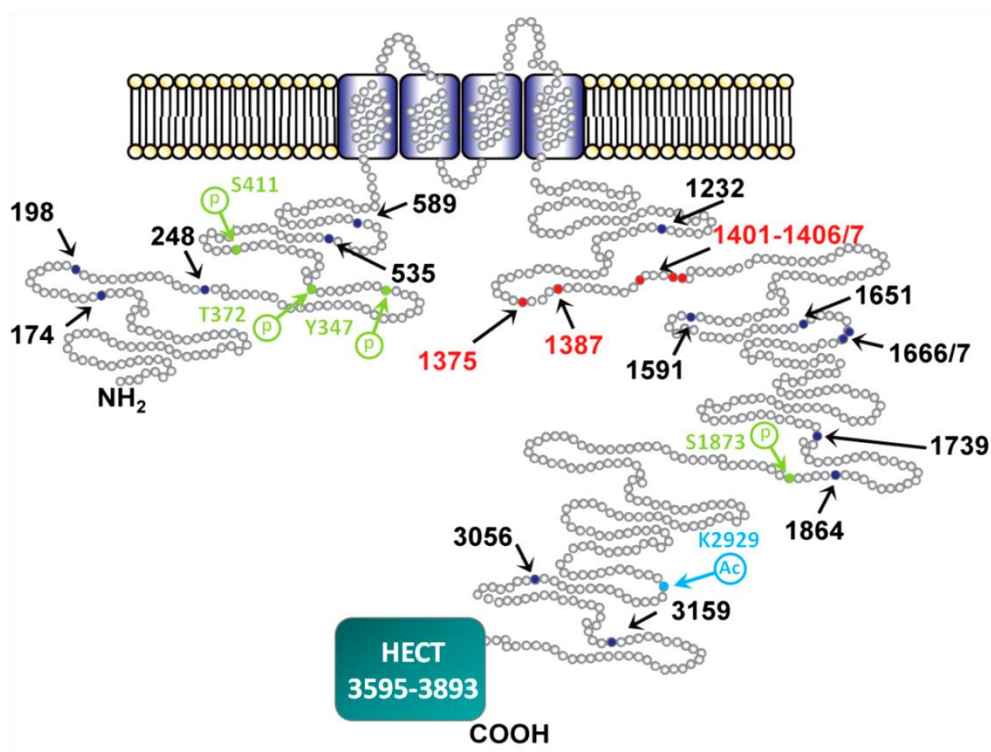


**Figure 1.9. Topological model of the ubiquitin transferase PfUT.** PfUT is a 3893 amino acids protein integrated to parasite's ER/Golgi membrane via four putative transmembrane domains. This HECT E3-type ubiquitin ligase contains a presumed N-terminal substrate binding region and a C-terminal HECT catalytic domain, responsible for ubiquitination. PfUT is phosphorylated at Y347, T372, S411

and S1873 (green) and acetylated at K2929 (blue). Black arrows point at the polymorphic residues. Red colour denotes polymorphisms conserved among different field isolates and laboratory strains, despite distinct geographic origins. Green “p” and blue “Ac” indicate a phosphoryl and an acetyl group, respectively. Adapted from Sanchez et al. (2014).

## 1.4. Genetic manipulation of *P. falciparum* genome

Genetic engineering of *P. falciparum* genome is critical for unravelling the mechanisms behind the reduced susceptibility to antimalarial drugs. Validation of a gene contribution to the resistance phenotype requires efficient tools enabling the modification of the parasite’s genome. Furthermore, uncovering the genes essential for *Plasmodium* pathogenesis could define new targets for malaria therapy (de Koning-Ward et al., 2015).

The genetic material of *P. falciparum* is organized into 14 linear chromosomes (23 Mb) contained in the nucleus, in addition to circular genomes found in the mitochondrion (6 kb) and apicoplast (35 kb) (Gardner et al., 2002). The GC content estimated to 19.4% (Gardner et al., 2002), classifies this human malaria parasite as one of the most AT-rich eukaryotes identified to date.

Adaptation of *P. falciparum* to continuous *in vitro* culture enables its genetic manipulation. The haploid genome of this apicomplexan parasite facilitates gene editing, as only a single copy needs to be targeted (Carvalho & Ménard, 2005). Another advantage includes accessibility to the fully sequenced genome of *P. falciparum* 3D7 strain (Chang et al., 2012). However, a particularly AT-rich genome composition often hinders the cloning of transfection vectors. Moreover, relatively low efficiency of transfection as well as low frequency of integration driven by certain integration methods may limit successful recombination events. Transfection of malaria parasite with a plasmid DNA is based on an electroporation primarily of the ring-stage forms. Transfected parasites are then selected for integration or episomal expression, by means of a drug resistance cassette carried in the plasmid backbone. The most frequently used selectable marker is a human dihydrofolate reductase (hDHFR), conferring resistance to the drug WR99210 (de Koning-Ward et al., 2015).

### 1.4.1. Genome editing tools

*Plasmodium* does not have a non-homologous end joining (NHEJ) machinery, used in other organisms to repair the DNA broken via double strand breaks (DSBs). Nevertheless, the parasite is capable of fixing the damaged DNA by accurate homologous recombination (HR), govern in the presence of a DNA template (Lee et al., 2014).

With recent advances in *P. falciparum* molecular genetics, numerous systems are available to modify the *P. falciparum* genome. These include integration of the transfection plasmid carrying

homologous DNA or “trace-free” editing, mediated by a single or double crossover event, respectively (Fig. 1.10) (de Koning-Ward et al., 2015).

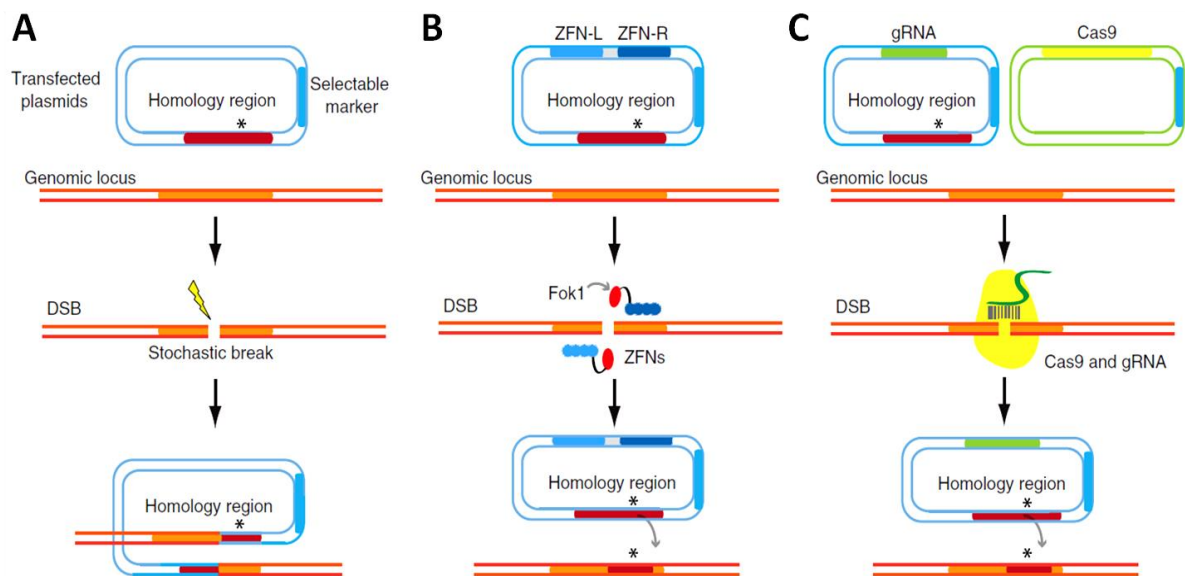


**Figure 1.10. Strategies for editing the *P. falciparum* genome.** **A.** Traditional engineering approach is based on the homology-directed repair of the spontaneous double strand breaks (DSBs) in DNA, near the target site (black star). Recombination between plasmid and chromosomal DNA occurs in a single crossover event. On the contrary, site-specific nucleases drive directed DSBs, followed by a homology-driven repair using the donor DNA (containing two homology arms flanking the gene of interest) via a double crossover recombination. **B.** Zinc-finger nuclease (ZFN)-based manipulation. A pair of ZFNs consists of ZFN-L and ZFN-R, each fused to a split FokI domain (red dot), carried on a single plasmid. Following expression, their dimerization assembles a functional enzyme, which induces DSB at the specified target site. **C.** CRISPR-Cas9-mediated editing relies on simultaneous expression of Cas9 endonuclease and the guide RNA, directing it to the target cleavage site. A repair template carrying a desired DNA modification is contained in the plasmid encoding the guide RNA. Adapted from Lee and Fidock (2014).

**Conventional approach** to manipulate the gene in *P. falciparum* involves the on and off drug-exposure cycles, for up to 3 months of culture before the desired recombination may occur. It is, nonetheless, applicable for gene disruption or allelic substitution (Fig. 1.10.A) (Lee & Fidock, 2014).

A modernized version of a classical approach, termed **selection linked integration (SLI)**, has been recently developed. SLI involves traditional homology-directed plasmid integration into the target locus, yet considerably improving the time-efficiency and success rate in obtaining transgenic parasites. Including a T2A skip peptide between the tagged gene of interest and a selectable marker provides separate expression of these two, even though they are regulated by the same endogenous promoter (Birnbaum et al., 2017).

The more precise, site-directed genome editing takes advantage of specific nucleases, which generate DSBs at the desired target sequence enabling various gene alterations. Among them are the **zinc finger nucleases** (ZFNs). These metalloenzymes comprise the catalytic domain of the FokI endonuclease and multiple zinc-finger proteins (DNA-binding domains). By inducing DSBs at the defined DNA site, the ZFNs trigger a template-guided homologous recombination (Fig. 1.10.B). Despite the time-efficiency and improved precision over the conventional method, the usage of ZFNs-mediated approach is limited by the cost and complexity of engineering the zinc-finger proteins (de Koning-Ward et al., 2015).

The *P. falciparum* genome editing has been revolutionized with the introduction of a robust and cost-effective technology, comprising the CRISPR (clustered regularly interspaced short palindromic repeats) and the accompanying Cas9 (CRISPR-associated protein 9) (Ghorbal et al., 2014). The **CRISPR-Cas9** system is based on the RNA-guided cleavage by Cas9 endonuclease, followed by the homologous end joining repair (Fig. 1.10.C). It has been adapted from the bacteria *Streptococcus pyogenes*, where it serves as a defense mechanism against viruses (Jinek et al., 2012). The guide RNA consists of 20 nucleotides, complementary to the target site, and a protospacer adjacent motif (PAM), present for cleavage. It also contains the scaffold sequence required for Cas9 binding, so called tracrRNA (Mali et al., 2013).

Alternative *P. falciparum* genome manipulation strategy allowing for multiple alteration of a single gene locus, includes the **Bxb1 integrase** system (Balabaskaran-Nina & Desai, 2018). Bxb1 catalyses the irreversible recombination between the chromosomal *attB* site and a donor *attP* site, carried on the plasmid along with the gene of interest. The system does not require drug selection. Nonetheless, generation of *P. falciparum* line containing a silent *attB* site integrated into a nonessential *cg6* gene (Nkrumah et al., 2006) or within an intron of the target gene (Balabaskaran-Nina & Desai, 2018) is a pre-requirement of this approach, restricting its application.

Although the genome sequence of *P. falciparum* has been analyzed, a considerable fraction of genes contained in it awaits functional investigation. High-throughput genetic screens contribute to unravelling the genes with critical roles for parasite's asexual blood stage development. This, in turn is advantageous for the design of novel drugs and vaccines against malaria infection. An example of such technology involves gene mutagenesis via insertion of **piggyBac transposable elements** (de Koning-Ward et al., 2015). *piggyBac* transposase mediates integration of a drug resistance cassette into random TTAA-target sites, highly abundant in the *P. falciparum* genome (Balu et al., 2005; Zhang et al., 2018).

Although applied efficiently in many eukaryotic systems, the **RNA interference** (RNAi) is not possible in *P. falciparum*, as the parasite lacks the necessary enzymes (Baum et al., 2009).

### 1.4.2. Conditional gene downregulation methods

The haploid nature of the *P. falciparum* genome hinders the classical knockout of genes displaying critical roles in the intraerythrocytic life cycle, as it may cause parasite death. Therefore, the functional dissection of supposedly essential genes should be approached through a conditional disruption. Various methodologies have been established to conditionally manipulate gene expression at the genome, transcript or protein level (de Koning-Ward et al., 2015).

One of the conditional DNA deletion systems includes the **Cre-loxP**. Site-specific Cre recombinase catalyses the excision of a DNA fragment located between the two *loxP* sites. The activity of Cre can be regulated by a tetracycline analogue, anhydrotetracycline (ATc). Removal of the ATc from the culture medium results in activation of weak tetracycline (Tet) promoter, thereby enhancing the levels of Cre-mediated recombination (Jones et al., 2016). Moreover, the **DiCre** (Dimerizable Cre) system has been developed as a more efficient alternative of the ATc-mediated Cre method. DiCre relies on the dimerization of the two halves of Cre, fused to the FKBP (FK506-binding protein) and FRB (FKBP-rapamycin binding ) proteins, driven by the presence of rapamycin (Knuepfer et al., 2017).

A conditional alteration of *P. falciparum* genes can be also applied on the transcriptional level. One of the examples embraces the ATc-regulated **Tet-Off** technology (Gossen & Bujard, 1992; Meissner et al., 2005). In this case, the promoter of the gene of interest is replaced by a weak one, containing numerous tetracycline operator (TetO) sites. Binding of the transcriptional transactivator domain (TRAD) to TetO initiates the gene expression. Exposure to ATc inhibits this interaction, in turn blocking the gene expression (Meissner et al., 2005).

A method implicating the posttranscriptional regulation of mRNA levels involves the use of metabolite-responsive self-cleaving **glmS ribozymes** (Prommana et al., 2013). These RNA molecules displaying catalytic activity are commonly found in bacterial genomes. They reside in the 5' UTRs of the genes implicated in production of glucosamine 6-phosphate (GlcN6P) (Lee & Lee, 2017). glmS ribozymes contain four domains (so called pseudoknots) of which P1 and P2 are involved in the recognition of GlcN6P, whereas P3 and P4 are required for structural stabilization (Roth et al., 2006). Glucosamine (GlcN)-induced self-cleavage of glmS ribozyme destabilizes the mRNA, in turn decreasing the produced protein levels. Therefore, by integrating the glmS ribozyme into the 3' untranslated region (UTR) of the gene of interest, its expression can be regulated in GlcN-dependent manner (Prommana et al., 2013).



Conditional downregulation on the protein level could be achieved via the **DD** (FKBP-based destabilization domain) (Robbins et al., 2017) or the **DDD** (DHFR-based destabilization domain) approaches (Cobb et al., 2017). The fusion of the protein of interest with either of these two domains leads to its ubiquitination-mediated degradation, through the endoplasmic reticulum-associated degradation (ERAD) pathway. The presence of stabilizing ligands (Shield 1 and trimethoprim, for the DD and DDD system, respectively) can reverse the degradation (Cobb et al., 2017; Robbins et al., 2017). Alternatively, the conditional aggregation domain (**CAD**)-based strategy could be employed as an inducible system for *P. falciparum* export proteins (Kuhn et al., 2010; Saridaki et al., 2008). Fusion of an export protein with CAD results in its aggregation inside the ER, and thereby inhibition of protein transport. The protein arrest can be reversed upon addition of an anti-aggregation ligand (AP21998) (Saridaki et al., 2008).

Finally, the diversity of available inducible systems is of high relevance, as the success of the approach chosen for manipulation of a particular gene is often uncertain. Furthermore, a transgenic line generated using one of the above described methodologies requires robust functional assays for the phenotypic characterization of the parasite (de Koning-Ward et al., 2015).

## 1.5. Aim of the study

Posttranslational modifications (PTMs) control numerous processes with fundamental roles for the biology and pathogenesis of the human malaria parasite. Although alterations in the PTMs have been associated with the reduced drug susceptibility in several eukaryotes, such correlations have not yet been extensively investigated in *Plasmodium*.

The purpose of this doctoral study was to gain a deeper insight into the role of specific PTMs in mediating *P. falciparum* events throughout its asexual life cycle. On the one hand, this thesis aimed to assess whether phosphorylation modulates the PfCRT-mediated resistance to chloroquine and quinine. The focus of the investigation was put on PfCRT's serine 33. The involvement of phosphorylation in this phenomenon has been addressed through chemical and genetic methods. On the other hand, this work aimed at understanding the physiological function of PfUT during parasite's intraerythrocytic development. Another objective was to validate the PfUT's association with parasite's altered responses to quinine and quinidine. To meet these goals a conditional downregulation as well as gene disruption have been attempted.

As phosphorylation and ubiquitination regulate numerous pathways critical for *P. falciparum* proliferation and survival, the mediators of these PTMs are attractive targets for drug discovery against malaria. Moreover, understanding the mechanisms underlying the PTM-mediated drug

resistance could limit or even prevent the resistance spread by implementation of novel antimalarial combination therapies. Therefore, results of the current study could contribute not only to gaining a profound knowledge concerning implication of the PTMs in parasite's biology, but also to identification of new targets for malaria therapy.

## 2. Materials and Methods

### 2.1. Materials

#### 2.1.1. Equipments

| Equipment                                  | Company                                     |
|--|---|
| Analytical scales                          | Sartorius, Göttingen                        |
| Autoclave ABT 120-5DM                      | Kern & Sohn, Balingen, Germany              |
| Autoclave 2540 EL                          | Tuttnauer, Breda, The Netherlands           |
| Blot scanner C-DiGit                       | Li-cor, Bad Homburg, Germany                |
| Camera S6X11                               | Rainbow CCTV, Irvine, CA, USA               |
| Centrifuge Biofuge fresco                  | Thermo Fisher Scientific, Dreieich, Germany |
| Centrifuge Biofuge pico                    | Thermo Fisher Scientific, Dreieich, Germany |
| Centrifuge J2-MC                           | Beckman Coulter, Krefeld, Germany           |
| Centrifuge Megafuge 1.0 R                  | Heraeus, Hanau, Germany                     |
| Centrifuge Megafuge 2.0 R                  | Heraeus, Hanau, Germany                     |
| Centrifuge Sorvall RC5B Plus               | Thermo Fisher Scientific, Dreieich, Germany |
| Electrophoresis power supply Power Pac 300 | Bio-Rad, München, Germany                   |
| Electrophoresis power supply Power Pac 200 | Bio-Rad, München, Germany                   |
| Electrophoresis power supply EPS 1001      | Amersham (GE Healthcare), München, Germany  |
| Electrophoresis power supply EPS 3501      | Amersham (GE Healthcare), München, Germany  |
| Electroporator Gene Pulser II              | Bio-Rad, München, Germany                   |
| Flow cytometer BD FACSCanto                | BD Biosciences, San Jose, CA, USA           |
| Freezer -20°C LGex 3410 MediLine           | Liebherr, Biberach, Germany                 |
| Freezer -80°C HERAfreeze                   | Thermo Fisher Scientific, Dreieich, Germany |
| Fridge LKexv 3910 MediLine                 | Liebherr, Biberach, Germany                 |
| Gas burner gasprofi 1 micro                | WLD-TEC                                     |
| Heating block NeoBlock Mono I              | NeoLab, Heidelberg, Germany                 |
| Ice machine                                | Ziegra, Isernhagen, Germany                 |
| Incubator Heraeus B12/UB12                 | Thermo Fisher Scientific, Dreieich, Germany |
| Light optical microscope Axio Lab.A1       | Zeiss, Jena, Germany                        |
| Liquid nitrogen tank MVE Cryosystem 6000   | Thermo Fisher Scientific, Dreieich, Germany |
| Liquid nitrogen tank LS 6000               | Taylor-Wharton, Husum, Germany              |
| Liquid nitrogen tank RS Series             | Taylor-Wharton, Husum, Germany              |
| Magnetic sorter VarioMACS                  | Miltenyi Biotec, Bergisch Gladbach, Germany |
| Magnetic stirrer RCT                       | IKA, Staufen, Germany                       |
| Magnetic stirrer COMBIMAG RCH              | IKA, Staufen, Germany                       |
| Magnetic stirrer HR 3001                   | Heidolph, Schwabach, Germany                |
| Microwave oven R940/94ST                   | Sharp, Hamburg, Germany                     |
| MiliQ water system Purist ultrapure        | Rephile, Germany                            |
| Particle counter                           | Beckman Coulter, Krefeld, Germany           |
| pH meter pH 7110                           | WTW, Weilheim, Germany                      |
| Pipetman Gilson P2, P20, P200, P1000       | Gilson, Limburg an der Lahn, Germany        |
| Pipetus Forty / Standard                   | Hirschmann, Eberstadt, Germany              |
| Plate reader FLUOstar OPTIMA               | BMG Labtech, Ortenberg, Germany             |
| Printer hp LaserJet 1300                   | Hewlett Packard, Heidelberg, Germany        |
| Rotors JA20.2, JA20.1                      | Beckman instruments, Palo Alto, CA, USA     |
| Rotors SS-34; GS-3 , SM24                  | DuPont Instruments, Bad Homburg, Germany    |

|  |   |
|--|---|
| Scanner Epson Perfection 2400                  | Epson America, Long Beach, CA, USA          |
| SDS PAGE XCell SureLock Mini-Cell              | Thermo Fisher Scientific, MA, USA           |
| Semi-dry transfer cell Trans-blot SD           | Bio-Rad, München, Germany                   |
| Shaker KS 501 digital                          | IKA, Staufen, Germany                       |
| Shaker incubator Innova 4000                   | New Brunswick, Wesseling-Berzdorf, Germany  |
| Shaker incubator Innova 4300                   | New Brunswick, Wesseling-Berzdorf, Germany  |
| Sonicator Sonoplus HD 2070                     | Bandelin, Berlin, Germany                   |
| Spectrophotometer UVIKON 923                   | Kontron instruments, Munich, Germany        |
| Sterile work bench Herasafe                    | Thermo Fisher Scientific, Dreieich, Germany |
| Sterile work bench SterilGard Class II         | The Baker company, Sanford, ME, USA         |
| Stop watch                                     | Roth, Karlsruhe, Germany                    |
| Thermocycler Labcycler                         | Sensoquest, Göttingen, Germany              |
| Thermal cycler ABI 7500 Real-Time PCR System   | Applied Biosystems, Foster City, CA, USA    |
| UV chamber GS Gene linker                      | Bio-Rad, München, Germany                   |
| UV table TFX-35M                               | Vilber Lourmat, Eberhardzell, Germany       |
| Vortex Genie 2                                 | Scientific Industries, Bohemia, NY, USA     |
| Waterbath 7A                                   | Julabo, Seelbach, Germany                   |
| Widefield fluorescent microscope Axiovert 200M | Carl Zeiss, Oberkochen                      |

## 2.1.2. Consumables

| Consumable  | Company  |
|---|--|
| 96-well plates, black / clear                           | Greiner Bio-One, Frickenhausen, Germany        |
| 96-well plates for qPCR, MicroAmp Fast (0.1 ml)         | Applied Biosystems, Foster City, CA, USA       |
| Acetate sealing foil for 96-well plate                  | Sarstedt, Nümbrecht, Germany                   |
| Aluminium foil  | Roth, Karlsruhe, Germany                       |
| Cell culture plater                                     | Greiner Bio-One, Kremsmünster, Germany         |
| Cellstar tubes  | Greiner bio one, Frickenhausen, Germany        |
| Cover slips   | Roth, Karlsruhe, Germany                       |
| Cryovials   | Nalgene®, Wiesbaden, Germany                   |
| Cuvettes  | Sarstedt, Nümbrecht, Germany                   |
| Electroporation cuvettes Gene Pulser                    | Bio-Rad, München, Germany                      |
| Eppendorf tubes   | Sarstedt, Nümbrecht, Germanx                   |
| Eppendorf LoBind tubes                                  | Sigma-Aldrich, Darmstadt, Germany              |
| Falcon polypropylene round-bottom tubes                 | BD Biosciences, Bedford, MA, USA               |
| Filter systems 500 ml                                   | Corning, Kaiserslautern, Germany               |
| Filters Millex GS (0.2 µm)                              | Merck Millipore, Darmstadt, Germany            |
| Filter tips P20, P200, P1000                            | Greiner Bio-One, Frickenhausen, Germany        |
| Gloves TouchNTuff                                       | Ansell, München, Germany                       |
| Immersion oil   | Zeiss, Jena, Germany                           |
| MACS CS column  | Miltenyi Biotec, Bergisch Gladbach, Germany    |
| Object slides   | Marienfeld, Lauda-Königshofen, Germany         |
| Parafilm  | Bemis, Londonerry, UK                          |
| PCR softtubes 0.25 ml                                   | Biozym Scientific, Hessisch Oldendorf, Germany |
| PCR strip tubes & domed caps                            | BioMedical Instruments, Zoellnitz, Germany     |
| Petri dishes (10 ml diameter)                           | Greiner Bio-one, Frickenhausen, Germany        |
| Petri-dishes (25 ml diameter)                           | Greiner Bio-one, Frickenhausen, Germany        |
| Pipette tips  | Corning incorporation, Bodenheim, Germany      |
| Plastic pipettes (1 ml; 2 ml; 5 ml; 10 ml; 25 ml; 50ml) | Corning incorporation, Bodenheim, Germany      |

PVDF membrane  
Sterile filtration devices  
Thermo well PCR  
Transfer pipettes

Bio-Rad, München, Germany  
Corning incorporation, Bodenheim, Germany  
Corning incorporation, Bodenheim, Germany  
Sarstedt, Nümbrecht, Germany

### 2.1.3. Chemicals

| Chemicals                                  | Company   |
|--|---|
| 2-Mercaptoethanol                          | Sigma-Aldrich, Darmstadt, Germany               |
| 2-Propanol                                 | Sigma-Aldrich, Darmstadt, Germany               |
| Acetic acid                                | Honeywell Fluka, Schwerte, Germany              |
| Acrylamid (30%) Mix 29:1                   | AppliChem, Darmstadt, Germany                   |
| Agar-Agar                                  | Roth, Karlsruhe, Germany                        |
| Agarose Molecular Biology Grade            | BIORON, Ludwigshafen, Germany                   |
| Albumin Fraction V (BSA)                   | AppliChem, Darmstadt, Germany                   |
| Ammonium peroxodisulfate (APS)             | Roth, Karlsruhe, Germany                        |
| Ampicilin sodium salt                      | Roth, Karlsruhe, Germany                        |
| Brilliant blue R250                        | Roth, Karlsruhe, Germany                        |
| Bromophenol Blue sodium salt               | SERVA, Heidelberg, Germany                      |
| Calcium chloride dihydrate                 | Sigma-Aldrich, Darmstadt, Germany               |
| Chlorophorm                                | VWR International, Darmstadt, Germany           |
| Dimethyl sulfoxide (DMSO)                  | Merck, Darmstadt, Germany                       |
| Dithiotreitol (DTT)                        | Sigma-Aldrich, Darmstadt, Germany               |
| Dry ice                                    | Zentrallager UniKlinikum Heidelberg             |
| EDTA                                       | AppliChem, Darmstadt                            |
| Ethanol (99%)                              | Zentrallager UniKlinikum Heidelberg             |
| Ethidium bromide                           | Sigma-Aldrich, Darmstadt, Germany               |
| Formaldehyde                               | Sigma-Aldrich, Darmstadt, Germany               |
| G418 disulfate salt                        | Sigma-Aldrich, Darmstadt, Germany               |
| Gelatin from cold water fish skin (40-50%) | Sigma-Aldrich, Darmstadt, Germany               |
| Gentamicin                                 | c.c.pro, Oberdorla, Germany                     |
| Giemsa staining solution                   | Roth, Karlsruhe, Germany                        |
| Glucosamine hydrochloride                  | Sigma-Aldrich, Darmstadt, Germany               |
| Glucose                                    | Roth, Karlsruhe, Germany                        |
| Glycerol                                   | Sigma-Aldrich, Darmstadt, Germany               |
| Glycine                                    | AppliChem, Darmstadt, Germany                   |
| Glutaraldehyde (25%)                       | Merck, Darmstadt, Germany                       |
| H <sub>2</sub> O <sub>2</sub> (30%)        | Honeywell Fluka, Schwerte, Germany              |
| Heparin sodium salt                        | Sigma-Aldrich, Darmstadt, Germany               |
| Hoechst 33342                              | Life technologies, CA, USA                      |
| Hypoxanthine                               | c.c.pro, Oberdorla, Germany                     |
| IC <sub>50</sub> drugs:                    |   |
| Chloroquine diphospahte salt               | Sigma-Aldrich, Darmstadt, Germany               |
| Quinine hydrochloride                      | Sigma-Aldrich, Darmstadt, Germany               |
| Quinidine sulfate salt dihydrate           | Sigma-Aldrich, Darmstadt, Germany               |
| Pyrimethamine                              | Sigma-Aldrich, Darmstadt, Germany               |
| Immersion oil                              | Waldeck, Münster, Germany                       |
| Methanol                                   | VWR International, Darmstadt, Germany           |
| Paraformaldehyde (16%), EM Grade           | Electron Microscopy Sciences, Hatfield, PA, USA |

|                              |  |
|------------------------------|--|
| PBS tablets                  | Sigma-Aldrich, Darmstadt, Germany                    |
| Protease inhibitor           | Roche, Basel, Switzerland                            |
| Potassium chloride           | Sigma-Aldrich, Darmstadt, Germany                    |
| RPMI 1640                    | Gibco, Darmstadt, Germany                            |
| Saponin                      | SERVA, Heidelberg, Germany                           |
| SeaKem LE agarose            | Biozym Scientific, Hessisch Oldendorf, Germany       |
| Skim milk powder             | Honeywell Fluka, Schwerte, Germany                   |
| Sodium chloride              | Sigma-Aldrich, Darmstadt, Germany                    |
| Sodium dodecyl sulfate (SDS) | AppliChem, Darmstadt, Germany                        |
| Sodium deoxycholate          | Sigma-Aldrich, Darmstadt, Germany                    |
| Sodium fluoride              | Sigma-Aldrich, Darmstadt, Germany                    |
| Sodium hydroxide             | Sigma-Aldrich, Darmstadt, Germany                    |
| Sorbitol                     | Sigma-Aldrich, Darmstadt, Germany                    |
| Sucrose                      | AppliChem, Darmstadt, Germany                        |
| TEMED                        | Roth, Karlsruhe, Germany                             |
| Tris                         | Roth, Karlsruhe, Germany                             |
| Triton X-100                 | Merck, Darmstadt, Germany                            |
| TRIzol reagent               | Ambion - Thermo Fisher Scientific, Dreieich, Germany |
| Tryptone/Peptone             | Roth, Karlsruhe, Germany                             |
| Tween 20                     | Roth, Karlsruhe, Germany                             |
| Verapamil hydrochloride      | Sigma-Aldrich, Darmstadt, Germany                    |
| WR99210                      | Jacobus Pharmaceuticals, Princeton, NJ, USA          |
| Yeast extract                | Roth, Karlsruhe, Germany                             |

## 2.1.4. KITS

| KIT  | Company                                     |
|--|---|
| BM chemiluminescence blotting substrate POD      | Roche, Mannheim, Germany                    |
| CloneJET PCR Cloning Kit                         | Thermo Fisher Scientific, Dreieich, Germany |
| DNeasy Blood & Tissue Kit                        | Qiagen, Hilden, Germany                     |
| FastStart Universal SYBR Green Master (Rox)      | Roche, Mannheim, Germany                    |
| Gel Extraction/PCR Purification Kit              | Qiagen, Hilden, Germany                     |
| High Pure Plasmid Isolation Kit                  | Roche, Mannheim, Germany                    |
| In-Fusion® HD Cloning Kit                        | Clontech Laboratories, USA                  |
| Plasmid MaxiPrep Kit                             | Qiagen, Hilden, Germany                     |
| SuperScript® III First-Strand Synthesis Supermix | Thermo Fisher Scientific, Dreieich, Germany |
| DNA-free Kit – DNase Treatment and Removal       | Thermo Fisher Scientific, Dreieich, Germany |

## 2.1.5. Biological material

### 2.1.5.1. Antibodies

| Antibody                            | Source | Company                                     |
|-------------------------------------|--------|---|
| Anti- $\alpha$ -tubulin, monoclonal | Mouse  | Sigma Aldrich, München, Germany             |
| Anti-HA (12CA5), monoclonal         | Mouse  | Roche, Mannheim, Germany                    |
| Anti-PfUT (SAB 654), C-terminal     | Rabbit | Signalway Antibody, College Park, MD, USA   |
| Anti-PfUT (Thermo 1-2a), N-terminal | Rabbit | Thermo Fisher Scientific, Dreieich, Germany |

|   |            |  |
|---|------------|--|
| Anti-BiP, polyclonal                                    | Rabbit     | Kindly provided by J. Przyborski (Pesce et al., 2008)    |
| Anti-PfERC, polyclonal                                  | Rabbit     | Kindly provided by J. Przyborski (Adisa et al., 2001)    |
| Anti-PfERD2, polyclonal                                 | Rabbit     | Kindly provided by J. Przyborski                         |
| Anti-Ub (FL-76), polyclonal                             | Rabbit     | Santa Cruz Biotech., Heidelberg, Germany                 |
| Anti-PfCRT, polyclonal                                  | Guinea Pig | Eurogentec, Köln, Germany                                |
| Anti-mouse-POD  | Goat       | Jackson ImmunoResearch, Suffolk, UK                      |
| Anti-rabbit-POD   | Goat       | Jackson ImmunoResearch, Suffolk, UK                      |
| Anti-guine pig-POD                                      | Donkey     | Jackson ImmunoResearch, Suffolk, UK                      |
| Alexa Fluor 488 anti-mouse IgG                          | Goat       | Invitrogen - Thermo Fisher Scientific, Dreieich, Germany |
| Alexa Fluor 546 anti-mouse IgG                          | Goat       |  |
| Alexa Fluor 488 anti-rabbit IgG                         | Goat       | Invitrogen - Thermo Fisher Scientific, Dreieich, Germany |
| Alexa Fluor 546 anti-rabbit IgG                         | Goat       |  |
| Anti-mouse IgG, 10 nm colloidal gold conjugate (GA1004) | Goat       | Boster Biological Technology, Pleasanton, CA, USA        |
| Anti-rabbit protein A 10nm gold                         | Goat       | CMC UMC, Utrecht, The Netherlands                        |

#### 2.1.5.2. Enzymes

| Enzyme                      | Company   |
|-----------------------------|---|
| EuroTaq Polymerase          | BioCat, Heidelberg, Germany                     |
| Phusion Polymerase          | Fermentas, Germany                              |
| Restriction Enzymes         | New England Biolabs, Frankfurt am Main, Germany |
| Shrimp Alkaline Phosphatase | New England Biolabs, Frankfurt am Main, Germany |
| T4 Ligase                   | Thermo Fisher Scientific, Dreieich, Germany     |

#### 2.1.5.3. Fluorescent dyes

| Fluorescent Dye | Company                                     |
|-----------------|---|
| Hoechst 33342   | Thermo Fisher Scientific, Dreieich, Germany |
| SYBR Green I    | Sigma Aldrich, München, Germany             |

#### 2.1.5.4. Size markers and loading dyes

| Marker                                   | Company  |
|--|--|
| GeneRuler 1 Kb plus DNA ladder           | Ambion - Thermo Fisher Scientific, Dreieich, Germany     |
| PageRuler Plus Prestained protein ladder | Ambion - Thermo Fisher Scientific, Dreieich, Germany     |
| HiMark Pre-Stained HMW Protein Standard  | Invitrogen - Thermo Fisher Scientific, Dreieich, Germany |
| RNA Gel Loading Dye (2x)                 | Ambion - Thermo Fisher Scientific, Dreieich, Germany     |

### 2.1.5.5. Plasmids

All the plasmids used in this study are described in Appendix II.

| Plasmid                       | Origin   |
|-------------------------------|--|
| pUF1-Cas9                     | Provided by Dr. Jose-Juan Lopez-Rubio, Montpellier, France           |
| pL6-HA-glmS                   | Generated by Dr. Cecilia Sanchez, Heidelberg, Germany                |
| pL6-B                         | Provided by Dr. Jose-Juan Lopez-Rubio, Montpellier, France           |
| pSLI-TGD                      | Provided by Dr. Tobias Spielmann, Hamburg, Germany                   |
| pSLI-APEX2                    | Provided by Dr. Markus Ganter, Heidelberg, Germany                   |
| pL6-PfUT-HA-glmS-UTguide1     | Generated by Monika Jankowska-Döllken in this study                  |
| pL6-HECT-C2S-HA-glmS-UTguide1 | Generated by Monika Jankowska-Döllken in this study                  |
| pSLI-TGD-PfUT                 | Generated by Monika Jankowska-Döllken in this study                  |
| pL6-B-AIEx-UTguide2           | Generated by Monika Jankowska-Döllken in this study                  |
| pL6-B-AIEx-UTguide3           | Generated by Monika Jankowska-Döllken in this study                  |
| pL6-PfUT-BirA-myc-UTguide1    | Generated by Monika Jankowska-Döllken in this study                  |
| pL6-BirA-myc-PfUT-UTguide4    | Generated by Alicia Miranda Moraga (Lehramtsstudentin) in this study |
| pSLI-PfUT-APEX2               | Generated by Alicia Miranda Moraga (Lehramtsstudentin) in this study |

### 2.1.5.6. Oligonucleotides

The oligonucleotides used in this study were purchased from Thermo Fisher Scientific or Eurofins. They were designed and tested for T<sub>m</sub>, predicted dimers formation and 3'-end stability using IDT OligoAnalyzer 3.1 Tool (<https://eu.idtdna.com/calc/analyzer>)

#### Primers used for cloning, colony PCR and sequencing:

(*blue*: enzyme restriction sites; *green*: homology regions for In Fusion cloning; *red*: desired mutations)

| No. | Name                       | Sequence  |
|-----|----------------------------|---|
| 1   | UT-12580- SpeI-for         | <b>GGACTAGT</b> TTAATGAAAGTTGTTAAGAAGGAG                            |
| 2   | UT-13040-BssHII-rev        | <b>TTGGCGCGCC</b> AGAAAG <b>GGAAAA</b> ATTCTTTTGGC                  |
| 3   | UT-3'UTR-NarI-for          | <b>ATGCGGCGCC</b> TTTTGTTTGCGACCCGATG                               |
| 4   | UT-3'UTR-AflIII-rev        | <b>CAGTCTTAAG</b> TCTTTAATGTATATGTCCTTGAC                           |
| 5   | UT-guide1-for              | <b>TAAGTATATAATATTA</b> AAGAAAGTGAAAAGTTCTTT <b>GTTT</b> AGAGCTAGAA |
| 6   | UT-guide1-rev              | <b>TTCTAGCTCTAAAACA</b> AAAGAACTTTTCACTTTCTT <b>AATATTATATACTTA</b> |
| 7   | UT-guide1-rev-short        | TAAAACAAAGAACTTTTCACTTTC  |
| 8   | UT-12367-for               | ATCTGCCCTACCTAATAATGG   |
| 9   | UT-3'UTR-rev               | AACATTTGGGGGAATCTCTC  |
| 10  | UT-3'UTR-rev-2             | AAATACTCTTAGGAACCTTAAACC  |
| 11  | UT-12265-SpeI-for          | <b>ACTAGT</b> TAGATATACGAACGATTCAATTAC                              |
| 12  | UT-12614-C2S-for           | TACCAAGTGTGATGACTT <b>CTAC</b>                                      |
| 13  | UT-12614-C2S-rev           | GTAG <b>GAAG</b> TCATCACACTTGGTA                                    |
| 14  | BirA-myc-BssHII-for        | GAT <b>GCGCGC</b> CTATGAAAGATAATACAGTACC                            |
| 15  | BirA-myc-linker-BssHII-for | <b>GCGCGC</b> ATGGAGCCGCTATGAAAG                                    |
| 16  | BirA-myc-NarI-rev          | CAAC <b>GCGCGC</b> CTAGATTATTAATAAGCTTTCA                           |
| 17  | UT-61-NotI-for             | <b>GCGGCCGC</b> TAAATGGAGATGAATCTGAAATGG                            |



|    |                        |  |
|----|------------------------|--|
| 18 | UT-498-Mlul-rev        | ACGCGTCTACCTACAACCTCATTTATCC                       |
| 19 | UT-548-rev             | GCATAAACTCCCATATGCTCTTG                            |
| 20 | UT-5'UTR-for           | TCTTTATTTCTACATCATGCTTTAAG                         |
| 21 | UT-3893-ext-SacII-for  | TCCGCGGTCTAAATACTATACGCAAGATATG                    |
| 22 | UT-4759-ext-AflIII-rev | AGAGCTTAAGACTACCAGATTTCATCATCCTC C                 |
| 23 | UT-shield-for          | ATAAACGT AATGACCCGAA                               |
| 24 | UT-shield-rev          | TTCGGGTCATTCACGTTTAT                               |
| 25 | UT-guide3-for          | TAAGTATATAATATTATAAATGTGAACGACCCGAAGTTTTAGAGCTAGAA |
| 26 | UT-guide3-rev          | TTCTAGCTCTAAAAGTTCGGGTCGTTACATTTATAATATTATATACTTA  |
| 27 | UT-guide3-rev-short    | TAAAACTTCGGGTCGTTCAACA                             |
| 28 | UT-3863-for            | GTAATAACATGAAGGAATATAATATG                         |
| 29 | UT-5'UTR-SpeI-for      | ACTAGTTTTTGCAGTTCATACATATATCTGTG                   |
| 30 | UT-5'UTR-AflIII-rev    | CTTAAGTTATTCTTTAACTAAAATTATATATATATTATACTTAAAGC    |
| 31 | UT-2-NotI-for          | GCGGCCGCTTGAAGAAATACTTGCTCTTTGAA                   |
| 32 | UT-2-SacII-rev         | CCGCGGACTACCTACAACCTCATTTATCC                      |
| 33 | BirA-myc-AflIII-for    | CTTAAG CT ATG AAA GAT AAT ACA GTA CC               |
| 34 | BirA-NotI-4Nf-rev      | GCGGCCGCTAGATGATGAAATAAGCTTTCCAG                   |
| 35 | UT-guide4-for          | TAAGTATATAATATTTGAAGAAATACTTGCTTTTTTTTTAGAGCTAGAA  |
| 36 | UT-guide4-rev          | TTCTAGCTCTAAAACAAAAAGCAAGTATTTCTTCAATATTATATACTTA  |
| 37 | UT-guide4-rev-short    | TAAACAAAAAGCAAGTATTTCTTC                           |
| 38 | UT-12580-NotI-for      | GCGGCCGCCTTAATGAAAGTTGTTAAGAAGG                    |
| 39 | UT-13040-Mlul-rev      | ACGCGTAGAAAGTGAAAGTTCTTTTGGC                       |
| 40 | APEX2-BssHII-for       | GCGCGCGGAAAGTCTTACCCAAGTGTGAG                      |
| 41 | APEX2-NarI-rev         | GGCGCCGGCATCAGCAAACCCAAGC                          |
| 42 | pJET-for               | CGACTCACTATAGGGAGAGCGGC                            |
| 43 | pJET-rev               | AAGAACATCGATTTTCCATGGCAG                           |
| 44 | pL6-guide-for          | GTAACCAAAATGCATAATTTTCC                            |
| 45 | pL6-guide-rev          | TAGGAAATAATAAAAAAGCACC                             |
| 46 | pL6- HA-glmS-5'-for    | ATTTAACTATATACTATGGAATAC                           |
| 47 | pL6- HA-glmS-5'-rev    | TATTGAGAAAAATAAGAACAAGAC                           |
| 48 | pL6-HA-glmS-3'-for     | ATCACATGATCTTCCAAAAACATG                           |
| 49 | pL6-HA-glmS-3'-rev     | TAAACCAATAGATAAAATTTGTAGAG                         |
| 50 | pSLI-4seq-for          | TCGTATGTTGTGTGGAATTGTG                             |
| 51 | pSLI-GFP-rev           | CACTGACAGAAAATTTGTGCC                              |

#### Primers used for qPCR:

| No. | Name                 | Sequence                 |
|-----|----------------------|--------------------------|
| 52  | UT-10-for            | TACTTGCTTTTTGAGAATTCCCAG |
| 53  | UT-309-rev           | ATTGCTCAAACCTCCGTCAG     |
| 54  | $\beta$ -tubulin-for | TGATGTGCGCAAGTGATCC      |
| 55  | $\beta$ -tubulin-rev | TCCTTTGTGGACATTCTCCTC    |

#### 2.1.5.7. *E. coli* strains

| Strain                   | Origin   |
|--------------------------|--|
| <i>E. coli</i> PMC 103   | Provided by Prof. Alan Cowman (Doherty et al., 1993) |
| <i>E. coli</i> XL10 Gold | Agilent Technologies, Böblingen, Germany             |

#### 2.1.5.8. *P. falciparum* strains

| Strain  | Origin   |
|---|--|
| <i>P. falciparum</i> 3D7                      | The Netherlands (D Walliker et al., 1987)                                      |
| <i>P. falciparum</i> 3D7 PfUT-HA- <i>glmS</i> | Generated by Monika Jankowska-Döllken in this study                            |
| <i>P. falciparum</i> 3D7 SLI-TGD-PfUT         | Generated by Monika Jankowska-Döllken in this study                            |
| <i>P. falciparum</i> Dd2                      | Indochina  |
| <i>P. falciparum</i> Dd2 PfCRT S33A/D/E       | Generated by Dr. Sonia Moliner Cubel (PhD thesis 2016) and Dr. Cecilia Sanchez |
| <i>P. falciparum</i> HB3                      | Honduras (Bhasin & Trager, 1984)   |

#### 2.1.6. Buffers, media and solutions

| Buffer/medium/solution        | Composition  |
|-------------------------------|--|
| Albumax I                     | 5% (w/v) Albumax I<br>in RPMI 1640 with 25 mM HEPES and L-Glutamine (Gibco)<br>filter sterilized   |
| Ampicillin Stock, 1000x       | 100 mg/ml in ddH <sub>2</sub> O  |
| Blocking Solution             | 5% (w/v) skimmed milk in PBS   |
| Cell Culture Media            |  |
| <u>Complete Medium</u>        | 10% Human A Serum<br>0.2 µg/ml Gentamycin<br>0.1 mM Hypoxanthine<br>in RPMI 1640 with 25 mM HEPES and L-Glutamine (Gibco)  |
| <u>Transfectants Medium</u>   | 5% Human A Serum<br>0.25% Albumax I<br>0.2 µg/ml Gentamycin<br>0.2 mM Hypoxanthine<br>in RPMI 1640 with 25 mM HEPES and L-Glutamine (Gibco)  |
| Coomassie Destaining Solution | 20% Methanol<br>7% Acetic Acid   |
| Coomassie Staining Solution   | 50% Methanol<br>10% Acetic Acid<br>0.5% Coomassie Blue R-250   |
| Cytomix                       | 120 mM KCl<br>0.15 mM CaCl <sub>2</sub><br>10 mM K <sub>2</sub> HPO <sub>4</sub> /KH <sub>2</sub> PO <sub>4</sub> , pH 7.6<br>25 mM HEPES/2 mM EGTA, pH 7.6<br>5 mM MgCl <sub>2</sub> in ddH <sub>2</sub> O<br>Adjusted to pH 7.6 with KOH |

|                                   |   |
|-----------------------------------|---|
|                                   | Filter sterilized   |
| DNA Loading Buffer (6x)           | 60% Glycerol<br>60 mM EDTA<br>0.25% Bromophenol Blue  |
| DSM1                              | 10 mM in 20% DMSO (v/v)   |
| Fixation Solution                 | 1x PBS<br>4% Paraformaldehyde (PFA)<br>0.0075% Glutaraldehyde (GA)  |
| Freezing Solution                 | 6.2 M Glycerol<br>0.14 M Na-Lactate<br>0.5 mM KCl<br>in ddH <sub>2</sub> O, adjusted to pH 7.2 with 0.5 M NaHCO <sub>3</sub><br>Filter sterilized   |
| G418                              | 50 mg/ml in RPMI  |
| IC <sub>50</sub> Lysis Buffer     | 20 mM Tris base<br>Adjusted to pH 7.4 with concentrated HCl<br>5 mM EDTA<br>0.008% (w/v) Saponin<br>0.08% (w/v) Triton X-100<br>Vacuum filtered, stored at RT   |
| LB Medium                         | 1% (w/v) tryptone/peptone<br>0.5% (w/v) yeast extract<br>0.5% (w/v) NaCl<br>Autoclaved  |
| LB Agar                           | 10 g tryptone/peptone<br>5 g yeast extract<br>5 g NaCl<br>15 g agar<br>in 1 L ddH <sub>2</sub> O, autoclaved  |
| MACS Buffer                       | 2 mM EDTA in 1x PBS, autoclaved<br>0.5% (w/v) BSA added prior to use  |
| NZY <sup>+</sup> Broth            | 1% (w/v) NZ amine (casein hydrolysate)<br>0.5% (w/v) yeast extract<br>0.5% (w/v) NaCl<br>pH adjusted to 7.5 with NaOH, autoclaved<br>Prior to use the following filter-sterilized supplements were added:<br>12.5 mM MgCl <sub>2</sub><br>12.5 mM MgSO <sub>4</sub><br>0.4% (w/v) Glucose |
| PBS                               | 1 tablet (Sigma-Aldrich) per 200 ml ddH <sub>2</sub> O  |
| Permeabilization Solution         | 0.1% Triton-100 in 1x PBS   |
| Permeabilization/Quenching Buffer | 0.1% Triton-100 and 125 mM Glycine in 1x PBS  |
| Protease Inhibitors (PI)          | 0.002% (w/v) Leupeptin<br>0.005% (w/v) Aprotinin<br>100 μM PMSF   |
| Protein Loading Buffer (2x)       | 3% (w/v) SDS<br>250 mM Tris pH 6.8<br>20% Glycerol<br>0.1% Bromophenol blue   |
| Protein Lysis Buffer              | 0.07% (w/v) Saponin in PBS  |

|                          |   |
|--------------------------|---|
|                          | Protease inhibitors   |
| RIPA Buffer              | 50 mM Tris pH 7.5<br>150 mM NaCl<br>5 mM EDTA<br>50 mM NaF (sodium fluoride)<br>0.5% NaDOC (sodium deoxycholate)<br>0.1% SDS<br>1% Triton X-100<br>Prior to use: 2 mM DTT, 100 mM PMSF, Protease Inhibitors |
| RNA Running Buffer (20x) | 41.86 g MOPS<br>6.8 g NaOAc<br>3.8 g EDTA<br>In 500 ml ddH <sub>2</sub> O   |
| RNase Solution           | 0.3 mg/ml RNase A in 1x PBS   |
| SDS-PAGE Running Buffer  | 25 mM Tris<br>250 mM Glycine<br>0.1% (w/v) SDS  |
| SDS-PAGE Transfer Buffer | 39 mM Tris<br>48 mM Glycine<br>0.038% (w/v) SDS   |
| SOB Medium               | 20 g Tryptone/Peptone<br>5 g Yeast Extract<br>0.5 g NaCl<br>5 g MgSO <sub>4</sub> x 7 H <sub>2</sub> O<br>In 1 L ddH <sub>2</sub> O, autoclaved   |
| SOC Medium               | SOB + 20 mM D-Glucose, filter sterilized<br>Stored at -20°C   |
| Sorbitol Lysis Solution  | 5% (w/v) D-sorbitol in ddH <sub>2</sub> O, filter sterilized  |
| Stripping Buffer         | 1x PBS<br>2% SDS<br>100 mM β-Mercaptoethanol  |
| Super Broth (SB)         | 35 g Tryptone/Peptone<br>30 g Yeast Extract<br>5 g NaCl<br>In 1 L ddH <sub>2</sub> O, autoclaved  |
| TAE Buffer, 1x           | 4 mM Tris-Acetate<br>1 mM EDTA, pH 8  |
| TE Buffer                | 10 mM Tris/HCl, pH 8<br>1 mM EDTA<br>In ddH <sub>2</sub> O<br>Filter sterilized   |
| Thawing Solution I       | 12% NaCl in ddH <sub>2</sub> O, filter sterilized/autoclaved  |
| Thawing Solution II      | 1.6% NaCl in ddH <sub>2</sub> O, filter sterilized/autoclaved   |
| Thawing Solution III     | 0.9% NaCl<br>0.2% Glucose<br>In ddH <sub>2</sub> O<br>Filter sterilized   |
| WR99210 Stock            | 10 mM in 20% DMSO (v/v)   |
| WR99210 Working Solution | 20 μM in RPMI 1640 with 25 mM HEPES and L-Glutamine   |

## 2.1.7. Computer software and databases

| Software                     | Origin  |
|------------------------------|---|
| 7500 Software v2.0.6.        | Applied Biosystems, Foster City, CA, USA  |
| BD FACSDiva Software         | BD Biosciences, San Jose, CA, USA   |
| BioEdit                      | <a href="http://www.mbio.ncsu.edu/BioEdit/bioedit">http://www.mbio.ncsu.edu/BioEdit/bioedit</a>             |
| FIJI Image Analysis          | <a href="http://fiji.sc/Fiji">http://fiji.sc/Fiji</a>   |
| Flowing Software 2.5.1       | Cell Imaging Core, Turku Centre for Biotechnology, Finland  |
| GATCViewer                   | GATC Biotech, Konstanz, Germany   |
| ImageJ                       | <a href="https://imagej.nih.gov/ij/">https://imagej.nih.gov/ij/</a>   |
| Image Studio Digits 4.0      | LI-COR Biosciences – GmbH, Bad Homburg, Germany   |
| KERN Microscope VIS Software | KERN & SOHN GmbH, Balingen, Germany   |
| MS Office                    | Microsoft Corporation, CA USA   |
| Mendeley                     | Mendeley Ltd.   |
| OPTIMA                       | BMG Labtech, Offenburg, Germany   |
| PlasmoDB                     | <a href="http://plasmodb.org/plasmo/">http://plasmodb.org/plasmo/</a>                                       |
| Protopacer Workbench         | <a href="http://www.protopacer.com/">http://www.protopacer.com/</a>   |
| Serial Cloner 2.6            | <a href="http://serialbasics.free.fr/Serial_Cloner.html">http://serialbasics.free.fr/Serial_Cloner.html</a> |
| Sigma Plot 13.0              | Systat Software Inc.  |
| SnapGene Viewer 2.8.2        | GSL Biotech LLC, Chicago, IL, USA   |

## 2.2. Methods

### 2.2.1. Parasitology

#### 2.2.1.1. *In vitro* cultivation of *P. falciparum*

Intraerythrocytic stages of *P. falciparum* were maintained in continuous blood culture according to standard protocols (Trager & Jensen, 1976). Parasites were cultured in complete RPMI medium at 37°C under an atmosphere of 5% O<sub>2</sub>, 3% CO<sub>2</sub>, 92% N<sub>2</sub> and 95% humidity. Human A+ erythrocytes were diluted to 2-4% hematocrit. Transfected parasites kept under selective drug pressure were fed with Transfectants Medium, supplemented with Albumax and containing high Hypoxanthine concentrations. Medium was changed at least every second day or more often if needed. Cultures were monitored regularly by methanol-fixed Giemsa-stained thin blood smears. Parasitemia, defined as a percentage of parasite-infected erythrocytes was kept between 0.1% to 5%, unless specified otherwise for particular experiments.

#### 2.2.1.2. Parasites freezing and thawing

Parasite culture selected for cryopreservation was adjusted to 3-5% ring stage parasitemia. The culture was centrifuged at 900 x g for 2 min and supernatant was discarded. The pellet was resuspended in 1/3 volume of freezing solution added dropwise and incubated for 5 min at RT.

Subsequently, another 4/3 volume of freezing solution was added slowly, then mixed carefully. The suspension was transferred to cryogenic vials and frozen at -80°C. For long term storage, samples were kept in liquid nitrogen.

For thawing of the cryopreserved parasites, the frozen cryovial was warmed up in a 37°C water bath for 30 sec. 200 µl of Thawing Solution I were added, mixed and the suspension was transferred to a 15 ml falcon tube. Then, 9 ml of Thawing Solution II were added slowly, the sample was centrifuged at 900 x g for 2min and the supernatant was discarded. Finally, 7 ml of Thawing Solution III were slowly added, the sample was centrifuged again and the supernatant was discarded. The pellet was resuspended in 14 ml of pre-warmed complete RPMI medium and transferred to a culture dish containing 500 µl of fresh erythrocytes.

### 2.2.1.3. Parasites synchronization

#### **Sorbitol:**

Ring stage parasites were synchronized by sorbitol treatment (Lambros & Vanderberg, 1979), based on the differential permeability of parasite-infected erythrocytes membrane. Due to the structural modifications induced by the parasite, the erythrocyte membrane of mature parasite stages (late trophozoites and schizonts) is permeable to sorbitol, resulting in parasite death caused by osmotic shock. Since uninfected RBC and ring stage-infected RBC lack the new permeation pathways they survive sorbitol treatment.

Briefly, parasite culture was collected and centrifuged at 900 x g for 2 min. The pellet was resuspended in 10 ml of pre-warmed 5% D-sorbitol solution and incubated for 5 min at 37°C. Cells were then centrifuged and the supernatant discarded. The pellet was resuspended in 14 ml of pre-warmed complete RPMI medium and transferred to a culture dish.

#### **Heparin:**

For a tight synchronization of parasite cultures, a combination of sorbitol and heparin treatments has been applied. Heparin reversibly inhibits invasion of merozoites into the erythrocyte (Boyle et al., 2010; Kobayashi & Kato, 2016). This property allows to manipulate the window during which merozoites can invade erythrocytes by adding and washing heparin out.

Parasites were synchronized with sorbitol to narrow down the synchronization window. Afterwards, parasites were cultured in the presence of 50U/ml heparin until the majority of parasites were at the schizont stage. Heparin was then removed from cultures for approximately 4 h to allow schizont rupture followed by erythrocytes invasion by released merozoites. After that, heparin was re-added to cultures for a couple of hours in order to block any further invasion events.

#### 2.2.1.4. Magnetic purification of late stage parasites

*P. falciparum* trophozoite and schizont stages were purified from ring stages and uninfected RBC using the magnetic activated cell sorting (MACS) system. This approach is based on the paramagnetic properties of hemozoin present in late parasite stages facilitating their purification by magnetic cell sorting (Paul et al., 1981). The MACS column was washed twice with MACS buffer pre-warmed to 37°C and inserted into the VarioMACS separator. The parasite cultures were resuspended and applied to the top of the column. The flow was adjusted to 1 drop every 3 sec. Afterwards, the column was washed with MACS buffer until the flow-through was clear. The column was then removed from the magnetic field and the late-stage infected erythrocytes were eluted with 12 ml of MACS buffer. The cells were centrifuged at 900 x g for 2 min and the pellet was resuspended in the appropriate buffer according to the experiment the cells were going to be used for.

#### 2.2.1.5. Transfection of *P. falciparum*

##### **Preparation of DNA:**

Approx. 100 µg of each transfection plasmid DNA were precipitated with 1/10 volume of 3M sodium acetate and 2.5 volumes of 100% ethanol and incubated at -20°C for at least 30 min. Samples were centrifuged at 17000 x g at 4°C for 30 min, washed with 0.5 ml 70% and centrifuged again for 10 min. Pellet was air-dried, resuspended in 30 µl of sterile TE-Buffer and stored at -20°C until needed. Prior to transfection, 370 µl of sterile cytomix were mixed with the 30 µl of plasmid.

##### **Preparation of parasite culture:**

*P. falciparum* ring stage parasites at 3-5% parasitemia were transfected by electroporation, as previously described (Wu et al., 1995). Parasites were synchronized using sorbitol treatment one cycle before transfection.

##### **Transfection:**

Parasite culture was centrifuged at 900 x g for 2 min and the supernatant was discarded. 200 µl of pellet were mixed by pipetting with the previously prepared 400 µl of plasmid DNA/cytomix mixture. The sample was then transferred to an electroporation cuvette and electroporated using the Gene Pulser II Electroporator (Bio-Rad) at 0.310 kV and 950 µF for 7-12 msec. Afterwards, the electroporated sample was immediately transferred to a culture dish containing 14 ml of transfection medium and 500 µl of fresh erythrocytes.

##### **Drug selection:**

Starting one day after transfection the positive drug selection was applied for the next seven days, where both, transfection medium and respective drugs were exchanged daily. Afterwards, medium was changed every 2-3 days and once per week culture was supplemented with 100 µl of fresh erythrocytes. Selection took 3 to 5 weeks until the parasites were visible again on the blood smears.

Part of the transfectant culture was cryopreserved (chapter 2.2.1.2) and the rest used for further characterization. The concentrations of the drugs used for the selection are listed below:

| Drug    | Stock conc. | Final conc. | System            |
|---------|-------------|-------------|-------------------|
| DSM1    | 10mM        | 1.5µM       | CRISPR-Cas9       |
| WR99210 | 20µM        | 5nM         | CRISPR-Cas9 / SLI |
| G418    | 50mg/ml     | 400µg/ml    | SLI               |

#### **CRISPR-Cas9:**

DMS1 and WR99210 were used simultaneously to select for the parasites carrying the pUF1-Cas9 and pL6 vector, respectively.

#### **SLI:**

WR99210 was used to select for the parasites carrying the pSLI plasmid. Transfectants obtained after 3 to 5 weeks of selection were first cryopreserved and then adjusted to three independent cultures of 1-4% parasitemia and 5% hematocrit in 5 ml of transfection medium. These cultures were then pressured for 2 weeks with neomycin (G418) to select for the parasites having integrated the construct (integrants). Proper integration leads to disruption of the targeted gene. Therefore, only the parasites that have integrated the neomycin phosphotransferase marker are able to grow in the presence of G418 (Birnbaum et al., 2017). For the first 10 days of selection medium and G418 were changed daily, afterwards every 2 days. After 14-16 days of selection, cultures were cultivated without G418 until parasites reappeared. Cultures were then cryopreserved. WR99210 was re-added to the culture medium for 2 more cycles. Parasites were then used for further characterization. In case of failure of recovering parasites after G418 selection in 6 independent attempts, the gene can be assumed to be essential (Birnbaum et al., 2017).

### **2.2.1.6. Cloning by limiting dilution**

Once the desired mutation or integration has been detected in transfectant culture, clones from the corresponding parasite line representing homogenous populations can be obtained by limiting dilution. Clonal parasite populations were cultivated in 96-well plate at 2% hematocrit, with an initial inoculum of 0.25 to 0.5 parasites per well. Individual clones in single wells were detected by microscopic examination of blood smears after 2 to 4 weeks of cultivation.

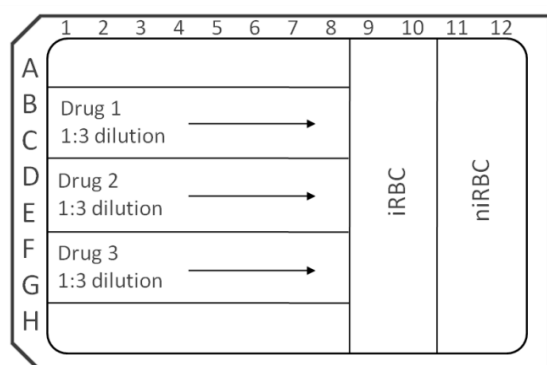
Parasitemia of the parental line was carefully determined as a prerequisite for successful preparation of dilution series. The total number of parasites in the starting culture was calculated from the parasitemia, taking into account that 0.5 ml of packed blood (100% hematocrit) is considered to contain roughly  $5 \times 10^9$  erythrocytes.



On this basis, a starting solution of  $10^6$  parasites per ml was prepared. It was subsequently diluted via 1:10 dilution series until  $10^1$  parasites per ml. This was further diluted via 1:2 dilution steps to two final working solutions of 5 and 2.5 parasites per ml (with final volume of 10 ml for each dilution). 200  $\mu$ l uninfected fresh erythrocytes were added to those two solutions (final hematocrit of 2%). The samples were repeatedly inverted to ensure proper mixing. 100  $\mu$ l of these suspensions were seeded into 96-well plates (V-shape bottom), resulting in 0.5 or 0.25 parasite per well. Parasites were cultured without drug selection in transfection medium exchanged every 2-3 days until parasite appearance, taking between 2 to 5 weeks. A dark color of the blood and yellowish medium were usually indicative of parasitized wells and this observation was further confirmed by microscopic analysis. Subsequently, the contents of parasitized wells were transferred to small culture plates to increase parasite numbers for freeze-downs and further investigations.

#### 2.2.1.7. Growth inhibition assay and $IC_{50}$ determination

*In vitro* parasite susceptibility to various compounds was assessed using SYBR Green-based growth inhibition assay (Smilkstein et al., 2004). To compare drug sensitivity profiles of different *P. falciparum* strains, the 50% inhibitory concentrations ( $IC_{50}$ ) were determined in SigmaPlot by fitting the dose-response curve to the four parameter Hill equation. All assays were performed in black 96-well plates using synchronous ring stage parasite culture at 0.5% parasitemia and 1.5% hematocrit in final volume of 100  $\mu$ l per well, in duplicates for each drug concentration. The uninfected RBC and untreated infected RBC, both at 1.5% final hematocrit, served in each plate as negative and positive control, respectively. Drugs tested in assay were prepared as 4x concentrated working solutions in RPMI 1640 medium and stored at  $-20^{\circ}\text{C}$  for no longer than two months. 50  $\mu$ l of a respective drug was added to the top well containing 50  $\mu$ l of culture medium and mixed thoroughly. The 1:3 serial dilutions were performed using multichannel pipette by transferring 25  $\mu$ l of the solution from each well to next rows containing 50  $\mu$ l of culture medium (Fig. 2.1).



| Drug / substance | Stock conc. | Final conc. in the first well |
|------------------|-------------|-------------------------------|
| CQ               | 6 $\mu$ M   | 1.5 $\mu$ M                   |
| QN               | 11 $\mu$ M  | 2.75 $\mu$ M                  |
| QD               | 6 $\mu$ M   | 1.5 $\mu$ M                   |
| PYR              | 1 mM        | 166 $\mu$ M                   |
| ML-7             | 500 $\mu$ M | 83 $\mu$ M                    |
| GlcN             | 1.6 M       | 400 mM                        |

**Figure 2.1. Experimental plate scheme and concentrations of substances used in the growth inhibition assay.** 50  $\mu$ l of stock solution were added to the first row, containing culture medium. After mixing, drug solution was transferred in 1:3 dilution (25  $\mu$ l) to the next rows. 25  $\mu$ l of drug solution were discarded from the first and last row. 50  $\mu$ l of parasite or erythrocyte culture were

added per well and plate was incubated for 72h. RBC – infected red blood cells, niRBC – non-infected red blood cells, CQ – chloroquine, QN – quinine, QD – quinidine, PYR – pyrimethamine, ML-7 – kinase inhibitor, GlcN – glucosamine.

The 25 µl drug solution from the final row was discarded, as well as 25 µl of the drug solution from the first row, resulting in a volume of 50 µl in each well of the plate. Finally, 50 µl of the parasite culture adjusted to 0.5% parasitemia and 3% hematocrit was added to each well resulting in final volume of 100 µl of parasite culture at 0.5% parasitemia and 1.5% hematocrit. Plates were incubated for 72h in the standard incubation conditions. Plates were then wrapped in aluminium foil and frozen at -80°C overnight. Afterwards, plates were thawed at RT for at least 2h and incubated with 100 µl/well of Lysis Buffer containing SYBR Green I (1x) for 1h in the darkness. SYBR Green binds to DNA resulting in emission of green light at 520 nm after excitation with blue light at 485 nm. Fluorescence intensities correlate with increases in parasitic DNA contents. Parasites content in respective wells of the 96-well plate was measured using the FLUOstar OPTIMA fluorescence plate reader operated under following parameters: excitation 485 nm, emission 520 nm, gain 1380, 10 flashes/well, top optic.

## 2.2.2. Microbiology and molecular biology

### 2.2.2.1. Preparation of electrocompetent *E. coli*

10 ml of Super Broth (SB) medium were inoculated with the electro-competent PMC 103 *E. coli* cells by scratching the frozen glycerol stock of bacterial culture and incubated overnight at 37°C with shaking at 200 rpm. The next day, 600 ml of SB medium were inoculated with 6 ml of overnight culture and incubated for 3.5 h at 37°C under shaking conditions (200 rpm). The culture was then centrifuged at 6000 x g for 10 min at 4°C. All the following steps were carried out on ice using pre-chilled solution. The pellet was resuspended in an equal volume of sterile water and centrifuged at 4000 rpm for 15 min at 4°C. This washing step was repeated twice. The pellet was then resuspended in an equal volume of 10% glycerol and centrifuged at 4000 rpm for 15 min at 4°C. The supernatant was discarded and the remaining pellet was resuspended in 1.2 ml of 10% glycerol. 50 µl of cell suspensions were aliquoted into pre-chilled Eppendorf tubes and stored at -80°C.

### 2.2.2.2. Transformation of *E. coli*

#### **Transformation of PMC 103 electrocompetent cells by electroporation**

The 50 µl aliquots of PMC 103 cells were thawed on ice and gently mixed with 150 µl of 10% glycerol. 10 µl of DNA were added to cells and transferred to pre-chilled electroporation cuvette. Electroporation was performed at 2500 V. 1 ml of pre-warmed SOC medium was immediately added to the cuvette. The mixture was then transferred to 15 ml falcon tube and incubated for 1 h at 37°C

with shaking at 200 rpm. Finally, the bacterial suspension was pelleted or directly plated onto selective LB agar plates and incubated overnight at 37°C.

#### Transformation of XL10 Gold ultracompetent cells by heat shock

The 40 µl aliquot of chemocompetent XL-10-Gold ultracompetent cells (Agilent Technologies) were thawed on ice and gently mixed with 1.6 µl of β-mercaptoethanol. The cell suspension was incubated for 10 min on ice and gently swirled every 2 min. 10 µl of DNA were added and the mixture was incubated for another 30 min on ice. Sample was then subjected to a heat shock for 30 sec at 42°C, followed by 2 min cooling down on ice. Afterwards, 0.9 ml of pre-warmed NZY<sup>+</sup> medium was mixed with transformed cells, transferred to 15 ml falcon tube and incubated for 1 h at 37°C with shaking at 200 rpm. Finally, the bacterial suspension was plated onto selective LB agar plates and incubated overnight at 37°C.

#### 2.2.2.3. Genomic DNA isolation from *P. falciparum*

To release *P. falciparum* parasites from erythrocytes, 14 ml of trophozoite- and schizont-stage culture at 3-5% parasitemia were centrifuged at 900 x g for 2 min. The supernatant was discarded, whereas the pellet was washed in PBS and centrifuged again. The pellet was then lysed in freshly prepared 0.1% saponin for 3 min on ice, followed by centrifugation at 2600 x g for 8 min. The pellet was washed 2-3 times in PBS until the supernatant was clear, then resuspended in 200 µl of PBS and transferred to 1.5 ml Eppendorf tube.

The genomic DNA was isolated using the DNeasy Blood & Tissue Kit (Qiagen). Briefly, the parasites were lysed with 200 µl AL buffer in presence of 20 µl of proteinase K, vortexed and incubated at 56°C for 10 min. Then, 200 µl of ethanol (99%) were added and the mixture was vortexed thoroughly. The mixture was then transferred to a DNeasy spin column and centrifuged at 6000 x g for 1 min. The flow-through was discarded and 500 µl of AW1 buffer were added, followed by a centrifugation at 6000 x g for 1 min. Again, the flow-through was discarded and 500 µl of AW2 buffer were added, followed by a centrifugation at 17000 x g for 3 min. The column was then transferred to a fresh 1.5 ml Eppendorf tube. To elute the DNA, 30 µl of ddH<sub>2</sub>O were loaded onto the membrane and incubated for 1 min at RT, followed by a centrifugation 6000 x g for 1 min. The genomic DNA was stored at -20°C.

#### 2.2.2.4. Polymerase Chain Reaction (PCR)

The amplification of the DNA fragments used for cloning was performed using the **Phusion High-Fidelity DNA Polymerase**. The PCR reaction mix and thermocycling conditions were as follows:

| Master Mix 1              |              | Thermocycling conditions                |      |          |
|---------------------------|--------------|---|------|----------|
| Buffer 5x                 | 10 $\mu$ l   | Initial denaturation                    | 94°C | 10 min   |
| dNTPs 2mM                 | 5 $\mu$ l    | Denaturation<br>Annealing<br>Elongation | 94°C | 45 sec   |
| Forward primer 50 $\mu$ M | 0.5 $\mu$ l  |   | X °C | 45 sec   |
| Reverse primer 50 $\mu$ M | 0.5 $\mu$ l  |   | 68°C | 1 min/kb |
| DNA template              | 1 $\mu$ l    | } x 30                                  |      |          |
| Phusion                   | 0.5 $\mu$ l  |   |      |          |
| H <sub>2</sub> O MilliQ   | 32.5 $\mu$ l | Final elongation                        | 68°C | 10 min   |
| Final volume              | 50 $\mu$ l   | X = T <sub>m</sub> of primers - 5°C     |      |          |

The amplification of the DNA fragments for colony screening was performed using the **Taq DNA Polymerase**. The PCR reaction mix and thermocycling conditions were as follows:

| Master Mix 2               |              | Thermocycling conditions                |      |          |
|----------------------------|--------------|---|------|----------|
| Buffer 10x                 | 2.5 $\mu$ l  | Initial denaturation                    | 94°C | 10 min   |
| dNTPs 2mM                  | 2.5 $\mu$ l  | Denaturation<br>Annealing<br>Elongation | 94°C | 45 sec   |
| MgCl <sub>2</sub> 50 mM    | 1.25 $\mu$ l |   | X °C | 45 sec   |
| Forward primer* 50 $\mu$ M | 0.5 $\mu$ l  |   | 68°C | 1 min/kb |
| Reverse primer* 50 $\mu$ M | 0.5 $\mu$ l  | } x 30                                  |      |          |
| DNA template**             | variable     |   |      |          |
| Taq                        | 0.25 $\mu$ l | Final elongation                        | 68°C | 10 min   |
| H <sub>2</sub> O MilliQ    | 17.5 $\mu$ l | Hold                                    | 4°C  | $\infty$ |
| Final volume               | 25 $\mu$ l   | X = T <sub>m</sub> of primers - 5°C     |      |          |

\* Colony PCR screening was performed using a vector flanking primer and a gene specific primer or both vector flanking primers.

\*\* A single colony was picked with a yellow tip, streaked onto a replica plate (selective agar plate) and shortly dipped in Eppendorf PCR tube containing 25  $\mu$ l of Master Mix 2. The yellow tip was removed and the PCR tube was directly used for amplification in a thermal cycler. The replicate agar plate was incubated at 37°C overnight.

#### 2.2.2.5. Agarose gel electrophoresis

Agarose is widely used for the separation of DNA and RNA molecules according to their size and charge. The resolution of the nucleic acid bands is dependent on the concentration of the agarose gel.

##### DNA

0.8 to 2 % agarose gels were prepared by dissolving appropriate amounts of agarose in 1x Tris-acetate-EDTA (TAE) buffer by boiling in a microwave. Gel was subsequently cooled down to 55°C, supplemented with ethidium bromide (EtBr) and poured into a gel cast. A comb was inserted to create wells and the gel was left to solidify. The completely solidified gel was transferred to an electrophoresis chamber filled with 1x TAE buffer. DNA samples were mixed with 6x DNA loading dye and loaded into the wells of the gel. A 1 kb Plus DNA Ladder was run alongside the samples as a size marker. Electrophoresis was carried out at RT at constant voltage of 90 to 140 V, depending on size

of the gel. DNA was visualized under UV light and captured using a DC120 Zoom Digital camera (Kodak).

#### RNA

0.28 g of Biozym SeaKem LE Agarose were dissolved in 2 ml of 20x RNA running buffer and 30 ml of ddH<sub>2</sub>O, by boiling in a microwave, resulting in 0.7% gel. Gel was cooled down to 55°C, supplemented with 8 ml of formaldehyde (to maintain the denaturated form of RNA) and 0.5 µl of EtBr and poured into a gel cast. RNA samples were mixed with RNA loading buffer (Ambion - Thermo Fisher Scientific), heated for 3 min at 65°C and loaded into the wells of the gel. Electrophoresis was carried out at constant voltage of 60 V in RNA running buffer. RNA was visualized under UV light and captured using a DC120 Zoom Digital camera (Kodak).

#### 2.2.2.6. DNA extraction from agarose gel

The extraction and purification of DNA fragments from the agarose gel was performed using the QIAquick Gel Extraction Kit (Qiagen) according to manufacturer's instructions. Briefly, the DNA fragments were excised from the agarose gel and dissolved in QG buffer (1:3 w/v ratio) at 50°C. Isopropanol was then added to precipitate the DNA and the sample was loaded onto a QIAquick spin column and centrifuged at 17000 x g. DNA bound to the membrane was washed with PE buffer and subsequently eluted with 30 µl of ddH<sub>2</sub>O and stored at -20°C.

#### 2.2.2.7. Determination of nucleic acid concentration and purity

The concentration of nucleic acids was analyzed using the spectrophotometer UVIKON 923 (Kontron Instruments). The absorbance spectrum from 230 to 300 nm was measured for 1:100 diluted sample with ddH<sub>2</sub>O used as a blank. The nucleic acid **concentration** was determined taking into account that absorbance at 260 nm ( $A_{260}$ ) of 1.0 equals 50 ng/µl of pure dsDNA or 40 ng/µl of pure RNA:

$$\text{DNA conc. [ng/}\mu\text{l]} = A_{260} \times 50 \text{ ng/}\mu\text{l} \times \text{dilution factor}$$

$$\text{RNA conc. [ng/}\mu\text{l]} = A_{260} \times 40 \text{ ng/}\mu\text{l} \times \text{dilution factor}$$

To evaluate nucleic acid **purity**, the  $A_{260}/A_{280}$  ratio was calculated:

$$\text{Pure DNA: } A_{260}/A_{280} = 1.8$$

$$\text{Pure RNA: } A_{260}/A_{280} = 2.0$$

#### 2.2.2.8. Restriction enzymes digestion

PCR products and vectors were digested using respective restriction enzymes and buffers (NEB). When the digestion was performed with two enzymes in the same reaction, buffers and enzyme concentrations were used according to the recommendations generated by NEB Double Digest

Finder at <https://nebcloner.neb.com>. The restriction digestion reactions of plasmid DNA and PCR products were set up as follows:

| Control digestion  |        | Digestion of vector/insert for cloning |       |
|--------------------|--------|--|-------|
| DNA                | 1 µg   | DNA                                    | 20 µg |
| NEB buffer         | 1 µl   | NEB buffer                             | 5 µl  |
| Enzyme 1           | 0.4 µl | Enzyme 1                               | 1 µl  |
| Enzyme 2           | 0.4 µl | Enzyme 2                               | 1 µl  |
| ddH <sub>2</sub> O | x µl   | ddH <sub>2</sub> O                     | x µl  |
| Final volume       | 10 µl  | Final volume                           | 30 µl |

Control digestions were incubated for 1.5 h, whereas digestion of vectors and inserts for cloning for 4 h at temperature optimal for each restriction enzyme.

#### 2.2.2.9. Dephosphorylation of DNA ends

Thermosensitive Alkaline Phosphatase (TSAP) catalyses the removal of 5' phosphate groups from DNA ends, preventing the recircularization of linearized plasmid DNA during ligation. All linearized vectors used for cloning were dephosphorylated prior to their use in ligation reactions. After 4 h of plasmid DNA digestion, 1 µl of TSAP (Promega) was added directly to the reaction mix and incubated for 1 h at 37°C, followed by inactivation for 15 min at 74°C. The sample was then loaded on 0.8% agarose gel, followed by plasmid DNA extraction using QIAquick Gel Extraction Kit (Qiagen).

#### 2.2.2.10. Ligation of DNA fragments

##### Ligation into pJET1.2/blunt

As an intermediate cloning step, some of the inserts used in this work were cloned into the pJET1.2/blunt plasmid. Ligation was performed using CloneJET PCR Cloning Kit (Fermentas) following the manufacturer's instructions:

| Components                                  |        |
|---|--------|
| Reaction Buffer 2X                          | 5 µl   |
| Insert                                      | 3.5 µl |
| DNA blunting enzyme                         | 0.5 µl |
| → Incubate 5 min at 70°C, then chill on ice |        |
| pJET1.2/blunt cloning vector                | 0.5 µl |
| T4 DNA Ligase                               | 0.5 µl |
| Final volume                                | 10 µl  |

The final ligation mixture (10 µl) was incubated at RT for 30 min. The reaction was directly transformed into *E. coli* PMC 103 electrocompetent cells.

### T4 DNA ligase

The vectors and DNA fragments ligated using the T4 DNA ligase were previously digested with the adequate restriction enzymes and purified using the QIAquick gel extraction kit (Qiagen). The ligation reaction was set as follows:

| <b>Components</b>        |                             |
|--------------------------|-----------------------------|
| T4 DNA Ligase Buffer 10x | 1 $\mu$ l                   |
| Linear vector DNA        | 30-150 ng (0.5 $\mu$ l)     |
| Insert DNA               | 5:1 molar ratio over vector |
| T4 DNA Ligase            | 1 $\mu$ l                   |
| ddH <sub>2</sub> O       | x $\mu$ l                   |
| Final volume             | 10 $\mu$ l                  |

The ligation reaction was incubated at 16°C overnight and transformed into *E. coli* PMC 103 electrocompetent cells on the following day.

### In Fusion cloning of guide RNA

The In Fusion Cloning technology has been used to insert the guide RNA into the pL6 plasmids. The pL6 vector of interest was digested with the BtgZI enzyme for 3-4 h at 60°C, dephosphorylated and purified with the QIAquick gel extraction kit. The primers consisting of the guide RNA sequences flanked by the homologous to the vector sequences necessary for In Fusion recombination were diluted to 100  $\mu$ M. 4.5  $\mu$ l of each primer (forward and reverse) were mixed together with 1  $\mu$ l of NEB buffer #2. The mixture was heated for 5 min at 95°C, cooled down to 25°C in a step-wise manner and kept on ice until use for the ligation reaction. The ligation reaction was set as follows:

| <b>Components</b>                 |             |
|-----------------------------------|-------------|
| Vector (200 ng)                   | 0.5 $\mu$ l |
| Hybridized primers (1:5 dilution) | 3.5 $\mu$ l |
| In Fusion Enzyme Mix              | 1 $\mu$ l   |
| Final volume                      | 5 $\mu$ l   |

The reaction mixture was incubated 15 min at 50°C and then kept on ice until its transformation into XL-10 Gold cells.

## 2.2.2.11. Plasmid DNA isolation

### Small-scale isolation (Miniprep)

The small-scale DNA plasmid isolation from bacteria was performed using the High Pure Plasmid Isolation Kit (Roche) according to the manufacturer's instructions. A single colony was inoculated into 10 ml of LB medium with 100  $\mu$ g/ml ampicillin and incubated overnight at 37°C with shaking at 200 rpm. The overnight cultures were centrifuged at 2600 x g for 5 min at RT. Pellets were resuspended in suspension buffer, followed by incubation with lysis buffer for 5 min at RT. The lysed solution was

treated with chilled binding buffer for 5 min on ice, followed by centrifugation at 17000 x g for 10 min at 4°C. The supernatant was loaded onto the High Pure filter tube and centrifuged at 17000 x g for 1 min at RT. After two washing steps, the DNA was eluted with 50 µl of ddH<sub>2</sub>O and stored at -20°C.

#### **Big-scale isolation (Maxiprep)**

The big-scale DNA plasmid isolation from bacteria was performed using the Plasmid Maxi Kit (Qiagen) according to the manufacturer's instructions. A single colony was inoculated into 3 ml of SB medium with 100 µg/ml ampicillin and incubated for 6-8 h at 37°C with shaking at 200 rpm. The starter culture was then diluted 1:1000 in SB (i.e. 400 µl in 400 ml) containing 100 µg/ml ampicillin and incubated overnight at 37°C under 200 rpm shaking. The overnight bacterial culture was pelleted by centrifugation at 6000 x g for 15 min at 4°C, mixed with resuspension buffer and lysed by 5 min incubation at RT with lysis buffer. Lysis was stopped by addition of chilled neutralization buffer followed by 20 min incubation on ice. Samples were centrifuged at 15000 x g for 30 min at 4°C and the supernatant was loaded onto the pre-equilibrated column and run through the resin by gravity flow. After washing, DNA was eluted, precipitated with isopropanol and centrifuged at 15000 x g for 30 min at 4°C. The pellet was washed with chilled 70% ethanol and centrifuged at 15000 x g for 20 min at 4°C. The DNA pellet was then air-dried, resuspended in an appropriated amount of ddH<sub>2</sub>O and stored at -20°C.

#### **2.2.2.12. DNA sequencing**

The sequencing of the DNA samples was performed by GATC Biotech (Konstanz, Germany), later acquired by Eurofins Genomics (Ebersberg, Germany). The samples were prepared as follows:

|               |                     |
|---------------|---------------------|
| Plasmids:     | 20 µl, 30-100 ng/µl |
| PCR products: | 20 µl, 10-50 ng/µl  |
| Primers:      | 20 µl, 10 pmol/µl   |

The GATC Viewer and Serial Cloner softwares were used to analyze the obtained sequences.

#### **2.2.2.13. Total RNA extraction from *P. falciparum***

To release *P. falciparum* parasites from erythrocytes, 36 ml of trophozoite- and schizont-stage culture at 3-5% parasitemia were centrifuged at 4°C for 2 min at 900 x g with brake-off at 130 x g. The supernatant was discarded, whereas the pellet was resuspended in 5 ml of freshly prepared ice cold 0.2% saponin and incubated for 3 min on ice. PBS was added up to 25 ml and the tubes were centrifuged for 8 min at 3000 x g at 4°C. The supernatant was discarded and the pellet was washed with ice cold PBS and centrifuged again. The supernatant was discarded and 1-2 ml of Trizol were added to the pellet, mixed thoroughly by vortexing, and directly frozen at -80°C overnight. The



samples were then thawed at 37°C and transferred to 1.5 ml Eppendorf tubes. 200 µl of chloroform were added per 1 ml of Trizol, the mixture was vigorously hand-shaken, incubated for 3 min at RT and centrifuged at 10500 x g for 30 min at 4°C. The upper aqueous phase containing mostly RNA was carefully collected and transferred to a fresh 1.5 ml Eppendorf LoBind tube. 500 µl of isopropanol were added per 1 ml of Trizol to the aqueous phase, the mixture was incubated at -80°C for at least 30 min and subsequently centrifuged at 10500 x g for 10 min at 4°C. The pellet was washed with cold 70% ethanol and centrifuged at 10500 x g for 10 min at 4°C. The RNA pellet was then air-dried at RT to eliminate any trace of ethanol, and dissolved in 30 µl of ribonuclease-free water. The concentration was measured by spectrophotometry and the RNA was stored at -80°C. The integrity of the extracted RNA was assessed on a denaturing agarose gel (0.7% agarose).

#### 2.2.2.14. DNase treatment

The possible genomic DNA contamination was removed from the freshly isolated RNA samples using the DNA-free Kit – DNase Treatment and Removal (Invitrogen). Briefly, 5 µg of RNA were mixed with 1.5 µl of 10X DNase I Buffer and 1 µl DNase I, adjusted to a total volume of 15 µl with nuclease-free water. The mixture was gently shaken by hand and incubated at 37°C for 30 min. 2 µl of DNase Inactivation Reagent were added and incubated for 5 min at RT. The mixture was centrifuged at 10000 rpm for 2 min at 4°C, the supernatant was transferred to a fresh Eppendorf LoBind tube and stored at -80°C if not used directly for cDNA synthesis.

#### 2.2.2.15. Reverse transcription

The cDNA was synthesized using the SuperScript III First-Strand Synthesis SuperMix (Invitrogen). Briefly, 6 µl (~2 µg) of DNase-treated RNA were mixed with 1 µl of 50 µM oligo(dT)<sub>20</sub> and 1 µl of annealing buffer, incubated for 5 min at 65°C, followed by 2 min chilling on ice. Subsequently, 10 µl of 2x First-Strand Reaction Mix and 2 µl of the SuperScript III/RNaseOUT Enzyme Mix were added to the RNA mixture and incubated for 50 min at 50°C. The reaction was terminated by 5 min incubation at 85°C, followed by 1 min cooling on ice. The cDNA concentration was measured by spectrophotometry and adjusted to 50 ng/µl. The cDNA was stored at -20°C.

#### 2.2.2.16. Quantitative real-time PCR

Quantitative real-time PCR was performed using an ABI 7500 Real-Time PCR detection system and the FastStart Universal SYBR Green Master (Rox). Samples were analyzed in a MicroAmp Fast 96-well plate, in technical triplicates (each containing 200 ng of cDNA), using primer pairs for target (PfUT) and reference genes (β-tubulin) and including H<sub>2</sub>O as a negative control. The qPCR reaction mix and thermocycling conditions were as follows:

| Master Mix              |        | Thermocycling conditions                              |      |        |
|-------------------------|--------|---|------|--------|
| SYBR Green Master (Rox) | 10 µl  | Uracyl N-Glycosylase activity                         | 50°C | 2 min  |
| Forward primer 50µM     | 0.2 µl | Polymerase activation                                 | 95°C | 10 min |
| Reverse primer 50µM     | 0.2 µl | Primer-dependent amplification and real-time analysis | 95°C | 15 sec |
| cDNA (50ng/ µl)         | 4 µl   |   | 55°C | 15 sec |
| H <sub>2</sub> O        | 5.6 µl |   | 60°C | 45 sec |
| Final volume            | 20 µl  | + melting curve                                       |      |        |

Data were analyzed using delta-delta Ct method taking into account primers efficiencies.

### Determination of primer efficiency

A validation experiment consisting of five points of cDNA dilution (400 ng, 200 ng, 100 ng, 50 ng and 25 ng) was run for target and reference gene in triplicates, with H<sub>2</sub>O as a negative control. For each primer pair (target or reference gene) Ct values were plotted on a standard curve against the log of the cDNA concentrations. The linear regression was fitted to calculate the slope. Primer efficiency was then determined as  $10^{(-1/\text{slope})}$  and used for comparative Ct calculations. A slope of -3.32 gives a primer efficiency value of 2, indicating a 100% efficiency. This means that in every PCR cycle, the amount of DNA will be doubled. Good primer efficiency is assumed to be between 1.95 and 2.05, with 95% and 105% efficiency, respectively (Bio-Rad Laboratories, 2006; Eurogentec, 2008).

## 2.2.3. Biochemistry and cell biology

### 2.2.3.1. Preparation *P. falciparum* protein extracts

*P. falciparum* trophozoite stages at parasitemia of 5-10% were purified using the MACS system. After elution of infected erythrocytes from the column, samples were centrifuged for 2 min at 900 x g and pellets were washed once with PBS. Infected erythrocytes were then resuspended in 1 ml of Protein Lysis Buffer to remove red blood cell material. After 3 min incubation on ice, samples were centrifuged for 1 min at 17000 x g at 4°C and washed 3 times in ice cold PBS containing protease inhibitors. Parasites were then lysed in 4 pellet volumes of RIPA buffer containing 10 µg/ml DNase I for 30 min on ice, vortexed in between incubation time, and centrifuged for 20 min at 17000 x g at 4°C. Protein lysates (supernatant) were transferred to a fresh Eppendorf tube, resuspended in 1:1 ratio with 2x Protein Loading Buffer containing β-mercaptoethanol and stored at -20°C.

### 2.2.3.2. SDS-PAGE electrophoresis

Protein samples were analyzed by SDS-PAGE electrophoresis. Before being loaded on the SDS-PAGE gel, samples were heated at 37°C for 5-10 min. The PageRuler Plus Prestained (10 to 250 kDa) or HiMark Pre-Stained HMW Protein Standard (31 to 460 kDa) were used as protein ladders. Samples were loaded on NuPAGE Tris-Acetate 3-8% gradient gels or self-made gels. Gels were run at 150 V

and 40 mA for approx. 1.5 h in Tris-Acetate SDS running buffer (NuPAGE) or Tris-Glycine SDS running buffer. Self-made SDS-PAGE gels were prepared as follows:

| <b>Resolving gel</b> | <b>8%</b> | <b>10%</b> | <b>12%</b> | <b>Stacking gel</b> | <b>4%</b> |
|----------------------|-----------|------------|------------|---------------------|-----------|
| ddH <sub>2</sub> O   | 4.68 ml   | 3.96 ml    | 3.35 ml    | ddH <sub>2</sub> O  | 3.45 ml   |
| 1.5M Tris pH 8.6     | 2.50 ml   | 2.50 ml    | 2.50 ml    | 1M Tris pH 6.8      | 630 µl    |
| 10% SDS              | 100 µl    | 100 µl     | 100 µl     | 10% SDS             | 50 µl     |
| 30% Acrylamid        | 2.66 ml   | 3.33 ml    | 4.00 ml    | 30% Acrylamid       | 830 µl    |
| 10% APS (fresh)      | 100 µl    | 100 µl     | 100 µl     | 10% APS (fresh)     | 50 µl     |
| TEMED                | 6 µl      | 6 µl       | 6 µl       | TEMED               | 5 µl      |
| Final volume         | 10 ml     | 10 ml      | 10 ml      | Final volume        | 5 ml      |

### 2.2.3.3. Coomassie staining

To visualize proteins after SDS-PAGE electrophoresis gels were soaked in Coomassie Staining Solution for 10 min with shaking, followed by washing in Coomassie Destaining Solution with regular solvent changes until the background was clear and protein bands could be easily distinguished.

### 2.2.3.4. Western blot

After SDS-PAGE electrophoresis was completed, proteins were transferred from the gel onto an Immun-Blot PVDF membrane (Bio-Rad) using XCell II Blot Module. The gel was transferred onto 2 sponges and 2 Whatman papers pre-soaked in Transfer Buffer. The PVDF membrane was activated with methanol for at least 30 sec, briefly rinsed in ddH<sub>2</sub>O and transferred onto the gel. Another 2 Whatman papers and 3 sponges pre-soaked in Transfer Buffer were transferred on top of the membrane. The assembled “blotting sandwich” was then placed in a blotting chamber. The upper chamber was filled with transfer buffer, completely covering the blotting sandwich, whereas the lower chamber was filled with ddH<sub>2</sub>O to dissipate heat during the transfer. Wet transfer was run for 1h at 230 mA and 30 V. Afterwards, the membrane was blocked in 5% milk overnight at 4°C with gentle agitation. The following day, the membrane was incubated with the respective primary antibody diluted in 1% BSA for 1h at RT on roller, followed by 3 washes (3 x 10 min) with PBST (0.1% Tween in PBS) and 30 min blocking in 5% milk. Incubation with a secondary antibody diluted in 1% BSA was carried out for 30 min at RT on roller, followed by 3 washes (3 x 10 min) with PBST. The protein ladder was marked on the membrane using LICOR WesternSure Pen, followed by 5 min incubation with freshly prepared Developing Solution (BM chemiluminescence blotting substrate POD, Roche; 2 ml of solution A mixed with 20 µl of solution B). Signal was captured using the LiCor C-DiGit Blot Scanner and images were processed using Image Studio software. The dilutions of the antibodies used for Western blot were as follows:

| <b>Antibody</b>                             | <b>Dilution</b> |
|---|-----------------|
| Anti- $\alpha$ -tubulin (mouse)             | 1:1000          |
| Anti-HA (mouse)                             | 1:1000          |
| Anti-PfUT, C-terminal, SAB 654 (rabbit)     | 1:1000          |
| Anti-PfUT, N-terminal, Thermo 1-2a (rabbit) | 1:1000          |
| Anti-PfCRT (guinea pig)                     | 1:1000          |
| Anti-Ub (rabbit)                            | 1:2000          |
| Anti-mouse-POD                              | 1:10000         |
| Anti-rabbit-POD                             | 1:10000         |
| Anti-guinea pig-POD                         | 1:5000          |

### 2.2.3.5. Western blot membrane stripping

In order to remove antibodies from the western blot membrane for its reprobing, the membrane was incubated with Stripping Buffer for 30 min at RT on roller, followed by 3 washes (3 x 10 min) with PBST (0.1% Tween in PBS).

### 2.2.3.6. Immunofluorescence assay (IFA)

Parasites at trophozoite stage were either purified using the MACS system or collected unpurified from erythrocytes at parasitemia of 5-10%. Samples were centrifuged at 900 x g for 2 min. Erythrocytes were washed in PBS, followed by fixation in 4% PFA and 0.0075% GA for 30 min at RT with rotation. Samples were then washed twice with PBS and kept at 4°C or directly incubated with 0.1% Triton X-100 and 125 mM Glycine for 15 min at RT with rotation. All the following treatments were conducted at RT with rotation. 3% BSA in PBS was used as blocking buffer and as antibodies dilution buffer. Samples were blocked for at least 2 h, followed by primary antibody staining for 1.5 h (or at 4°C overnight). Cells were then washed in 3% BSA in PBS 3 times for 15 min, followed by secondary antibody staining for 45 min in the dark. Samples were then washed with PBS 3 times for 15 min, including addition of 5  $\mu$ M Hoechst to the final wash. Cells were resuspended in PBS and stored at 4°C until imaging. Samples were imaged using Carl Zeiss Axiovert 25 widefield microscope using objective with 63x magnification. Images were acquired and processed in FIJI. The dilutions of the antibodies used for IFAs were as follows:

| <b>Antibody</b>                             | <b>Dilution</b> |
|---|-----------------|
| Anti-HA (mouse)                             | 1:1000          |
| Anti-PfUT, C-terminal, SAB 654 (rabbit)     | 1:1000          |
| Anti-PfUT, N-terminal, Thermo 1-2a (rabbit) | 1:1000          |
| Anti-BiP (rabbit)                           | 1:1000          |
| Anti-PfERC (rabbit)                         | 1:500           |
| Anti-PfERD2 (rabbit)                        | 1:500           |
| Alexa Fluor 488 anti-mouse IgGs             | 1:1000          |
| Alexa Fluor 546 anti-rabbit IgGs            | 1:500           |

### 2.2.3.7. Transmission electron microscopy (TEM)

Immunogold-labelled samples for transmission electron microscopy (TEM) were prepared according to the Tokuyasu method (Cyrklaff et al., 2011). For this purpose, erythrocytes infected with the *P. falciparum* at trophozoite stage (36 ml culture, 2% hematocrit, 5% parasitemia) were purified from uninfected red blood cells using MACS system. After elution from the column, parasitized erythrocytes were centrifuged for 2 min at 900 x g and the pellet was washed twice with 1x PHEM. PHEM buffer contains Pipes, Hepes, EGTA and MgSO<sub>4</sub> and is commonly used to preserve cell structure for immuno-labelling. The sample was fixed in 4% PFA and 0.016% GA in 1x PHEM buffer for 1h at RT under agitation and subsequently washed twice in 1x PHEM. Pellet was resuspended in 1:1 ratio in 1x PHEM followed by embedding in 10-12% gelatine. Sample was incubated for 5 min at 37°C, shortly pelleted and solidified on ice. Gelatinized sample was cut into small cubes (around 1 mm<sup>3</sup>) and infused with 2.3 M sucrose solution for cryo-protection (at 4°C with light agitation overnight). The cubes were mounted on metal pins with excess of sucrose solution and frozen in liquid nitrogen. Subsequently, the frozen cubes were sectioned using the cryo-ultramicrotome (Leica, UCT6), melted on a drop of sucrose/methyl cellulose solution (2.3 M / 1.5%) and mounted onto TEM grids coated with Formvar film. Immuno-labelling was preceded by incubation in 50 mM glycine in PBS for 30 min to quench the remains of free aldehyde fixatives, followed by soaking in blocking buffer containing 1.5% BSA and 0.1% fish skin gelatine in 1x PBS for 30 min. This blocking buffer was also used as a dilution buffer for antibodies. Tokuyasu cryo-sections were labelled with primary mouse anti-HA antibody (dilution 1:1) for 1 h at RT and washed 5 times 3 min in the quenching buffer. Subsequent labelling with secondary goat anti-mouse antibody coupled to 10 nm colloidal gold (dilution 1:20) was carried out for 1 h at RT followed by washing 3 times in quenching buffer and 3 times in ddH<sub>2</sub>O, for 3 min each. Cryo-sections were then fixed in 1% glutaraldehyde for 5 min at RT, followed by washing 5 times for 3 min in ddH<sub>2</sub>O. To enhance the contrast and to embed the sample, the sections were washed in a mixture of uranyl acetate and methyl cellulose (1.8% / 0.8 %) and air dried. Specimens were examined and images recorded using Jeol JEM-1400 transmission electron microscope.

ER/Golgi complex was determined as membranous compartments adjacent to nuclei, including the margin of 50 nm at each side of a membrane for the accuracy of labelling that takes into consideration the cumulative length of the primary and secondary antibodies and the size of the protein A gold marker.

The distribution of gold particles was analyzed stereologically (Lucocq, 1994) according to their subcellular localization in the infected red blood cell on several micrographs. For this purpose, a

square grid with known spacing was placed over each of the micrographs to facilitate the quantification of gold hits and the number of line intersections which define the area of a compartment. For each compartment, **gold counts** were determined and depicted as percentage of the total number of gold particles in the analyzed area, as well as was the **compartment area** presented as percentage of the total analyzed area. Subsequently, the ratios of gold counts per compartment area were generated for each subcellular region to obtain the number of gold hits per unit area. These values were then depicted as a proportion of total gold signal measured across all analyzed compartments of several micrographs.

#### 2.2.3.8. Flow cytometry based analysis

Flow cytometry measurement of parasite DNA stained with SYBR Green offers the opportunity to study intraerythrocytic development of malaria parasites. It takes advantage of the fact that erythrocytes lack DNA, showing clear separation between *P. falciparum* infected and uninfected red blood cells. Therefore, based on the DNA content of parasite it is possible to quantify parasitemia and distinguish parasites at different stages (Grimberg, 2011).

The staining procedure was performed as described by Ganter et al. (2017). Parasites were fixed in 4% PFA and 0.0075% GA at 4°C overnight. Samples were then washed several times with PBS and stored in PBS at 4°C. 200 µl of each sample were transferred to a 96-well V-bottom plate, centrifuged for 2 min at 900 x g and permeabilized with 200 µl of 0.1% Triton X-100 for 8 min at RT. Cells were washed twice with PBS, and subsequently treated with 200 µl of 0.3 mg/ml RNase A for 30 min at 37°C. Samples were then washed twice with PBS and kept at 4°C until staining. Cells were incubated with 200 µl of SYBR Green I (1:2000 in PBS) for 20 min at RT in the dark. Stained samples were then washed twice with PBS, transferred to FACS tubes containing 1 ml of cold PBS and run on a BD FACSCanto flow cytometer. SYBR Green fluorescence was detected in the fluorescein isothiocyanate (FITC) channel. For each sample 50 000 events were recorded and analyzed using Flowing Software. The FSC-H versus FSC-A plot was first used to discriminate doublets from single cells. Singlets gate was further used for analysis of FITC positive events. The unstained sample served as a negative control used for gating of uninfected erythrocytes.

##### 2.2.3.8.1. Determination of parasitemia and multiple-infections

Parasitemia was quantified as a ratio of FITC positive cells representing infected erythrocytes to the total number of red blood cells analyzed per one flow cytometry measurement.

SYBR Green staining allows not only to determine the total number of infected red blood cells in population (parasitemia), but also to distinguish between single, double, and triple *P. falciparum* infections (Bei et al., 2010). The flow cytometer is however unable to differentiate between the

signal emitted by a red blood cell infected with two ring stage parasites versus the signal of a single di-nucleated trophozoite (already after the first round of nuclear division). Therefore, for analysis of multiple infections it is crucial to use highly synchronized ring stage parasite cultures. The populations of singly-, doubly- and triply-infected erythrocytes were determined via a defined gating on dot plot and histogram (Fig 2.2).

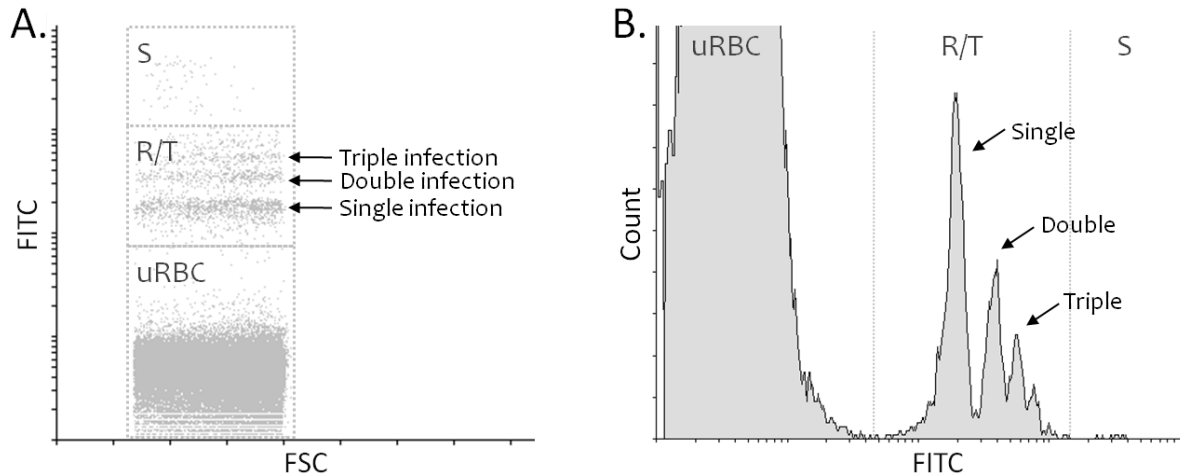


**Figure 2.2. Flow cytometry gating.** FITC channel was used to gate populations of uninfected red blood cells (uRBC), ring/trophozoite-stage parasites (R/T) and schizonts (S) on dot plot (A) and histogram (B). Parasitemia is expressed as a percentage of parasites (S + R/T) in all analyzed events (S + R/T + uRBC). Ring-stage parasites can be used for analysis of single, double and triple infections.

#### 2.2.3.8.2. Quantification of parasite multiplication rates (PMR)

The parasite multiplication rate (PMR) is the fold increase in parasitemia observed each new cycle of asexual growth (Chotivanich et al., 2000; Duncan et al., 2011). In order to determine the PMR, parasite cultures were synchronized using sorbitol and heparin treatments and diluted to 0.1% parasitemia at the trophozoite stage. 200  $\mu$ l of each of three independent biological replicates were collected every 48 h over 4 cycles, fixed, stained with SYBR Green (chapter 2.2.3.8) and run on a BD FACSCanto flow cytometer. Data were analyzed using Flowing Software, Excel and Sigma Plot 13. Data points were plotted in a scatter plot depicting parasitemia expressed as the natural logarithm over the time of 4 replicative cycles. The linear regression was then fitted and the PMR was quantified as:

$$PMR = e^a,$$

where  $a$  corresponds to the slope of the linear regression.

#### 2.2.3.8.3. Determination of merozoites number

The number of merozoites generated per schizont was determined via flow cytometric analysis of the DNA content in rupturing schizonts. Parasites were synchronized using sorbitol and heparin treatments. Samples were collected, fixed, stained with SYBR Green (chapter 2.2.3.8) and run on a BD FACSCanto flow cytometer. Data were analyzed using Flowing Software and Sigma Plot 13. The merozoites number was expressed as a mean fluorescence emitted by a population of schizonts containing multiple DNA copy numbers, divided by a mean intensity obtained for a population of singly-infected red blood cells, with a single DNA copy number.

$$\text{Merozoites number} = \frac{\text{mean fluorescence intensity of schizonts}}{\text{mean fluorescence intensity of singly-infected erythrocytes}}$$

The populations of schizonts and singly-infected erythrocytes were determined via a defined gating strategies (Fig 2.2).

#### 2.2.3.8.4. Determination of asexual life cycle duration

Cell cycle progression of *P. falciparum* can be tracked using flow cytometry, by quantification of the increase in DNA content over time. Parasite cultures were synchronized to a 4 h window using sorbitol and heparin treatments, and adjusted to 0.5% ring stage parasitemia. The cell cycle length was analyzed as previously described (Ganter et al., 2017), by measuring the parasite DNA content (C-value) at 4 h intervals over the 66h post invasion. At each time point, 200 µl of each of three independent biological replicates were collected, fixed, stained (chapter 2.2.3.8) and run on a BD FACSCanto. Data were analyzed using Flowing Software, Excel and Sigma Plot 13. The C-value was quantified by dividing the total parasite mean fluorescence intensity at particular time point by the mean intensity of a single infection from the first time point.

$$C\text{-value} = \frac{\text{parasites mean fluorescence intensity}}{\text{mean intensity of a single infection from the first time point}}$$

The visible drop of the C-value after reaching the peak at schizont stage indicates the beginning of a new cycle.

#### 2.2.3.8.5. Egress and invasion assay

Parasites were synchronized to the 4 h window using sorbitol and heparin treatments and adjusted to 0.3% parasitemia at schizont stage and 2% hematocrit. The experiment was carried out in 96-well flat bottom plates with 200 µl-sample volume in triplicates. The first time point was collected 2-4 h prior to schizont rupture. At each time point (every 2-4 h), the whole plate was collected, washed twice with PBS and fixed in 4% PFA and 0.0075% GA at 4°C overnight. Samples were then washed



with PBS, stained with SYBR Green (chapter 2.2.3.8) and run on a BD FACSCanto flow cytometer. Data were analyzed using Flowing Software, Excel and Sigma Plot 13. Data points were plotted in a line and scatter plot of parasitemia versus the time post invasion. The efficiency of merozoites egress from mature schizonts (egress efficiency) was depicted as a percentage of schizont parasitemia (Fig. 2.2, gate S) over the time post invasion. The efficiency of released merozoites to invade red blood cells (invasion efficiency) was shown as a percentage of ring parasitemia (Fig. 2.2, gate R) over the time post invasion (A. S. Paul et al., 2015b).

#### 2.2.3.8.6. Merozoites attachment assay

Merozoites attachment assay was performed to determine whether the increased invasion efficiency was associated with a stronger attachment of merozoites to erythrocytes or if it occurred at a later stage of the invasion process. The merozoite entry to the host cell is an actin-dependent process. Therefore, an inhibitor of actin polymerization, cytochalasin D, has been used to separate the two events (attachment and invasion). Cytochalasin D (cyt. D) allows merozoites to attach to erythrocytes but it blocks their entry (Egan et al., 2015; Paul et al., 2015)

Parasites were synchronized to the 4 h window using sorbitol and heparin treatments and adjusted to 0.3% parasitemia at schizont stage and 2% hematocrit. For each clone, three independent biological replicates were prepared in three different conditions: Ø cyt. D (invasion), 1 µM cyt. D (attachment), 50 U/ml heparin (negative control; no attachment or invasion). 200 µl per sample were transferred to 96-well flat bottom plates (1 plate per time point). Plates were collected at 0 h (schizont rupture), 1 h, 4 h, and 7 h post invasion. At each time point, the whole plate was collected, and fixed in 10 volumes of 2% GA and 0.116 M sucrose (e.g. 100 µl sample per 1 ml fixative) at 4°C overnight. All washing steps and staining solutions were supplemented with 0.116 M sucrose. Samples were then washed with PBS, stained with SYBR Green (chapter 2.2.3.8) and run on a BD FACS Canto flow cytometer. Data were analyzed using Flowing Software, Excel and Sigma Plot 13. Data were presented as a comparison of merozoites attachment to erythrocytes (+ cyt. D) and invasion to ring stage parasites (Ø cyt. D) at different time points post invasion. Heparin served as negative control for background subtraction.

#### 2.2.4. *In vitro* development of resistance to quinine

*In vitro* development of drug resistance using laboratory strains enables the detection of its determinants, before resistance emerges in the field. The gradual increase of selective pressure induces potential adaptive mutations conferring resistance to the applied drug (Oduola et al., 1988; Witkowski et al., 2010). Once the drug pressured strain reaches the desired level of resistance, the

parasite's genome is sequenced. This procedure aims to identify new mutations potentially involved in the acquired resistance to quinine and/or other unrelated antimalarials (Rathod et al., 1997).

This approach was attempted in *P. falciparum* Dd2 strain, chosen as experimental line due to its high mutation rate, which increases the probability of obtaining the mutants (Bopp et al., 2013; Rathod et al., 1997). The ultimate goal was to develop the parasite line resistant at least to 2  $\mu$ M quinine. This concentration represents ten times the IC<sub>50</sub> value determined for quinine in Dd2 strain. Parasites were treated with quinine, which concentration was increased in a step-by-step fashion. The experiment was conducted in multiple 50 ml cell culture flasks containing a filter cap, with a starting inoculum of  $5 \times 10^9$  parasitized red blood cells. The initial treatment dose amounted to 200 nM, corresponding to quinine's IC<sub>50</sub> in Dd2. Development of resistance was determined by measuring the increase in IC<sub>50</sub> values for quinine (QN) and its stereoisomer quinidine (QD), along with chloroquine (CQ) serving as a control. Parasite samples were regularly cryopreserved, as so called "freeze-downs". When necessary (e.g. after culture contamination), the freeze-downs were brought back to the culture and immediately subjected to the selective drug pressure. The experiment was carried out over a period of over one year until reaching the quinine exposure dose of 2  $\mu$ M.

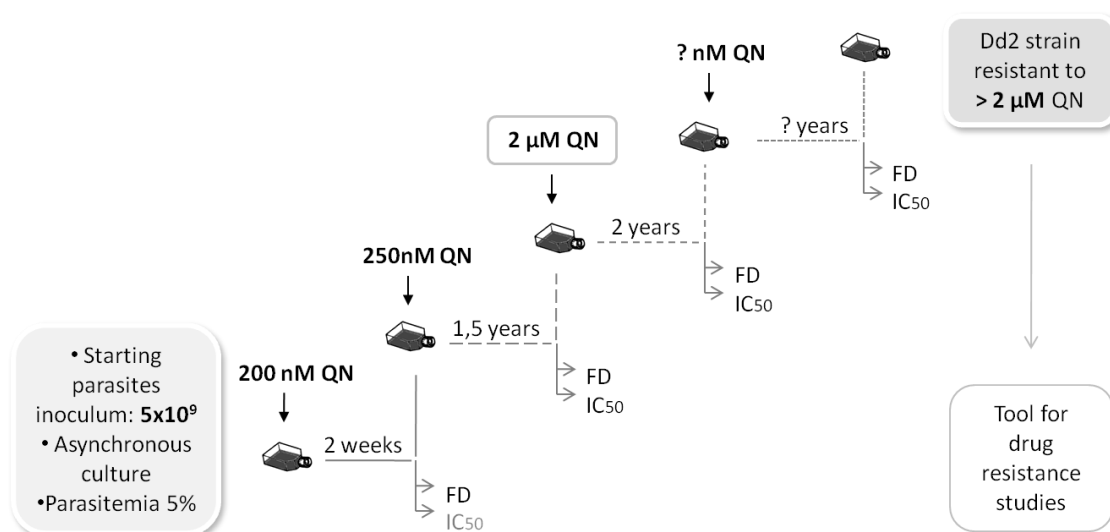


**Figure 2.3. Schematic representation of *in vitro* development of strain resistant to high quinine concentrations.** Parasites were exposed to gradually increasing concentrations of quinine (QN), starting from 200 nM until reaching at least 2  $\mu$ M treatment dose. Progress of acquired resistance was monitored via IC<sub>50</sub> measurements. FD – freeze-down.

### 2.2.5. Data analysis

The data analysis and display were performed using Excel 2010 and SigmaPlot 13.0.

## 3. Results

### 3.1. Analysis of the role of PfCRT phosphorylation at S33 in resistance to chloroquine and quinine

Reversible protein phosphorylation plays a key role in regulation of many cellular processes, including, among others, modulation of the activity of a transporter (Foster et al., 2006; Ramamoorthy et al., 2011; Stolarczyk et al., 2011). The chloroquine resistance transporter PfCRT is phosphorylated at various sites, including S33, S411, T416 and S420 (Kuhn et al., 2010; Lasonder et al., 2012; Solyakov et al., 2011). Phosphorylation of threonine 416 has been shown to direct the trafficking of PfCRT from the ER to the digestive vacuolar membrane (Kuhn et al., 2010). However, the functional roles of the other modifications remain unclear. The purpose of this project was to investigate the role of phosphorylation of serine 33 in the drug resistance-mediating function of PfCRT.

#### 3.1.1. The kinase inhibitor ML-7 reduces chloroquine and quinine resistance

In a previous study conducted by Dr. Cecilia Sanchez, a range of protein kinase and phosphatase inhibitors was screened for the activity on accumulation of chloroquine in the *P. falciparum* chloroquine resistant strain Dd2 (unpublished data). Among the tested inhibitors, only ML-7, W-7 and H-89 showed a significant increase in the uptake of chloroquine by Dd2 strain, with p values of <0.001, 0.003 and 0.004, respectively (One Way ANOVA, Holm-Sidak test). ML-7 has been previously identified as an inhibitor of a serine/threonine protein kinase PfCK2 $\alpha$  (casein kinase 2) (Graciotti et al., 2014; Holland et al., 2009). W-7, a calmodulin-dependent protein kinase inhibitor, was shown to block the activity of PfPKB (protein kinase B-like enzyme) (Vaid & Sharma, 2006). H-89 is a known inhibitor of the cyclic AMP-dependent protein kinase catalytic subunit PfPKA-C (Syn et al., 2001). Interestingly, all three compounds are structurally related derivatives of naphthalene- and isoquinoline-sulfonamides (Fig. 3.1).

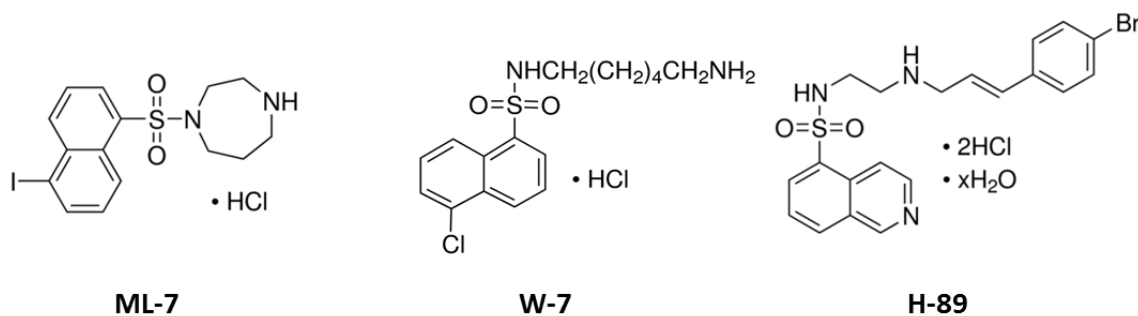


**Figure 3.1. Chemical structures of the 3 inhibitors with a significant impact on chloroquine accumulation in *P. falciparum* chloroquine resistant Dd2 strain.**

Of the three inhibitors with a statistically significant impact on the chloroquine accumulation in the Dd2 strain, ML-7 was selected for further analysis in the current study. The dose-response curves have been generated to evaluate the inhibitory effect of ML-7 on the parasite growth (Fig. 3.2.A). The  $IC_{50}$  values of  $19 \pm 3 \mu M$  and  $37 \pm 5 \mu M$  were determined for *P. falciparum* Dd2 and HB3 strains, respectively. A maximum ML-7 concentration not affecting the development of Dd2 parasites was estimated to be  $1 \mu M$  and was subsequently used in the growth inhibition assay together with chloroquine (CQ) and quinine (QN). A ML-7 concentration of  $2.5 \mu M$ , with a mildly toxic effect on the parasite growth, has also been tested along with the two mentioned quinoline drugs. Presence of ML-7 resulted in a significantly ( $p < 0.001$ ) increased susceptibility of a resistant Dd2 strain to these drugs, with  $IC_{50}$  values for CQ ranging from  $129 \pm 5 nM$  in the absence of inhibitor, to  $82 \pm 6 nM$  and  $83 \pm 9 nM$  in the presence of  $1 \mu M$  and  $2.5 \mu M$  ML-7, respectively. As for QN, the  $IC_{50}$  values ranged from  $305 \pm 8 nM$  in the absence of inhibitor, to  $140 \pm 9 nM$  and  $167 \pm 24 nM$  in the presence of  $1 \mu M$  and  $2.5 \mu M$  ML-7, respectively (Fig. 3.2.B and C). Presence of ML-7 did not affect the CQ and QN response levels of a sensitive strain HB3. An antifolate drug, pyrimethamine (PYR) has been used as a control (Fig. 3.2.D). PYR targets the parasite's dihydrofolate reductase (DHFR) and resistance to PYR is conferred by point mutations in the enzyme (Oguike et al., 2016). Treatment with ML-7 had no influence on the responsiveness of Dd2 and HB3 to PYR, with average  $IC_{50}$  values of  $30 \pm 2 \mu M$  and  $11 \pm 2 \mu M$ , respectively.

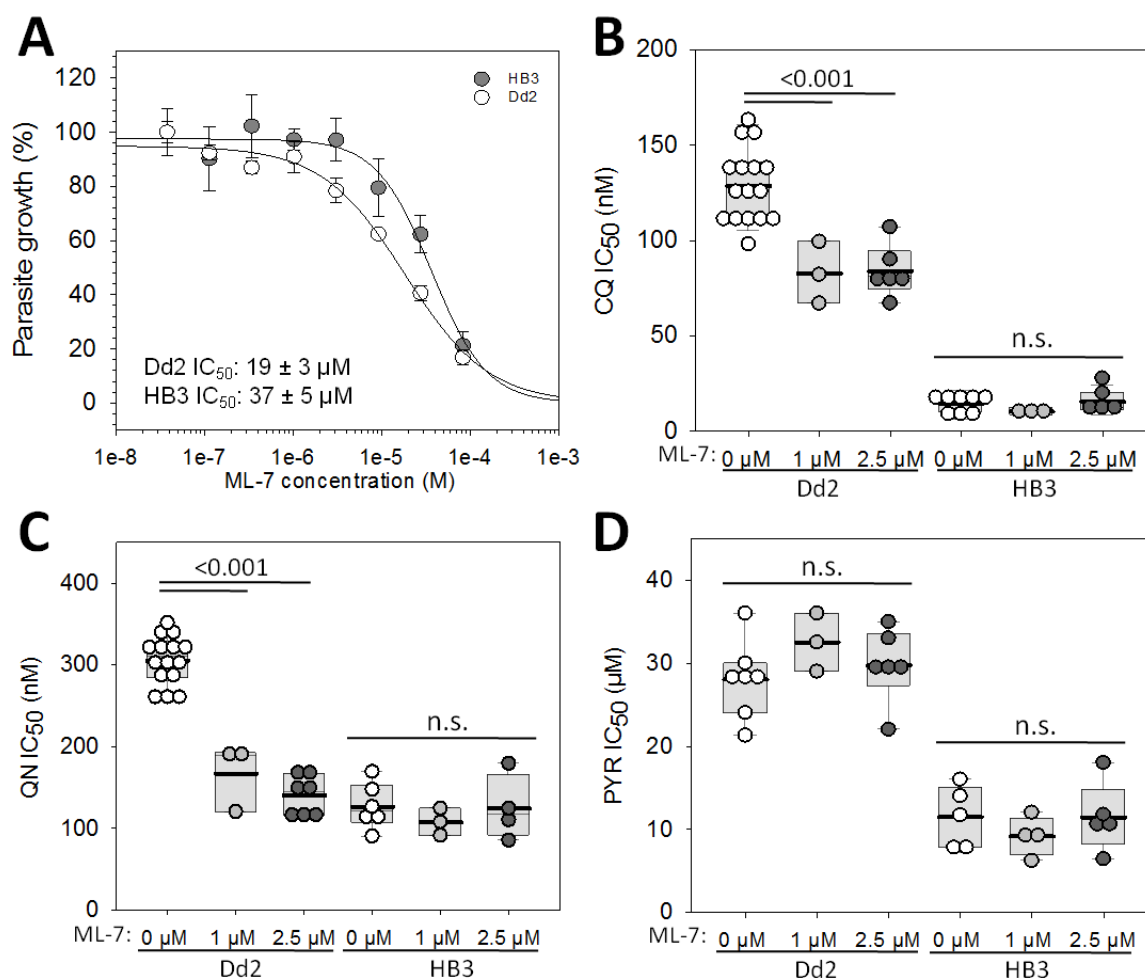


**Figure 3.2. Characterization of kinase inhibitor ML-7.** **A.** ML-7 dose-response curves. Inhibition of parasite growth in the presence of increasing ML-7 concentrations was measured for Dd2 and HB3 strains and is depicted as mean  $\pm$  SEM of four independent biological replicates. **B–D.** Responsiveness of Dd2 and HB3 to selected antimalarial drugs in the presence and absence of 1  $\mu M$  and 2.5  $\mu M$  ML-7. Half-maximal inhibitory concentrations ( $IC_{50}$ ) were determined for **B.** chloroquine (CQ), **C.** quinine (QN) and **D.** pyrimethamine (PYR). Each symbol represents an independent biological replicate. A box plot analysis of each data set is shown in grey. A thick black line indicates the mean value. Statistical significance between the data sets was calculated using One Way ANOVA Holm-Sidak test; n.s. – not significant.

### 3.1.2. Phosphorylation of PfCRT's serine 33 modulates chloroquine and quinine responsiveness

To assess the role of phosphorylation in PfCRT function, the CRISPR-Cas9 genome editing technology (Ghorbal et al., 2014) was applied to replace PfCRT serine 33 by alanine, glutamic acid or aspartic acid (Fig. 3.3.A). Serine (S) substitution by alanine (A) prevents potential phosphorylation. Mutation to glutamic acid (E) or aspartic acid (D), the negatively charged amino acids, mimics phosphorylation of a serine residue. S33 mutant lines have been generated by Dr. Sonia Moliner Cubel and Dr. Cecilia

Sanchez. Several clones were isolated for each mutant line, namely B5 and B6 for S33A mutant, F8, C8 and B10 for S33E mutant, and A11, F8 and G8 for S33D mutant.

The growth inhibition assays were performed for Dd2 wild type and mutant lines to verify the drug resistance-mediating function of PfCRT. Drug responsiveness was measured for chloroquine (CQ) and quinine (QN), along with pyrimethamine (PYR) as a control (Fig. 3.3.B-D). A significant ( $p<0.001$ ) increase in the susceptibility to chloroquine has been observed for S33A clones, B5 and B6, with  $IC_{50}$  values of  $80 \pm 4$  nM and  $72 \pm 5$  nM, respectively, in comparison to Dd2 WT with  $IC_{50}$  values of  $131 \pm 5$  nM. S33E clones, F8, C8 and B10, revealed an intermediate phenotype between the Dd2 wild type and S33A mutants with chloroquine  $IC_{50}$  values of  $102 \pm 3$  nM,  $108 \pm 4$  nM and  $105 \pm 4$  nM, and a significance of  $p=0.001$ ,  $p=0.006$  and  $p=0.027$ , respectively. S33D clones, A11, F8 and G8 displayed a chloroquine resistance phenotype not significantly different from the Dd2, with  $IC_{50}$  values of  $137 \pm 6$  nM,  $134 \pm 6$  nM and  $130 \pm 4$  nM, respectively. A chloroquine sensitive strain HB3 exhibited  $IC_{50}$  value of  $14 \pm 2$  nM. Regarding the quinine resistance phenotype, similar trends in drug responsiveness as for chloroquine have been observed. S33A clones, B5 and B6, showed a significant reduction ( $p<0.001$ ) in resistance to quinine, with  $IC_{50}$  values of  $202 \pm 7$  nM and  $193 \pm 13$  nM, respectively, in comparison to Dd2 WT with  $IC_{50}$  values of  $311 \pm 9$  nM. S33E mutation resulted in an intermediate quinine resistance phenotype, with  $IC_{50}$  values of  $234 \pm 11$  nM,  $228 \pm 10$  nM and  $220 \pm 16$  nM, for clones F8, C8 and B10, respectively, with a significance of  $p<0.001$  for each of the clones. S33D mutants, A11, F8 and G8, showed again a phenotype not significantly different from Dd2, with quinine  $IC_{50}$  values of  $310 \pm 19$  nM,  $314 \pm 13$  nM and  $299 \pm 14$  nM, respectively. The quinine  $IC_{50}$  value of HB3 strain analyzed in parallel was  $127 \pm 11$  nM. In contrast to varying responses to chloroquine and quinine, there was no significant difference in the responsiveness of Dd2 and mutants to pyrimethamine, with an average  $IC_{50}$  value of  $27 \pm 2$  nM.

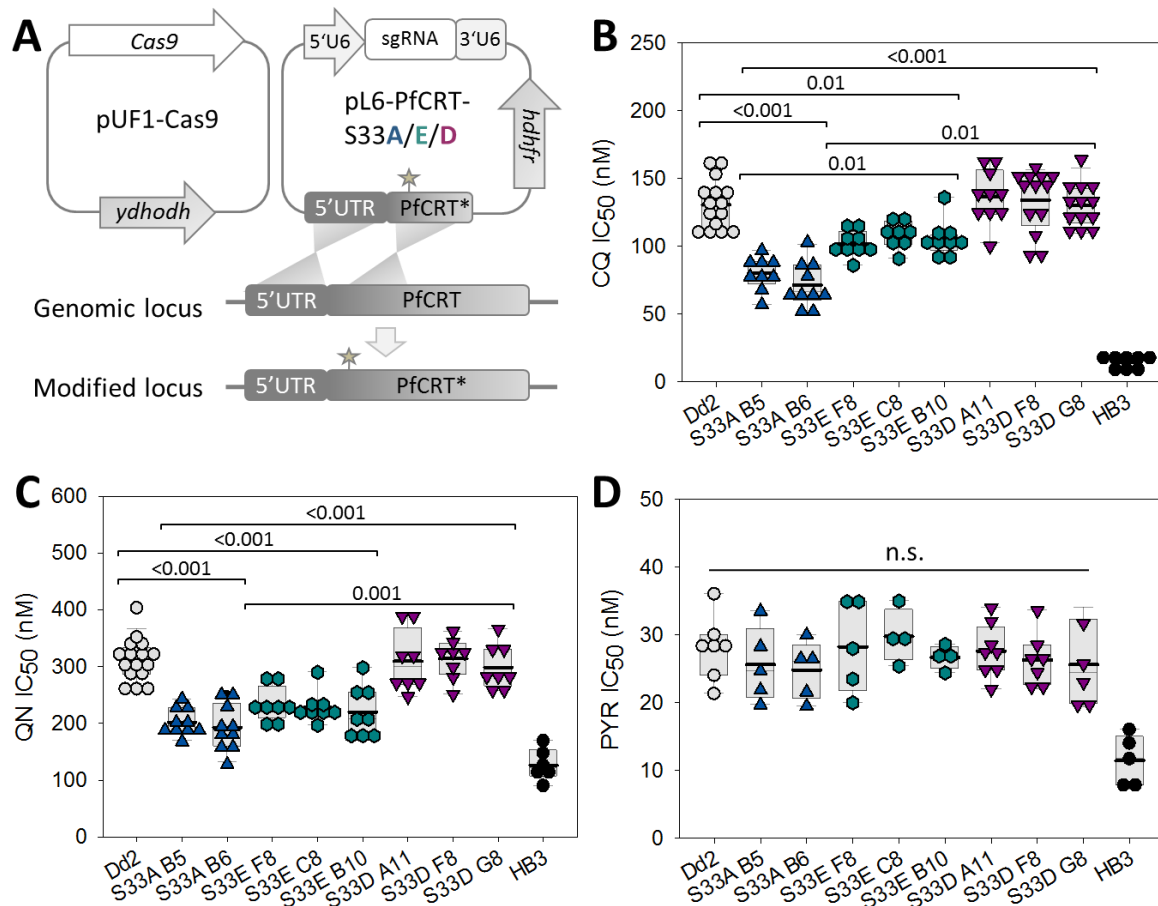


**Figure 3.3. CRISPR-Cas9-mediated mutagenesis of *PfCRT* locus and responsiveness of the mutants to selected antimalarials.** **A.** Schematic representation of the CRISPR-Cas9-based strategy to replace serine (S) at position 33 by alanine (A), glutamic acid (E) or aspartic acid (D) in the *PfCRT* locus. Mutant lines were generated by Dr. Sonia Moliner Cubel and Dr. Cecilia Sanchez. **B-D.** Drug responsiveness of the *PfCRT* S33 mutants, the parental strain Dd2 and HB3. Half-maximal inhibitory concentrations (IC<sub>50</sub>) were determined for **B.** chloroquine (CQ), **C.** quinine (QN) and **D.** pyrimethamine (PYR). Each symbol represents an independent biological replicate. A box plot analysis of each data set is shown in grey. A thick black line indicates the mean value. Statistical significance between the data sets was calculated using One Way ANOVA Holm-Sidak test; n.s. – not significant. Data in **B** and **C** were generated together with Marina Müller.

### 3.1.3. Multiplication rate variation in the *PfCRT* S33 mutants

Acquiring resistance against a drug is often associated with fitness cost (Felger & Beck, 2008; Schneider & Escalante, 2013). Different *pfprt* alleles have been previously shown to confer various impact on the parasite fitness (Mita et al., 2004; Petersen et al., 2015). To assess whether *PfCRT* S33 mutations carry a fitness cost for the parasite, growth of the respective mutants in a co-culture with Dd2 wild type was examined in a fitness assay (Fig. 3.4.A). S33A and S33E mutants revealed a fitness advantage in relation to Dd2 wild type parasites, as a proportion of these *PfCRT* mutants increased over time, with slopes of linear regression determined to be 1.057 and 1.025, respectively. The

fitness of the S33D clones analyzed over 20 cycles was comparable with the Dd2 wild type, with a slope of the regression line of -0.171.

To better understand the differences in fitness between Dd2 wild type and PfCRT S33 mutants, the parasite multiplication rates (PMRs) were determined for each clone (Fig. 3.4.B). For this purpose, pre-synchronized parasites were cultured for 4 replicative cycles during which samples were collected every 48 h at the trophozoite stage. PMR of each clone was expressed as a fold increase in parasitemia measured over time. The PMR for Dd2 and HB3 of  $11 \pm 1$  and  $7 \pm 1$ , respectively, were consistent with the results of previous studies (Murray et al., 2017; Reilly et al., 2007). S33A clones, B5 and B6, exhibited a significant increase ( $p < 0.001$ ) in PMR, with values of  $18 \pm 1$  and  $19 \pm 1$ , respectively. Similar results were observed for S33E clones, F8, C8 and B10, with PMR of  $19 \pm 1$ ,  $17 \pm 1$  and  $19 \pm 1$ , respectively, with a significance of  $p < 0.001$  for each clone. The multiplication rates obtained for S33D clones, A11, F8 and G8, with values of  $12 \pm 1$ ,  $12 \pm 1$  and  $12 \pm 1$ , respectively, were not significantly different from the Dd2 wild type.

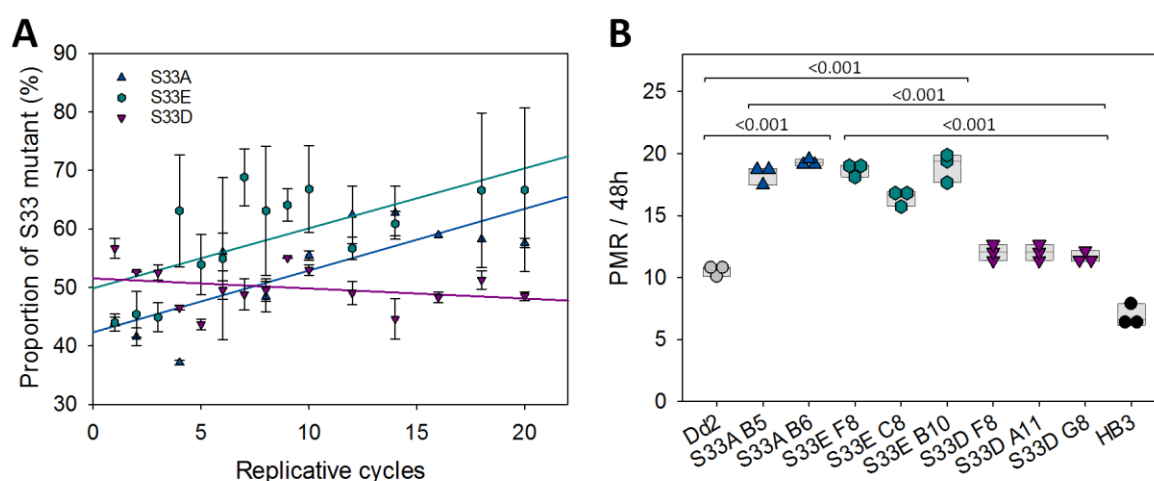


**Figure 3.4. Characterization of the growth of PfCRT S33 mutants.** **A.** Effect of PfCRT S33 mutations on the parasite fitness. Dd2 WT and S33 mutants were mixed at ~1:1 ratio and cultivated for 20 cycles. The allelic proportions of serine (S) over alanine (A), glutamic acid (E) or aspartic acid (D) were measured by pyrosequencing. The proportion of S33 mutants co-cultured with Dd2 WT over time is presented at the Y axis. Results were fit to a linear regression model of the relative proportion of the wild type over the mutated S33 alleles over time. For each clonal line data is shown as the mean  $\pm$  SEM of three independent mixed cultures. Fitness assays for S33A, S33E and S33D mutants were performed by Dr. Sonia Moliner Cubel, Chinha Xoumpholphakdy and Dr. Britta Nyboer, respectively. **B.** Parasite multiplication rates (PMR) of Dd2 wild type and PfCRT S33 mutant lines. PMR of each clone represented by three independent biological replicates was determined as a fold increase in parasitemia per 48h, measured over 4 cycles. A box plot analysis of each data set is shown in grey. Statistical significance between the data sets was calculated using One Way ANOVA Holm-Sidak test.



### 3.1.4. Fitness advantage of PfCRT S33 mutants results from an increased numbers of merozoites

Different factors of parasite intraerythrocytic development can affect parasite multiplication rates, one of the measures of parasite fitness. These include the cell cycle duration, numbers of merozoites generated per schizont, or efficiency of red blood cell invasion (Chotivanich et al., 2000; Ganter et al., 2017; Garg et al., 2015). The above-mentioned aspects were taken into account to address the observed differences in the multiplication rates between the Dd2 wild type and PfCRT S33 mutants. Since the different clones of a particular PfCRT S33 mutant displayed comparable results, as presented in previous sections, in some of the following experiments, a representative clone of each mutant has been selected for further investigations. To begin with, the length of the cell cycle has been investigated. For this purpose, the parasite DNA content, referred to as the “C-value”, was measured in samples collected in 4 h intervals throughout the replicative cycle. The intraerythrocytic cycle duration of both Dd2 wild type and S33 mutants was determined to be 44h, as estimated from the peak of mitotic activity (Fig. 3.5.A). Interestingly, C-values obtained at 44 h post invasion differed for each clone, indicating that different numbers of merozoites have developed in mature schizonts. Therefore, numbers of merozoites generated per schizont were further analyzed, as a potential reason of differences in multiplication rates observed for the clones (Fig. 3.5.B). Numbers of merozoites per schizont quantified for Dd2 and HB3, with values of  $15 \pm 1$  and  $11 \pm 1$ , respectively, were consistent with previous reports (Reilly et al., 2007). S33A clones, B5 and B6, showed a significant increase ( $p < 0.001$ ) in merozoites numbers, with values of  $19 \pm 1$  and  $20 \pm 1$ , respectively. Similar results have been observed for S33E clones, F8, C8 and B10, with merozoites numbers of  $18 \pm 1$ ,  $17 \pm 1$  and  $18 \pm 1$ , respectively, and with a significance of  $p < 0.001$ . The numbers of merozoites obtained for S33D clones, A11, F8 and G8, of  $16 \pm 1$ ,  $16 \pm 1$  and  $16 \pm 1$ , respectively, were not significantly different from Dd2 wild type.

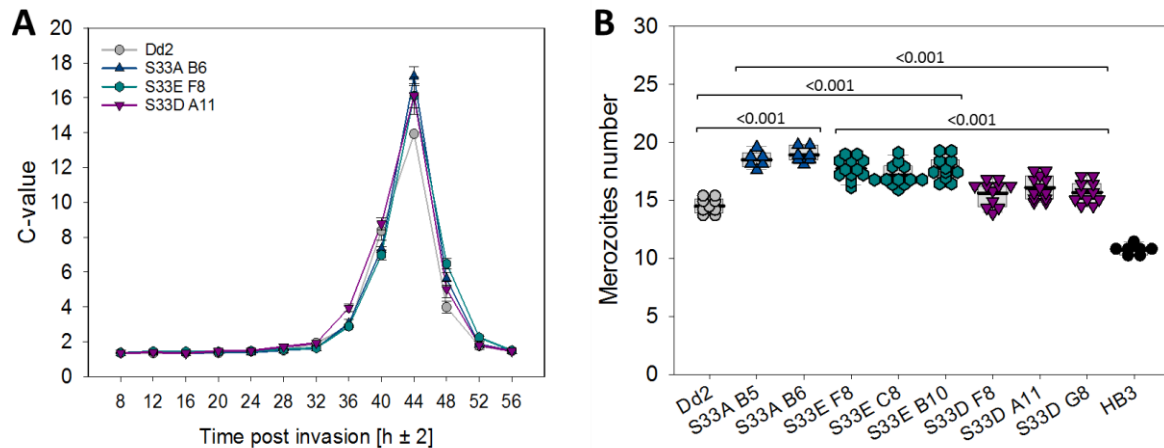


**Figure 3.5. Comparison of cell cycle length and merozoites numbers in Dd2 wild type and PfCRT S33 mutant lines. A.** The cell cycle length expressed as an increase in the parasite DNA copy number (C-value) measured over time. The drop in the C-value after reaching the peak indicates the beginning of a new cycle. For each clone, each time point represents a mean  $\pm$  SEM of three independent biological replicates. **B.** Number of merozoites generated per schizont determined using flow cytometry. Each symbol represents an independent biological replicate. A box plot analysis of each data set is shown in grey. A thick black line indicates the mean value. Statistical significance between the data sets was calculated using One Way ANOVA Holm-Sidak test.

Furthermore, the differences in multiplication rates may also derive from an altered parasite egress or invasion. Release, also known as egress, of daughter merozoites from a mature schizont and the subsequent invasion of new red blood cells are two tightly coordinated processes, essential for parasite replication (Collins et al., 2017; Koch & Baum, 2016). To assess whether alterations in multiplication rates of PfCRT S33 mutants are associated with egress or invasion events, mature schizonts at initially identical parasitemia were allowed to rupture and re-invade fresh erythrocytes and were monitored in 2 h intervals. Egress efficiency is depicted as parasitemia of schizonts decreasing over time with the gradual release of merozoites from rupturing mature schizonts as a new cycle begins (Fig. 3.6.A). Invasion efficiency is presented as parasitemia of ring stage parasites increasing over time with the merozoites invading new red blood cells (Fig. 3.6.B). While no difference in egress efficiency has been observed between Dd2 wild type and PfCRT S33 mutants, clone S33A B6 displayed a significant increase in invasion efficiency in relation to other clones, for up to 49 h post invasion (p.i.), with  $p \leq 0.001$  (according to One Way ANOVA Holm-Sidak test). Since the cell cycle length of Dd2 and PfCRT mutants was estimated to be 44 h (Fig. 3.5.A), a time point of 49 h p.i. corresponds to the first 5 h of a new replicative cycle. Although the difference in ring parasitemia between S33A B6 mutant and Dd2 wild type was slightly reduced at subsequent time points, it remained significant, ranging between  $p=0.003$  and  $p=0.019$ . In contrast, after 49 h p.i. the differences in invasion efficiencies of S33A B6 and S33E F8 clones were statistically non-significant. Invasion efficiency of S33A B6 was significantly higher in comparison to S33D A11 mutant during all analyzed time points, with  $p \leq 0.001$ .

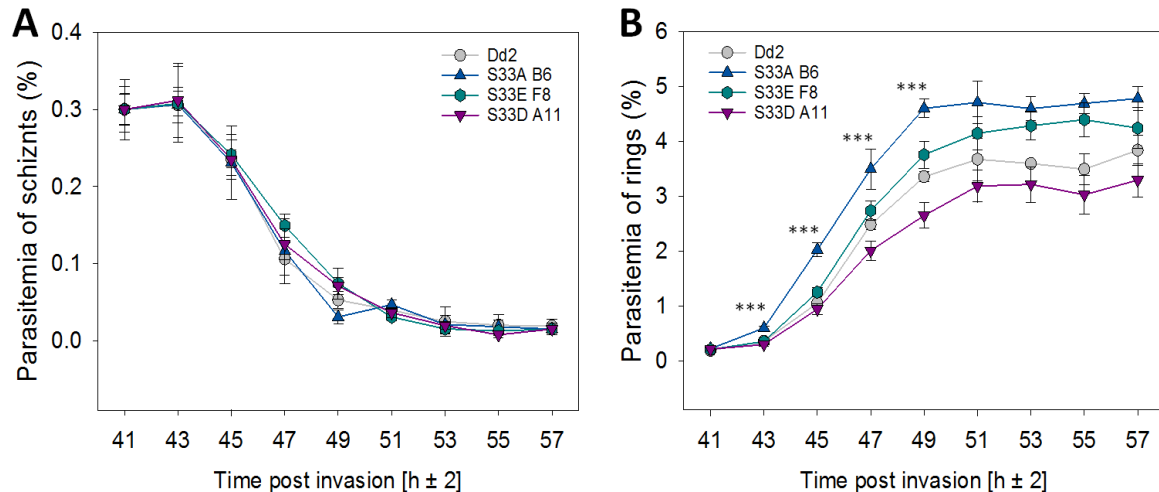


**Figure 3.6. Egress and invasion efficiencies of Dd2 parental line and PfCRT S33 mutants.** **A.** Egress efficiency presented as a parasitemia of schizonts decreasing over time. **B.** Invasion efficiency depicted as a parasitemia of ring stage parasites increasing over time. The mean  $\pm$  SD of three independent biological replicates are shown. \*\*\* indicates a significant difference in parasitemia of clone S33A B6 in relation to Dd2 WT, S33E F8 and S33D A11, with  $p \leq 0.001$ , according to One Way ANOVA Holm-Sidak test.

Prior to invasion, the merozoite attaches to the erythrocytes surface. Subsequently, it reorientates and forms a tight junction with the erythrocyte membrane, enabling its actin-based entry into the host cell (Field et al., 1993; Koch & Baum, 2016). To determine whether the increase in invasion efficiency observed for PfCRT S33A mutant already occurred during merozoite attachment to the red blood cell surface or later in the invasion process, a merozoites attachment assay was performed. To distinguish between the two events (attachment or invasion) an inhibitor of actin polymerization, cytochalasin D (cyt. D), has been used (Egan et al., 2015; Paul et al., 2015). In the absence of cyt. D, the parasites are able to invade erythrocytes, whereas addition of cyt. D results in only attachment of merozoites to the red blood cell surface, as their entry is blocked. Parasites were synchronized to a 4 h window at mature schizont stage. Following schizont rupture (time point: 0 h), parasitemias of released merozoites attaching to (+ cyt. D) or invading (- cyt. D) new red blood cells were monitored at 1, 4 or 7 h post invasion (p.i.). As shown in Figure 3.7, no significant differences were observed in both attachment and invasion between the analyzed clones at 0 h p.i. At the subsequent time points, merozoites of PfCRT S33A B6 mutant seemed to have higher attachment in comparison to other clones, but only at 4 h p.i. the difference was statistically significant (Fig. 3.7.A). Regarding invasion, S33A B6 displayed significant increase ( $p < 0.001$ ) in invasion at 1 and 4 h p.i. in relation to all other clones (Fig. 3.7.B), confirming results depicted in Figure 3.6.B. At 7 h p.i. S33A B6 showed significantly higher invasion than Dd2 WT and S33D A11 ( $p = 0.006$  and  $p = 0.001$ , respectively), but no more than S33E F8, what is also consistent with previous findings.

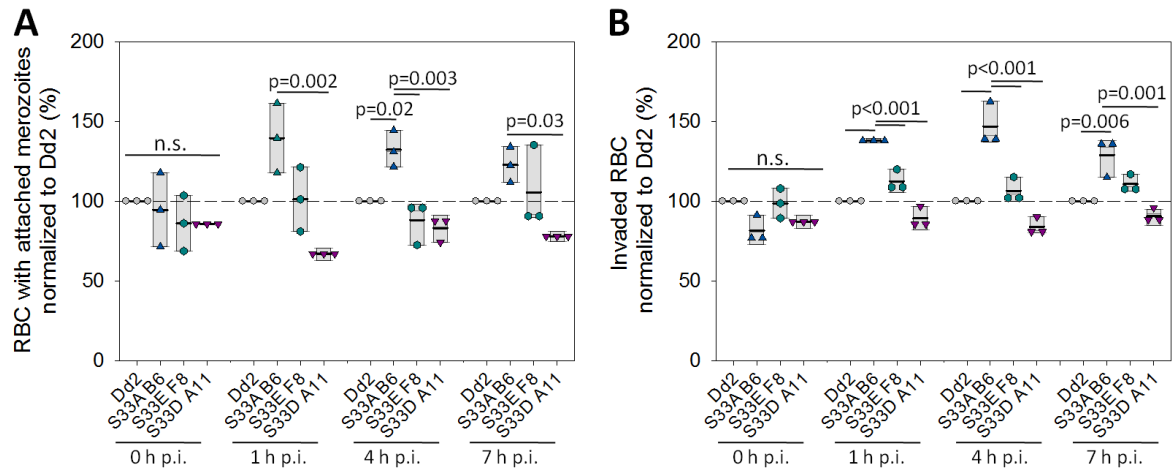


**Figure 3.7. Flow cytometry-based analysis of merozoites attachment and invasion events in Dd2 parental line and PfCRT S33 mutants. A.** Merozoites attachment to the RBC surface measured in the presence of 1  $\mu$ M cytochalasin D. **B.** Merozoites invasion into RBC measured in the absence of cytochalasin D. Results are presented as parasitemia over respective time points: 0, 1, 4 and 7 h post invasion (p.i.), corresponding to parasites age of 41-1 h p.i., 43-3 h p.i., 2-6 h p.i. and 5-9 h p.i., respectively. Data were normalized at each time point to the Dd2 WT. Each symbol represents an independent biological replicate. A box plot analysis of each data set is shown in grey. A thick black line indicates the mean value. Statistical significance between the data sets was calculated using One Way ANOVA Holm-Sidak test; n.s. – not significant.

## 3.2. Functional characterization of PfUT in parasite's asexual life cycle

Ubiquitination is a crucial posttranslational modification regulating numerous cellular processes via labelling of substrate proteins with mono-, multi- and polyubiquitin chains (Suryadinata et al., 2014). A HECT E3 ubiquitin ligase, termed *Plasmodium falciparum* ubiquitin transferase (PfUT), has been suggested as a novel candidate gene for multifactorial resistance to quinine (Sanchez et al., 2014). However, both PfUT's role in the reduced quinine responsiveness and its physiological function in the parasite remain unclear. Therefore, this chapter aims to provide an insight into a better understanding of a biological role of PfUT in the asexual life cycle of *P. falciparum*.

### 3.2.1. Conditional knockdown of PfUT using glmS ribozyme system

Multiple genetic tools are available to study the function of *Plasmodium* genes (Prommana et al., 2013; Ghorbal et al., 2014; Jones et al., 2016; Kirchner et al., 2016; Birnbaum et al., 2017; Balabaskaran-Nina & Desai, 2018). Since ubiquitination is a key regulator of many cellular processes, the components of the ubiquitination pathway, including PfUT, are likely critical for the parasite's survival. Interestingly, an ortholog of PfUT in a murine malaria model *Plasmodium berghei* was annotated as indispensable for parasite asexual blood stages, as determined in the large pool of barcoded gene-deletion mutants (Bushell et al., 2017). Taking the above into account, a knockout attempt of a likely essential gene would have had a lethal effect for haploid blood stage *Plasmodium* parasites. Therefore, in order to link the parasite phenotype to a controlled PfUT abundance, a conditional knockdown approach has been chosen over a conventional knockout strategy.

#### 3.2.1.1. Generation of PfUT-HA-glmS parasite line

To assess the role of PfUT in the asexual life cycle of *P. falciparum*, a conditional gene knockdown using the glucosamine inducible glmS ribozyme system was attempted (Elsworth et al., 2014; Prommana et al., 2013). The CRISPR-Cas9 genome editing technology (Ghorbal et al., 2014) has been applied to incorporate the triple hemagglutinin (HA) tag and the glmS ribozyme within the 3' untranslated region of PfUT (Fig. 3.8.A). PfUT-HA-glmS line has been generated in *P. falciparum* 3D7 quinine-sensitive strain via a double-crossover homologous recombination between the transfection vector pL6-PfUT-HA-glmS-UTR bearing two homology regions and the *pfut* locus. Three clones termed 5G, 6E and 11B were isolated from the parental line via limiting dilution and used for further characterization. Correct integration of 3xHA and glmS ribozyme into the endogenous PfUT locus was confirmed by PCR amplification and Sanger sequencing (Fig. 3.8.B and C). Multiple attempts to obtain a transgenic parasite line in *P. falciparum* Dd2 quinine-resistant strain were unsuccessful.

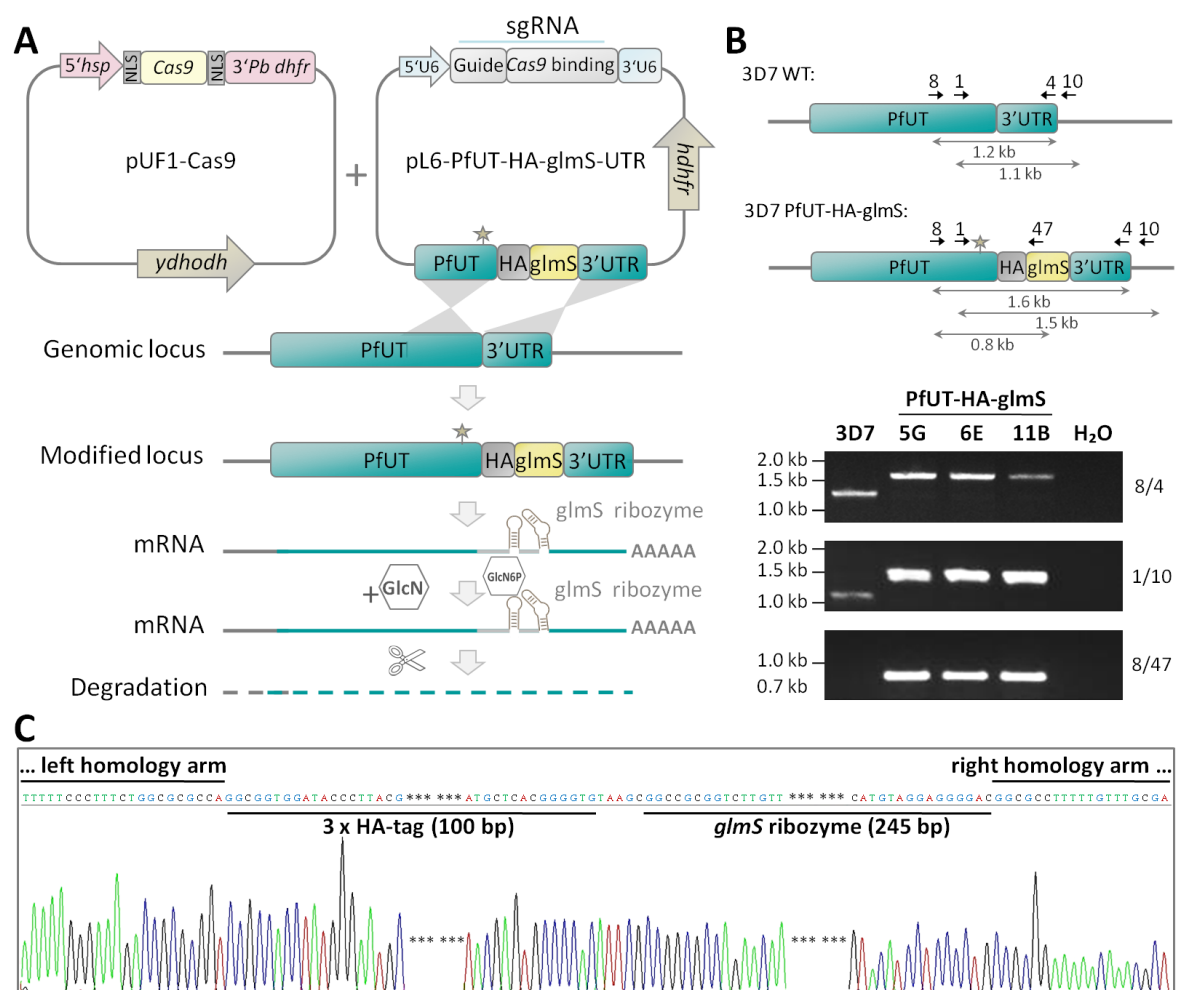


**Figure 3.8. CRISPR-Cas9-mediated integration of HA-glmS into PfUT locus.** **A.** Schematic representation of the CRISPR-Cas9-based strategy used to incorporate sequences of HA and glmS ribozyme at the 3' end of the endogenous PfUT gene. Glucosamine (GlcN) added to the culture medium is taken up by the parasite and converted to the glucosamine-6-phosphate (GlcN6P). Binding of GlcN6P stimulates self-cleavage of glmS ribozyme, leading to mRNA destabilization and downregulation of the target protein. **B.** Results of PCR amplification for wild type and the three PfUT-HA-glmS clones (5G, 6E and 11B). The expected sizes of PCR products (primer pairs: 8/4, 1/10 and 8/47) are indicated. Primers 8 and 10 are located, respectively, upstream and downstream of the homology regions (PfUT and 3' UTR). **C.** Representative DNA sequence chromatogram of one of the PfUT-HA-glmS clones showing a correct integration of triple HA and glmS ribozyme sequences between the two homology regions.

### 3.2.1.2. Determination of optimal glucosamine concentrations

Prior to validation of the glmS ribozyme system in the PfUT-HA-glmS parasites, dose dependent growth curves were performed for the *P. falciparum* 3D7 wild type line in order to determine the optimal conditions of GlcN treatment (Fig. 3.9). Several GlcN concentrations were tested, ranging from 1.25 to 10 mM. The maximal concentration at which parasites still retained normal growth and morphology was 5 mM GlcN. Therefore, it has been chosen for further characterization of the PfUT-HA-glmS mutants.

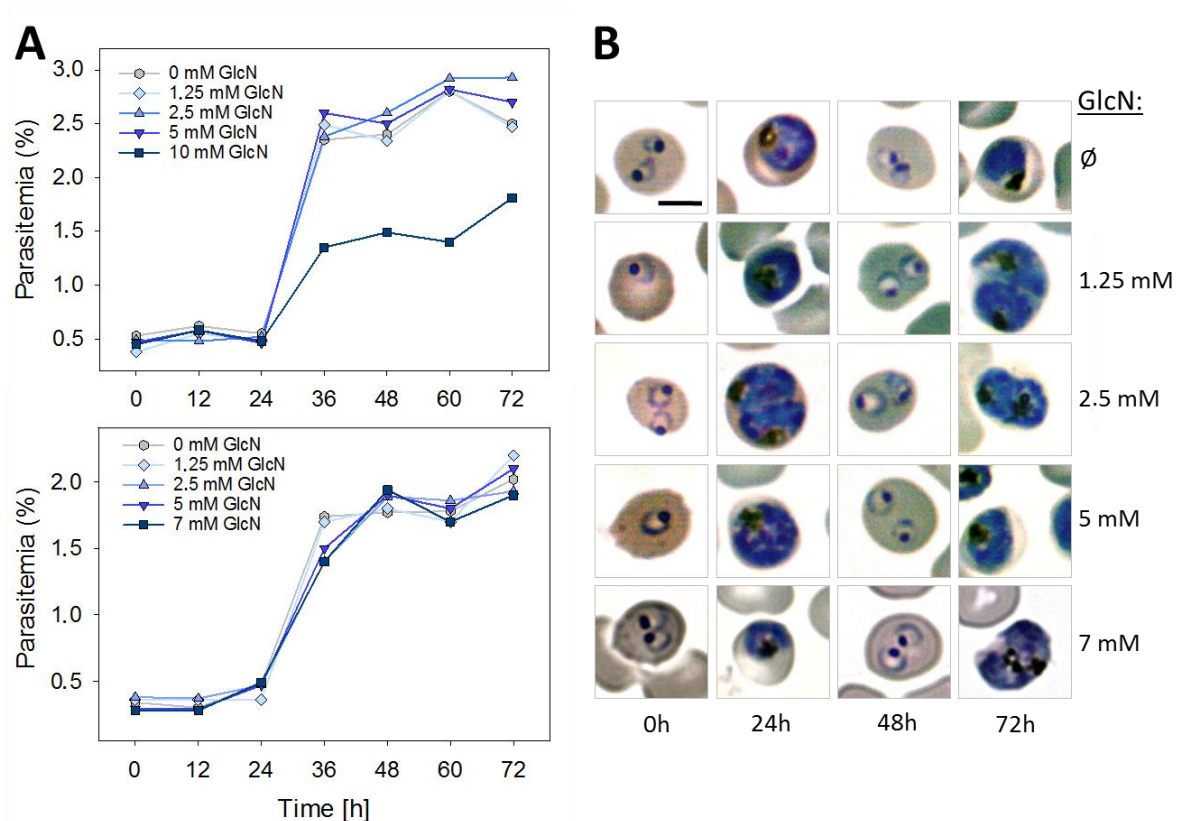


**Figure 3.9. Effect of GlcN treatment on the growth and morphology of *P. falciparum* 3D7 wild type.** **A.** Growth of the 3D7 wild type parasites in the presence of various GlcN concentrations measured over 72h in two independent experiments (top and bottom panel). Parasitemia was estimated from Giemsa-stained thin blood smears. **B.** Morphology of the 3D7 wild type parasites in the Giemsa-stained thin blood smears analyzed at various GlcN concentrations over 72h of treatment. Scale bar: 5  $\mu$ m.

### 3.2.1.3. PfUT is overexpressed in the HA-glmS mutant line

Glucosamine-induced downregulation of PfUT levels was assessed on both transcript and protein levels, as the glmS ribozyme is a RNA-based gene regulatory system, mediating glucosamine dependent reduction of protein expression (Prommana et al., 2013).

First, the *pfut* mRNA levels were analyzed via a reverse transcription quantitative PCR (RT-qPCR) using primer pairs specific to the N-terminal part of PfUT gene and an internal reference gene,  $\beta$ -tubulin. A validation experiment in which a dilution series of cDNA was amplified using primers targeting PfUT and  $\beta$ -tubulin determined their respective efficiencies to 1.95 and 2.01, indicating qPCR amplification efficiencies of 98% and 100%, respectively (Fig. 3.10.A). According to its transcription profile (Bozdech et al., 2003; Llinás et al., 2006), PfUT is relatively equally expressed throughout the intraerythrocytic cycle, with a slight decrease in late schizonts and merozoites. Taking that into account, total RNA was then extracted from the trophozoite stage parasites cultured in the presence or absence of 5 mM glucosamine (GlcN) and subjected to RT-qPCR analysis. The levels of

*pfut* mRNA in untreated PfUT-HA-glmS line were found to be significantly increased by approx. 2-fold in relation to the wild type parasites, with  $p < 0.001$  according to One Way ANOVA Holm-Sidak test (Fig. 3.10.B). Exposure of mutant parasites to 5 mM GlcN resulted in a significant reduction of *pfut* transcripts in relation to untreated PfUT-HA-glmS parasites, with  $p < 0.001$ . Glucosamine treatment did not affect the *pfut* mRNA levels in 3D7 wild type strain.

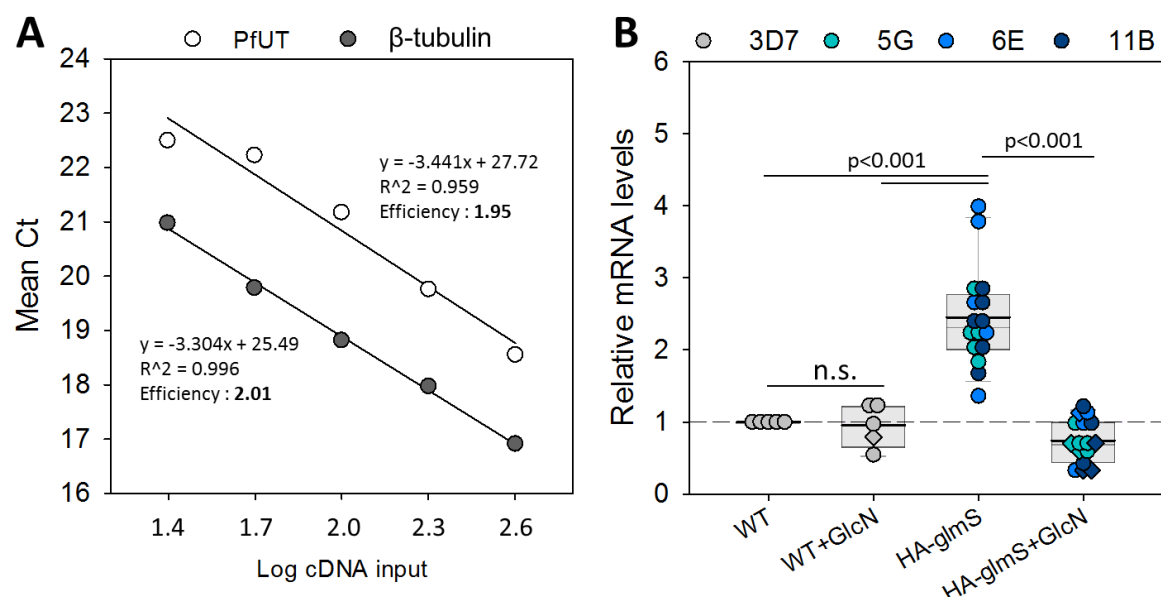


**Figure 3.10. RT-qPCR analysis of the *pfut* transcript levels in 3D7 WT and PfUT-HA-glmS line. A.** Determination of RT-qPCR primer pairs efficiencies. A series of cDNA 2-fold dilutions was amplified using primer pairs specific for the target (PfUT) and the housekeeping gene ( $\beta$ -tubulin). Results were plotted as mean Ct values of triplicates (each dot) against the log of cDNA input and fitted to the linear regression model. Primers efficiencies of 1.95 for PfUT and 2.01 for  $\beta$ -tubulin were quantified from the slope, indicating the qPCR amplification efficiency of 98% and 100%, respectively. **B.** RT-qPCR measurement of *pfut* mRNA levels in trophozoite stage 3D7 WT and PfUT-HA-glmS parasites in the presence and absence of 5 mM glucosamine (GlcN). GlcN treatment for 120 h, corresponding to the 3<sup>rd</sup> replicative cycle, is indicated as circles, whereas the 48 h exposure is marked with rhombus shape. RT-qPCR data were analyzed using the delta-delta Ct method normalized to  $\beta$ -tubulin and relative to untreated 3D7 WT. Results for the three clones of PfUT-HA-glmS line (5G, 6E and 11B) are pooled together and shown as “HA-glmS”, yet depicting values for individual clones with a blue scale colour code. Each symbol represents an independent biological replicate. A box plot analysis of each data set is shown in grey. A thick black line indicates the mean value. Statistical significance between the data sets was calculated using One Way ANOVA Holm-Sidak test; n.s. – not significant.

To determine whether changes observed for PfUT on the transcript level correlate with the protein levels, a western blot analysis was performed. For this purpose, protein extracts of trophozoite stage parasites cultured in the presence or absence of 5 mM glucosamine (GlcN) were immunoblotted with antibodies against HA-tag, as well as C- and N-terminal ends of PfUT. Anti- $\alpha$ -tubulin was used in parallel as a loading control. Western blot analysis displayed bands of approx. 460 kDa and 50 kDa corresponding to the predicted size of PfUT and  $\alpha$ -tubulin, respectively (Fig. 3.11.A). Densitometric



quantification of signal intensity using anti-HA antibody revealed around 40% reduction in PfUT-HA protein abundance in the mutant line exposed to GlcN, with a significance of  $p < 0.001$  as estimated by t-test (Fig. 3.11.B). Interestingly, the PfUT protein levels detected in PfUT-HA-glmS line using antibodies raised against its C-terminal and N-terminal domains were found to be increased by approx. 2-fold in relation to 3D7 WT parasites, with a significance of  $p < 0.001$  in case of N-terminal labelling (Fig. 3.11.C and D). Since the use of C-terminal antibody resulted in unspecific binding (Fig. 3.11.A, middle panel), the immunoblots stained with anti-C-terminal PfUT have been aligned to the ones labelled with anti-HA to verify which of the two bands corresponds to the PfUT (data not shown). As a result, the lower band has been chosen for quantification of signal intensity. Exposure to GlcN led to a significant decrease of PfUT protein levels with  $p$  values of 0.02 and  $p < 0.001$ , as determined by probing with C-terminal and N-terminal PfUT, respectively (Fig. 3.11.C and D). Glucosamine treatment did not influence the PfUT protein levels in 3D7 WT strain.

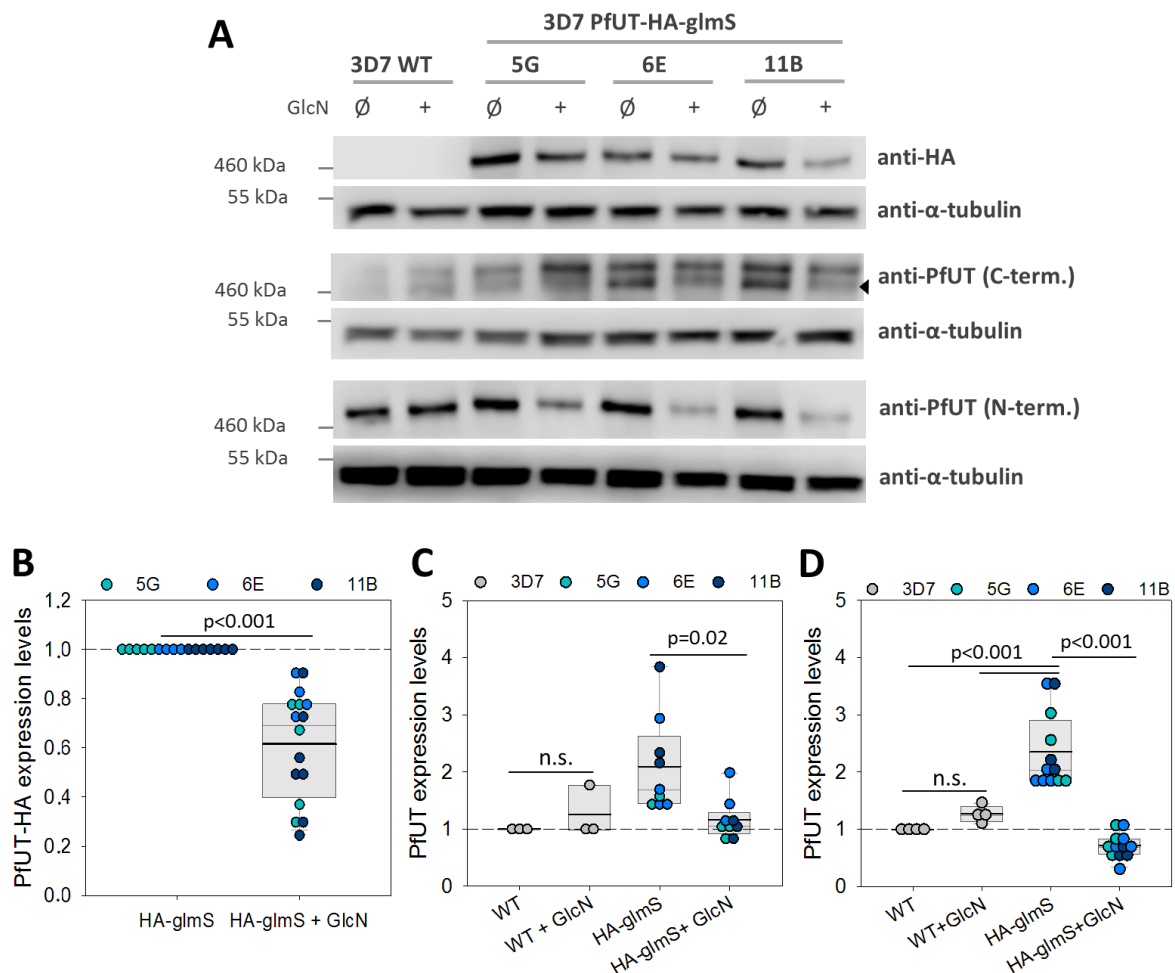


**Figure 3.11. Western blot analysis of PfUT expression levels in 3D7 WT and PfUT-HA-glmS parasites.** **A.** Protein lysates were prepared from late trophozoites cultured for 120 h in the presence or absence of 5 mM GlcN. Proteins were resolved in 3-8% Tris-Acetate SDS-PAGE and immunoblotted with antibodies against HA-tag (mouse, 1:1000; top panel), residues 3654 to 3875 of the C-terminal

domain of PfUT (rabbit, 1:1000; middle panel) and residues 473 to 712 of the N-terminal PfUT (rabbit, 1:1000; bottom panel) along with  $\alpha$ -tubulin (mouse, 1:1000) as a loading control. Representative western blots are shown. An uncropped view of the western blot membranes can be found in Appendix I, Fig. I.3. **B.-D.** The intensities of the bands in the western blots in part A were analyzed using LI-COR Image Studio Digits 4.0 software and normalized to  $\alpha$ -tubulin. Data for the three clones of PfUT-HA-glmS line (5G, 6E and 11B) is pooled together and shown as “HA-glmS”, yet depicting values for individual clones with a blue scale colour code. The downregulation levels of PfUT-HA in mutant line upon GlcN treatment in relation to HA-glmS untreated were quantified using anti-HA (**B**). The PfUT expression levels relative to untreated 3D7 WT (“WT”, grey dots) were determined for immunoblots labelled with C-terminal PfUT (lower band indicated with a black arrowhead) (**C**) and N-terminal PfUT (**D**). Exposure of parasites to 5 mM GlcN for 48 h revealed results comparable to 120 h treatment (data not shown). Each symbol represents an independent biological replicate. A box plot analysis of each data set is shown in grey. A thick black line indicates the mean value. Statistical significance between the data sets was calculated using t-test (**B**) or One Way ANOVA Holm-Sidak test (**C** and **D**); n.s. – not significant.

### 3.2.1.4. PfUT-HA localizes to the ER/Golgi complex

PfUT has previously been shown to localize to the parasite’s ER/Golgi complex in wild type parasites (Sanchez et al., 2014). To verify whether the localization of PfUT in the mutant line was affected by a C-terminal integration of HA-glmS, immunofluorescence assays (IFA) were performed. To assure the specificity of the commercially available anti-HA antibody, which was intended to be tested in colocalization with respective ER/Golgi markers, it was first colocalized with N- and C-terminal PfUT antibodies used in the above mentioned study of Sanchez et al. As shown in Figure 3.12, staining of HA was absent in the 3D7 WT, but it overlapped with a signal for both, N- and C-terminal PfUT in the HA-glmS transgenic line, thus proving the specificity of the tested antibodies.

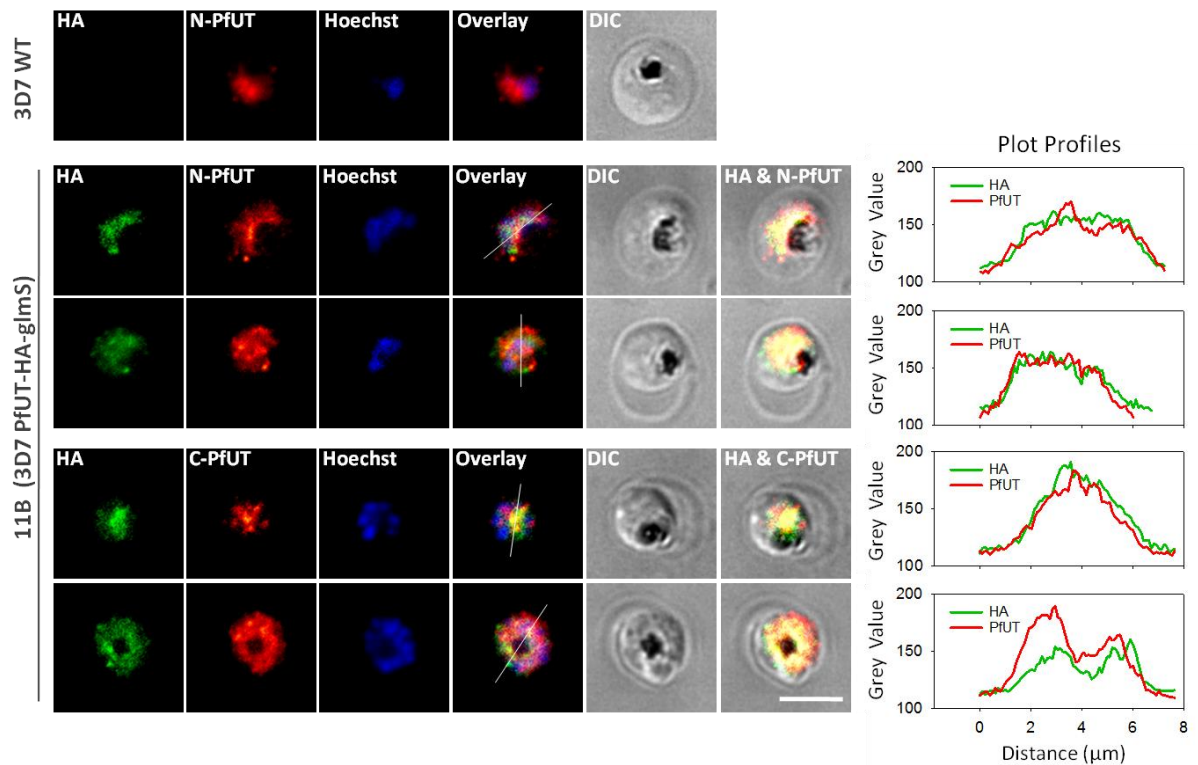


**Figure 3.12. Colocalization of HA and PfUT primary antibodies by indirect immunofluorescence assay (IFA).** Late stage *P. falciparum*-infected erythrocytes were fixed and labelled with anti-HA (mouse, 1:1000) along with N-terminal PfUT (rabbit, 1:1000) or C-terminal PfUT (rabbit, 1:1000). Secondary antibody staining was carried out using anti-mouse Alexa Fluor 488 (green) and anti-rabbit Alexa Fluor 546 (red). The nuclei were visualized with Hoechst (blue). Overlay of the green, red and blue channels, as well as the differential interference contrast (DIC) are shown. Additional merge of green and red channels together with DIC and plot profiles are included for a better presentation of signals colocalization. 3D7 WT (top panel) lacking a HA-tag served as a control for specificity of anti-HA staining in PfUT-HA-glmS line. Scale bar: 5 μm.

Subsequently, localization of PfUT-HA in the mutant line was analyzed via IFA by a colocalization with ER markers, BiP and ERC, as well as with a Golgi marker, ERD2. The results of the colocalization studies confirmed the previously demonstrated partial colocalization of PfUT with indicated ER/Golgi markers (Fig. 3.13).

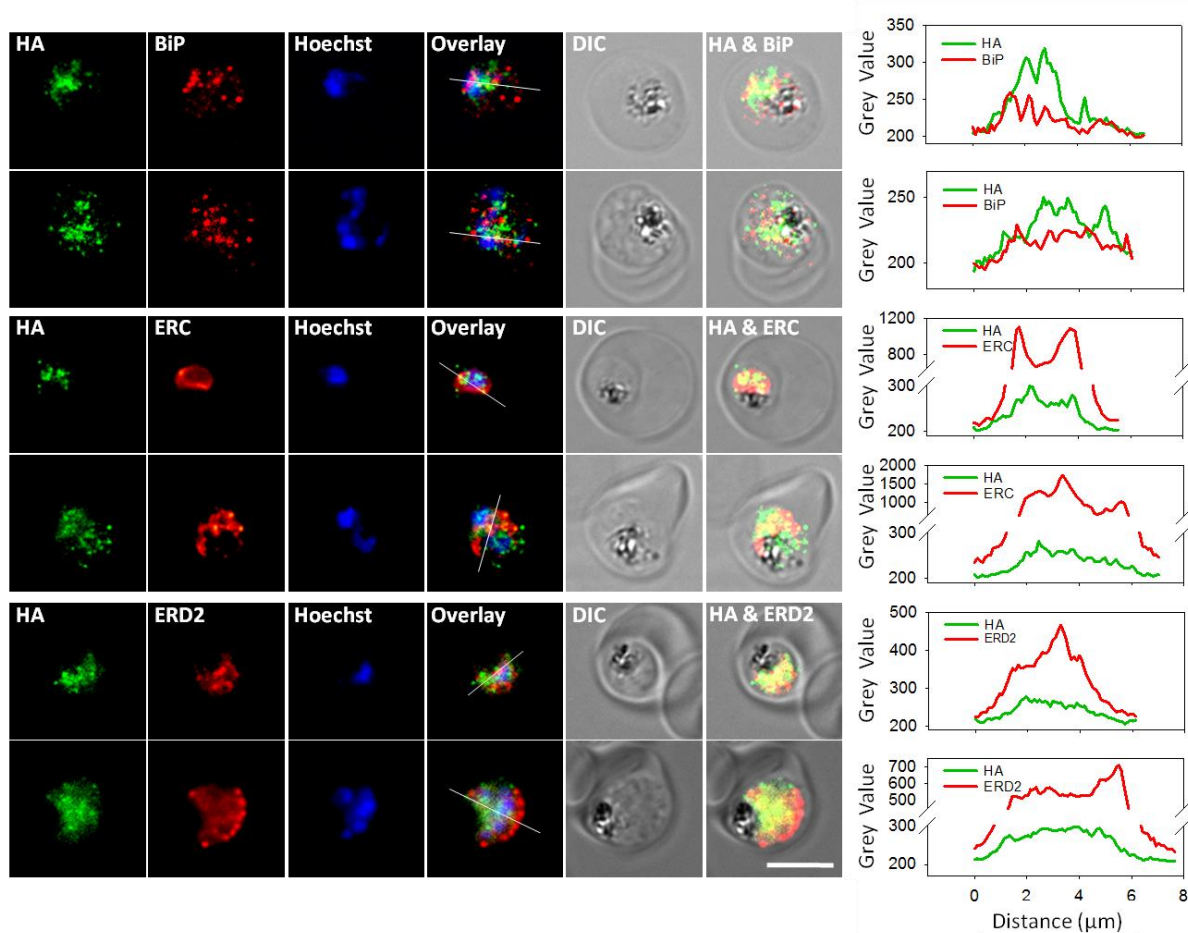


**Figure 3.13. Colocalization of PfUT-HA with ER and Golgi markers by indirect immunofluorescence assay (IFA).** Late stage *P. falciparum*-infected erythrocytes were fixed and labelled with anti-HA (mouse, 1:1000) along with one of the ER markers, BiP (rabbit, 1:1000) or ERC (rabbit, 1:500), or with a Golgi marker ERD2 (rabbit, 1:500). Secondary antibody staining was carried out using anti-mouse Alexa Fluor 488 (green) and anti-rabbit Alexa Fluor 546 (red). The nuclei were visualized with Hoechst (blue). Overlay of the green, red and blue channels, as well as the differential interference contrast (DIC) are shown. Additional merge of green and red channels together with DIC and plot profiles are included for a better presentation of signals colocalization. Scale bar: 5  $\mu$ m.

The sub-cellular localization of PfUT-HA was further attempted by immuno-electron microscopy. Cryo-preserved Tokuyasu sections of erythrocytes infected with late trophozoite stage PfUT-HA-glms parasites were consecutively labelled with anti-HA and gold conjugated secondary antibody and examined via transmission electron microscopy (TEM). No abnormalities in the morphology of the parasites were observed in the HA-glms line with a reference to the published TEM images of wild type *P. falciparum* parasites (Muregi et al., 2011; Sanchez et al., 2014; Sherling et al., 2017). Although a minor unspecific labelling was detectable in some areas of the cell, the vast majority of the gold particles accumulated in the region of the ER/Golgi complex, membranous compartments adjacent to nuclei (Fig. 3.14.A). The gold labelling was quantified by estimating the distribution of gold particles across the area of their subcellular localization in several recorded micrographs. This analysis exposed the specificity of gold counts in ER/Golgi complex over the other subcellular

compartments (Fig. 3.14.B), with a significance of  $p < 0.001$  assessed by One Way ANOVA Holm-Sidak test.

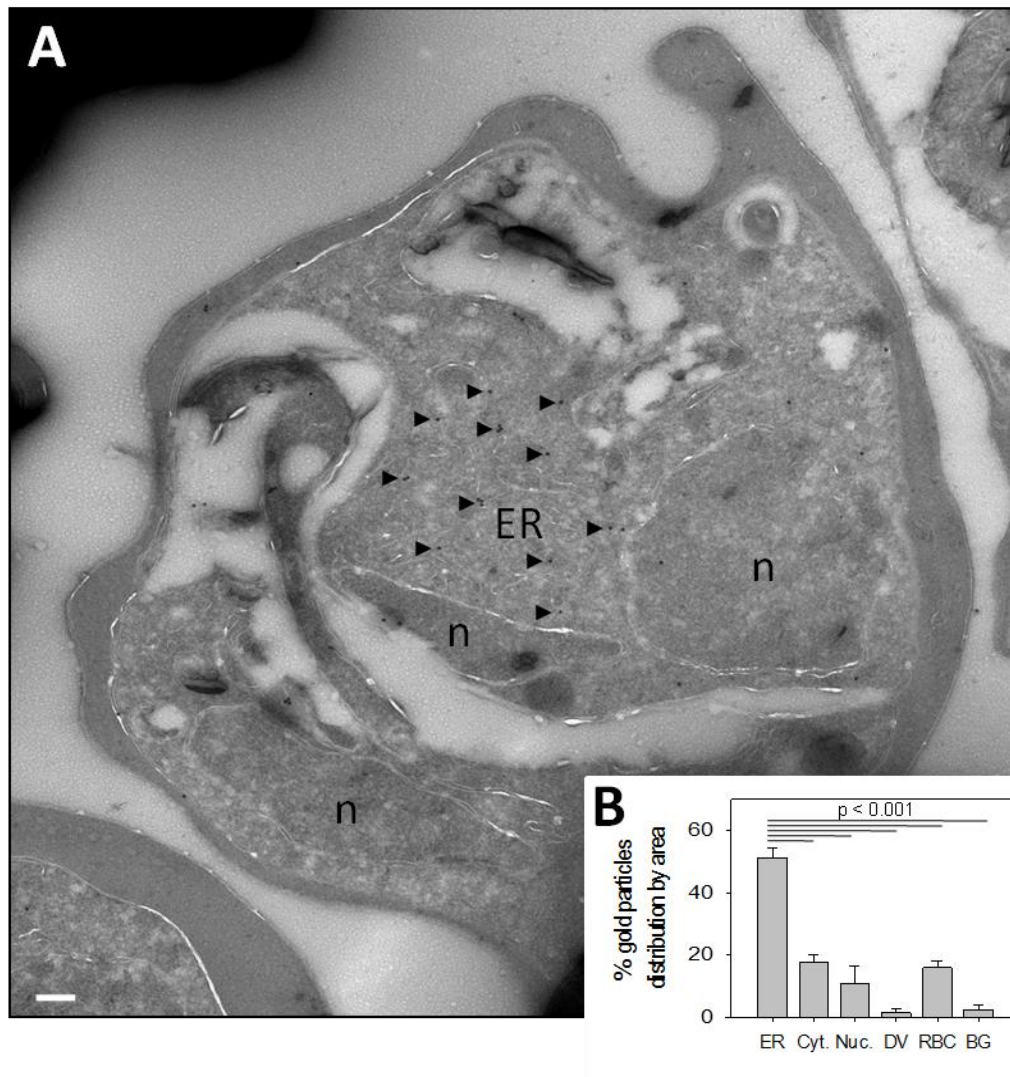


**Figure 3.14. Immunogold subcellular localization of PfUT-HA by transmission electron microscopy (TEM).** **A.** A representative electron micrograph depicting the localization of PfUT-HA in the parasite's ER/Golgi complex (ER) as indicated by accumulation of the vast majority of gold particles (black arrowheads). Infected erythrocytes samples prepared according to the Tokuyasu approach were labelled with anti-HA (mouse, 1:1), followed by staining with anti-mouse antibody coupled to 10 nm colloidal gold (goat, 1:20). n - nucleus. Scale bar: 200 nm. **B.** Quantification of EM immunogold labelling. The distribution of gold in particular regions of the infected erythrocyte to the total analyzed area was determined in 5 micrographs. Gold particles were significantly more present in areas of ER/Golgi complex (ER) than in other subcellular compartments, including the parasite's cytoplasm (Cyt.), nucleus (Nuc.), digestive vacuole (DV), red blood cell cytosol (RBC) and non cellular background (BG). Data is shown as the mean  $\pm$  SEM. Statistical significance between the data sets was calculated using One Way ANOVA Holm-Sidak test.

These results confirm the localization of PfUT-HA indicated earlier via IFA (Fig. 3.14.A) and are consistent with previously reported immuno-electron microscopic localization of PfUT in the wild type parasites (Sanchez et al., 2014).

### 3.2.1.5. PfUT-HA-glmS line displays a reduced growth phenotype

Growth curves analysis was performed to assess whether integration of HA-glmS, resulting in PfUT overexpression, impacted the parasite proliferation. Parasite growth expressed as an increase in parasitemia was measured for 3D7 WT and PfUT-HA-glmS line in the presence and absence of 5 mM GlcN over 168 h, corresponding to 4 replicative cycles (Fig. 3.15.A). Interestingly, growth of the HA-glmS transgenic line, compared to 3D7 WT was significantly reduced in the absence of GlcN, with  $p < 0.001$  according to F-test statistics. The impaired growth of PfUT-HA-glmS parasites was partially rescued upon GlcN treatment, with a significance of  $p = 0.02$ , in relation to untreated mutants. The presence of GlcN had no effect on the growth of the 3D7 WT. Despite the differences observed in the growth of 3D7 WT and PfUT-HA-glmS line, the parasites appeared morphologically normal throughout the whole experiment (data not shown).

To further verify these findings, the parasite multiplication rates (PMR) per 48 h were determined for each clone throughout the 168 h of experimental duration (Fig. 3.15.B). PMRs were expressed as a fold increase in parasitemia measured over time. The multiplication rate for 3D7 WT was estimated to be  $8 \pm 1$  regardless the GlcN presence, consistent with previous reports (Murray et al., 2017). GlcN untreated PfUT-HA-glmS clones 5G, 6E and 11B displayed a significantly lower PMR ( $p < 0.001$ ), with values of  $5 \pm 1$ ,  $6 \pm 1$  and  $5 \pm 1$ , respectively. Exposure of the HA-glmS transgenic line to GlcN resulted in an increase in PMR of clones 5G, 6E and 11B, with values of  $8 \pm 1$ ,  $8 \pm 1$  and  $8 \pm 1$ , respectively, with significance of  $p = 0.02$ ,  $p = 0.01$  and  $p = 0.02$ , in relation to respective untreated clones. These results support the findings from the growth curve analysis.

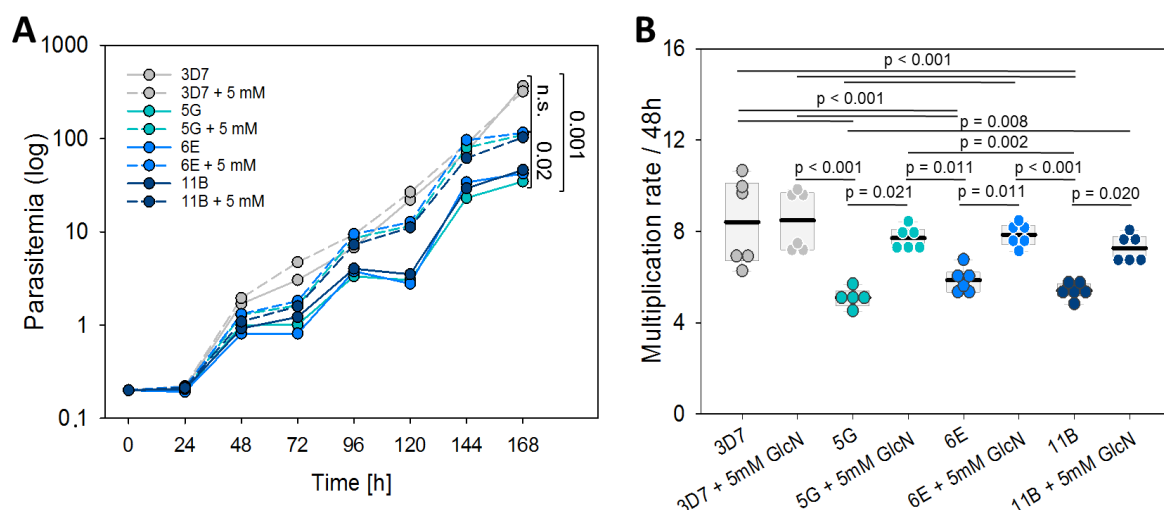


**Figure 3.15. Growth and multiplication rates of *P. falciparum* 3D7 WT and PfUT-HA-glmS mutant lines. A.** Growth of the 3D7 WT and PfUT-HA-glmS parasites (represented by three individual clones: 5G, 6E and 11B) measured over 168h in the presence and absence of 5mM GlcN. Each symbol depicts a mean of three independent biological replicates. Statistical significance between the growth curves was assessed with F-test. **B.** Parasite multiplication rate (PMR) for each clone was determined as a



fold increase in parasitemia per 48h, measured over 4 cycles. Each symbol represents an independent biological replicate. A box plot analysis of each data set is shown in grey. A thick black line indicates the mean value. Statistical significance between the data sets was calculated using One Way ANOVA Holm-Sidak test.

### 3.2.1.6. The impaired growth of the PfUT-HA-glmS line results from an extended cell cycle duration

Several features of parasite intraerythrocytic development were taken into consideration to address the impaired growth and reduced PMR of PfUT-HA-glmS clones in the absence of GlcN. First, numbers of merozoites generated per schizont were determined, as a decreased merozoite number may lead to reduced invasion and consequently a decrease in parasitemia. Since the nuclear division in *P. falciparum* occurs asynchronously, the number of merozoites produced per schizont ranges between 8 and 24 (Reilly et al., 2007; Garg et al., 2015). No differences in the number of merozoites have been observed between the 3D7 WT and the PfUT-HA-glmS clones, with the average number of 19 merozoites, irrespective of GlcN presence (Fig. 3.16.A).

The impaired growth phenotype may also arise from the differences in multiple infections of erythrocytes. Multiply-infected erythrocyte refers to a red blood cell containing more than one parasite. Invasion of a single erythrocyte by up to seven merozoites is commonly observed in patient samples. However, only up to three parasites are capable of maturation until the schizont stage (Orjih, 2014). A triple infection of a single erythrocyte compared with three separate singly-infected red blood cells gives the impression of reduced overall parasitemia, although the number of parasites in both events is equal. Therefore, to assess whether multiply-infected erythrocytes were preferable to single infections, being a cause of the reduced growth, the proportions of single, double and triple infections were quantified for the 3D7 WT and the PfUT-HA-glmS parasites. The singly parasitized red blood cells were the majority among all the types of infections, however, no differences have been observed in quantities of singly-, doubly, and triply-infected erythrocytes between the 3D7 WT and the PfUT-HA-glmS line (Fig. 3.16.B).

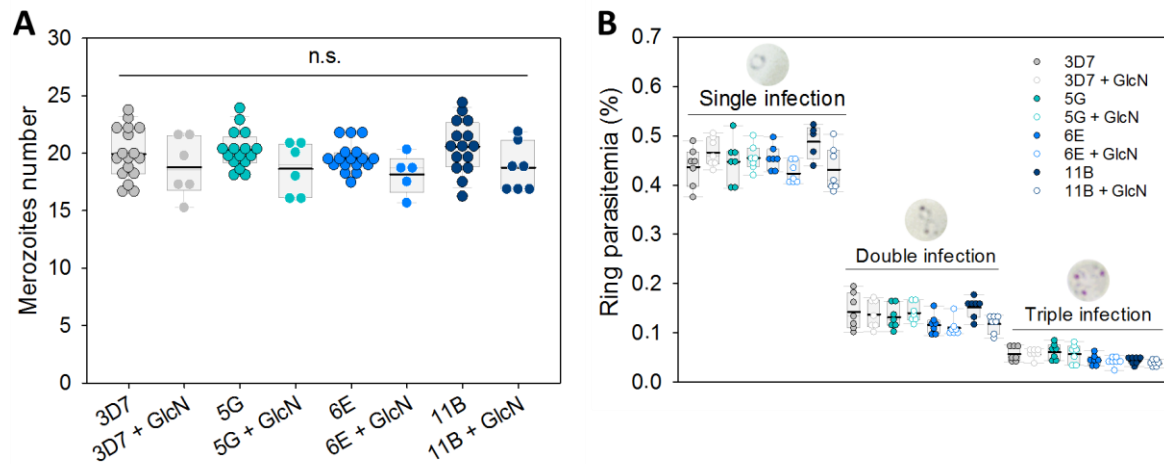


**Figure 3.16. Analysis of merozoites numbers and multiply-infected erythrocytes in 3D7 WT and PfUT-HA-glmS parasites.** **A.** Number of merozoites generated per schizont determined using flow cytometry in the presence and absence of 5mM GlcN. **B.** Singly-, doubly- and triply-infected red blood cells expressed as percentage of ring-stage parasitemia measured by flow cytometry. Each symbol represents an independent biological replicate. A box plot analysis of each data set is shown in grey. A thick black line indicates the mean value. Statistical significance between the data sets was calculated using One Way ANOVA Holm-Sidak test; n.s. – not significant.

Another possible factor that could have influenced the growth of the HA-glmS transgenic parasites is the length of intraerythrocytic cycle. To investigate whether there were differences in the duration of cell cycle of 3D7 WT and PfUT-HA-glmS line, the DNA content in these parasites was measured over time post invasion. For this purpose, samples of parasites synchronized to a 4 h window were collected in 4 h intervals. The DNA content was expressed as a DNA copy number (C-value). The wild type parasites C-value starts to increase around 28-32 h post invasion, with the beginning of parasite DNA replication in the S phase (Fig. 3.17.A). The length of 3D7 WT was estimated to be 48 h, identified by a sudden drop in C-value, in agreement with the previous studies (Bozdech et al., 2003; Van Biljon et al., 2018). The asexual life cycle of the PfUT-HA-glmS line, however, was extended for approximately 8 h in the absence of GlcN, due to an apparent elongation of S phase (Fig. 3.17.A). Exposure to GlcN in the 1<sup>st</sup> replication cycle had no influence on the cell cycle time of either 3D7 WT or PfUT-HA-glmS line, resulting still in 48 h and 56 h cycle, respectively (Fig. 3.17.B). Interestingly, parasites treatment with GlcN prolonged up to the 3<sup>rd</sup> cycle resulted in a 4 h shorter cycle length for mutants, comparative to the 1<sup>st</sup> cycle (Fig. 3.17.C and D). The duration of the 3D7 WT cycle was unaffected by 144 h GlcN exposure. The peak of C-value corresponds to the number of merozoites at the schizont stage parasites, reflecting the data depicted in Figure 3.16.A. There was no difference in the numbers of merozoites measured for 3D7 WT and PfUT-HA-glmS parasites, irrespective of the time of GlcN exposure (Fig. 3.17.A-C).



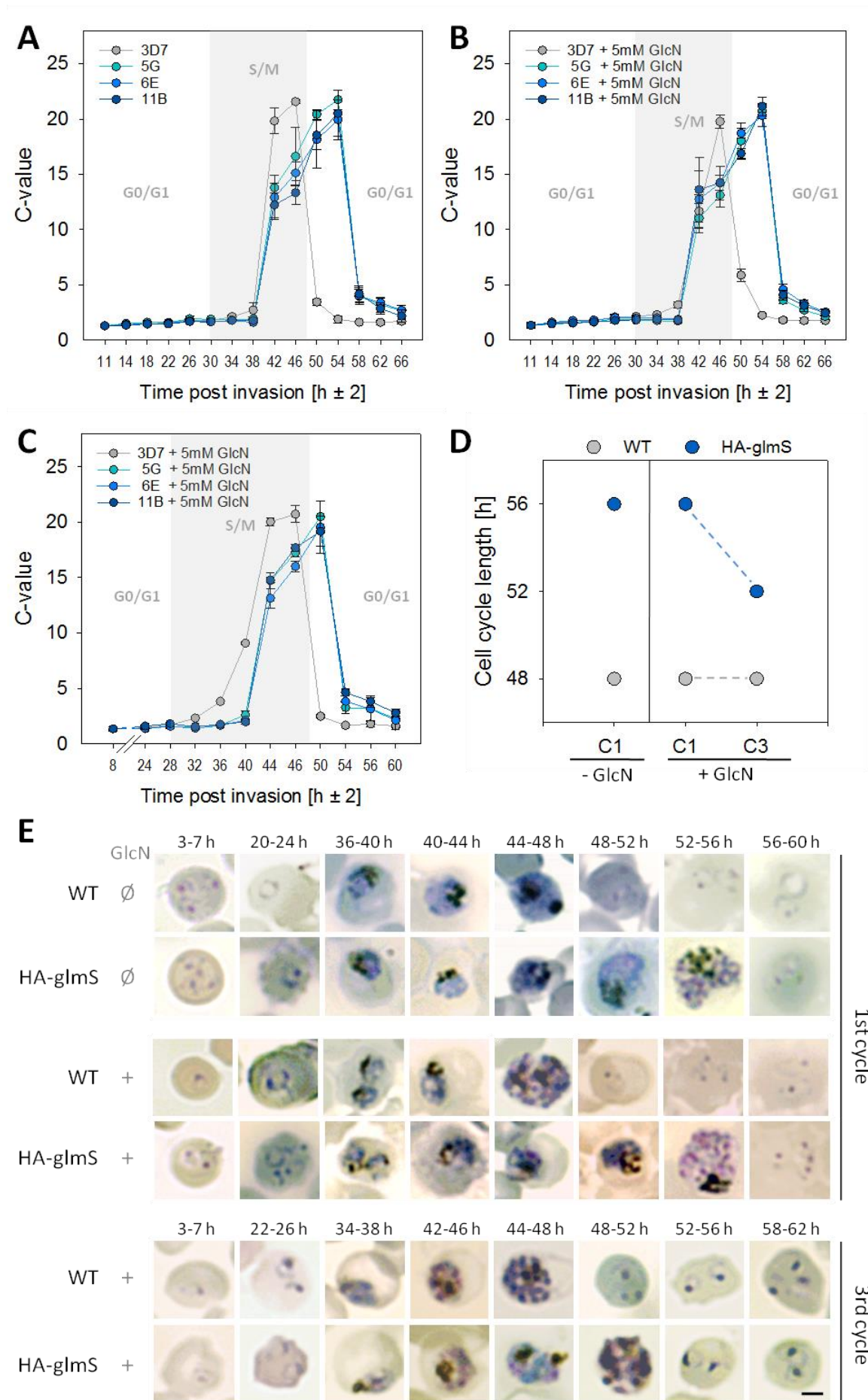


**Figure 3.17. Analysis of cell cycle length and morphology of 3D7 WT and PfUT-HA-glmS parasites.** The cell cycle length expressed as an increase in the parasite DNA copy number (C-value) over time was measured for tightly synchronized parasites (4 h window) in the absence of GlcN (**A**), as well as in the presence of 5 mM GlcN in the 1<sup>st</sup> (**B**) and 3<sup>rd</sup> (**C**) replicative cycle. The drop in the C-value after reaching the peak indicates the beginning of a new cycle. For each clone at each time point a mean  $\pm$  SEM of three independent biological replicates is shown. G0/G1 and S/M phases of the 48 h intra-erythrocytic cell cycle of 3D7 WT are also indicated, to better display the differences observed in the mutant line. **D.** Graph summarizing panels A, B and C, presented as a final cell cycle length of 3D7 WT and PfUT-HA-glmS parasites measured in the 1<sup>st</sup> (C1) and 3<sup>rd</sup> cycle (C3) in the presence or absence of GlcN. **E.** Morphology of the parasites in the Giemsa-stained thin blood smears analyzed in the absence of GlcN ("Ø", top 2 panels), as well as in presence of 5 mM GlcN in the 1<sup>st</sup> ("+", middle 2 panels) and 3<sup>rd</sup> cycle ("+", bottom 2 panels), depicted for selected time points. Scale bar: 2  $\mu$ m.

Giemsa-stained thin blood smears revealed morphologically normal appearance of transgenic and wild type parasites at all analyzed time points, regardless of GlcN presence, simultaneously exhibiting the elongated S phase of PfUT-HA-glmS parasites (Fig. 3.17.E).

### 3.2.1.7. Analysis of the ubiquitination patterns

In order to understand the mechanism underpinning the phenotype of PfUT-HA-glmS parasites described in previous sections, the identification of PfUT's biological substrates is crucial. To address this issue, the ubiquitination patterns of the 3D7 WT have been compared with those of the mutant line via a western blot analysis, both in presence and absence of 5 mM GlcN. Ubiquitinated proteins were detected by immunoblotting with a polyclonal anti-ubiquitin antibody. As shown in Figure 3.18, no obvious differences in the ubiquitination patterns were found between 3D7 WT and the three PfUT-HA-glmS clones, 5G, 6E and 11B, irrespective of GlcN presence.

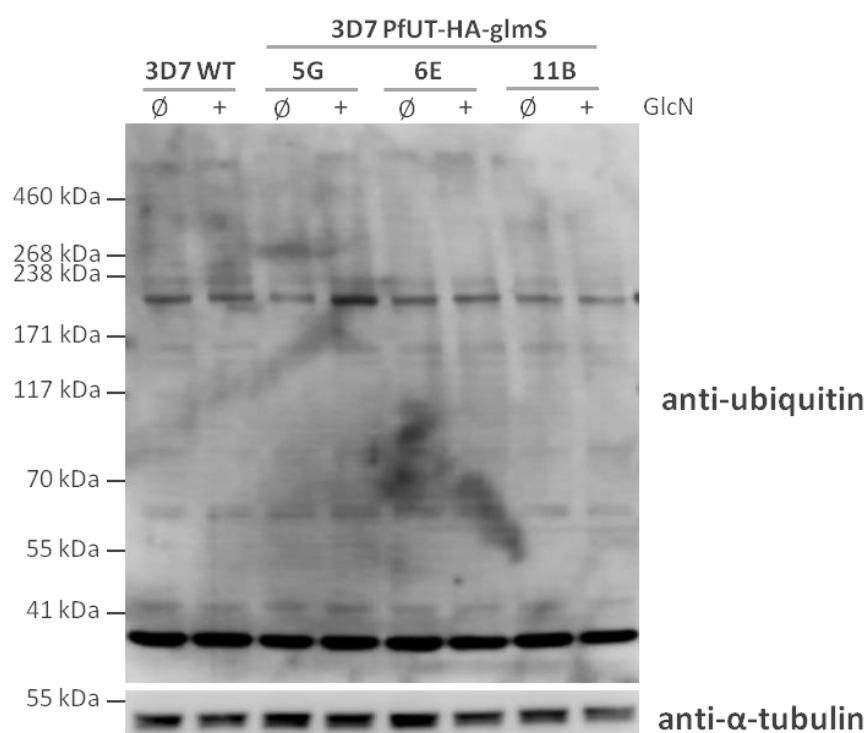


**Figure 3.18. Western blot analysis of ubiquitination patterns in 3D7 wild type and PfUT-HA-glmS parasites.** Protein lysates were prepared from late trophozoite stage parasites pre-cultured for 120 h under standard conditions in the presence or absence of 5 mM GlcN. Proteins were resolved via 3-8% Tris-Acetate SDS-PAGE followed by immunoblotting with polyclonal anti-ubiquitin antibody (rabbit, 1:1000).  $\alpha$ -tubulin (50 kDa) was used as a loading control.

### 3.2.1.8. Investigating PfCRT as a substrate of PfUT

A genetic linkage analysis conducted on the progeny of a genetic cross between a resistant Dd2 and a sensitive HB3 strain revealed an association between PfUT and a resistant PfCRT variant in altering the parasite responses to quinine (Sanchez et al., 2014). Moreover, it has been shown that PfCRT traffics to the digestive vacuolar membrane via ER/Golgi complex (Kuhn et al., 2010), prompting to hypothesize that PfCRT might be a substrate of PfUT. Therefore, a potential role of PfCRT as PfUT's target has been investigated via a western blot analysis. In a number of studies, the molecular weight of PfCRT has ranged from 38 to 50 kDa, depending on the PfCRT variant and SDS-PAGE conditions (Cooper et al., 2002; Johnson et al., 2008; Valderramos et al., 2010; Shahinas et al., 2013; Sanchez et al., 2014). Most likely due to the specific SDS-PAGE conditions (Tris-Acetate, 3-8% gradient gel) applied in this experiment, the size of the detected PfCRT corresponded to ~38 kDa (Fig. 3.19.A). Densitometry of western blot bands revealed that, regardless of GlcN presence, the levels of PfCRT abundance in the 3D7 WT were not significantly different from those in the HA-glmS transgenic line carrying the overexpressed PfUT variant (Fig 3.19.B).

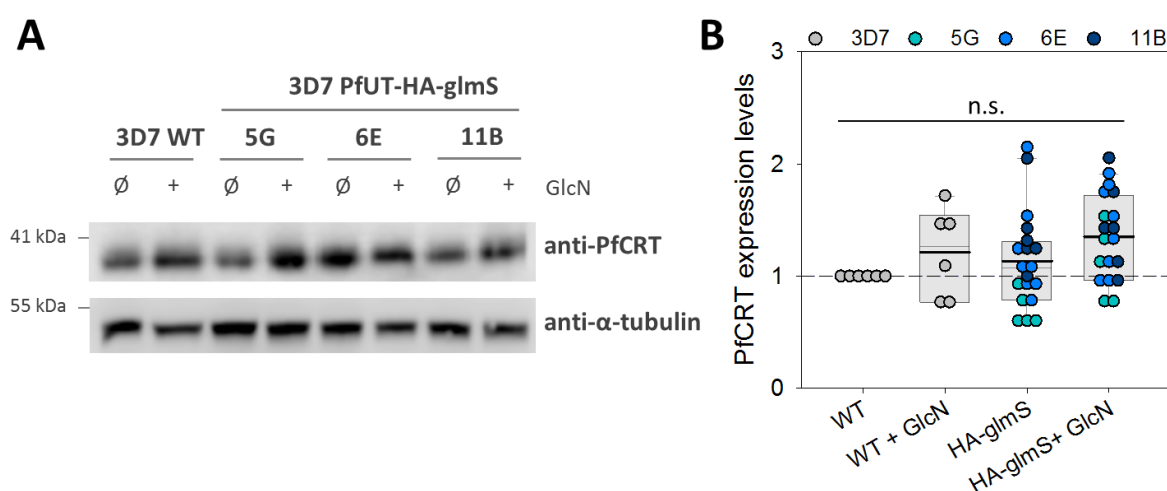


**Figure 3.19. Western blot analysis of PfCRT expression levels in 3D7 wild type and PfUT-HA-glmS parasites.** **A.** Protein lysates prepared from late trophozoites pre-cultured for 120 h in the presence or absence of 5 mM GlcN were resolved in 3-8% SDS-PAGE followed by immunoblotting with antibody raised against peptide MKFASKNNQKNSSK of the N-terminal PfCRT (guinea pig, 1:1000).  $\alpha$ -tubulin with an expected size of 50 kDa served as a loading control. **B.** The intensities of the bands in the western blots were analyzed using LI-COR Image Studio Digits 4.0 software. Data was normalized

to  $\alpha$ -tubulin. Results for the three clones of PfUT-HA-glmS line (5G, 6E and 11B) are pooled together and shown as “HA-glmS”, yet depicting values for individual clones with a blue scale colour code. The PfCRT expression levels were quantified in relation to the untreated 3D7 WT (“WT”, grey dots). Each symbol represents an independent biological replicate. A box plot analysis of each data set is shown in grey. A thick black line indicates the mean value. Statistical significance between the data sets was calculated using One Way ANOVA Holm-Sidak test; n.s. – not significant.

### 3.2.1.9. PfUT-HA-glmS parasites are more susceptible to quinine and quinidine

PfUT has been identified as a novel candidate gene that might contribute to multi-factorial resistance to quinine (Sanchez et al., 2014). To validate the association of PfUT with altered quinine responsiveness, growth inhibition assays were conducted for 3D7 WT and PfUT-HA-glmS line carrying the overexpressed PfUT variant. The half-maximal (50%) inhibitory concentrations ( $IC_{50}$ ) were determined for a comparison of drug resistance phenotypes for respective parasite lines. Drug responsiveness was measured for quinine, along with two other quinoline drugs, quinidine and chloroquine. Although quinidine is not an effective antimalarial drug, as a stereoisomer of quinine, it should, supposedly, show similar trend in results. Chloroquine was used as a control drug, since the main determinant of chloroquine resistance is a mutated PfCRT variant, whereas the 3D7 WT parasites are carrying the sensitive alleles (Valderramos et al., 2010). Therefore, parasites of the 3D7 genetic background tested in this growth inhibition assay should display a comparable responsiveness to chloroquine.

Genomic integration of the HA-glmS sequence to the PfUT locus resulted in a significantly increased ( $p < 0.001$ ) susceptibility of HA-glmS transgenic line to quinine in the absence of GlcN, with  $IC_{50}$  values of  $74 \pm 4$  nM,  $61 \pm 2$  nM and  $64 \pm 3$  nM, for the three PfUT-HA-glmS clones, 5G, 6E and 11B, respectively, in comparison to  $94 \pm 4$  nM determined for 3D7 WT (Fig. 3.20.A). Similarly, a significant reduction ( $p < 0.001$ ) in resistance to quinidine has been observed for clones 5G, 6E and 11B with  $IC_{50}$  values of  $25 \pm 2$  nM,  $19 \pm 1$  nM and  $22 \pm 1$  nM, respectively, in relation to 3D7 WT with a  $IC_{50}$  of  $36 \pm 2$  nM. However, the chloroquine sensitivity profile of PfUT-HA-glmS clones was not significantly different from 3D7 WT, with an average  $IC_{50}$  value of  $11 \pm 1$  nM. Treatment with 5 mM GlcN further reduced the response levels of HA-glmS mutants to quinine. HA-glmS clones, 5G, 6E and 11B, displayed significantly lower ( $p < 0.001$ ) quinine  $IC_{50}$  values of  $34 \pm 4$  nM,  $35 \pm 3$  nM and  $42 \pm 1$  nM, respectively, than 3D7 WT with  $68 \pm 6$  nM (Fig. 3.20.B). Regarding quinidine response levels, clones 5G, 6E and 11B were significantly ( $p < 0.001$ ) more sensitive to quinidine exposure, with  $IC_{50}$  values of  $15 \pm 1$  nM,  $14 \pm 1$  nM and  $17 \pm 1$  nM, respectively, in comparison to 3D7 WT with  $IC_{50}$  value of  $26 \pm 2$

nM. The chloroquine  $IC_{50}$  values with an average of  $10 \pm 1$  nM, again, revealed no significant difference between 3D7 WT and PfUT-HA-glmS clones.

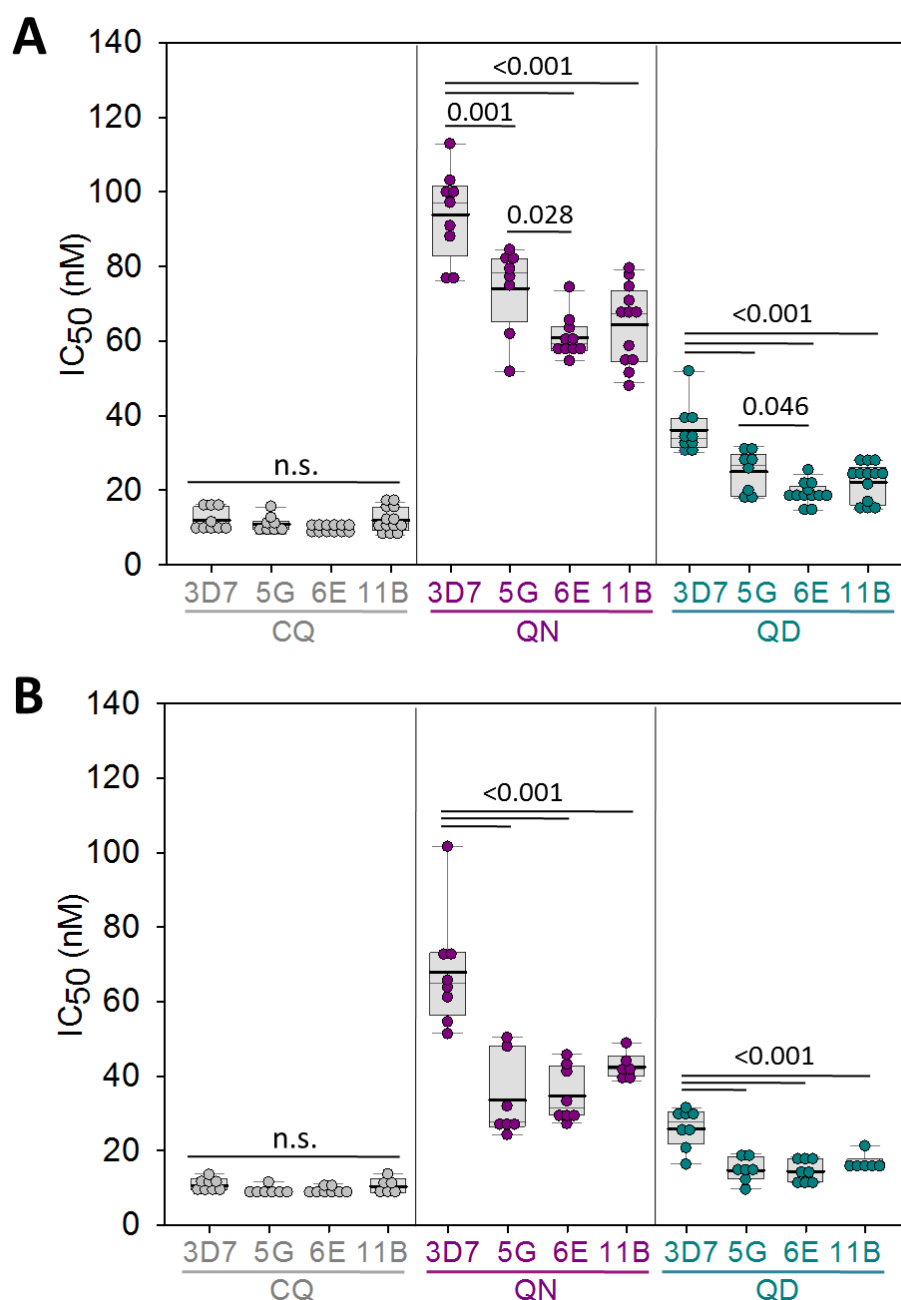


**Figure 3.20. Growth inhibition assays of 3D7 wild type and PfUT-HA-glmS parasites in the absence (A) and presence (B) of 5 mM GlcN.** Half-maximal inhibitory concentrations ( $IC_{50}$ ) were determined for chloroquine (CQ, control drug), quinine (QN) and quinidine (QD, stereoisomer of QN). Each symbol represents an independent biological replicate. A box plot analysis of each data set is shown in grey. A thick black line indicates the mean value. Statistical significance between the data sets consisting of at least 6 independent measurements was calculated using One Way ANOVA Holm-Sidak test; n.s. – not significant.

The outcome of the growth inhibition assay performed in the presence of 5 mM GlcN (Fig. 3.20.B) must be taken with caution, since GlcN could have a slightly toxic effect at the indicated concentration in this experiment. The set-up of an assay in a 96-well plate containing parasite culture and serial drug dilutions incubated for 72 h in 37°C may lead to medium evaporation, which would, in turn, increase the final GlcN concentration in each well to levels harmful for the parasite (as previously shown in Figure 3.9.A). The growth response curves conducted for GlcN in the *P. falciparum* 3D7 strain revealed an  $IC_{50}$  value of  $9.1 \pm 0.4$  mM (data not shown). 5 mM GlcN was the highest concentration at which parasites displayed unaffected growth. It suggests that an increase in local GlcN concentration above 5 mM due to medium evaporation during the course of experiment might have negative effects on the parasite. For that reason, the drug responsiveness of the WT and HA-glmS transgenic parasites was also measured in the presence of 2.5 mM GlcN (Appendix I, Fig. I.4). The data showed a similar trend to the results obtained for untreated parasites depicted in Figure 3.20.A. However, due to the limited number of repetitions ( $n=3-4$ ), the differences between the WT and HA-glmS line were not significant. Quinine  $IC_{50}$  values were estimated to be  $60 \pm 10$  nM,  $48 \pm 12$  nM and  $60 \pm 8$  nM for clones 5G, 6E and 11B, respectively, and  $82 \pm 11$  nM for 3D7 WT. The responsiveness of the parasites to quinidine was represented by  $IC_{50}$  values of  $22 \pm 5$  nM,  $16 \pm 3$  nM and  $21 \pm 5$  nM for clones 5G, 6E and 11B, respectively, in comparison to  $32 \pm 3$  nM for 3D7 WT. All parasites displayed comparable responses to the chloroquine treatment, with an average  $IC_{50}$  value of  $11 \pm 1$  nM.

### 3.2.2. Inactivation of PfUT's HECT catalytic domain

The extended cell cycle length of the PfUT-HA-glmS line may have resulted from an overexpressed PfUT regulating the abundance, activity or trafficking of its substrates, any of which might be involved in control of parasite proliferation. Another possible explanation of the observed phenotype, assuming targeting proteins for degradation as the main function of PfUT, is that integration of HA-glmS could affect the stability and/or activity of HECT catalytic domain, resulting in a dominant negative phenotype, most likely due to accumulation of PfUT's substrates which escaped degradation in the proteasome. Nonetheless, it cannot be ruled out that both overexpressed and catalytically inactive version of HECT domain could lead to a dominant negative PfUT effect.

To investigate the hypothesis of PfUT's negative dominance, an active cysteine site of its HECT catalytic domain has been replaced by a serine residue by means of the CRISPR-Cas9 genome editing technology, maintaining the presence of HA-glmS at the C-terminus of PfUT to allow for comparison between the two transgenic lines (Fig. 3.21.A). An active cysteine site is located 32-36 amino acids upstream of the C-terminal end of HECT domain (Huibregtse et al., 1995), which in case of PfUT

corresponds to the cysteine at position 3860. As already mentioned in the introduction part (chapter 1.3.3), E3 type ubiquitin ligases belonging to the HECT family, including PfUT, form a thioester intermediate with a target protein via an active cysteine residue of their catalytic domains, before a final labelling of the substrate with a ubiquitin molecule. The cysteine active site is therefore critical for their ubiquitinating function. Replacement of cysteine to serine deactivates HECT domain by depriving it of redox activity, yet retaining the hydrophilic properties and structure of the residue (Fig. 3.21.B).

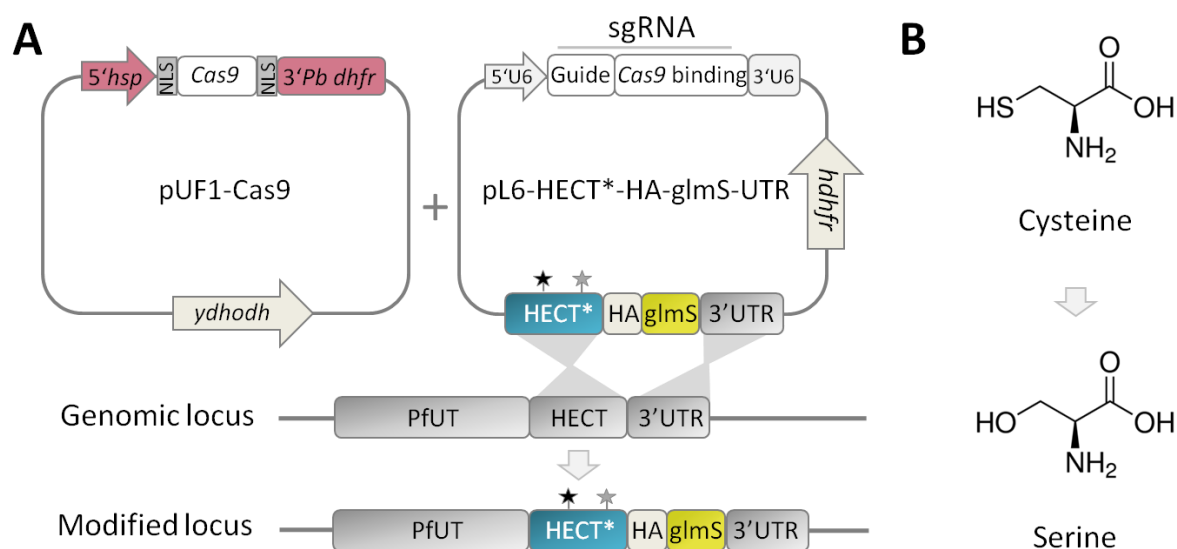


**Figure 3.21. CRISPR-Cas9-mediated replacement of an active cysteine site of the PfUT's HECT catalytic domain.** **A.** Schematic representation of the CRISPR-Cas9-based strategy to replace the active cysteine (Cys) at position 3860 by serine (Ser) in the PfUT locus. The homology region referred to as HECT\*, carrying a Cys3860Ser mutation (black star) and a shield mutation (grey star) has been integrated via a double crossover homologous recombination at a PfUT locus. A guide RNA targeting the Cas9 endonuclease to a recognition and cleavage site was the one successfully used in generation of PfUT-HA-glmS line (chapter 3.2.1.1). **B.** Chemical structures of the cysteine and its amino acid replacement, serine.

The *P. falciparum* 3D7 strain was transfected with pL6-HECT\*-HA-glmS and pUF1-Cas9 vectors on three independent occasions. Following the two months of drug selection, no re-appearance of parasites has been observed in any of the three transfection events. This result might be an indication of a detrimental role of the inactivation of a HECT catalytic domain in the protein possibly essential for the parasite intraerythrocytic development.

### 3.2.3. PfUT disruption using SLI-TGD system

A conditional knockdown strategy using the glmS ribozyme system was not efficient enough to conclude whether PfUT is essential in *P. falciparum* blood stages. Therefore, to further investigate

the role of PfUT in parasite asexual life cycle, a recently developed approach, termed selection-linked integration mediated targeted gene disruption (SLI-TGD), was undertaken (Birnbaum et al., 2017). SLI-TGD generates a gene knockout by a single crossover homologous recombination between the construct and the N-terminal region of the gene of interest. Following the transfection and selection with WR99210, parasites carrying the plasmid were successfully recovered in *P. falciparum* 3D7 strain, but not in Dd2 strain. Transfectants were then pressured with neomycin to select for parasites which had integrated the pSLI-TGD-PfUT construct. Since disruption of the targeted gene results in expression of GFP and neomycin phosphotransferase, only integrants are able to survive the neomycin selection. The failure in parasites recovery after neomycin selection is indicative of a potentially essential gene (Birnbaum et al., 2017). The six independent attempts to recover integrants after neomycin selection were unsuccessful, suggesting that PfUT might be essential for *P. falciparum* blood stage growth.

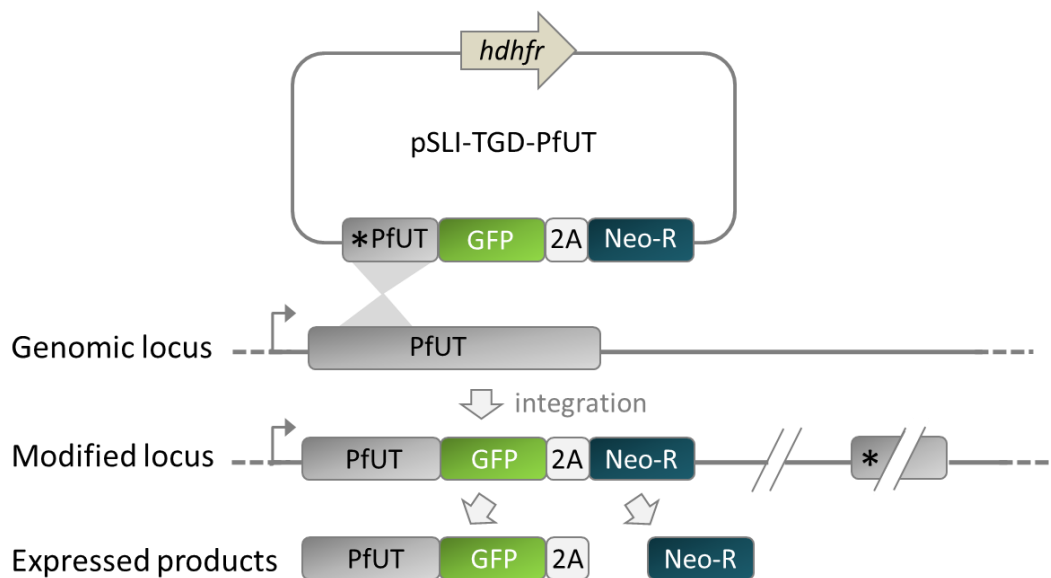


**Figure 3.22. Schematic of the SLI-TGD strategy.** The pSLI-TGD-PfUT vector has been integrated via a single crossover homologous recombination at a N-terminal PfUT locus. A skip peptide (2A) included between GFP and Neo-R (neomycin phosphotransferase resistance gene) leads to expression of Neo-R separately from GFP-tagged PfUT. A stop codon (\*) was inserted at the beginning of homology region to prevent undesired expression of Neo-R from an episome and to ensure the gene knockout after recombination. *hdhfr* – human dihydrofolate reductase gene.



## 4. Discussion and Outlook

### 4.1. Unravelling the role of PfCRT phosphorylation at position S33 in resistance to chloroquine and quinine

The chloroquine resistant transporter PfCRT is a well characterized drug-metabolite carrier associated with conferring resistance to quinoline drugs (Bray et al., 2005; Juge et al., 2015). The natural function of PfCRT is, however, still not fully understood. Posttranslational modifications, including palmitoylation and phosphorylation, seem to be responsible for modulating the role of this transporter in the parasite (Jones et al., 2012; Kuhn et al., 2010). Out of the four phosphorylation sites in this phosphoprotein, namely S33, S411, T416 and S420, only the threonine at position 416 has been linked to PfCRT's trafficking to the digestive vacuole, whereas the relevance of the other three residues has so far remained unknown. The present study attempts to understand the role of serine 33 phosphorylation in context of drug resistance.

#### 4.1.1. Phosphorylation of PfCRT's serine 33 modulates chloroquine and quinine responsiveness

The role of phosphorylation in the drug resistance mediating function of PfCRT has been evaluated from two perspectives. On the one hand, chemistry-based approach was used to block various protein kinases and phosphatases. On the other hand, genetic engineering has been implemented to modify the serine 33 phosphorylation site.

First, a screen of a range of kinase and phosphatase inhibitors revealed three compounds, ML-7, W-7 and H-89 (Fig. 3.1), which presence significantly increased accumulation of chloroquine in the *P. falciparum* Dd2 strain, carrying a resistant variant of PfCRT (Dr. Cecilia Sanchez, publication under review). A representative of the three inhibitors with a comparable influence on chloroquine accumulation, ML-7, was tested for an effect on the resistance profile of the Dd2 strain, and it significantly sensitized Dd2 parasites to chloroquine (CQ) and quinine (QN) (Fig. 3.2). These results provided the first evidence of phosphorylation being involved in modulating drug responsiveness in parasites bearing a mutant PfCRT background. However, the inhibitors of protein kinases used to regulate the levels of phosphorylation are often not specific and may cause various cellular effects, leading to misinterpretation of the observed phenotypes. For instance, although ML-7 is classified in humans as a selective mammalian myosin light chain kinase inhibitor (MLCK) (Isemura et al., 1991; Xiong et al., 2017), it also inhibits CK2 $\alpha$  and PKA (Holland et al., 2009; McKenzie et al., 2018), whereas in *P. falciparum* it blocks PfCK2 $\alpha$  (Graciotti et al., 2014; Holland et al., 2009). W-7 targets human

MLCK (Pinna & Cohen, 2005) and parasite PfPKB (Vaid & Sharma, 2006). H-89 blocks an activity of parasite and mammalian PKA (Syn et al., 2001; Warriar et al., 2007) as well as mammalian MSK1, PKB $\alpha$ , SGK, RSK1, RSK2, ROCK2, AMPK, CHK1 and MLCK (Limbutara et al., 2019; Raina et al., 2009). Noteworthy, although human MLCK, a target of all three inhibitors, lacks an ortholog in *P. falciparum*, it shares a high homology with parasite's calcium-dependent protein kinase family, including PfCDPK5.

Then, to link the drug resistance phenotype specifically with a PfCRT phosphorylation, a genetic manipulation has been undertaken. CRISPR-Cas9-mediated PfCRT serine 33 substitutions aiming to prevent or mimic phosphorylation in *P. falciparum* Dd2 strain, further supported the above observations, exposing the dependency of drug responsiveness on a variant of PfCRT 33 residue. As anticipated based on the outcome of the chemical approach, phosphorylation-defective alanine mutants (S33A) displayed significantly increased susceptibility to CQ and QN, in comparison to Dd2 strain bearing a phosphorylated serine 33 (Fig. 3.3). Similar observations regarding regulatory influence of phosphorylation in context of drug resistance have been made in human ABC transporters, of which non-phosphorable alanine mutants displayed an increased sensitivity to drugs (Germann et al., 1996; Xie et al., 2008). Replacement of serine by a glutamic and aspartic acid, respectively, partially and fully mimicked the phosphorylation of serine 33. The differences in drug responses of these two negatively charged amino acids could be attributed to their chemical structure. A non-phosphorylated aspartic acid (D) appears chemically more similar to a phosphoserine, than a glutamic acid (E) does; therefore the phosphorylation mimicry effect of S33D mutants was stronger than of S33E. Moreover, PfCRT's localization and protein levels were comparable regardless of the variant of amino acid residue at position 33 (Dr. Cecilia Sanchez and Dr. Sonia Moliner Cubel, publication under review). Therefore, the differences observed in drug susceptibilities between the respective mutants are likely associated with the physiological function of PfCRT.

To get an insight into the mechanism underlying the above findings, a substitution of serine by a non-phosphorable alanine or one of the two amino acids mimicking phosphorylation, was reproduced in *Xenopus laevis* oocytes expressing the Dd2 variant of PfCRT (Dr. Britta Nyboer; publication under review). The oocyte heterologous expression system, commonly applied for characterisation of membrane transporters, allows to determine substrate affinity ( $K_m$ ) and maximum transport velocity ( $V_{max}$ ) (Krishna & Woodrow, 1999). While the pH of the digestive vacuole and cytoplasm of the parasite is approx. 5.2 and 7.2, respectively (Kuhn et al., 2007), it is inverse in the oocyte system, where the oocyte cytosol and extracellular medium exhibit a pH of 5.0-6.0 and 7.0-7.2, respectively (Martin et al., 2009). Therefore, oocyte uptake assays reflect parasite efflux of the compounds from

the digestive vacuole. Keeping that in mind, CQ uptake assays in oocytes revealed a comparable transport velocity of Dd2 WT and S33D mutant, in contrast to S33A and S33E mutants, with noticeably reduced and intermediate uptake velocities, respectively (Dr. Britta Nyboer, publication under review). The described results confirm the study performed in the parasite, additionally indicating a role of PfCRT serine 33 phosphorylation as a regulator of transport velocity in this drug and metabolite carrier. Nevertheless, to rely on the oocytes data, one would need to provide an evidence of PfCRT being phosphorylated in the oocyte system, e.g. via immunoblotting with a phospho-antibody or by phosphoproteomic analysis (work in progress).

Taking these findings together, kinase inhibition as well as lack of a phosphorylation site, both resulted in increased CQ accumulation and enhanced susceptibility to CQ and QN. As the phosphorylation of PfCRT was directly linked to the drug resistance-mediating activity of this transporter, it motivated the identification of a responsible kinase. To investigate which of approximately 90 *P. falciparum* kinases (Doerig et al., 2008) is implicated in regulation of drug resistance mediating function of PfCRT, the protein-protein interaction methods such as Bio-ID, co-immunoprecipitation or yeast-two-hybrid screen, could be applied to reveal potential kinase candidates. Then, to verify the ability of these kinases to phosphorylate PfCRT and in particular its S33, they could be subjected to an *in vitro* kinase assays using a synthetic peptide of the N-terminal PfCRT region as a substrate, and a mutant peptide containing alanine replacement to serine at position 33, as a control. The yeast two-hybrid assays (performed in the lab by Anne Christin Roth, Dr. Cecilia Sanchez and Dr. Sonia Moliner Cubel) revealed a serine/threonine protein kinase (PF11\_0488 / PF3D7\_1148000) as an interacting partner of a C-terminal domain of PfCRT, but none of kinases targeting the N-terminal PfCRT. On the other hand, one could potentially use bioinformatics tools, such as PKIS (Zou et al., 2013) or PhosphoPredict (Song et al., 2017), designed to identify the kinases responsible for experimentally verified phosphorylation sites. However, these are so far available only for human catalyzing phosphorylation enzymes, and their predictability of *P. falciparum* kinases should therefore be taken with caution. Ultimately, as *Plasmodium* kinases are interesting antimalarial drug targets and they show relatively low sequence homology with their mammalian orthologs (Doerig, 2004), the inhibitor of the identified kinase could potentially be administered in combination therapies with chloroquine and quinine, preserving the usage of these long appreciated antimalarials.

#### 4.1.2. Fitness advantage of PfCRT S33 mutants results from the increased numbers of merozoites

As conferring resistance to drugs is often associated with fitness cost for the parasite (Walliker, 2005; Felger & Beck, 2008), the fitness of PfCRT S33 mutants was put under investigation. In the absence of drug pressure, alanine and glutamic acid mutants, with a sensitive and an intermediate resistance phenotype, respectively, were significantly fitter than Dd2 wild type and the aspartic acid mutant (Fig. 3.4.A). Fitness of the latter was comparable to Dd2 wild type. The fitness advantage of alanine and glutamic acid mutants was reflected by an increase in parasite multiplication rates (PMR) (Fig. 3.4.B), arising from the corresponding changes in merozoite numbers and their invasion efficiencies (Fig. 3.5 - 3.7).

Divergences in PMR arising from changes in cell cycle length, numbers of generated merozoites or erythrocyte invasion efficiency are commonly observed between the laboratory adapted *P. falciparum* strains differing in drug resistance background (Murray et al., 2017) as well as in field isolates causing distinct levels of malaria severity (Chotivanich et al., 2000). For example, a comparison of multidrug resistant (Dd2) and a sensitive wild type (HB3) strain revealed that the latter is characterized by longer cell cycle duration, a lower merozoite numbers and reduced invasion rates (Reilly et al., 2007).

A causal link between altered resistance profile, fitness and altered merozoites viability has also been notified in another mediator of chloroquine and quinine resistance, encoded by *mdr1* gene, a P-glycoprotein homolog 1, which similarly to PfCRT localizes to the digestive vacuole membrane (Cowman et al., 1991). Resistance acquired by parasites bearing either mutated alleles or multiple *mdr1* copy numbers incurred reduced fitness, associated with lower parasite multiplication rates and diminished merozoites viability (Hayward et al., 2005; Preechapornkul et al., 2009; Reed et al., 2000). These *in vitro* observations are consistent with results of several epidemiological studies reporting that after the selective pressure is removed, parasites conferring resistance may be put at a competitive disadvantage, as seen by drug sensitivity increasing over time (Thaithong et al., 1988; Liu et al., 1995; Kublin et al., 2003; Mita et al., 2004).

As the physiological function of PfCRT has still to be established, it is not clear how PfCRT S33 mutations might lead not only to the altered drug responses but also to such a pronounced effect on parasite overall fitness. Considering the differences in CQ transport velocity between the mutants, it cannot be ruled out that there are also variations in transport velocity of the natural substrates of this carrier. Assuming that the natural substrate of PfCRT is toxic for the parasite, its reduced

transport rate would result in lower levels of the toxic compound in the cytoplasm. Therefore, the parasite could direct its resources into enhanced proliferation, leading to increased merozoite numbers. Furthermore, if the natural substrate is a metal ion, its accumulation in the food vacuole could stimulate the activity of certain enzymes, such as aminopeptidases. In turn, this could result in higher levels of basic amino acids and peptides, derived from host haemoglobin digestion (Juge et al., 2015; Martin et al., 2009; Patzewitz et al., 2012), which could be further utilized for synthesis of parasites' own proteins. Metabolomic analysis conducted for PfCRT S33 mutants (Dr. Cecilia Sanchez, unpublished data) revealed a significant increase in levels of various tri- and tetrapeptides in S33A and S33E mutants in relation to S33D clone, and a significant reduction in content of some dipeptides in S33A mutant. Therefore, one of the possible mechanisms underlying the fitness variation in S33 mutants might be associated with altering amino acid-generating pathways, present both in digestive vacuole and in cytoplasm (Dalal & Klemba, 2007). One of the cytoplasmic aminopeptidases localizing to the parasite's apical organelles is *P. falciparum* dipeptidyl aminopeptidase 3 (DPAP3), the activity of which has been shown to be important for parasite proliferation and critical for merozoites attachment and invasion events (Lehmann et al., 2018). DPAP3 is most abundant in late schizont and merozoite stages and its knockout results in significantly decreased numbers of ring-infected erythrocytes (Lehmann et al., 2018). The expression of DPAP3 coincides with the transcription profile of PfCRT (Bozdech et al., 2003). Nevertheless, a lack of correlation between PfCRT's RNA and protein levels cannot be ruled out, and should be validated experimentally. Interestingly, another member of this family essential for parasite proliferation, namely dipeptidyl aminopeptidase 1 (DPAP1), localizes to parasite's digestive vacuole (Klemba et al., 2004). Moreover, before trafficking to its final destination, a proenzyme form of DPAP1 is found in the parasitophorous vacuole of mature schizonts (Klemba et al., 2004). Although at reduced levels, DPAP1 pro-form retains its activity (Wang et al., 2011), suggesting that similarly to DPAP3, it might be involved in modulating parasite egress and the following red blood cell invasion.

Secretion of different proteins from apical organelles prior to egress is known to be mediated by two signalling proteins, plant-like calcium-dependent protein kinase PfCDPK5 (Absalon et al., 2018; Dvorin et al., 2010) and cGMP-dependent protein kinase PfPKG (Collins et al., 2013), the knockouts of which block the egress. Attention should be paid to PfCDPK5, as it was mentioned before as an ortholog of mammalian MLCK targeted by all three kinase inhibitors tested in the present study. Other kinases with a potential role in phosphorylation of PfCRT S33 could include either a cyclin-dependent PfCrk-5 or an orphan protein kinase PfPK7, as disruption of these important for schizogony kinases resulted in reduced growth rates, linked to decreased numbers of merozoites formed per schizont (Dorin-Semblat et al., 2008; Dorin-Semblat et al., 2013). Furthermore, several

studies draw attention to the role of calcium signalling pathways in merozoites development and invasion (Garcia, 1999; McCallum-Deighton & Holder, 1992). Noteworthy, a calcium-binding calmodulin, which is an activator among others of PfPKB (Silva-Neto et al., 2002; Vaid & Sharma, 2006; Vaid et al., 2008), similarly to DPAP3 localizes to parasite's apical region, and its inhibition was shown to block schizonts maturation and merozoites invasion (Garcia, 1999). Therefore, it would be rational to compare calcium levels in PfCRT S33 mutants. Potentially elevated calcium levels in S33A mutant could increase the activity of one of the kinases implicated in regulation of parasite proliferation, through a signalling cascade. This might theoretically explain the enhanced invasion rates of merozoites. Thus, it could be speculated that the same kinase which phosphorylates PfCRT's S33 residue is also implicated in regulation of intraerythrocytic development and invasion of merozoites. In that case, the activity of this kinase in S33A mutant could potentially be reinforced into intensified mediation of schizont maturation, egress and invasion events. This in turn could possibly upregulate DPAPs and likely other proliferation-controlling enzymes, leading to increased numbers of viable merozoites.

Another hypothesis may comprise the involvement of the lipid metabolism in the observed fitness variation, since the aforementioned metabolic profiling of S33 mutants revealed also differences in the abundance of certain lipids. Both alanine and glutamic acid mutants displayed significantly less phosphatidylcholines (PC) and lysophospholipids (LPL), than the aspartic acid mutant, which likely corresponds to Dd2 WT (not included in analysis), as could be assumed based on the similarities in fitness and drug resistance profile. Notably, none of these lipids was detectable in the case of PfCRT knockdown. During intraerythrocytic growth, parasite requires considerable amounts of lipids, among the others for the formation of membrane networks and development of daughter merozoites. *P. falciparum*, by synthesizing these lipids *de novo* or acquiring them from the host cell, shows a high adaptability of its lipids synthesis pathways in response to various disturbances (Gulati et al., 2015; Wein et al., 2018). Interestingly, analysis of serum lipid profiles in malaria-positive patients revealed lower levels of lipids and lipoproteins present in *Plasmodium*-infected group compared to healthy individuals (Visser et al., 2013) and more pronounced lipid alterations in severe than in uncomplicated malaria cases (Mfonkeu et al., 2010; Mohanty et al., 1992; Njoku et al., 2001). Although high-density lipoprotein cholesterol (HDL) is essential for *P. falciparum* survival *in vitro*, another study demonstrated that the parasite's development is promoted at lower HDL concentrations (Imrie et al., 2004). These studies suggest that reduced levels of certain lipids may actually facilitate parasites' proliferation, thus their potential correlation with increased merozoites numbers cannot be excluded.

Biological mechanisms influencing changes in lipid profiles during malaria infection may be both host- and parasite-related. A host-related decrease of plasma lipoproteins accompanying various acute diseases is likely caused by their migration into tissues due to increased capillary permeability (Visser et al., 2013); whereas, the parasite-related changes in lipid levels seem to be associated with heme detoxification into hemozoin, taking place in the parasite's digestive vacuole (Fitch et al., 1999; Fong & Wright, 2013; Hänscheid et al., 2007; Pandey et al., 2003; Pisciotta et al., 2007). The role of neutral lipids in mediating the formation of hemozoin has been supported by transmission electron micrographs illustrating hemozoin crystals within lipid nanospheres (Pisciotta et al., 2007). These lipids, albeit, were not the ones found significantly affected in the metabolomic profiling of PfCRT S33 mutants. Most likely, since there is no correlation between levels of total hemozoin and *P. falciparum* sensitivity to CQ (Zhang et al., 1999), a demand for the neutral lipid bodies surrounding hemozoin crystals is then comparable in sensitive and resistant strains. On the other hand, the situation changes under drug pressure. Since CQ and QN are targeting the heme detoxification pathway, presence of these drugs results in accumulation of toxic heme and reduction of hemozoin levels in sensitive strains, in contrast to CQ resistant strains, which may even elevate hemozoin production (Orjih et al., 1994). Heme overload in drug susceptible strains in turn results in increased hemolysis (release of haemoglobin) of parasitized red blood cells. Prior to the hemolysis, osmotic fragility and passive permeability are increasing, whereas ATPase-dependent transport of sodium ions is decreasing. These changes are caused by esterification of fatty acids to membrane phospholipids, which alters the fluidity of the phospholipid bilayer, by changing its unsaturation degree (Holz, 1977). Noteworthy, S33A and S33E mutants exhibit significantly reduced levels of those esterified fatty acids, precisely of phosphatidylcholines (PCs). Moreover, some of the fatty acids are known to enhance the activity of adenylate cyclases generating cAMP, which further influence cAMP-dependent protein kinases. Phosphorylating activity of these kinases was shown to modify the membrane proteins interacting with phospholipid bilayer, consequently changing membrane fluidity and barrier properties (Holz, 1977; Wang & Oram, 2007). One could therefore assume that altered lipid levels might be potentially related to the disturbed function of PfCRT, due to phosphorylation-defective 33 residues in these mutants. A natural function of PfCRT as a lipid transporter could also be considered, since as shown on example of two human lipid transporters, ACBA1 and CD36, phosphorylation can influence the lipid changes mediated by these carriers (Glatz et al., 2010; Wang & Oram, 2007). This supposition, however, still does not explain the alterations of merozoite numbers observed in S33 mutants.

Another assumption takes into consideration that PfCRT may interact with one of the enzymes hydrolysing phosphatidylcholine (PC) in the parasite. It happens that lysophospholipase A (LPLA;

PF14\_0017 or PF3D7\_1401500) implicated in PC hydrolysis, was found in the STRING functional protein association network ([www.string-db.org](http://www.string-db.org)) as one of the PfCRT's interacting partners (Appendix I, Fig. I.1). This enzyme which has been shown as dispensable in *P. berghei*, facilitates a release of fatty acids (FA) from lysophospholipids (LPL), which also have been found at reduced levels in S33A and S33E mutants. LPL in turn are products of hydrolysis of PC and phospholipids (PL) catalyzed by a phospholipase A (PLA) (Flammersfeld et al., 2018). Noteworthy, the conversion of phosphatidylethanolamine (PE, precursor of PC) to PC by PE-methyltransferase (PEMT) requires serine, which can be taken up either from the host or from the haemoglobin degradation in digestive vacuole (Flammersfeld et al., 2018), linking the latter again to phospholipid synthesis pathway. Furthermore, it has been shown that phospholipases may both activate and be activated by kinases. On the one hand, phospholipases are regulated by some kinases, such as PKC (Exton, 1997). On the other hand, by hydrolysing phospholipids, activated phospholipase generates unsaturated fatty acids, the presence of which, as already mentioned earlier, stimulates the kinase which in turn again activates phospholipase, forming a positive feedback loop (Exton, 1997; Holz, 1977; Wang & Oram, 2007). A possibility of LPLA being regulated by phosphorylation is highlighted by a presence of serine active site in this enzyme (Flammersfeld et al., 2018). Interestingly, it has been shown that blocking the function of phospholipase C, which further activates PfPKB, resulted in impaired invasion (Vaid et al., 2008). Another study reports that the activity of *P. falciparum* phospholipase A2 has been inhibited by exposure to chloroquine, quinine, and the artemisinin derivative, arteether (Zidovetzki et al., 1993), suggesting that the phospholipid catabolism pathway may indeed be associated with PfCRT-mediated resistance to chloroquine and quinine.

The results of this study showed that fitness advantage incurred by S33A and S33E mutants was due to increased numbers of merozoites, which displayed better invasion efficiencies (Fig. 3.5-3.7). Although the differences in merozoites attachment to the red blood cell membrane were not significant, a trend similar to the results of the invasion assay could be detected. The lack of significance is observed likely due to a spread of attachment results for each analyzed clone, in comparison to quite similar range of values within a clone in case of invasion assay. These differences may arise from the fact that attaching merozoites, whose invasion is blocked by the presence of cytochalasin D, may detach before fixation, causing a bigger data variation within replicates of the same clone. Taking this into consideration, one possible explanation of increased attachment and invasion rates could be again linked to changes in lipid profiles. While during the attachment of merozoites to the erythrocyte membrane the composition of phospholipids remains relatively unchanged, the ratio of unsaturated fatty acids chains to the saturated ones within these phospholipids rises significantly (Holz, 1977; Vial et al., 2003; Flammersfeld et al., 2018), changing the



membrane fluidity and further facilitating invasion. Interestingly, it has been reported that with progression through the parasite's cell cycle, PC contents decreases, whereas the level of unsaturation of fatty acids remarkably increases (Wunderlich et al., 1991). It is therefore tempting to speculate that this process might be enhanced in S33A and S33E mutants. Although the differences in the lipid saturation state could not be distinguished in metabolomic profiling, one could attempt to resolve them via lipidom analysis.

Taking into account all the observations regarding lipid metabolism in the parasite, a simplified model is being proposed towards unravelling the mechanism underlying fitness variation between PfCRT S33 mutants (Fig. 4.1). The present model draws attention to the possibility that a kinase which phosphorylates PfCRT S33 is also a regulator of a lipid pathway, where it regulates LPLA, either directly or by activating another enzyme in PC hydrolysis cascade. Since the S33A mutant lacks a phosphorylation site, the activity of the kinase regulating it might be intensified towards the phospholipid catabolism pathway. It could potentially lead to upregulation of some of the pathway components, ultimately resulting in enhanced hydrolysis of PC and its intermediate degradation product LPL to free fatty acids. To test this hypothesis one could compare the relative expression levels of LPLA via qPCR and Western Blot. Additionally, this enzyme could be overexpressed in *P. falciparum* Dd2 strain and the resulting transfectants examined for the fitness advantage and for an associated increase in merozoites numbers. Alternatively, LPLA could be also targeted with a specific inhibitor and tested whether or not it affects parasite invasion.

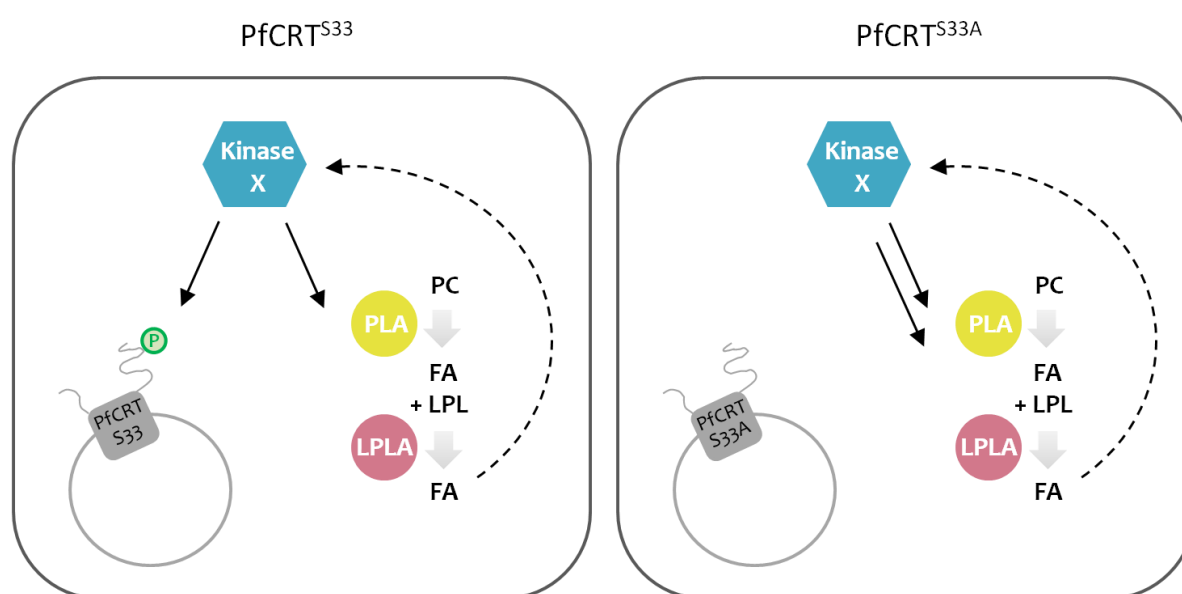


**Figure 4.1. A simplified model illustrating possible changes in parasite's lipid profile depending on PfCRT S33 phosphorylation.** Left panel: PfCRT S33 (WT). Right panel: PfCRT S33A. **Kinase X** – yet undefined kinase, **PLA** – phospholipase A, **LPLA** – lysophospholipase A, **PC** – phosphatidylcholine, **FA** – fatty acids, **LPL** – lysophospholipids, **P** – phospho-serine 33.

The model does not include the involvement of a kinase in generating increased merozoites numbers. It is possible that schizont maturation and merozoites invasion are either directly stimulated by an indicated kinase, or that responsibility lies on the side of FA hydrolysed from PC, which may further modulate the activity of other kinases implicated in control of these processes.

As the here described phenotype of PfCRT S33 mutants was obtained in the absence of selective pressure, it would be interesting to see how these clones behave upon exposure to chloroquine and quinine, to develop a full picture of the effect of phosphorylation-defective substitutions on parasite's drug resistance profile.

To confirm that these findings are not a result of a technical issue, being either a random selection of clones exhibiting stronger phenotype among the whole pool of recombinant parasites or potential experimental errors, performing the complementation studies could be considered. This would comprise the replacement of alanine in S33A mutants back to serine, followed by a comparison of the phenotype of such a recombinant strain to Dd2 WT. Alternatively, all the S33 mutants could be generated in the chloroquine sensitive and quinine semi-resistant *P. falciparum* 3D7 strain. Although the resistance profile of these mutants might differ remarkably, the fitness variation would rather be expected to reflect the observations made in Dd2 strain. Furthermore, since a genetic cross between the resistant Dd2 strain and sensitive HB3 has been already performed obtaining a progeny varying with regard to resistance profile as well as growth patterns (Sanchez et al., 2014), the sensitive fast growers could be selected. A subsequent QTL analysis could potentially identify genes contributing to this phenotype.

One may also wonder why various parasite strains carry a phosphorable serine at PfCRT's position 33 (PlasmoDB) if replacing it by alanine seems to be more advantageous. As commonly known, laboratory observations do not always reflect the field studies. It is important to bear in mind that by increasing invasion rates, the parasite may enhance its virulence, leading to the host death and thereby jeopardizing its own survival.

Many studies have shown that mutations could be beneficial or that the presence of a protein critical, albeit, only within a particular parasite stage (Helm et al., 2010; Kenthirapalan et al., 2016; Rathnapala et al., 2017). It therefore would be interesting to investigate whether the S33A mutant, displaying increased invasion rates, would further increase gametogenesis, and in turn enhancing transmission to a mosquito vector, alter the sporogony and finally increase the efficiency of parasites in mammalian host. Although the S33A mutant has a fitness advantage in parasite's blood stage, it might be only a stage-specific effect, and a transmission to the subsequent stages might be blocked,

as observed for the parasites resistant to atovaquone (Goodman et al., 2016). Such scenario would render the kinase phosphorylating PfCRT S33 even more attractive as a drug target.

## 4.2. Functional characterization of PfUT in the parasite's asexual life cycle

The HECT E3 ubiquitin ligase PfUT is one of the components of the ubiquitination pathway, crucial for *P. falciparum* intraerythrocytic development. It localizes to the membrane of the ER/Golgi complex with the N- and C-terminal ends presumably facing the parasite's cytosol (Sanchez et al., 2014). Although several studies have suggested that PfUT might be post-translationally modified by phosphorylation (Pease et al., 2013) and acetylation (Cobbold et al., 2016), the functional significance of those modifications is so far unknown. The *S. cerevisiae* homolog, an ubiquitin fusion degradation protein 4 (UFD4), is involved in the proteasome-mediated proteolysis of its targets, a nucleotide excision repair protein RAD4 (Ju & Xie, 2006) and DNA repair helicase RAD25 (Bao et al., 2015). However, the role of PfUT in *P. falciparum* blood stages and the substrates of this ubiquitin ligase remain to be resolved. Furthermore, PfUT has been suggested to play a role in altered responses to quinine and quinidine in certain genetic backgrounds (Sanchez et al., 2014). Nevertheless, these findings require further validation. The present study was designed to gain a deeper insight into the physiological function of PfUT in the parasite's development, as well as its association with resistance to quinine.

### 4.2.1. Overexpression of PfUT results in cell cycle lengthening of PfUT-HA-glmS parasites

Aiming to verify the essentiality of PfUT in *P. falciparum* blood stages, the glmS ribozyme system was applied. Used to conditionally control the *pfut* expression, this method revealed on the one hand, the inefficiency of attempted *pfut* downregulation, and on the other hand, an increase in PfUT transcript correlated with protein levels (Fig. 3.10 and 3.11). An apparent 2-fold overexpression of PfUT resulted in an elongation of the cell cycle length of HA-glmS-tagged transgenic line (Fig. 3.17), which was further reflected in the impaired growth of these parasites.

The altered cellular mRNA levels may result either from changes in their transcription efficiency or mRNA stability. Transcription factors, which bind to the promoter or enhancer regions of a gene, control the rates of mRNA synthesis by either promoting or suppressing the DNA transcription (Latchman, 1993). On the other hand, the mRNA stability could potentially be influenced by multiple factors, including 5' mRNA capping (eukaryotes) or just 5' phosphorylation state (prokaryotes), polyadenylation of the mRNA 3' end, ribosome-mediated protection from RNases, formation of secondary structures proximal to the 5' and 3' ends or regulatory-protein factors (Liu et al., 1995; Grunberg-Manago, 1999; Condon, 2003; Sharp & Bechhofer, 2003; Collins et al., 2007; Schoenberg,

2007). As the glmS ribozyme used in the present study is a RNA molecule containing structure stabilization domains (chapter 1.4.2) (Lee & Lee, 2017), the herein observed increase of PfUT transcript levels could result from its C-terminal tagging with HA-glmS, enhancing mRNA stability of the mutant line. Moreover, the expression of GC-rich genes has been shown to be much more efficient than of GC-poor ones, containing identical promoters and UTR sequences, and resulted from an elevated steady-state mRNA levels of the first ones (Kudla et al., 2006). Therefore, as non-*Plasmodium* derived sequences of HA and glmS have notably high GC content (Appendix III.2), their presence could likely increase the stability of *pfut* mRNA. Although due to several biological factors a relationship between mRNA and the corresponding cellular protein levels might be poor, in nearly 80% of instances the variance in protein abundance correlates with underlying mRNA changes (Lee et al., 2011; Liu et al., 2016). This also seems to be the case for PfUT-HA-glmS, with a 2-fold increase in *pfut* transcripts reflected by a respective change in PfUT protein levels.

Despite the fact that the glmS system did not facilitate the efficient downregulation of PfUT, it revealed an impaired growth phenotype, presumably due to PfUT's overexpression. As shown in numerous reports, even though the efficiency of conditional systems does not always fulfil the expectations, they often display interesting phenotypes. For instance, previous studies revealed a phenotype resulting from a complete knockdown (Elsworth et al., 2014; Gabriel et al., 2018) or a partial downregulation (Bei et al., 2010; Beck et al., 2014). In contrast, less successful attempts have also been reported, including a gene knockout or full downregulation with no detrimental effect on the parasite (Cobb et al., 2017; Thériault & Richard, 2017; Wezena et al., 2018), no downregulation and no phenotype despite the presence of inducible system (Azevedo et al., 2012) and finally even a failure to integrate a tag (Azevedo et al., 2012). These divergent outcomes probably arise from the function affiliated to the gene product and its importance for the parasite's survival or in the most unfortunate case, simply to a lack of success in obtaining recombined parasites.

As discussed in the preceding chapter, an apparent slowed-down growth and reduction of parasite multiplication rates may result from the alteration of various aspects of parasitic development, including numbers of merozoite generated per schizont, multiple infections of a single erythrocyte or the duration of parasite's replicative cycle. The current study linked the reduced growth of the PfUT-HA-glmS line with its apparent prolongation of the intraerythrocytic cycle. The growth defect was partially rescued by glucosamine treatment, due to a shortening of the cell cycle length. This effect can probably be explained by an extension of the S phase in the mutant parasites. Nonetheless, the cause of the altered growth may possibly be also attributed to a delay in the transition from G1 to S phase. Considering that replication starts around 30 hours post invasion, and that at this stage of the cycle the DNA copy number equals one, a delayed duplication of a single nucleus may at first glance

escape one's attention. However, although these differences in doubling time between wild type and mutant lines may appear to be non-significant, their relevance cannot be definitively excluded. Interestingly, a delayed transition to the mitotic division has been associated with a reduced multiplication rate and fitness of artemisinin resistant parasites (Bunditvorapoom et al., 2018). Notably, a main determinant of artemisinin resistance is a mutated variant of PfKelch13, a substrate adaptor for an E3 ubiquitin ligase (Ariey et al., 2014). PfKelch13 was suggested to play a role in regulating ubiquitination (Mbengue et al., 2015) and was recently shown to be implicated in the control of DNA replication and repair (Gibbons et al., 2018). Moreover, a comparison of multidrug resistant and sensitive strains, Dd2 and HB3, respectively, depicted longer cycle duration, caused by extension of ring stage phase, and a decline in merozoite invasion rates in the latter (Reilly et al., 2007). While the DNA replication phase of PfUT-HA-glmS parasites seems to be extended in time leading to delayed egress and, hence, subsequent invasion, the attachment and invasion efficiencies were not yet particularly investigated. Nonetheless, the observed decrease in parasite multiplication rates might not only be due to cell cycle lengthening but also due to an altered efficiency of merozoite attachment or invasion into the red blood cell. Furthermore, in order to address the probable differences in timing of DNA replication between the wild type and mutant parasites, the bromodeoxyuridine (BrdU) cell proliferation assay could be attempted. This method, based on BrdU incorporation to the parasite's DNA, allows to track undergoing DNA synthesis using an anti-BrdU antibody (Claessens et al., 2018; Merrick, 2015). However, since *Plasmodium* parasites lack an enzyme capable of integrating BrdU to the DNA, namely a thymidine kinase, its expression is a requirement preceding the assay performance. This approach would clearly indicate not only divergences in the DNA replication dynamics, but also a potentially delayed G1 to S phase transition.

When it comes to phenotypic characterization of the PfUT-HA-glmS parasites, one has to account for the overexpressed PfUT variant. A brief screen of PlasmoDB database revealed that PfUT expression profiles are relatively low in comparison to other known *P. falciparum* genes (PlasmoDB), indicating that low levels might be sufficient to perform its functions in the asexual life cycle. Therefore, the abnormal expression of PfUT is likely to have deleterious effects on the parasite intraerythrocytic development, possibly resulting in a decelerated metabolism and in turn a prolongation of the cell cycle length, if not directly leading to the parasite's death. Nevertheless, as shown in numerous studies, overexpression of a E3 ubiquitin ligase may have both a conducive or a detrimental effect for an organism (Adler et al., 2018; Chen et al., 2017; Ito et al., 2017; Lin et al., 2015; Lu & Legerski, 2007; Melgar-Lesmes et al., 2018; Totland et al., 2017). Noteworthy, the overexpression of PfUT's minimal HECT domain (containing E2-binding site and catalytically active cysteine) conferred an increase in quinine resistance profile of strains with certain genetic backgrounds, not affecting susceptibility of

other ones (Sanchez et al., 2014). Although the growth patterns were not investigated, the results suggested that the expression of the HECT catalytic domain does not seem to be toxic for any of these parasite strains. Moreover, such an approach does not guarantee the specificity of ubiquitination, as a putative substrate binding region localizing to the N-terminus of PfUT is excluded from the experimental design. Therefore, to better understand the described here phenotype of the PfUT-HA-glms line, an overexpression of a wild type and a dominant-negative mutant of PfUT should be considered, aiming a phenotypic comparison of the obtained transfectants with the HA-glms transgenic parasites.

The overexpression, ideally of untagged PfUT would help to see whether the effect observed herein is only due to PfUT overexpression or if HA-glms tagging might have affected the conformation, structure and/or function of PfUT. To further support this investigation, it would be desirable to overexpress a dominant negative PfUT mutant, as by comparison with PfUT-HA-glms, it would reveal whether the phenotype of the latter results only from an increase in PfUT abundance or also due to its altered catalytic activity. To verify the possibility of PfUT's negative dominance, the CRISPR-Cas9 system was applied to replace an active cysteine by a serine residue, thus inactivating the PfUT's HECT catalytic domain. Failure to recover parasites in three independent trials after around two months of drug selection suggests that the cysteine active site might be critical for PfUT's function and its substitution in a likely essential protein lethal to the parasites. However, a technical issue as a reason for unrecovered parasites, such as transfection inefficiency, cannot be entirely excluded.

Due to its prominent size ( ~460 kDa), a fully functional PfUT cannot be expressed episomally. Nevertheless, overexpression of the endogenous PfUT could be achieved, for instance using a promoter swapping technique (Kaufmann & Knop, 2011; McCleary, 2009) to replace a native weak *pfut* promoter with another highly active during parasite blood stages. Another possibility includes the integration of a drug resistance cassette (such as human dihydrofolate reductase, conferring resistance to WR) downstream to the PfUT via a skip peptide. In a fashion analogous to the previously described SLI method (Birnbaum et al., 2017), both proteins would be under control of *pfut*'s promoter, albeit, due to the presence of a skip peptide, expressed apart from each other. This approach would allow the levels of PfUT expression to be regulated in a drug-dose dependent manner.

Localisation studies using immunofluorescence and immuno-electron microscopy revealed that PfUT-HA localizes to the ER/Golgi complex, consistent with the localization of this protein in the wild type parasites. Therefore, the differences in cell cycle duration are likely to arise from the overexpressed PfUT variant modulating the activity of its substrates, being it either degradation or regulatory role.

### 4.2.2. Investigating the biological substrates of PfUT

Understanding the mechanisms underlying the increase in cell cycle duration requires the identification of the proteins targeted by PfUT in the parasite. Addressing this issue by an analysis of ubiquitination patterns did not show any obvious differences between the 3D7 WT and PfUT-HA-glmS parasites. This approach, however, remains quite qualitative and should be addressed in a quantitative manner, i.e. by mass spectrometry analysis. Noteworthy, a polyclonal ubiquitin antibody (Ub FL-76 from Santa Cruz Biotechnology) used herein for immunoblotting has been discontinued by the supplier and replaced by a more specific monoclonal Ub P4D1, stated to provide a stronger signal. Therefore, as the antibody quality might have played a role in results obtained in this study, it would be worth repeating the experiment with the new recommended version. Moreover, the differences in abundance of ubiquitinated proteins may not be apparent under standard cell culture conditions, but might be revealed once the parasites are under stress. To test this hypothesis, one could conduct an analysis of protein ubiquitination elevated by heat shock or blocked activity of the proteasome. Increase of the cell culture temperature e.g. to 42°C or presence of the proteasome inhibitor, such as MG132, will surely augment accumulation of ubiquitinated proteins, possibly exposing PfUT's substrates.

The process of identifying substrates of a ubiquitin ligase encounters various challenging factors, including the dynamic nature of protein ubiquitination, weak and/or transient interactions between ligase and its substrate, multiplicity of substrates targeted by a single ligase (and *vice versa*) or the rapid degradation of many ubiquitinated proteins (Iconomou & Saunders, 2016). The possibility of low substrate abundance as well as a subcellular localization should also be taken into consideration before approaching identification of targets of a particular ubiquitin ligase, as they may respectively, hinder the identification or reveal false positive substrate-ligase interactions.

Numerous strategies could be applied in order to identify substrates of PfUT. These include **genetic screens** like yeast two-hybrid (Y2H), protein microarrays or high-throughput quantitative microscopy (high-content analysis, HCA), **mass spectrometry based-proteomics methods**, such as stable isotope labelling by amino acids in cell culture (SILAC), various configurations of affinity purification strategies (e.g. co-immunoprecipitation, co-IP, or tandem ubiquitin-binding entities, TUBEs), ubiquitin ligase trapping and proximity labelling or Gly-Gly (di-Gly) remnant affinity purification, and finally **integrated approaches** combining several of the available techniques (Iconomou & Saunders, 2016). Some of these methods have already been attempted for PfUT, whereas others are not even yet established for *Plasmodium*.



A compilation of yeast two-hybrid assays conducted in different studies, accessible on PlasmoDB, revealed a handful of PfUT-interacting partners. These include proteins critical for egress and/or invasion, such as merozoite surface protein MSP-1 and rhoptry neck protein RON2, essential for protein export EXP2, several so far uncharacterized proteins associated with transcription or translation and a proteasome beta subunit. Interestingly, a recent study has shown that EXP2 knockdown leads to a reduction of parasite growth and protein export (Charnaud et al., 2018), hence, an altered growth of PfUT-HA-glmS line may potentially result from EXP2 being regulated by overexpressed PfUT. The same might be true for MSP-1 and RON2, proteins associated with invasion and egress events. Although not listed among the hits presented on PlasmoDB, the chloroquine resistance marker protein PfCRMP, a putative chloroquine target in the nucleus, was found in a Y2H screen conducted by LaCount and colleagues (2005). Noteworthy, potential interacting partners of several HECT ubiquitin ligases indicated in various Y2H screens turned out to be their actual targets, thus supporting the usage of this method as a reasonable for identification of substrate proteins (Mitsui et al., 1999; Traweger et al., 2002).

Proximity dependent biotin labelling (BioID) is based on the fusion of a protein of interest (POI) with a biotin ligase (BirA\*) or ascorbate peroxidase (APEX2), which in the presence of biotin will label all the proteins directly interacting with or in close proximity to the POI. Biotinylated proteins can then be pulled down using streptavidin beads and identified by mass spectrometry. Multiple attempts to tag PfUT either with BirA or APEX2 were unsuccessful, possibly due to the size of the fusion proteins. Nevertheless, taking advantage of already generated HA-tagged PfUT, a co-immunoprecipitation coupled to mass spectrometry (co-IP-MS) analysis will be carried out in the near future. Moreover, the earlier mentioned diGly proteomics of ubiquitin-enriched proteins is also considered for future investigations. Conducting both methods will hopefully reveal targets of PfUT and, hence, unravel the mechanisms underpinning the herein described phenotype of PfUT-HA-glmS parasites. Alternatively, one could make use of an already overexpressed variant of PfUT in HA-glmS transgenic line, which is required for another affinity purification-based strategy, aiming to identify the E3 ubiquitin ligase substrates. This approach exploits the labelling of substrates with His-tagged ubiquitin followed by their pull down and a quantitative proteomic comparison of protein ubiquitination in wild type versus overexpressed ligase variants (Song et al., 2011). Proteins identified by mass spectrometry, in case of PfUT overexpression, would display enhanced incorporation of His-tagged ubiquitin in comparison to its WT variant, being likely substrates of this ubiquitin ligase.

The majority of protein-protein interaction networks will generate a list of upstream and downstream candidates, either mediating PfUT's function or being regulated by this ubiquitin ligase, respectively. Therefore, aiming to identify particularly the substrates of PfUT, enrichment of

ubiquitinated proteins, for example by means of TUBEs (Mata-Cantero et al., 2016) is desired and will be applied in future investigations. Furthermore, while identified in one of the above approaches interacting proteins will represent potential substrates of PfUT, their status as a “target protein” may require further validation, for example by co-IP followed by western blot analysis, immunofluorescence co-localization studies or *in vitro* ubiquitination assays.

The chloroquine resistance transporter PfCRT has been previously indicated as a potential substrate of PfUT, since both, although in particular genetic backgrounds, were associated with altered quinine and quinidine responses (Sanchez et al., 2014). This observation was further supported by the finding that PfCRT traffics to the digestive vacuole membrane via ER/Golgi complex (Kuhn et al., 2010). Contrary to expectations, the western blot analysis conducted in the current study displayed no differences in PfCRT protein abundance between the wild type and the overexpressed PfUT variant, regardless of glucosamine presence (Fig. 3.19). Nevertheless, one cannot rule out the possibility that the overexpression of PfUT does not affect PfCRT, whereas its reduced levels would. Since resistances to chloroquine or quinine have multifactorial natures, a mutational change or altered abundance of any of the resistance mediators may imbalance the relevant gene combinations. This, however, does not necessarily mean that all the components directly interact with each other; they may instead form a cascade of dependencies or potentially even reflect a cumulative effect of independent pathways. Moreover, although PfCRT was shown to be ubiquitinated by PfUT’s HECT domain in an *in vitro* ubiquitination assay, so were the immunoglobulins present in the assay due to elution conditions (Sanchez et al., 2014). This indicates a potentially unspecific reaction, likely arising from usage of solely the overexpressed HECT domain lacking a putative substrate binding site, instead of the whole fully functional PfUT. On top of that, one need to keep in mind that *in vitro* ubiquitination does not account for a cellular context, such as subcellular localization, mediation of posttranslational modifications or feedback regulation by deubiquitinating enzymes. Therefore, although it is possible that PfCRT is specifically targeted by PfUT, the aforementioned results have to be taken with caution. Furthermore, the same study of Sanchez and colleagues (2014) showed somewhat contradictory results regarding requirement of mutated variants of PfCRT and PfUT in the resistance of respective strains. While overexpression of mutant PfCRT in selected strains, bearing PfUT resistance alleles led to their increased susceptibility to quinine and quinidine, the presence of mutated variants of both genes in a group of analyzed field isolates and laboratory strains was associated with an opposite effect, namely an increase of quinine IC<sub>50</sub> values determined for these parasites (Sanchez et al., 2014). This might indicate that not only PfUT and PfCRT are required for quinine resistance and that interaction of one of these two with another resistance mediator, rather than their interaction with each other, influences the parasite’s sensitivity to quinine. A possible

cause of the observed differences in drug responsiveness of the analyzed strains has been related to a genetic variation found within a segment on chromosome 13 (Sanchez et al., 2014). The suggested region may contain one or more quinine resistance mediators, and although they are yet undefined a potential substrate of PfUT might be found among them. However, with so many uncertainties, at the moment the clear conclusions in this regard cannot be drawn.

Given that the overexpression of PfUT affects the length of the cell cycle of HA-glmS transgenic line, it is likely that among the substrates of this ubiquitin ligase one will find proteins involved in the control of parasite proliferation and cell cycle progression. Among the known regulators of these processes are cyclins, encoded by *pfcyc1-4* genes, as well as activated by them cyclin-dependent protein kinases (CDKs) and CKD-related kinases (CRKs) (Le Roch, 2003; Matthews et al., 2018). Interestingly, PfCYC1, an activator of a protein kinase 5 PfPK5 and a MO15-related kinase PfMRK, was shown to be critical for parasite proliferation (Robbins et al., 2017), whereas PfCYC3, another modulator of PfPK5 activity, was shown to be involved in the regulation of DNA replication initiation (Roques et al., 2015). Moreover, dormancy of artemisinin resistant parasites resulting from a prolongation of their ring phase through a delayed G1/S phase progression, was shown to be linked to a downregulation of PfCYC1 and PfCYC3, as well as of kinases activated by them, namely PfMRK and PfPK5 (Gray et al., 2016). Furthermore, it has been reported that PfPK5 is critical for both activation and maintenance of parasite's S phase (Graeser et al., 1996). Other possibilities include *cdc-2* related kinases PfCRK1, PfCRK3 and PfCRK4, as they were shown to have a crucial role for parasite growth and proliferation (Ganter et al., 2017; Halbert et al., 2010; Iwanaga et al., 2013). Among non-cyclin/CDK regulators of the cell cycle with a potential of being targeted by PfUT, one could consider plant-like calcium-dependent protein kinases (CDPKs), such as PfCDPK5 (Absalon et al., 2018) and PfCDPK7 (Kumar et al., 2014), the disruption of which has been associated with the blocked egress and altered proliferation, respectively. Another possible target could be a cyclic GMP-dependent protein kinase PfPKG, as it has been proven to play a crucial role in parasite egress and invasion (Alam et al., 2015; Ganter et al., 2017). A eukaryotic elongation factor 1A (eEF1A) could also be considered, as its knockout in *P. berghei* blood stages revealed associated with the G1 phase increase of the parasite cycle length of up to 4 h (Janse et al., 2003). Another interesting PfUT's substrate candidate might include the already mentioned in the preceding chapter dipeptidyl aminopeptidase DPAP3, shown to be important for parasite proliferation and merozoite invasion (Lehmann et al., 2018). The findings from other studies summarized here do not explain the mechanisms underlying the phenotype of PfUT-HA-glmS parasites, but highlight candidate proteins and biological processes which could be further examined using genetic manipulation methods.

Intriguingly, the STRING (Search Tool for the Retrieval of Interacting Genes/Proteins) database containing known and predicted protein-protein interactions, depicted in the network of PfUT, apart from a few components of a ubiquitin proteasome system, a plasmodial homologue of cell division cycle 48 (CDC48) (PFF0940c/PF3D7\_0619400) and a DNA repair protein RAD23 (PF10\_0114/PF3D7\_1011700) (Appendix I, Fig. I.2), the alteration of which could potentially affect parasite proliferation. CDC48 is associated with the ERAD pathway AAA-type ATPase, suggested to play degradative and regulatory roles in many processes, as well as to maintain the cellular homoeostasis (Chung et al., 2012; Imamura et al., 2012; Ponts et al., 2008a; Wang et al., 2015). Notably, in yeasts, CDC48 has been shown to be involved in the degradation of critical cell cycle regulators (Ye, 2006). RAD23 has been characterized as a linker of DNA repair and the ubiquitin/proteasome pathways, as it belongs to a nucleotide excision repair (NER) pathway (Gupta et al., 2016), but is also known to shuttle polyubiquitinated proteins to the 19S regulatory subunit of the proteasome (Kirkpatrick et al., 2005; Wang et al., 2015). A validation of these two proteins as substrates of PfUT, for instance via Western Blot and IFA, might be worth considering.

Another important finding might be a potential involvement of PfUT in tryptophan metabolism, with a special focus on biosynthesis of its derivative, indole-3-acetate, as suggested by MetaCyc Metabolic Pathway and KEGG (Kyoto Encyclopedia of Genes and Genomes) databases. It has been reported that various tryptophan-derived indolamines regulate the *P. falciparum* cell cycle by increasing the levels of cytosolic calcium (Beraldo & Garcia, 2005). Presence in the parasite culture medium of one of them, melatonin, as well as of its precursors, substantially increased maturation of young stages into schizonts followed by enhanced parasite invasion rates. Furthermore, melatonin was shown to activate phospholipase C (PLC), which generates inositol triphosphates (IP3) and in turn opens ER-localized IP3-sensitive calcium channels (Alves et al., 2011). The localization nearby the ER and a high likelihood of the cell cycle progression being regulated by this process prompts to speculate, that overexpressed PfUT reduces the levels of some of the tryptophan derivatives, in turn leading to slowed-down parasite maturation and decreased invasion efficiencies. To test this hypothesis, the cytosolic levels of calcium could be compared in WT and HA-glmS parasites, which one would expect to be decreased in the mutant line. Alternatively, a metabolomic analysis could be conducted. Noteworthy, the process described here associates lipid metabolism with the observed phenotype of PfUT-HA-glmS, which as suggested earlier could also be involved in the increased fitness of PfCRT S33 mutants. As in the case of an aforementioned phospholipid, namely phosphatidylcholine, a phospholipase A (PLA) facilitates the hydrolysis of phosphatidylinositol (PI) to lysophosphatidylinositol (LPI), which can be further processed to inositol and fatty acids (FA) by lysophospholipase A (LPLA) (Hurley & McCormick, 2008), much like in the case of the aforementioned

phosphatidylcholine (compare with Fig. 4.1 found in chapter 4.1.2). Thus, PfUT and PfCRT might be linked through the lipids catabolism pathway. This might possibly explain the dependency of the quinine resistance profile on the presence of mutant versions of both these genes. It is also worth mentioning that IP3 is a hydrolysis product of phosphatidylinositol bisphosphate (PIP2), which when phosphorylated by a phosphatidylinositol-3-kinase (PI3K) appears as phosphatidylinositol trisphosphate (PIP3). In turn, in the artemisinin resistant *P. falciparum* increased levels of PfPI3K and, hence, its product PIP3 were associated with a mutated variant of Kelch13 (a substrate adapter for a yet unidentified Cullin-RING E3 ubiquitin ligase), which mediates a reduction of the degradative polyubiquitination of PfPI3K (Coppée et al., 2018; Mbengue et al., 2015; Ng et al., 2017). Taken together, the information referred to in this paragraph suggest that regulation of the phospholipids synthesis and turnover might have a critical role for the parasite susceptibility to various antimalarial drugs.

Once the substrates of PfUT are identified, it will be of interest to determine the site of ubiquitination as well as the type and topology of ubiquitin chain linkages generated by PfUT. Some of the above exemplified methods may address this issue within the scope of the conducted approach (such as diGly proteomics), whereas the other ones will need additional effort. A variety of antibodies is available on the market, facilitating recognition of either diGly remnants (Lys-ε-Gly-Gly) produced by trypsin digestion (Kim et al., 2011; Wagner et al., 2011) or whole polyubiquitin chains (Matsumoto et al., 2010; Newton et al., 2008). Different polyubiquitin chain types are recognized by ubiquitin-binding-domains (UBDs) of distinct proteins and targeted to specific signalling pathways (chapter 1.3.3). For example, PfUT's substrates displaying lysine 48-linked polyubiquitin chains would indicate the role of this ubiquitin ligase in the proteasomal degradation, whereas, polyubiquitination through lysine 63 would suggest its involvement in non-degradative cellular processes, such as kinase activation, DNA damage tolerance, signal transduction or endocytosis (Hamilton et al., 2014; Suryadinata et al., 2014).

### 4.2.3. PfUT is likely essential for *P. falciparum* blood stages

The efficiency of the conditional glmS ribozyme system applied in the current study turned out to be below the expectations resulting on average in 40% and 70% downregulation of PfUT upon glucosamine exposure, as evaluated via anti-HA and anti-N-terminal PfUT staining, respectively. Although for various proteins such incomplete knockdown might be already sufficient to conclude about its importance for the parasite, in case of overexpressed PfUT, it only brings us close to the abundance levels of its wild type variant. Addressing this issue an alternative gene disruption strategy called SLI-TGD revealed that *pfut* was refractory to truncation. Such finding, according to the

designers of the system, is an indication of PfUT being likely essential (Birnbaum et al., 2017). However, a definite proof of PfUT indispensability is still missing and could be approached either chemically or via genetic engineering. While a non-genetic method to inactivate PfUT using selective inhibitors may seem to be straight forward, finding specific inhibitors exclusively targeting PfUT could be challenging. An interesting alternative appears to be a selective chemical labelling using Fluorophore-Assisted Laser Inactivation (FALI) technique, though it is not yet established in *Plasmodium* (Marks et al., 2004). Despite the fact that genetic manipulations may uncontrollably alter protein localization or function, as seen on the example of HA-glmS transgenic line, an implementation of another available conditional knockdown strategy (chapter 1.4.2) seems to be reasonable for controllable downregulation of PfUT, permitting to link the phenotype to the protein abundance. Alternatively, improvement of the glmS ribozyme strategy could be attempted to achieve more pronounced downregulation levels. As shown in Fig. 3.9, glucosamine concentration could not be increased over 5 mM, because of its toxicity for the parasite. However, one could consider an exchange of the glmS ribozyme by another riboswitch from the inducible self-cleavage ribozymes class (Felletti et al., 2016; Lee & Lee, 2017). Moreover, incorporation of double- or triple-tandem riboswitches may substantially improve the regulation of gene expression, likewise it occurs naturally in such multiple form in *Bacillus thuringiensis* (Zhou et al., 2016). Furthermore, for all likely essential genes according to the SLI-TGD, authors of the selection-lined integration (SLI) approach suggest to conduct their further functional analysis using knock sideways (KS) strategy (Birnbaum et al., 2017). KS relies on mislocalization of native proteins to another subcellular compartment via rapalog-induced dimerization of FRB\* and FKBP fusion proteins (Birnbaum et al., 2017).

A functional genomics study conducted by the research group of Dr. John Adams, based on the *piggyBac* transposon-mediated mutagenesis of the *P. falciparum* genome characterized PfUT as a gene dispensable for asexual blood-stage development (Zhang et al., 2018). The analysis was based on the mutagenesis index score (MIS) depending on the number of identified *piggybac* insertions relative to the possible target sites within a particular gene, and a mutagenesis fitness score (MFS) defining the mutant's growth fitness. While high MIS and low MFS qualifies mutant PfUT as a "growth winner" in the additionally performed *in vitro* growth screen, the herein described alteration of PfUT expression clearly revealed a contrary effect. Furthermore, according to their analysis essential genes have significantly enhanced expression levels throughout the intraerythrocytic cycle and their gene ontology (GO) functions are associated among others with cell cycle control, DNA replication, ER-associated ubiquitin-dependent protein catabolism or response to drugs. This contrasts the aforementioned findings that PfUT has relatively low and homogenous expression levels, with the data presented herein suggesting that it might be involved in cell cycle regulation. At

the same time, another study performed in *P. berghei* annotated PfUT as likely essential for asexual blood stage growth, based on the growth rates measurement of barcoded knockout mutants (Bushell et al., 2017). Nevertheless, a rodent malaria model does not necessarily reflect the observations made in a human pathogen, as *Plasmodium* harbours species-related differences in the genome (Frech & Chen, 2011). Given that *P. falciparum* encodes three other HECT ubiquitin ligases (PF3D7\_0628100, PF3D7\_0826100, PF3D7\_1119400) and approximately 50 E3-type or E3-like enzymes (Hamilton et al., 2014), they might potentially be capable of maintaining the ubiquitin-mediated cellular homeostasis in case of PfUT's absence. Hence, one cannot rule out the possibility that PfUT might not be essential for parasite's survival, yet still playing a crucial role in its development.

Another aspect potentially indicating the importance of PfUT for the parasite's intraerythrocytic life cycle concerns difficulties in terms of its genetic manipulation. Despite multiple attempts to diversely modify either the N- or C-terminus of PfUT (Appendix I, Fig. I.5), only the incorporation of a small HA-tag was successful. Inability to inactivate PfUT's HECT catalytic domain may further support the relevance of this ubiquitin ligase to be fully functional for parasite's viability. Nonetheless, it might not necessarily point to PfUT's indispensability, but instead be linked to the technical bottlenecks of working with *P. falciparum*. On the one hand, parasite genome with an AT content of 80.6% (Gardner et al., 2002) makes genetic engineering challenging and prone to errors. Another limitation includes the availability of the fully sequenced *P. falciparum* genome only for the 3D7 strain, restricting the design of efficient guide RNAs and instead increasing the risk of possible off-target sites of RNA-guided Cas9 endonuclease in other parasite strains. Presumably, this might be a reason why the HA-glms recombination was possible in the 3D7, but not in Dd2 strain, despite multiple attempts. In any case, one cannot rule out with complete confidence the possibility that the issue lies in parasites' genetic background carrying either the wild type or mutant PfUT variant, and alteration of the latter might be potentially more harmful for the drug resistant parasite, such as Dd2. Furthermore, efficiencies of the available transfection methods remain relatively low, representing a serious limitation for the successful genetic engineering-based experiment (Hasenkamp et al., 2012; Skinner-Adams et al., 2003). Although there is no universal rule regarding the number of gene truncation trials, which permit definitive conclusions about protein's indispensability, the reliance solely on inability to delete or disrupt a gene is a relatively poor indicator of its essentiality. Therefore, another attempt to conditionally downregulate PfUT appears to be desired for an unambiguous conclusion with respect to its significance for the parasite.

Based on PfUT interacting networks, it seems that the function of PfUT might be associated with the ERAD pathway and proteasomal degradation. However, the prominent size of the protein and the

fact that it is being post-translationally modified may indicate that PfUT has multiple, yet undefined roles. For example, a recently reported activity-based profiling of mammalian E3 ligases revealed one with an esterification activity (Pao et al., 2018). Interestingly, this particular E3 ligase displayed threonine selectivity and even contained two catalytic cysteines involved in thioester intermediate formation. Such an activity-based protein profiling has been already approached in *P. falciparum*, as shown on the example of PfUCH54, for which deubiquitinating and deneddylating activities were found (Artavanis-Tsakonas et al., 2006). Therefore, one could also consider attempting this technique to unravel the potential activities of PfUT.

#### 4.2.4. Association of PfUT with resistance to quinine and quinidine

PfUT has been previously suggested as a novel candidate gene of multifactorial resistance to QN, as it altered responses to this drug in parasite strains bearing mutated PfCRT background (Sanchez et al., 2014). Although *P. falciparum* 3D7 carries PfCRT sensitive alleles, it still shows a semi-resistance profile with regard to quinine. To that end, the PfUT-HA-glmS line was tested for responses to various quinoline drugs, revealing increased susceptibility to QN and QD, not affecting the CQ control. Given that QN targets the mature trophozoites and that the S phase of the PfUT-HA-glmS line is extended, it seems reasonable to observe an increased susceptibility of these parasites, as the drug had more time to act on their late stage forms. On the other hand, bearing in mind that QN blocks the haemoglobin detoxification pathway causing specific oxidative stress, in parasites with likely imbalanced homeostasis due to PfUT overexpression, QN might have even more pronounced toxic effect. Nonetheless, if the presence of QN increases protein oxidation, so does CQ, which also prevents hemozoin biocrystallization. Thus, the PfUT-HA-glmS parasites should also exhibit increased sensitivity towards CQ, yet they do not. However, in case of average IC<sub>50</sub> values at 10 nM the potential differences might be just difficult to detect. To test whether the observed differences in quinine responsiveness between WT and HA-glmS lines result from the prolonged drug-parasite contact or if it is rather a response of enhanced environmental toxicity, the measurements of IC<sub>50</sub> values could be repeated including a drug from other than the quinolines class of antimalarials. It would be beneficial not only to select a drug to which resistance is determined by a particular gene unlikely to be involved in responses to QN, but at the same time displaying higher IC<sub>50</sub> values for a transparent interpretation of results. No differences observed for additionally tested compounds might suggest that the observed herein phenotypic drug susceptibility of HA-glmS transgenic line is linked to the elongated exposure of late stage parasites to the drug.

For definitive proof of PfUT being implicated in resistance to quinine, an allelic exchange should be approached. Replacement of the five conserved polymorphic residues within PfUT (chapter 1.3.3, Fig.



1.9) in the resistant Dd2 strain by the sensitive alleles from 3D7 strain, followed by analysis of the drug responsiveness profiles of these mutants could possibly validate whether or not this HECT ubiquitin ligase is associated with resistance to the mentioned quinoline drug. Multiple CRISPR-Cas9-mediated attempts to generate allelic exchange mutants were unsuccessful, likely due to potential RNA-guided off-target effects in the Dd2 strain, for which the genomic sequence is not fully resolved.

An alternative method for the identification of drug resistance determinants may be the *in vitro* development of resistance forced by a gradual increase of drug pressure in the parasite culture (Menard et al., 2015; Nzila & Mwai, 2010; Oduola & Bowdre, 1988; Witkowski et al., 2009). The progress of the resistance rising due to the emergence of adaptive mutations could be monitored via  $IC_{50}$  measurements. Whole genome sequencing would then reveal the genes associated with the notably reduced drug susceptibility, which might include factors commonly found in field isolates, but also genes so far not linked to the drug resistance profile. Although the development of a quinine resistant line has been attempted in *P. falciparum* Dd2 strain, it did not prove successful. In fact, the increase of the quinine  $IC_{50}$  values has been observed along with the applied pressure, but parasite freezing-thawing events (required, for example, after unfortunate culture contamination) revealed a significant drop in the quinine response, almost to the initial levels, which raised again upon exposure to high QN doses (Appendix I, Fig. I.6). Interestingly, parasites under treatment seemed to grow slower than the untreated control culture, yet still appeared morphologically healthy despite the applied concentration of the drug (data not shown). This might be an indication of adaptive epigenetic changes driving parasite's survival under pressure, rather than the development of mutations. Several reports have demonstrated that *P. falciparum* is capable of directing transcriptional responses as an adaptation to changing environmental conditions (Merrick & Duraisingh, 2010; Rovira-Graells et al., 2012) and that it maintains the epigenetic memory to ensure its survival (Chookajorn et al., 2007; Voss et al., 2014). Therefore, it could be interesting to conduct a transcriptomic analysis of these quinine pressured parasites aiming to identify factors responsible for their intriguing phenotype. If PfUT is indeed associated with quinine resistance then this analysis could potentially reveal one of PfUT's interacting partners. As aforementioned, the experiment was carried out using a Dd2 strain as a "baseline", bearing mutated variants of PfCRT and PfUT and displaying moderate levels of quinine resistance. Numerous studies have shown that strains already resistant to at least one drug are more amenable to give rise to the resistance to another drug (Nzila & Mwai, 2010). Hence, for future investigations, one could consider to use a parasite strain with resistance already developed but against a drug other than quinine.

It has just recently been revealed that quinine targets a component of the *P. falciparum* purine salvage pathway, a purine nucleoside phosphorylase PfPNP (Dziekan et al., 2019). Since in various

organisms PNP is also involved in nicotinate and nicotinamide metabolism (MetaCyc and KEGG databases), which in turn is associated with tryptophan metabolism, theoretically there might be an indirect connection between the PfUT and PfPNP, so that the PfUT-mediated alteration of this pathways could potentially assure parasite's resistance to quinine. It has been suggested that *P. falciparum* nicotinamide adenine dinucleotide (NAD<sup>+</sup>) pathway relies on the uptake of exogenous nicotinic acid and nicotinamide, which in most eukaryotes are biosynthesized from tryptophan (O'Hara et al., 2014). Nevertheless, the NAD metabolism is not yet fully understood in *P. falciparum*, and since resistant parasites have been shown to maintain enhanced metabolic flexibility (Carey et al., 2017), it is possible that the parasite contains a parallel biosynthetic pathway, which is utilized differently by sensitive and resistant parasites.

Apart from the previously mentioned alteration of the cell cycle G1 phase and Kelch13-mediated increase of PIP3 levels, resistance to artemisinin is also associated with an upregulation of genes encoding unfolded protein response (UPR), including arrest of protein translation, increased production of chaperons and degradation of unfolded and misfolded proteins (Dogovski et al., 2015; Mok et al., 2015). Resistance to quinine might be likewise associated with an increased ability to manage oxidative stress and alteration of the genes involved in cell cycle regulation. PfUT could potentially play a role in mediating the resistance, as indicated by similarities of the cellular processes implicated in reduced artemisinin susceptibility and the ones influenced by PfUT. PfUT seems not only to control the cell cycle progression and the levels of indole-derivative indirectly regulating production of IP3, but its localization at ER/Golgi suggests that it might be also implicated in modulation of ER homeostasis via UPR. Along the same lines, PfUT partially colocalizes with proteins belonging to the UPR pathway, namely BiP and ERC (Fig. 3.13), which were upregulated in artemisinin resistant parasites (Mok et al., 2015; Paloque et al., 2016). To investigate these speculations one could challenge the quinine resistant parasites (e.g. Dd2 or an *in vitro* developed resistant strain) with compounds causing oxidative damage and inducing ER stress, such as H<sub>2</sub>O<sub>2</sub> and DTT, respectively (Rocamora et al., 2018). If the mechanism underlying quinine susceptibility is indeed associated with stress responses to the oxidative damage and the UPR, then these parasites should also reveal resistance to the mentioned inhibitors.

Unravelling the importance of PfUT for the parasite development as well as its contribution to the quinine resistance might make PfUT an interesting drug target candidate. A drug therapy consisting of quinine combined with a PfUT inhibitor could potentially preserve an application of this valuable antimalarial drug.

## 5. Conclusion

This project was undertaken to evaluate the impact of phosphorylation and ubiquitination on the intraerythrocytic development and drug susceptibility of the human malaria parasite *P. falciparum*. Phosphorylation of PfCRT's serine 33 has been shown to regulate the drug resistance-mediating function of this transporter. A natural progression of this work is to identify the kinase implicated in this phenomenon. Provided that the defined kinase exhibits no homology to human enzymes or at least distinct binding sites for potential inhibitors, it could be a valuable target of antimalarial agents. Combination therapy comprising the kinase inhibitor and chloroquine or quinine could potentially reduce or prevent the further spread of resistance to these valuable drugs.

The second major finding concerns the PfUT-mediated regulation of the parasite cycle progression. Nevertheless, a comprehensive understanding of the mechanisms underpinning the cell cycle lengthening of the transgenic PfUT-HA-glmS line requires identification of natural substrates of PfUT. Such an investigation might also reveal other cellular functions of this prominent HECT E3 ubiquitin ligase. Although mutant parasites displayed altered responses to quinine and quinidine, a direct proof of PfUT's association with the reduced susceptibility to these quinolines requires further efforts. Nonetheless, given the importance of the ubiquitin-proteasome pathway in controlling fundamental aspects of *P. falciparum* biology, its components, including PfUT, are appealing targets for malaria therapeutic intervention.

## 6. References

- Absalon, S., Blomqvist, K., Rudlaff, R. M., DeLano, T. J., Pollastri, M. P., & Dvorin, J. D. (2018). Calcium-Dependent Protein Kinase 5 is required for release of egress-specific organelles in *Plasmodium falciparum*. *mBio*, 9(1), e00130-18. <https://doi.org/10.1128/MBIO.00130-18>
- Achan, J., Talisuna, A. O., Erhart, A., Yeka, A., Tibenderana, J. K., Baliraine, F. N., ... D'Alessandro, U. (2011). Quinine, an old anti-malarial drug in a modern world: role in the treatment of malaria. *Malaria Journal*, 10(1), 144. <https://doi.org/10.1186/1475-2875-10-144>
- Adisa, A., Albano, F. R., Reeder, J., Foley, M., & Tilley, L. (2001). Evidence for a role for a *Plasmodium falciparum* homologue of Sec31p in the export of proteins to the surface of malaria parasite-infected erythrocytes. *Journal of Cell Science*, 113(12), 2177–2185. Retrieved from <http://jcs.biologists.org/content/114/18/3377>
- Adler, G., Mishra, A. K., Maymon, T., Raveh, D., & Bar-Zvi, D. (2018). Overexpression of Arabidopsis ubiquitin ligase AtPUB46 enhances tolerance to drought and oxidative stress. *bioRxiv*, 379859. <https://doi.org/10.1101/379859>
- Aggarwal, S., Kandpal, M., Asthana, S., & Yadav, A. K. (2017). Perturbed signaling and role of posttranslational modifications in cancer drug resistance. *Drug Resistance in Bacteria, Fungi, Malaria, and Cancer*, (January 2018), 1–629. <https://doi.org/10.1007/978-3-319-48683-3>
- Ahmad, S., & Glazer, R. I. (1993). Expression of the antisense cDNA for protein kinase C alpha attenuates resistance in doxorubicin-resistant MCF-7 breast carcinoma cells. *Molecular Pharmacology*, 43(6), 858-862. Retrieved from <http://molpharm.aspetjournals.org/content/43/6/858>
- Alam, M. M., Solyakov, L., Bottrill, A. R., Flueck, C., Siddiqui, F. A., Singh, S., ... Tobin, A. B. (2015). Phosphoproteomics reveals malaria parasite Protein Kinase G as a signalling hub regulating egress and invasion. *Nature Communications*, 6(1), 7285. <https://doi.org/10.1038/ncomms8285>
- Alves, E., Bartlett, P. J., Garcia, C. R. S., & Thomas, A. P. (2011). Melatonin and IP3-induced Ca<sup>2+</sup> release from intracellular stores in the malaria parasite *Plasmodium falciparum* within infected red blood cells. *The Journal of Biological Chemistry*, 286(7), 5905–12. <https://doi.org/10.1074/jbc.M110.188474>
- Antony, H. A., & Parija, S. C. (2016). Antimalarial drug resistance: An overview. *Tropical Parasitology*, 6(1), 30–41. <https://doi.org/10.4103/2229-5070.175081>
- Aravind, L., Iyer, L. M., Wellems, T. E., & Miller, L. H. (2003). *Plasmodium* biology: genomic gleanings. *Cell*, 115(7), 771–85. [https://doi.org/10.1016/S0092-8674\(03\)01023-7](https://doi.org/10.1016/S0092-8674(03)01023-7)
- Ardiani, A., Goyke, A., & Black, M. E. (2009). Mutations at serine 37 in mouse guanylate kinase confer resistance to 6-thioguanine. *Protein Engineering, Design & Selection: PEDS*, 22(4), 225–32. <https://doi.org/10.1093/protein/gzn078>
- Ariey, F., Witkowski, B., Amaratunga, C., Beghain, J., Langlois, A.-C., Khim, N., ... Ménard, D. (2014). A molecular marker of artemisinin-resistant *Plasmodium falciparum* malaria. *Nature*, 505(7481), 50–5. <https://doi.org/10.1038/nature12876>
- Arrow, K. J., Panosian, C., & Gelband, H. (2004). Saving Lives, Buying Time: Economics of Malaria Drugs in an Age of Resistance. *Library of Congress Cataloging-in-Publication Data* (Vol. 388). Retrieved from <http://www.nap.edu/catalog/11017.html>

- Artavanis-Tsakonas, K., Misaghi, S., Comeaux, C. A., Catic, A., Spooner, E., Duraisingh, M. T., & Ploegh, H. L. (2006). Identification by functional proteomics of a deubiquitinating/deNeddylating enzyme in *Plasmodium falciparum*. *Molecular Microbiology*, 61(5), 1187–1195. <https://doi.org/10.1111/j.1365-2958.2006.05307.x>
- Artavanis-Tsakonas, K., Weihofen, W. A., Antos, J. M., Coleman, B. I., Comeaux, C. A., Duraisingh, M. T., ... Ploegh, H. L. (2010). Characterization and structural studies of the *Plasmodium falciparum* ubiquitin and Nedd8 hydrolase UCHL3. *Journal of Biological Chemistry*, 285(9), 6857–6866. <https://doi.org/10.1074/jbc.M109.072405>
- Azevedo, M. F. de, Gilson, P. R., Gabriel, H. B., Simões, R. F., Angrisano, F., Baum, J., ... Wunderlich, G. (2012). Systematic analysis of fkbp inducible degradation domain tagging strategies for the human malaria parasite *Plasmodium falciparum*. *PLoS ONE*, 7(7). <https://doi.org/10.1371/JOURNAL.PONE.0040981>
- Baer, K., Klotz, C., Kappe, S. H. I., Schnieder, T., & Frevert, U. (2007). Release of hepatic *Plasmodium yoelii* merozoites into the pulmonary microvasculature. *PLoS Pathogens*, 3(11), e171. <https://doi.org/10.1371/journal.ppat.0030171>
- Balabaskaran-Nina, P., & Desai, S. A. (2018). Diverse target gene modifications in *Plasmodium falciparum* using Bxb1 integrase and an intronic attB. *Parasites & Vectors*, 11(1), 548. <https://doi.org/10.1186/s13071-018-3129-5>
- Balu, B., Shoue, D. A., Fraser, M. J., Adams, J. H., & Adams, J. H. (2005). High-efficiency transformation of *Plasmodium falciparum* by the lepidopteran transposable element piggyBac. *Proceedings of the National Academy of Sciences of the United States of America*, 102(45), 16391–6. <https://doi.org/10.1073/pnas.0504679102>
- Bange, T., Sigismund, S., Penengo, L., & Polo, S. (2007). The ubiquitination code: a signalling problem. *Cell Division*, 2(1), 11. <https://doi.org/10.1186/1747-1028-2-11>
- Bao, X., Johnson, J. L., & Rao, H. (2015). Rad25 protein is targeted for degradation by the Ubc4-Ufd4 pathway. *The Journal of Biological Chemistry*, 290(13), 8606–12. <https://doi.org/10.1074/jbc.M114.618793>
- Baum, J., Papenfuss, A. T., Mair, G. R., Janse, C. J., Vlachou, D., Waters, A. P., ... de Koning-Ward, T. F. (2009). Molecular genetics and comparative genomics reveal RNAi is not functional in malaria parasites. *Nucleic Acids Research*, 37(11), 3788–98. <https://doi.org/10.1093/nar/gkp239>
- Beaudenon, S., Dastur, A., & Huibregtse, J. M. (2005). Expression and Assay of HECT Domain Ligases. *Methods in Enzymology*, 398, 112–125. [https://doi.org/10.1016/S0076-6879\(05\)98011-7](https://doi.org/10.1016/S0076-6879(05)98011-7)
- Beck, J. R., Muralidharan, V., Oksman, A., & Goldberg, D. E. (2014). PTEX component HSP101 mediates export of diverse malaria effectors into host erythrocytes. *Nature*, 511(7511), 592–5. <https://doi.org/10.1038/nature13574>
- Bei, A. K., Brugnara, C., & Duraisingh, M. T. (2010). *In vitro* genetic analysis of an erythrocyte determinant of malaria infection. *The Journal of Infectious Diseases*, 202(11), 1722–1727. <https://doi.org/10.1086/657157>
- Bei, A. K., Desimone, T. M., Badiane, A. S., Ahouidi, A. D., Dieye, T., Ndiaye, D., ... Duraisingh, M. T. (2010). A flow cytometry-based assay for measuring invasion of red blood cells by *Plasmodium falciparum*. *American Journal of Hematology*, 85(4), 234–7. <https://doi.org/10.1002/ajh.21642>

- Beraldo, F. H., & Garcia, C. R. S. (2005). Products of tryptophan catabolism induce  $\text{Ca}^{2+}$  release and modulate the cell cycle of *Plasmodium falciparum* malaria parasites. *Journal of Pineal Research*, 39(3), 224–230. <https://doi.org/10.1111/j.1600-079X.2005.00249.x>
- Bhasin, V. K., & Trager, W. (1984). Gametocyte-forming and non-gametocyte-forming clones of *Plasmodium falciparum*. *The American Journal of Tropical Medicine and Hygiene*, 33(4), 534–7. Retrieved from <http://www.ncbi.nlm.nih.gov/pubmed/6383092>
- Bio-Rad Laboratories. (2006). Real-Time PCR Applications Guide. *www.bio-Rad.com*, 1–105. <https://doi.org/10.1007/s13181-011-0177-z>
- Birnbaum, J., Flemming, S., Reichard, N., Blancke Soares, A., Mes, P., Jonscher, E., ... Spielmann, T. (2017). A genetic system to study *Plasmodium falciparum* protein function. <https://doi.org/10.1038/nmeth.4223>
- Blasco, B., Leroy, D., & Fidock, D. A. (2017). Antimalarial drug resistance: linking *Plasmodium falciparum* parasite biology to the clinic. *Nature Medicine*, 23(8), 917–928. <https://doi.org/10.1038/nm.4381>
- Bloiland, P. B. (2001). Anti-infective drug resistance surveillance and containment team. Drug resistance in malaria. *World Health Organization*. Retrived from <http://www.who.int/iris/handle/10665/66847>
- Blomqvist, K., DiPetrillo, C., Strega, V. A., Pine, S., & Dvorin, J. D. (2017). Receptor for Activated C-Kinase 1 (PfRACK1) is required for *Plasmodium falciparum* intra-erythrocytic proliferation. *Molecular and Biochemical Parasitology*, 211, 62–66. <https://doi.org/10.1016/j.molbiopara.2016.10.002>
- Bopp, S. E. R., Manary, M. J., Bright, A. T., Johnston, G. L., Dharia, N. V, Luna, F. L., ... Winzeler, E. A. (2013). Mitotic evolution of *Plasmodium falciparum* shows a stable core genome but recombination in antigen families. *PLoS Genetics*, 9(2), e1003293. <https://doi.org/10.1371/journal.pgen.1003293>
- Boyle, M. J., Wilson, D. W., Richards, J. S., Riglar, D. T., Tetteh, K. K. A., Conway, D. J., ... Beeson, J. G. (2010). Isolation of viable *Plasmodium falciparum* merozoites to define erythrocyte invasion events and advance vaccine and drug development. *Proceedings of the National Academy of Sciences of the United States of America*, 107(32), 14378–83. <https://doi.org/10.1073/pnas.1009198107>
- Bozdech, Z., Llinás, M., Pulliam, B. L., Wong, E. D., Zhu, J., & DeRisi, J. L. (2003). The transcriptome of the intraerythrocytic developmental cycle of *Plasmodium falciparum*. *PLoS Biology*, 1(1), e5. <https://doi.org/10.1371/journal.pbio.0000005>
- Bray, P. G., Martin, R. E., Tilley, L., Ward, S. A., Kirk, K., & Fidock, D. A. (2005). Defining the role of PfCRT in *Plasmodium falciparum* chloroquine resistance. *Molecular Microbiology*, 56(2), 323–333. <https://doi.org/10.1111/j.1365-2958.2005.04556.x>
- Bruce-Chwatt, L. J. (1962). Classification of antimalarial drugs in relation to different stages in the life-cycle of the parasite: commentary on a diagram. *Bulletin of the World Health Organization*, 27(2), 287–90. Retrieved from <http://www.ncbi.nlm.nih.gov/pubmed/14016124>
- Bunditvorapoom, D., Kochakarn, T., Kotanan, N., Modchang, C., Kümpornsinsin, K., Loesbanluechai, D., ... Chookajorn, T. (2018). Fitness loss under amino acid starvation in artemisinin-resistant *Plasmodium falciparum* isolates from Cambodia. *Scientific Reports*, 8(1), 12622. <https://doi.org/10.1038/s41598-018-30593-5>

- Bushell, E., Gomes, A. R., Sanderson, T., Anar, B., Girling, G., Herd, C., ... Billker, O. (2017). Functional profiling of a *Plasmodium* genome reveals an abundance of essential genes. *Cell*, 170(2), 260–272.e8. <https://doi.org/10.1016/j.cell.2017.06.030>
- Carey, M. A., Papin, J. A., & Guler, J. L. (2017). Novel *Plasmodium falciparum* metabolic network reconstruction identifies shifts associated with clinical antimalarial resistance. *BMC Genomics*, 18(1), 543. <https://doi.org/10.1186/s12864-017-3905-1>
- Carlton, J. M. (2018). Malaria parasite evolution in a test tube: Experimental evolution studies reveal drug targets and resistance mechanisms. *Science*, 359(6372), 2017–2018.
- Carvalho, T. G., & Ménard, R. (2005). Manipulating the *Plasmodium* genome. *Current Issues in Molecular Biology*, 7(1), 39–56. Retrieved from <https://www.ncbi.nlm.nih.gov/pubmed/15580779>
- Chang, H. H., Park, D. J., Galinsky, K. J., Schaffner, S. F., Ndiaye, D., Ndir, O., ... Hartl, D. L. (2012). Genomic sequencing of *Plasmodium falciparum* malaria parasites from Senegal reveals the demographic history of the population. *Molecular Biology and Evolution*, 29(11), 3427–3439. <https://doi.org/10.1093/molbev/mss161>
- Charnaud, S. C., Kumarasingha, R., Bullen, H. E., Crabb, B. S., & Gilson, P. R. (2018). Knockdown of the translocon protein EXP2 in *Plasmodium falciparum* reduces growth and protein export. *PLoS ONE*, 13(11), e0204785. <https://doi.org/10.1371/journal.pone.0204785>
- Chavchich, M., Gerena, L., Peters, J., Chen, N., Cheng, Q., & Kyle, D. E. (2010). Role of pfmdr1 amplification and expression in induction of resistance to artemisinin derivatives in *Plasmodium falciparum*. *Antimicrobial Agents and Chemotherapy*, 54(6), 2455–64. <https://doi.org/10.1128/AAC.00947-09>
- Chen, S., Zhao, H., Wang, M., Li, J., Wang, Z., Wang, F., ... Ahammed, G. J. (2017). Overexpression of E3 ubiquitin ligase gene AdBiL contributes to resistance against chilling stress and leaf mold disease in tomato. *Frontiers in Plant Science*, 8, 1109. <https://doi.org/10.3389/fpls.2017.01109>
- Chookajorn, T., Dzikowski, R., Frank, M., Li, F., Jiwani, A. Z., Hartl, D. L., & Deitsch, K. W. (2007). Epigenetic memory at malaria virulence genes. *Proceedings of the National Academy of Sciences of the United States of America*, 104(3), 899–902. Retrieved from <https://www.ncbi.nlm.nih.gov/pubmed/17209011>
- Chotivanich, K., Udomsangpetch, R., Simpson, J. A., Newton, P., Pukrittayakamee, S., Looareesuwan, S., & White, N. J. (2000). Parasite multiplication potential and the severity of *falciparum* malaria. *The Journal of Infectious Diseases*, 181(3), 1206–1209. <https://doi.org/10.1086/315353>
- Chung, D.-W. D., Ponts, N., Cervantes, S., & Le Roch, K. G. (2009). Post-translational modifications in *Plasmodium*: More than you think! *Molecular and Biochemical Parasitology*, 168(2), 123–134. <https://doi.org/10.1016/J.MOLBIOPARA.2009.08.001>
- Chung, D.-W. D., Ponts, N., Prudhomme, J., Rodrigues, E. M., & Le Roch, K. G. (2012). Characterization of the ubiquitylating components of the human malaria parasite's protein degradation pathway. *PLoS One*, 7(8), e43477. <https://doi.org/10.1371/journal.pone.0043477>
- Church, L. W., Le, T. P., Bryan, J. P., Gordon, D. M., Edelman, R., Fries, L., ... Hoffman, S. L. (1997). Clinical manifestations of *Plasmodium falciparum* malaria experimentally induced by mosquito challenge. *The Journal of Infectious Diseases*, 175(4), 915–20. Retrieved from <http://www.ncbi.nlm.nih.gov/pubmed/9086149>

- Claessens, A., Harris, L. M., Stanojcic, S., Chappell, L., Stanton, A., Kuk, N., ... Merrick, C. J. (2018). RecQ helicases in the malaria parasite *Plasmodium falciparum* affect genome stability, gene expression patterns and DNA replication dynamics. *PLoS Genetics*, 14(7), e1007490. <https://doi.org/10.1371/journal.pgen.1007490>
- Cobb, D. W., Florentin, A., Fierro, M. A., Krakowiak, M., Moore, J. M., & Muralidharan, V. (2017). The Exported Chaperone PfHsp70x Is Dispensable for the *Plasmodium falciparum* Intraerythrocytic Life Cycle. *mSphere*, 2(5), e00363-17. <https://doi.org/10.1128/mSphere.00363-17>
- Cobbold, S. A., Santos, J. M., Ochoa, A., Perlman, D. H., & Llinás, M. (2016). Proteome-wide analysis reveals widespread lysine acetylation of major protein complexes in the malaria parasite. *Scientific Reports*, 6, 19722. <https://doi.org/10.1038/srep19722>
- Collins, C. R., Hackett, F., Atid, J., Tan, M. S. Y., & Blackman, M. J. (2017). The *Plasmodium falciparum* pseudoprotease SERA5 regulates the kinetics and efficiency of malaria parasite egress from host erythrocytes. *PLoS Pathogens*, 13(7), e1006453. <https://doi.org/10.1371/journal.ppat.1006453>
- Collins, C. R., Hackett, F., Strath, M., Penzo, M., Withers-Martinez, C., Baker, D. A., & Blackman, M. J. (2013). Malaria parasite cGMP-dependent protein kinase regulates blood stage merozoite secretory organelle discharge and egress. *PLoS Pathogens*, 9(5), e1003344. <https://doi.org/10.1371/journal.ppat.1003344>
- Collins, J. A., Irnov, I., Baker, S., & Winkler, W. C. (2007). Mechanism of mRNA destabilization by the glmS ribozyme. *Genes & Development*, 21(24), 3356–68. <https://doi.org/10.1101/gad.1605307>
- Condon, C. (2003). RNA processing and degradation in *Bacillus subtilis*. *Microbiology and Molecular Biology Reviews : MMBR*, 67(2), 157–74. <https://doi.org/10.1128/MMBR.67.2.157-174.2003>
- Cooper, R. A., Ferdig, M. T., Su, X., Ursos, L. M. B., Mu, J., Nomura, T., ... Wellem, T. E. (2002). Alternative mutations at position 76 of the vacuolar transmembrane protein PfCRT are associated with chloroquine resistance and unique stereospecific quinine and quinidine responses in *Plasmodium falciparum*. *Molecular Pharmacology*, 61(1), 35–42. Retrieved from <https://www.ncbi.nlm.nih.gov/pubmed/11752204>
- Cooper, R. A., Lane, K. D., Deng, B., Mu, J., Patel, J. J., Wellem, T. E., ... Ferdig, M. T. (2007). Mutations in transmembrane domains 1, 4 and 9 of the *Plasmodium falciparum* chloroquine resistance transporter alter susceptibility to chloroquine, quinine and quinidine. *Molecular Microbiology*, 63(1), 270–282. <https://doi.org/10.1111/j.1365-2958.2006.05511.x>
- Coppée, R., Jeffares, D. C., Sabbagh, A., & Clain, J. (2018). Structural evolutionary analysis predicts functional sites in the artemisinin resistance malaria protein. *bioRxiv*. <https://doi.org/10.1101/346668>
- Counihan, N. A., Kalanon, M., Coppel, R. L., & de Koning-Ward, T. F. (2013). *Plasmodium* rhoptry proteins: why order is important. *Trends in Parasitology*, 29(5), 228–36. <https://doi.org/10.1016/j.pt.2013.03.003>
- Cowman, A. F., Karcz, S., Galatis, D., & Culvenor, J. G. (1991). A P-glycoprotein homologue of *Plasmodium falciparum* is localized on the digestive vacuole. *The Journal of Cell Biology*, 113(5), 1033–42. Retrieved from <http://www.ncbi.nlm.nih.gov/pubmed/1674943>
- Cui, L., Mharakurwa, S., Ndiaye, D., Rathod, P. K., & Rosenthal, P. J. (2015). Antimalarial drug resistance: Literature review and activities and findings of the ICEMR network. *The American Journal of Tropical Medicine and Hygiene*, 93(3\_Suppl), 57–68. <https://doi.org/10.4269/ajtmh.15-0007>



- Cyrklaff, M., Bisseye, C., Simporé, J., Frischknecht, F., Kilian, N., Sanchez, C. P., & Lanzer, M. (2011). Hemoglobins S and C interfere with actin remodeling in *Plasmodium falciparum*-infected erythrocytes. *Science*, 334(6060), 1283–1286. <https://doi.org/10.1126/science.1213775>
- Dalal, S., & Klemba, M. (2007). Roles for two aminopeptidases in vacuolar hemoglobin catabolism in *Plasmodium falciparum*. *The Journal of Biological Chemistry*, 282(49), 35978–87. <https://doi.org/10.1074/jbc.M703643200>
- de Koning-Ward, T. F., Gilson, P. R., & Crabb, B. S. (2015). Advances in molecular genetic systems in malaria. *Nature Reviews Microbiology*, 13(6), 373–387. <https://doi.org/10.1038/nrmicro3450>
- Demas, A. R., Sharma, A. I., Wong, W., Early, A. M., Redmond, S., Bopp, S., ... Wirth, D. F. (2018). Mutations in *Plasmodium falciparum* actin-binding protein coronin confer reduced artemisinin susceptibility. *Proceedings of the National Academy of Sciences of the United States of America*, 115(50), 12799–12804. <https://doi.org/10.1073/PNAS.1812317115>
- Dharia, N. V., Plouffe, D., Bopp, S. E. R., González-Páez, G. E., Lucas, C., Salas, C., ... Winzeler, E. A. (2010). Genome scanning of Amazonian *Plasmodium falciparum* shows subtelomeric instability and clindamycin-resistant parasites. *Genome Research*, 20(11), 1534–44. <https://doi.org/10.1101/gr.105163.110>
- Doerig, C. (2004). Protein kinases as targets for anti-parasitic chemotherapy. *Biochimica et Biophysica Acta (BBA) - Proteins and Proteomics*, 1697(1–2), 155–168. <https://doi.org/10.1016/j.bbapap.2003.11.021>
- Doerig, C., Billker, O., Haystead, T., Sharma, P., Tobin, A. B., & Waters, N. C. (2008). Protein kinases of malaria parasites: an update. *Trends in Parasitology*, 24(12), 570–577. <https://doi.org/10.1016/j.pt.2008.08.007>
- Doerig, C., Rayner, J. C., Scherf, A., & Tobin, A. B. (2015). Post-translational protein modifications in malaria parasites. *Nature Reviews Microbiology*, 13(3), 160–172. <https://doi.org/10.1038/nrmicro3402>
- Dogovski, C., Xie, S. C., Burgio, G., Bridgford, J., Mok, S., McCaw, J. M., ... Tilley, L. (2015). Targeting the cell stress response of *Plasmodium falciparum* to overcome artemisinin resistance. *PLoS Biology*, 13(4), e1002132. <https://doi.org/10.1371/journal.pbio.1002132>
- Doherty, J. P., Lindeman, R., Trent, R. J., Graham, M. W., & Woodcock, D. M. (1993). *Escherichia coli* host strains SURE and SRB fail to preserve a palindrome cloned in lambda phage: improved alternate host strains. *Gene*, 124(1), 29–35. Retrieved from <http://www.ncbi.nlm.nih.gov/pubmed/8440479>
- Dorin-Semblat, D., Carvalho, T. G., Nivez, M.-P., Halbert, J., Pouillet, P., Semblat, J.-P., ... Doerig, C. (2013). An atypical cyclin-dependent kinase controls *Plasmodium falciparum* proliferation rate. *Kinome*, 1, 4–16. <https://doi.org/10.2478/kinome-2013-0001>
- Dorin-Semblat, D., Sicard, A., Doerig, C., Ranford-Cartwright, L., & Doerig, C. (2008). Disruption of the PfPK7 gene impairs schizogony and sporogony in the human malaria parasite *Plasmodium falciparum*. *Eukaryotic Cell*, 7(2), 279–85. <https://doi.org/10.1128/EC.00245-07>
- Duncan, C. J. A., Sheehy, S. H., Ewer, K. J., Douglas, A. D., Collins, K. A., Halstead, F. D., ... Ellis, R. D. (2011). Impact on malaria parasite multiplication rates in infected volunteers of the protein-in-adjuvant vaccine AMA1-C1/Alhydrogel+CPG 7909. *PLoS One*, 6(7), e22271. <https://doi.org/10.1371/journal.pone.0022271>

- Duraisingh, M. T., & Cowman, A. F. (2005). Contribution of the *pfmdr1* gene to antimalarial drug-resistance. *Acta Tropica*, 94(3 SPEC. ISS.), 181–190. <https://doi.org/10.1016/j.actatropica.2005.04.008>
- Dvorin, J. D., Martyn, D. C., Patel, S. D., Grimley, J. S., Collins, C. R., Hopp, C. S., ... Duraisingh, M. T. (2010). A plant-like kinase in *Plasmodium falciparum* regulates parasite egress from erythrocytes. *Science*, 328(5980), 910–2. <https://doi.org/10.1126/science.1188191>
- Dziekan, J. M., Yu, H., Chen, D., Dai, L., Wirjanata, G., Larsson, A., ... Nordlund, P. (2019). Identifying purine nucleoside phosphorylase as the target of quinine using cellular thermal shift assay. *Science Translational Medicine*, 11(473), eaau3174. <https://doi.org/10.1126/scitranslmed.aau3174>
- Egan, E. S., Jiang, R. H. Y., Moechtar, M. A., Barteneva, N. S., Weekes, M. P., Nobre, L. V., ... Duraisingh, M. T. (2015). A forward genetic screen identifies erythrocyte CD55 as essential for *Plasmodium falciparum* invasion. *Science*, 348(6235), 711–4. <https://doi.org/10.1126/science.aaa3526>
- Elsworth, B., Matthews, K., Nie, C. Q., Kalanon, M., Charnaud, S. C., Sanders, P. R., ... de Koning-Ward, T. F. (2014). PTEX is an essential nexus for protein export in malaria parasites. *Nature*, 511(7511), 587–591. <https://doi.org/10.1038/nature13555>
- Emery, S. J., Baker, L., Ansell, B. R. E., Mirzaei, M., Haynes, P. A., McConville, M. J., ... Jex, A. R. (2018). Differential protein expression and post-translational modifications in metronidazole-resistant *Giardia duodenalis*. *GigaScience*, 7(4). <https://doi.org/10.1093/gigascience/giy024>
- Eurogentec. (2008). qPCR guide. *www.eurogentec.com*, 1–68. <https://doi.org/10.1038/nprot.2007.70>
- Exton, J. H. (1997). New developments in phospholipase D. *The Journal of Biological Chemistry*, 272(25), 15579–82. <https://doi.org/10.1074/JBC.272.25.15579>
- Felger, I., & Beck, H.-P. (2008). Fitness costs of resistance to antimalarial drugs. *Trends in Parasitology*, 24(8), 331–333. <https://doi.org/10.1016/j.pt.2008.05.004>
- Felletti, M., Stifel, J., Wurmthaler, L. A., Geiger, S., & Hartig, J. S. (2016). Twister ribozymes as highly versatile expression platforms for artificial riboswitches. *Nature Communications*, 7, 12834. <https://doi.org/10.1038/ncomms12834>
- Ferdig, M. T., Cooper, R. a, Mu, J., Deng, B., Joy, D. a, Su, X., & Wellems, T. E. (2004). Dissecting the loci of low-level quinine resistance in malaria parasites. *Molecular Microbiology*, 52(4), 985–97. <https://doi.org/10.1111/j.1365-2958.2004.04035.x>
- Ferreira, P. E., Holmgren, G., Veiga, M. I., Uhlén, P., Kaneko, A., & Gil, J. P. (2011). PfMDR1: mechanisms of transport modulation by functional polymorphisms. *PLoS ONE*, 6(9), e23875. <https://doi.org/10.1371/journal.pone.0023875>
- Field, S. J., Pinder, J. C., Clough, B., Dluzewski, A. R., Wilson, R. J. M., & Gratzer, W. B. (1993). Actin in the merozoite of the malaria parasite, *Plasmodium falciparum*. *Cell Motility and the Cytoskeleton*, 25(1), 43–48. <https://doi.org/10.1002/cm.970250106>
- Filisetti, D., Théobald-Dietrich, A., Mahmoudi, N., Rudinger-Thirion, J., Candolfi, E., & Frugier, M. (2013). Aminoacylation of *Plasmodium falciparum* tRNA<sup>Asn</sup> and insights in the synthesis of asparagine repeats. *Journal of Biological Chemistry*, 288(51), 36361–36371. <https://doi.org/10.1074/jbc.M113.522896>

- Fitch, C. D. (2004). Ferriprotoporphyrin IX, phospholipids, and the antimalarial actions of quinoline drugs. *Life Sciences*, 74(16), 1957–1972. <https://doi.org/10.1016/j.lfs.2003.10.003>
- Fitch, C. D., Cai, G., Chen, Y.-F., & Shoemaker, J. D. (1999). Involvement of lipids in ferriprotoporphyrin IX polymerization in malaria. *Biochimica et Biophysica Acta (BBA) - Molecular Basis of Disease*, 1454(1), 31–37. [https://doi.org/10.1016/S0925-4439\(99\)00017-4](https://doi.org/10.1016/S0925-4439(99)00017-4)
- Flammersfeld, A., Lang, C., Flieger, A., & Pradel, G. (2018). Phospholipases during membrane dynamics in malaria parasites. *International Journal of Medical Microbiology*, 308(1), 129–141. <https://doi.org/10.1016/J.IJMM.2017.09.015>
- Fong, K. Y., & Wright, D. W. (2013). Hemozoin and antimalarial drug discovery. *Future Medicinal Chemistry*, 5(12), 1437. <https://doi.org/10.4155/FMC.13.113>
- Foster, J. D., Cervinski, M. A., Gorentla, B. K., & Vaughan, R. A. (2006). Regulation of the dopamine transporter by phosphorylation. *Handbook of Experimental Pharmacology*, (175), 197–214. Retrieved from <http://www.ncbi.nlm.nih.gov/pubmed/16722237>
- Frech, C., & Chen, N. (2011). Genome comparison of human and non-human malaria parasites reveals species subset-specific genes potentially linked to human disease. *PLoS Computational Biology*, 7(12), e1002320. <https://doi.org/10.1371/journal.pcbi.1002320>
- Gabriel, H. B., Azevedo, M. F., Kimura, E. A., Katzin, A. M., Gabriel, H. B., Azevedo, M. F., ... Katzin, A. M. (2018). *Plasmodium falciparum* parasites overexpressing farnesyl diphosphate synthase/geranylgeranyl diphosphate synthase are more resistant to risedronate. *Memórias Do Instituto Oswaldo Cruz*, 113(10). <https://doi.org/10.1590/0074-02760180174>
- Ganter, M., Goldberg, J. M., Dvorin, J. D., Paulo, J. A., King, J. G., Tripathi, A. K., ... Duraisingh, M. T. (2017). *Plasmodium falciparum* CRK4 directs continuous rounds of DNA replication during schizogony. *Nature Microbiology*, 2, 1–34. <https://doi.org/10.1038/nmicrobiol.2017.17>
- Garcia, C. R. S. (1999). Calcium homeostasis and signaling in the blood-stage malaria parasite. *Parasitology Today*, 15(12), 488–491. [https://doi.org/10.1016/S0169-4758\(99\)01571-9](https://doi.org/10.1016/S0169-4758(99)01571-9)
- Gardner, M. J., Hall, N., Fung, E., White, O., Berriman, M., Hyman, R. W., ... Barrell, B. (2002). Genome sequence of the human malaria parasite *Plasmodium falciparum*. *Nature*, 419(6906), 498–511. <https://doi.org/10.1038/nature01097>
- Garg, S., Agarwal, S., Dabral, S., Kumar, N., Sehrawat, S., & Singh, S. (2015). Visualization and quantification of *Plasmodium falciparum* intraerythrocytic merozoites. *Systems and Synthetic Biology*, 9(1), 23–6. <https://doi.org/10.1007/s11693-015-9167-9>
- Germann, U. A., Chambers, T. C., Ambudkar, S. V., Licht, T., Cardarelli, C. O., Pastan, I., & Gottesman, M. M. (1996). Characterization of phosphorylation-defective mutants of human P-glycoprotein expressed in mammalian cells. *The Journal of Biological Chemistry*, 271(3), 1708–16. <https://doi.org/10.1074/JBC.271.3.1708>
- Ghorbal, M., Gorman, M., Macpherson, C. R., Martins, R. M., Scherf, A., & Lopez-Rubio, J.-J. (2014). Genome editing in the human malaria parasite *Plasmodium falciparum* using the CRISPR-Cas9 system. *Nature Biotechnology*, 32(8). <https://doi.org/10.1038/nbt.2925>
- Gibbons, J., Button-Simons, K. A., Adapa, S. R., Li, S., Pietsch, M., Zhang, M., ... Jiang, R. H. Y. (2018). Altered expression of K13 disrupts DNA replication and repair in *Plasmodium falciparum*. *BMC Genomics*, 19(1), 849. <https://doi.org/10.1186/s12864-018-5207-7>

- Glatz, J. F. C., Luiken, J. J. F. P., & Bonen, A. (2010). Membrane fatty acid transporters as regulators of lipid metabolism: implications for metabolic disease. *Physiological Reviews*, 90(1), 367–417. <https://doi.org/10.1152/physrev.00003.2009>
- Goodman, C. D., Siregar, J. E., Mollard, V., Vega-Rodríguez, J., Syafruddin, D., Matsuoka, H., ... McFadden, G. I. (2016). Parasites resistant to the antimalarial atovaquone fail to transmit by mosquitoes. *Science*, 352(6283), 349–53. <https://doi.org/10.1126/science.aad9279>
- Gossen, M., & Bujard, H. (1992). Tight control of gene expression in mammalian cells by tetracycline-responsive promoters. *Proceedings of the National Academy of Sciences of the United States of America*, 89(12), 5547–51. <https://doi.org/10.1073/pnas.89.12.5547>
- Graciotti, M., Alam, M., Solyakov, L., Schmid, R., Burley, G., Bottrill, A. R., ... Tobin, A. B. (2014). Malaria protein kinase CK2 (PfCK2) shows novel mechanisms of regulation. *PLoS One*, 9(3), e85391. <https://doi.org/10.1371/journal.pone.0085391>
- Graeser, R., Wernli, B., Franklin, R. M., & Kappes, B. (1996). *Plasmodium falciparum* protein kinase 5 and the malarial nuclear division cycles. *Molecular and Biochemical Parasitology*, 82(1), 37–49. [https://doi.org/10.1016/0166-6851\(96\)02716-8](https://doi.org/10.1016/0166-6851(96)02716-8)
- Gray, K.-A., Gresty, K. J., Chen, N., Zhang, V., Gutteridge, C. E., Peatey, C. L., ... Cheng, Q. (2016). Correlation between cyclin dependent kinases and artemisinin-induced dormancy in *Plasmodium falciparum* in vitro. *PLoS One*, 11(6), e0157906. <https://doi.org/10.1371/journal.pone.0157906>
- Grimberg, B. T. (2011). Methodology and application of flow cytometry for investigation of human malaria parasites. *Journal of Immunological Methods*, 367(1–2), 1–16. <https://doi.org/10.1016/j.jim.2011.01.015>
- Grunberg-Manago, M. (1999). Messenger RNA stability and its role in control of gene expression in bacteria and phages. *Annual Review of Genetics*, 33(1), 193–227. <https://doi.org/10.1146/annurev.genet.33.1.193>
- Gulati, S., Eklund, E. H., Ruggles, K. V., Chan, R. B., Jayabalasingham, B., Zhou, B., ... Fidock, D. A. (2015). Profiling the essential nature of lipid metabolism in asexual blood and gametocyte stages of *Plasmodium falciparum*. *Cell Host and Microbe*, 18(3), 371–381. <https://doi.org/10.1016/j.chom.2015.08.003>
- Gupta, B., Xu, S., Wang, Z., Sun, L., Miao, J., Cui, L., & Yang, Z. (2014). *Plasmodium falciparum* multidrug resistance protein 1 (pfmrp1) gene and its association with in vitro drug susceptibility of parasite isolates from north-east Myanmar. *The Journal of Antimicrobial Chemotherapy*, 69(8), 2110–7. <https://doi.org/10.1093/jac/dku125>
- Gupta, D. K., Patra, A. T., Zhu, L., Gupta, A. P., & Bozdech, Z. (2016). DNA damage regulation and its role in drug-related phenotypes in the malaria parasites. *Scientific Reports*, 6, 23603. <https://doi.org/10.1038/srep23603>
- Halbert, J., Ayong, L., Equinet, L., Roch, K. Le, Hardy, M., Goldring, D., ... Doerig, C. (2010). A *Plasmodium falciparum* transcriptional cyclin-dependent kinase-related kinase with a crucial role in parasite proliferation associates with histone deacetylase activity. *Eukaryotic Cell*, 9(6), 952. <https://doi.org/10.1128/EC.00005-10>
- Hamilton, M. J., Lee, M., & Roch, K. G. Le. (2014). The ubiquitin system: an essential component to unlocking the secrets of malaria parasite biology. *Molecular Biosystems*, 10(4), 715–723. <https://doi.org/10.1039/c3mb70506d>

- Hänscheid, T., Egan, T. J., & Grobusch, M. P. (2007). Haemozoin: from melatonin pigment to drug target, diagnostic tool, and immune modulator. *Lancet Infectious Diseases*, 7(10), 675–685. [https://doi.org/10.1016/S1473-3099\(07\)70238-4](https://doi.org/10.1016/S1473-3099(07)70238-4)
- Hasenkamp, S., Russell, K. T., & Horrocks, P. (2012). Comparison of the absolute and relative efficiencies of electroporation-based transfection protocols for *Plasmodium falciparum*. <https://doi.org/10.1186/1475-2875-11-210>
- Hayward, R., Saliba, K. J., & Kirk, K. (2005). *pfmdr1* mutations associated with chloroquine resistance incur a fitness cost in *Plasmodium falciparum*. *Molecular Microbiology*, 55(4), 1285–1295. <https://doi.org/10.1111/j.1365-2958.2004.04470.x>
- Helm, S., Lehmann, C., Nagel, A., Stanway, R. R., Horstmann, S., Llinas, M., & Heussler, V. T. (2010). Identification and characterization of a liver stage-specific promoter region of the malaria parasite *Plasmodium*. *PLoS One*, 5(10), e13653. <https://doi.org/10.1371/journal.pone.0013653>
- Henriques, G., Hallett, R. L., Beshir, K. B., Gadalla, N. B., Johnson, R. E., Burrow, R., ... Sutherland, C. J. (2014). Directional selection at the *pfmdr1*, *pfcr1*, *pfubp1*, and *pfap2mu* loci of *Plasmodium falciparum* in Kenyan children treated with ACT. *Journal of Infectious Diseases*, 210(12), 2001–2008. <https://doi.org/10.1093/infdis/jiu358>
- Henriques, G., van Schalkwyk, D. A., Burrow, R., Warhurst, D. C., Thompson, E., Baker, D. A., ... Sutherland, C. J. (2015). The Mu subunit of *Plasmodium falciparum* clathrin-associated adaptor protein 2 modulates in vitro parasite response to artemisinin and quinine. *Antimicrobial Agents and Chemotherapy*, 59(5), 2540–7. <https://doi.org/10.1128/AAC.04067-14>
- Holland, Z., Prudent, R., Reiser, J.-B., Cochet, C., & Doerig, C. (2009). Functional analysis of protein kinase CK2 of the human malaria parasite *Plasmodium falciparum*. *Eukaryotic Cell*, 8(3), 388–97. <https://doi.org/10.1128/EC.00334-08>
- Holz, G. G. (1977). Lipids and the malarial parasite. *Bulletin of the World Health Organization*, 55(2–3), 237–248. Retrieved from <https://www.ncbi.nlm.nih.gov/pmc/articles/PMC2366759/>
- Huibregtse, J. M., Scheffner, M., Beaudenon, S., & Howley, P. M. (1995). A family of proteins structurally and functionally related to the E6-AP ubiquitin-protein ligase. *Proceedings of the National Academy of Sciences*, 92(7), 2563–2567. <https://doi.org/10.1073/pnas.92.7.2563>
- Hunt, P., Afonso, A., Creasey, A., Culleton, R., Sidhu, A. B. S., Logan, J., ... Cravo, P. (2007). Gene encoding a deubiquitinating enzyme is mutated in artesunate- and chloroquine-resistant rodent malaria parasites. *Molecular Microbiology*, 65(1), 27–40. <https://doi.org/10.1111/j.1365-2958.2007.05753.x>
- Hurley, B. P., & McCormick, B. A. (2008). Multiple roles of phospholipase a 2 during lung infection and inflammation. *Infection and Immunity*, 76(6), 2259–2272. <https://doi.org/10.1128/IAI.00059-08>
- Iconomou, M., & Saunders, D. N. (2016). Systematic approaches to identify E3 ligase substrates. *The Biochemical Journal*, 473(22), 4083–4101. <https://doi.org/10.1042/BCJ20160719>
- Imamura, S., Yabu, T., & Yamashita, M. (2012). Protective role of cell division cycle 48 (CDC48) protein against neurodegeneration via ubiquitin-proteasome system dysfunction during zebrafish development. *The Journal of Biological Chemistry*, 287(27), 23047–56. <https://doi.org/10.1074/jbc.M111.332882>

- Imrie, H., Ferguson, D. J. P., Carter, M., Drain, J., Schiflett, A., Hajduk, S. L., & Day, K. P. (2004). Light and electron microscopical observations of the effects of high-density lipoprotein on growth of *Plasmodium falciparum* in vitro. *Parasitology*, 128(6), 577–584. <https://doi.org/10.1017/S0031182004005025>
- Imwong, M., Hien, T. T., Thuy-Nhien, N. T., Dondorp, A. M., & White, N. J. (2017). Spread of a single multidrug resistant malaria parasite lineage (*PfPailin*) to Vietnam. *The Lancet. Infectious Diseases*, 17(10), 1022–1023. [https://doi.org/10.1016/S1473-3099\(17\)30524-8](https://doi.org/10.1016/S1473-3099(17)30524-8)
- Isemura, M., Mita, T., Satoh, K., Narumi, K., & Motomiya, M. (1991). Myosin light chain kinase inhibitors ML-7 and ML-9 inhibit mouse lung carcinoma cell attachment to the fibronectin substratum. *Cell Biology International Reports*, 15(10), 965–972. [https://doi.org/10.1016/0309-1651\(91\)90146-A](https://doi.org/10.1016/0309-1651(91)90146-A)
- Issar, N., Roux, E., Mattei, D., & Scherf, A. (2008). Identification of a novel post-translational modification in *Plasmodium falciparum*: protein sumoylation in different cellular compartments. *Cellular Microbiology*, 10(10), 1999–2011. <https://doi.org/10.1111/j.1462-5822.2008.01183.x>
- Ito, M., Migita, K., Matsumoto, S., Wakatsuki, K., Tanaka, T., Kunishige, T., ... Nakajima, Y. (2017). Overexpression of E3 ubiquitin ligase tripartite motif 32 correlates with a poor prognosis in patients with gastric cancer. *Oncology Letters*, 13(5), 3131–3138. <https://doi.org/10.3892/ol.2017.5806>
- Iwanaga, T., Sugi, T., Kobayashi, K., Takemae, H., Gong, H., Ishiwa, A., ... Kato, K. (2013). Characterization of *Plasmodium falciparum* cdc2-related kinase and the effects of a CDK inhibitor on the parasites in erythrocytic schizogony. *Parasitology International*, 62(5), 423–430. <https://doi.org/10.1016/J.PARINT.2013.05.003>
- Iyer, G. R., Singh, S., Kaur, I., Agarwal, S., Siddiqui, M. A., Bansal, A., ... Malhotra, P. (2018). Calcium-dependent phosphorylation of *Plasmodium falciparum* serine repeat antigen 5 triggers merozoite egress. *The Journal of Biological Chemistry*, 293(25), 9736–9746. <https://doi.org/10.1074/jbc.RA117.001540>
- Janse, C. J., Haghparast, A., Sperança, M. A., Ramesar, J., Kroeze, H., Del Portillo, H. A., & Waters, A. P. (2003). Malaria parasites lacking eef1a have a normal S/M phase yet grow more slowly due to a longer G1 phase. *Molecular Microbiology*, 50(5), 1539–1551. <https://doi.org/10.1046/j.1365-2958.2003.03820.x>
- Janse, C. J., & Waters, A. P. (2007). The exoneme helps malaria parasites to break out of blood cells. *Cell*, 131(6), 1036–8. <https://doi.org/10.1016/j.cell.2007.11.026>
- Jinek, M., Chylinski, K., Fonfara, I., Hauer, M., Doudna, J. A., & Charpentier, E. (2012). A programmable dual RNA-guided DNA endonuclease in adaptive bacterial immunity. *Science*, 337(6096), 816. <https://doi.org/10.1126/SCIENCE.1225829>
- Johnson, D. J., Owen, A., Plant, N., Bray, P. G., & Ward, S. A. (2008). Drug-regulated expression of *Plasmodium falciparum* P-glycoprotein homologue 1: A putative role for nuclear receptors. *Antimicrobial Agents and Chemotherapy*, 52(4), 1438–1445. <https://doi.org/10.1128/AAC.01392-07>
- Jones, M. L., Collins, M. O., Goulding, D., Choudhary, J. S., & Rayner, J. C. (2012). Analysis of protein palmitoylation reveals a pervasive role in *Plasmodium* development and pathogenesis. *Cell Host & Microbe*, 12(2), 246–258. <https://doi.org/10.1016/j.chom.2012.06.005>

- Jones, M. L., Das, S., Belda, H., Collins, C. R., Blackman, M. J., & Treeck, M. (2016). A versatile strategy for rapid conditional genome engineering using loxP sites in a small synthetic intron in *Plasmodium falciparum*. *Scientific Reports*, 6(November 2015), 21800. <https://doi.org/10.1038/srep21800>
- Ju, D., & Xie, Y. (2006). A synthetic defect in protein degradation caused by loss of Ufd4 and Rad23. *Biochemical and Biophysical Research Communications*, 341(2), 648–652. <https://doi.org/10.1016/J.BBRC.2006.01.013>
- Juge, N., Moriyama, S., Miyaji, T., Kawakami, M., Iwai, H., Fukui, T., ... Moriyama, Y. (2015). *Plasmodium falciparum* chloroquine resistance transporter is a H<sup>+</sup>-coupled polyspecific nutrient and drug exporter. *Proceedings of the National Academy of Sciences of the United States of America*, 112(11), 3356–61. <https://doi.org/10.1073/pnas.1417102112>
- Kaufmann, A., & Knop, M. (2011). Genomic promoter replacement cassettes to alter gene expression in the yeast *Saccharomyces cerevisiae*. In *Methods in molecular biology*, Vol. 765, pp. 275–294. [https://doi.org/10.1007/978-1-61779-197-0\\_16](https://doi.org/10.1007/978-1-61779-197-0_16)
- Kehr, S., Jortzik, E., Delahunty, C., Yates, J. R., Rahlfs, S., & Becker, K. (2011). Protein S - glutathionylation in malaria parasites. *Antioxidants & Redox Signaling*, 15(11), 2855–2865. <https://doi.org/10.1089/ars.2011.4029>
- Kenthirapalan, S., Waters, A. P., Matuschewski, K., & Kooij, T. W. A. (2016). Functional profiles of orphan membrane transporters in the life cycle of the malaria parasite. *Nature Communications*, 7(1), 10519. <https://doi.org/10.1038/ncomms10519>
- Kim, W., Bennett, E. J., Huttlin, E. L., Guo, A., Li, J., Possemato, A., ... Gygi, S. P. (2011). Systematic and quantitative assessment of the ubiquitin-modified proteome. *Molecular Cell*, 44(2), 325–40. <https://doi.org/10.1016/j.molcel.2011.08.025>
- Kimura, E. A., Katzin, A. M., & Couto, A. S. (2000). More on protein glycosylation in the malaria parasite. *Parasitology Today*, 16(1), 38–39. [https://doi.org/10.1016/S0169-4758\(99\)01584-7](https://doi.org/10.1016/S0169-4758(99)01584-7)
- Kirchner, S., Power, B. J., & Waters, A. P. (2016). Recent advances in malaria genomics and epigenomics. *Genome Medicine*, 8(1), 92. <https://doi.org/10.1186/s13073-016-0343-7>
- Kirkpatrick, D. S., Denison, C., & Gygi, S. P. (2005). Weighing in on ubiquitin: the expanding role of mass spectrometry-based proteomics. *Nature Cell Biology*, 7(8), 750–757. Retrieved from <https://www.ncbi.nlm.nih.gov/pmc/articles/PMC1224607/>
- Klemba, M., Gluzman, I., & Goldberg, D. E. (2004). A *Plasmodium falciparum* dipeptidyl aminopeptidase I participates in vacuolar hemoglobin degradation. *The Journal of Biological Chemistry*, 279(41), 43000–7. <https://doi.org/10.1074/jbc.M408123200>
- Knuepfer, E., Napiorkowska, M., van Ooij, C., & Holder, A. A. (2017). Generating conditional gene knockouts in *Plasmodium* - a toolkit to produce stable DiCre recombinase-expressing parasite lines using CRISPR/Cas9. *Scientific Reports*, 7(1), 3881. <https://doi.org/10.1038/s41598-017-03984-3>
- Kobayashi, K., & Kato, K. (2016). A synchronization method using heparin for the *in vitro* culture of *Plasmodium falciparum*. *Parasitology International*. <https://doi.org/10.1016/J.PARINT.2016.02.014>

- Koch, M., & Baum, J. (2016). The mechanics of malaria parasite invasion of the human erythrocyte - towards a reassessment of the host cell contribution. *Cellular Microbiology*, 18(3), 319–29. <https://doi.org/10.1111/cmi.12557>
- Krishna, S., & Woodrow, C. J. (1999). Expression of parasite transporters in *Xenopus* oocytes. *Novartis Foundation Symposium*, 226, 126–39–44. Retrieved from <http://www.ncbi.nlm.nih.gov/pubmed/10645543>
- Kublin, J. G., Cortese, J. F., Njunju, E. M., Mukadam, R. A. G., Wirima, J. J., Kazembe, P. N., ... Plowe, C. V. (2003). Reemergence of chloroquine-sensitive *Plasmodium falciparum* malaria after cessation of chloroquine use in Malawi. *The Journal of Infectious Diseases*, 187(12), 1870–5. <https://doi.org/10.1086/375419>
- Kudla, G., Lipinski, L., Caffin, F., Helwak, A., & Zylicz, M. (2006). High guanine and cytosine content increases mRNA levels in mammalian cells. *PLoS Biology*, 4(6), 0933–0942. <https://doi.org/10.1371/journal.pbio.0040180>
- Kuhn, Y., Rohrbach, P., & Lanzer, M. (2007). Quantitative pH measurements in *Plasmodium falciparum*-infected erythrocytes using pHluorin. *Cellular Microbiology*, 9(4), 1004–1013. <https://doi.org/10.1111/j.1462-5822.2006.00847.x>
- Kuhn, Y., Sanchez, C. P., Ayoub, D., Saridaki, T., van Dorsselaer, A., & Lanzer, M. (2010). Trafficking of the phosphoprotein pfcr1 to the digestive vacuolar membrane in *Plasmodium falciparum*. *Traffic*, 11(2), 236–249. <https://doi.org/10.1111/j.1600-0854.2009.01018.x>
- Kumar, P., Tripathi, A., Ranjan, R., Halbert, J., Gilberger, T., Doerig, C., & Sharma, P. (2014). Regulation of *Plasmodium falciparum* development by Calcium-Dependent Protein Kinase 7 (PfCDPK7). *The Journal of Biological Chemistry*, 289(29), 20386. <https://doi.org/10.1074/JBC.M114.561670>
- Lakshmanan, V., Bray, P. G., Verdier-Pinard, D., Johnson, D. J., Horrocks, P., Muhle, R. A., ... Fidock, D. A. (2005). A critical role for PfCRT K76T in *Plasmodium falciparum* verapamil-reversible chloroquine resistance. *EMBO Journal*, 24(13), 2294–2305. <https://doi.org/10.1038/sj.emboj.7600681>
- Lambros, C., & Vanderberg, J. P. (1979). Synchronization of *Plasmodium falciparum* erythrocytic stages in culture. *The Journal of Parasitology*, 65(3), 418–20. Retrieved from <http://www.ncbi.nlm.nih.gov/pubmed/383936>
- Lasonder, E., Green, J. L., Camarda, G., Talabani, H., Holder, A. A., Langsley, G., & Alano, P. (2012). The *Plasmodium falciparum* schizont phosphoproteome reveals extensive phosphatidylinositol and cAMP-Protein Kinase A signaling. *Journal of Proteome Research*, 11(11), 5323–5337. <https://doi.org/10.1021/pr300557m>
- Lasonder, E., Green, J. L., Grainger, M., Langsley, G., & Holder, A. A. (2015). Extensive differential protein phosphorylation as intraerythrocytic *Plasmodium falciparum* schizonts develop into extracellular invasive merozoites. *PROTEOMICS*, 15(15), 2716–2729. <https://doi.org/10.1002/pmic.201400508>
- Latchman, D. S. (1993). Transcription factors: an overview. *International Journal of Experimental Pathology*, 74(5), 417–22. Retrieved from <http://www.ncbi.nlm.nih.gov/pubmed/8217775>
- Le Roch, K. G. (2003). Discovery of gene function by expression profiling of the malaria parasite life cycle. *Science*, 301(5639), 1503–1508. <https://doi.org/10.1126/science.1087025>



- Lee, A. H., Symington, L. S., & Fidock, D. A. (2014). DNA Repair mechanisms and their biological roles in the malaria parasite *Plasmodium falciparum*. *Microbiology and Molecular Biology Reviews*, 78(3), 469–486. <https://doi.org/10.1128/mmbr.00059-13>
- Lee, K.-Y., & Lee, B.-J. (2017). Structural and biochemical properties of novel self-cleaving ribozymes. *Molecules (Basel, Switzerland)*, 22(4). <https://doi.org/10.3390/molecules22040678>
- Lee, M. C., & Fidock, D. a. (2014). CRISPR-mediated genome editing of *Plasmodium falciparum* malaria parasites. *Genome Medicine*, 6(8), 63. <https://doi.org/10.1186/s13073-014-0063-9>
- Lee, M. V., Topper, S. E., Hubler, S. L., Hose, J., Wenger, C. D., Coon, J. J., & Gasch, A. P. (2011). A dynamic model of proteome changes reveals new roles for transcript alteration in yeast. *Molecular Systems Biology*, 7, 514. <https://doi.org/10.1038/msb.2011.48>
- Lehmann, C., Tan, M. S. Y., de Vries, L. E., Russo, I., Sanchez, M. I., Goldberg, D. E., & Deu, E. (2018). *Plasmodium falciparum* dipeptidyl aminopeptidase 3 activity is important for efficient erythrocyte invasion by the malaria parasite. *PLOS Pathogens*, 14(5), e1007031. <https://doi.org/10.1371/journal.ppat.1007031>
- Limbutara, K., Kelleher, A., Yang, C.-R., Raghuram, V., & Knepper, M. A. (2019). Phosphorylation changes in response to kinase inhibitor H89 in PKA-null cells. *Scientific Reports*, 9(1), 2814. <https://doi.org/10.1038/s41598-019-39116-2>
- Lin, D.-C., Xu, L., Chen, Y., Yan, H., Hazawa, M., Doan, N., ... Koeffler, H. P. (2015). Genomic and functional analysis of the E3 ligase PARK2 in Glioma. *Cancer Research*, 75(9), 1815–27. <https://doi.org/10.1158/0008-5472.CAN-14-1433>
- Liu, D. Q., Liu, R. J., Ren, D. X., Gao, D. Q., Zhang, C. Y., Qui, C. P., ... Tang, X. (1995). Changes in the resistance of *Plasmodium falciparum* to chloroquine in Hainan, China. *Bulletin of the World Health Organization*, 73(4), 483–6. Retrieved from <http://www.ncbi.nlm.nih.gov/pubmed/7554020>
- Liu, M. Y., Yang, H., & Romeo, T. (1995). The product of the pleiotropic *Escherichia coli* gene *csrA* modulates glycogen biosynthesis via effects on mRNA stability. *Journal of Bacteriology*, 177(10), 2663–72. Retrieved from <http://www.ncbi.nlm.nih.gov/pubmed/7751274>
- Liu, Y., Beyer, A., & Aebersold, R. (2016). On the dependency of cellular protein levels on mRNA abundance. *Cell*, 165(3), 535–550. <https://doi.org/10.1016/J.CELL.2016.03.014>
- Llinás, M., Bozdech, Z., Wong, E. D., Adai, A. T., & DeRisi, J. L. (2006). Comparative whole genome transcriptome analysis of three *Plasmodium falciparum* strains. *Nucleic Acids Research*, 34(4), 1166–1173. <https://doi.org/10.1093/nar/gkj517>
- Lorenz, S. (2018). Structural mechanisms of HECT-type ubiquitin ligases. *Biological Chemistry*, 399(2), 127. <https://doi.org/10.1515/hsz-2017-0184>
- Lu, X., & Legerski, R. J. (2007). The Prp19/Pso4 core complex undergoes ubiquitylation and structural alterations in response to DNA damage. *Biochemical and Biophysical Research Communications*, 354(4), 968–74. <https://doi.org/10.1016/j.bbrc.2007.01.097>
- Lucocq, J. (1994). Quantitation of gold labelling and antigens in immunolabelled ultrathin sections. *Journal of Anatomy*, 184(Pt 1), 1–13. Retrieved from <http://www.ncbi.nlm.nih.gov/pubmed/8157482>

- Macedo, C. S., Schwarz, R. T., Todeschini, A. R., Previato, J. O., & Mendonça-Previato, L. (2010). Overlooked post-translational modifications of proteins in *Plasmodium falciparum*: N- and O-glycosylation - A review. *Memorias Do Instituto Oswaldo Cruz*, 105(8), 949–956. Retrieved from <https://www.ncbi.nlm.nih.gov/pubmed/21225189>
- Maier, T., Güell, M., & Serrano, L. (2009). Correlation of mRNA and protein in complex biological samples. *FEBS Letters*, 583(24), 3966–3973. <https://doi.org/10.1016/J.FEBSLET.2009.10.036>
- Mali, P., Yang, L., Esvelt, K. M., Aach, J., Guell, M., DiCarlo, J. E., ... Church, G. M. (2013). RNA-guided human genome engineering via Cas9. *Science (New York, N.Y.)*, 339(6121), 823–6. <https://doi.org/10.1126/science.1232033>
- Marks, K. M., Braun, P. D., & Nolan, G. P. (2004). A general approach for chemical labeling and rapid, spatially controlled protein inactivation. *Proceedings of the National Academy of Sciences of the United States of America*, 101(27), 9982–7. <https://doi.org/10.1073/pnas.0401609101>
- Martin, R. E., Marchetti, R. V., Cowan, A. I., Howitt, S. M., Bröer, S., & Kirk, K. (2009). Chloroquine transport via the malaria parasite's chloroquine resistance transporter. *Science (New York, N.Y.)*, 325(5948), 1680–2. <https://doi.org/10.1126/science.1175667>
- Mata-Cantero, L., Azkargorta, M., Aillet, F., Xolalpa, W., LaFuente, M. J., Elortza, F., ... Rodriguez, M. S. (2016). New insights into host-parasite ubiquitin proteome dynamics in *P. falciparum* infected red blood cells using a TUBEs-MS approach. *Journal of Proteomics*, 139, 45–59. <https://doi.org/10.1016/J.JPROT.2016.03.004>
- Matsumoto, M. L., Wickliffe, K. E., Dong, K. C., Yu, C., Bosanac, I., Bustos, D., ... Dixit, V. M. (2010). K11-linked polyubiquitination in cell cycle control revealed by a K11 linkage-specific antibody. *Molecular Cell*, 39(3), 477–84. <https://doi.org/10.1016/j.molcel.2010.07.001>
- Matthews, H., Duffy, C. W., & Merrick, C. J. (2018). Checks and balances? DNA replication and the cell cycle in *Plasmodium*. *Parasites and Vectors*, 11(1), 1–13. <https://doi.org/10.1186/s13071-018-2800-1>
- Mbengue, A., Bhattacharjee, S., Pandharkar, T., Liu, H., Estiu, G., Stahelin, R. V., ... Haldar, K. (2015). A molecular mechanism of artemisinin resistance in *Plasmodium falciparum* malaria. *Nature*, 520(7549), 683–687. <https://doi.org/10.1038/nature14412>
- McCallum-Deighton, N., & Holder, A. A. (1992). The role of calcium in the invasion of human erythrocytes by *Plasmodium falciparum*. *Molecular and Biochemical Parasitology*, 50(2), 317–323. [https://doi.org/10.1016/0166-6851\(92\)90229-D](https://doi.org/10.1016/0166-6851(92)90229-D)
- McCleary, W. R. (2009). Application of promoter swapping techniques to control expression of chromosomal genes. *Applied Microbiology and Biotechnology*, 84(4), 641–648. <https://doi.org/10.1007/s00253-009-2137-y>
- McKenzie, A. J., William, T. F., Svec, K. V., & Howe, A. K. (2018). Protein Kinase A activity is regulated by actomyosin contractility during cell migration and is required for durotaxis. *bioRxiv*, (802). Retrieved from <https://www.biorxiv.org/content/10.1101/392399v1>
- Meissner, M., Krejany, E., Gilson, P. R., Koning-Ward, T. F. de, Soldati, D., & Crabb, B. S. (2005). Tetracycline analogue-regulated transgene expression in *Plasmodium falciparum* blood stages using *Toxoplasma gondii* transactivators. *Proceedings of the National Academy of Sciences of the United States of America*, 102(8), 2980. <https://doi.org/10.1073/PNAS.0500112102>

- Melgar-Lesmes, P., Luquero, A., Edelman, E., & Jiménez, W. (2018). Selective NDRP1 E3 ubiquitin ligase overexpression in inflammatory macrophages using functionalized carbon nanoparticles promotes fibrosis regression in cirrhotic mice. *Journal of Hepatology*, 68, S393–S394. [https://doi.org/10.1016/S0168-8278\(18\)31021-3](https://doi.org/10.1016/S0168-8278(18)31021-3)
- Menard, S., Haddou, T. Ben, Ramadani, A. P., Arie, F., Iriart, X., Beghain, J., ... Benoit-Vical, F. (2015). Induction of multidrug tolerance in *Plasmodium falciparum* by extended artemisinin pressure. *Emerging Infectious Diseases*, 21(10), 1733–1741. <https://doi.org/10.3201/eid2110.150682>
- Mendenhall, M. D., Richardson, H. E., & Reed, S. I. (1988). Dominant negative protein kinase mutations that confer a G1 arrest phenotype. *Proceedings of the National Academy of Sciences of the United States of America*, 85(June), 4426–4430. <https://doi.org/10.1073/pnas.85.12.4426>
- Merrick, C. J. (2015). Transfection with thymidine kinase permits bromodeoxyuridine labelling of DNA replication in the human malaria parasite *Plasmodium falciparum*. *Malaria Journal*, 14(1), 490. <https://doi.org/10.1186/s12936-015-1014-7>
- Merrick, C. J., & Duraisingh, M. T. (2010). Epigenetics in *Plasmodium*: what do we really know? *Eukaryotic Cell*, 9(8), 1150–8. <https://doi.org/10.1128/EC.00093-10>
- Mfonkeu, J. B. P., Gouado, I., Fotso Kuate, H., Zambou, O., Combes, V., Raymond Grau, G. E., & Amvam Zollo, P. H. (2010). Biochemical markers of nutritional status and childhood malaria severity in Cameroon. *British Journal of Nutrition*, 104(6), 886–892. <https://doi.org/10.1017/S0007114510001510>
- Miller, L. H., Ackerman, H. C., Su, X., & Wellems, T. E. (2013). Malaria biology and disease pathogenesis: insights for new treatments. *Nature Medicine*, 19(2), 156–67. <https://doi.org/10.1038/nm.3073>
- Mita, T., Kaneko, A., Lum, J. K., Zungu, I. L., Tsukahara, T., Eto, H., ... Tanabe, K. (2004). Expansion of wild type allele rather than back mutation in pfcrt explains the recent recovery of chloroquine sensitivity of *Plasmodium falciparum* in Malawi. *Molecular and Biochemical Parasitology*, 135(1), 159–163. [https://doi.org/10.1016/S0166-6851\(04\)00033-7](https://doi.org/10.1016/S0166-6851(04)00033-7)
- Mitsui, K., Nakanishi, M., Ohtsuka, S., Norwood, T. H., Okabayashi, K., Miyamoto, C., ... Ohtsubo, M. (1999). A novel human gene encoding HECT domain and RCC1-like repeats interacts with cyclins and is potentially regulated by the tumor suppressor proteins. *Biochemical and Biophysical Research Communications*, 122, 115–122. Retrieved from <https://www.ncbi.nlm.nih.gov/pubmed/10581175>
- Mohanty, S., Mishra, S. K., Das, B. S., Satpathy, S. K., Mohanty, D., Patnaik, J. K., & Bose, T. K. (1992). Altered plasma lipid pattern in *falciparum* malaria. *Annals of Tropical Medicine and Parasitology*, 86(6), 601–6. Retrieved from <http://www.ncbi.nlm.nih.gov/pubmed/1304701>
- Mok, S., Ashley, E. A., Ferreira, P. E., Zhu, L., Lin, Z., Chotivanich, K., ... Pukrittayakamee, S. (2015). Population transcriptomics of human malaria parasites reveals the mechanism of artemisinin resistance. *Science*, 347(6220), 431–435. <https://doi.org/10.1126/science.1260403>
- Mok, S., Liong, K.-Y., Lim, E.-H., Huang, X., Zhu, L., Preiser, P. R., & Bozdech, Z. (2014). Structural polymorphism in the promoter of *pfmrp2* confers *Plasmodium falciparum* tolerance to quinoline drugs. *Molecular Microbiology*, 91(5), 918–934. <https://doi.org/10.1111/mmi.12505>
- Müller, I. B., & Hyde, J. E. (2010). Antimalarial drugs: modes of action and mechanisms of parasite resistance. *Future Microbiology*, 5(12), 1857–1873. <https://doi.org/10.2217/fmb.10.136>

- Muregi, F. W., Ohta, I., Masato, U., Kino, H., & Ishih, A. (2011). Resistance of a rodent malaria parasite to a thymidylate synthase inhibitor induces an apoptotic parasite death and imposes a huge cost of fitness. *PloS One*, 6(6), e21251. <https://doi.org/10.1371/journal.pone.0021251>
- Murray, L., Stewart, L. B., Tarr, S. J., Ahouidi, A. D., Diakite, M., Amambua-Ngwa, A., & Conway, D. J. (2017). Multiplication rate variation in the human malaria parasite *Plasmodium falciparum*. *Scientific Reports*, 7(1), 1–8. <https://doi.org/10.1038/s41598-017-06295-9>
- Neafsey, D. E., Juraska, M., Bedford, T., Benkeser, D., Valim, C., Griggs, A., ... Wirth, D. F. (2015). Genetic diversity and protective efficacy of the RTS,S/AS01 malaria vaccine. *The New England Journal of Medicine*, 373(21), 2025–2037. <https://doi.org/10.1056/NEJMoa1505819>
- Newton, K., Matsumoto, M. L., Wertz, I. E., Kirkpatrick, D. S., Lill, J. R., Tan, J., ... Dixit, V. M. (2008). Ubiquitin chain editing revealed by polyubiquitin linkage-specific antibodies. *Cell*, 134(4), 668–78. <https://doi.org/10.1016/j.cell.2008.07.039>
- Ng, C. L., Fidock, D. A., & Bogyo, M. (2017). Protein degradation systems as anti-malarial therapeutic targets. *Trends in Parasitology*, 33(9), 731–743. <https://doi.org/10.1016/j.pt.2017.05.009>.Protein
- Njoku, O. U., Alumanah, E. O., & Meremikwu, C. U. (2001). Effect of *Azadirachta indica* extract on plasma lipid levels in human malaria. *Bollettino Chimico Farmaceutico*, 140(5), 367–70. Retrieved from <http://www.ncbi.nlm.nih.gov/pubmed/11680094>
- Nkrumah, L. J., Muhle, R. A., Moura, P. A., Ghosh, P., Hatfull, G. F., Jacobs, W. R., ... Fidock, D. A. (2006). Efficient site-specific integration in *Plasmodium falciparum* chromosomes mediated by mycobacteriophage Bxb1 integrase. *Nature Methods*, 3(8), 615–21. <https://doi.org/10.1038/nmeth904>
- Nkrumah, L. J., Riegelhaupt, P. M., Moura, P., Johnson, D. J., Patel, J., Hayton, K., ... Fidock, D. A. (2009). Probing the multifactorial basis of *Plasmodium falciparum* quinine resistance: evidence for a strain-specific contribution of the sodium-proton exchanger PfNHE. *Molecular and Biochemical Parasitology*, 165(2), 122–31. <https://doi.org/10.1016/j.molbiopara.2009.01.011>
- Nzila, A., & Mwai, L. (2010). *In vitro* selection of *Plasmodium falciparum* drug-resistant parasite lines. *The Journal of Antimicrobial Chemotherapy*, 65(3), 390–8. <https://doi.org/10.1093/jac/dkp449>
- O'Hara, J. K., Kerwin, L. J., Cobbold, S. A., Tai, J., Bedell, T. A., Reider, P. J., & Llinás, M. (2014). Targeting NAD<sup>+</sup> metabolism in the human malaria parasite *Plasmodium falciparum*. *PLoS One*, 9(4). <https://doi.org/10.1371/journal.pone.0094061>
- Oduola, A. M. J., & Bowdre, J. H. (1988). *Plasmodium falciparum*: Induction of resistance to mefloquine cloned strains by continuous drug exposure *in vitro*. *Experimental Parasitology*, 360, 354–360. Retrieved from <https://www.ncbi.nlm.nih.gov/pubmed/3056740>
- Oguike, M. C., Falade, C. O., Shu, E., Enato, I. G., Watila, I., Baba, E. S., ... Roper, C. (2016). Molecular determinants of sulfadoxine-pyrimethamine resistance in *Plasmodium falciparum* in Nigeria and the regional emergence of dhps 431V. *International Journal for Parasitology: Drugs and Drug Resistance*, 6(3), 220–229. <https://doi.org/10.1016/J.IJPDDR.2016.08.004>
- Okombo, J., & Chibale, K. (2018). Recent updates in the discovery and development of novel antimalarial drug candidates. *MedChemComm*, 9(3), 437–453. <https://doi.org/10.1039/c7md00637c>

- Olotu, A., Fegan, G., Wambua, J., Nyangweso, G., Leach, A., Lievens, M., ... Bejon, P. (2016). Seven-year efficacy of RTS,S/AS01 malaria vaccine among young African children. *New England Journal of Medicine*, 374(26), 2519–2529. <https://doi.org/10.1056/NEJMoa1515257>
- Orjih, A. U. (2014). Maturation of *Plasmodium falciparum* in multiply infected erythrocytes and the potential role in malaria pathogenesis. *Parasitology Research*, 113(11), 4045–4056. <https://doi.org/10.1007/s00436-014-4073-8>
- Orjih, A. U., Ryerse, J. S., & Fitch, C. D. (1994). Hemoglobin catabolism and the killing of intraerythrocytic *Plasmodium falciparum* by chloroquine. *Experientia*, 50(S1), 34–39. <https://doi.org/10.1007/BF01992046>
- Palogue, L., Ramadani, A. P., Mercereau-Puijalon, O., Augereau, J.-M., Benoit-Vical, F., Ashley, E., ... Chakrabarti, D. (2016). *Plasmodium falciparum*: multifaceted resistance to artemisinins. *Malaria Journal*, 15(1), 149. <https://doi.org/10.1186/s12936-016-1206-9>
- Pandey, A. V., Babbarwal, V. K., Okoyeh, J. N., Joshi, R. M., Puri, S. K., Singh, R. L., & Chauhan, V. S. (2003). Hemozoin formation in malaria: a two-step process involving histidine-rich proteins and lipids. *Biochemical and Biophysical Research Communications*, 308(4), 736–743. [https://doi.org/10.1016/S0006-291X\(03\)01465-7](https://doi.org/10.1016/S0006-291X(03)01465-7)
- Pao, K., Wood, N. T., Knebel, A., Rafie, K., Stanley, M., Mabbitt, P. D., ... Virdee, S. (2018). Activity-based E3 ligase profiling uncovers an E3 ligase with esterification activity. *Nature*. <https://doi.org/10.1038/s41586-018-0026-1>
- Park, D. J., Lukens, A. K., Neafsey, D. E., Schaffner, S. F., Chang, H., & Valim, C. (2012). Sequence-based association and selection scans identify drug resistance loci in the *Plasmodium falciparum* malaria parasite. *Proceedings of the National Academy of Sciences of the United States of America*, 109(32), 13052–13057. <https://doi.org/10.1073/pnas.1210585109>
- Pascual, A., Briolant, S., Pelleau, S., Bogueau, H., Hovette, P., Zettor, A., ... Pradines, B. (2013). In vitro susceptibility to quinine and microsatellite variations of the *Plasmodium falciparum* Na<sup>+</sup>/H<sup>+</sup> exchanger (Pf<sub>nh</sub>-1) gene: the absence of association in clinical isolates from the Republic of Congo. *Malaria Journal*, 10(1), 37. <https://doi.org/10.1186/1475-2875-10-37>
- Patzewitz, E.-M., Salcedo-Sora, J. E., Wong, E. H., Sethia, S., Stocks, P. A., Maughan, S. C., ... Müller, S. (2012). Glutathione transport: a new role for PfCRT in chloroquine resistance. *Antioxidants & Redox Signaling*, 19(7), 683–695. <https://doi.org/10.1089/ars.2012.4625>
- Paul, A. S., Saha, S., Engelberg, K., Jiang, R. H. Y., Coleman, B. I., Kosber, A. L., ... Duraisingh, M. T. (2015). Parasite calcineurin regulates host cell recognition and attachment by Apicomplexans. *Cell Host & Microbe*, 18(1), 49–60. <https://doi.org/10.1016/j.chom.2015.06.003>
- Paul, F., Roath, S., Melville, D., Warhurst, D. C., & Osisanya, J. O. (1981). Separation of malaria-infected erythrocytes from whole blood: use of a selective high-gradient magnetic separation technique. *Lancet*, 2(8237), 70–1. Retrieved from <http://www.ncbi.nlm.nih.gov/pubmed/6113443>
- Pease, B. N., Huttlin, E. L., Jedrychowski, M. P., Talevich, E., Harmon, J., Dillman, T., ... Chakrabarti, D. (2013). Global analysis of protein expression and phosphorylation of three stages of *Plasmodium falciparum* intraerythrocytic development. *Journal of Proteome Research*, 12(9), 4028–4045. <https://doi.org/10.1021/pr400394g>

- Perrett, C. A., Lin, D. Y.-W., & Zhou, D. (2011). Interactions of bacterial proteins with host eukaryotic ubiquitin pathways. *Frontiers in Microbiology*, 2, 143. <https://doi.org/10.3389/fmicb.2011.00143>
- Pesce, E.-R., Acharya, P., Tatu, U., Nicoll, W. S., Shonhai, A., Hoppe, H. C., & Blatch, G. L. (2008). The *Plasmodium falciparum* heat shock protein 40, Pfj4, associates with heat shock protein 70 and shows similar heat induction and localisation patterns. *The International Journal of Biochemistry & Cell Biology*, 40(12), 2914–2926. <https://doi.org/10.1016/j.biocel.2008.06.011>
- Peters, W. (1982). Antimalarial drug resistance: an increasing problem. *British Medical Bulletin*, 38(2), 187–92. Retrieved from <http://www.ncbi.nlm.nih.gov/pubmed/7052200>
- Petersen, I., Gabrysiewicz, S. J., Johnston, G. L., Dhingra, S. K., Ecker, A., Lewis, R. E., ... Fidock, D. A. (2015). Balancing drug resistance and growth rates via compensatory mutations in the *Plasmodium falciparum* chloroquine resistance transporter. *Molecular Microbiology*, 97(2), 381–395. <https://doi.org/10.1111/mmi.13035>
- Petersen, I., Eastman, R., & Lanzer, M. (2011). Drug-resistant malaria: molecular mechanisms and implications for public health. *FEBS Letters*, 585(11), 1551–62. <https://doi.org/10.1016/j.febslet.2011.04.042>
- Phillips, M. A., Burrows, J. N., Manyando, C., van Huijsduijnen, R. H., Van Voorhis, W. C., & Wells, T. N. C. (2017). Malaria. *Nature Reviews Disease Primers*, 3, 17050. <https://doi.org/10.1038/nrdp.2017.50>
- Pinna, L. A., & Cohen, P. T. W. (2005). Inhibitors of protein kinases and protein phosphates. *Springer Books*. Retrieved from <http://the-eye.eu/public/Books/Medical/texts/Inhibitors%20of%20Protein%20Kinases%20and%20Protein%20Phosphatases%20-%20L.%20Pinna%2C%20P.%20Cohen%20%28Springer%2C%202005%29%20WW.pdf>
- Pisciotta, J. M., Coppens, I., Tripathi, A. K., Scholl, P. F., Shuman, J., Bajad, S., ... Jr. (2007). The role of neutral lipid nanospheres in *Plasmodium falciparum* haem crystallization. *The Biochemical Journal*, 402(1), 197–204. <https://doi.org/10.1042/BJ20060986>
- Ponts, N., Fu, L., Harris, E. Y., Zhang, J., Chung, D.-W. D., Cervantes, M. C., ... Le Roch, K. G. (2013). Genome-wide mapping of DNA methylation in the human malaria parasite *Plasmodium falciparum*. *Cell Host & Microbe*, 14(6), 696–706. <https://doi.org/10.1016/j.chom.2013.11.007>
- Ponts, N., Yang, J., Chung, D. W. D., Prudhomme, J., Girke, T., Horrocks, P., & Le Roch, K. G. (2008). Deciphering the ubiquitin-mediated pathway in apicomplexan parasites: A potential strategy to interfere with parasite virulence. *PLoS One*, 3(6). <https://doi.org/10.1371/journal.pone.0002386>
- Porcar, I., Codoñer, A., Gómez, C. M., Abad, C., & Campos, A. (2003). Interaction of quinine with model lipid membranes of different compositions. *Journal of Pharmaceutical Sciences*, 92(1), 45–57. <https://doi.org/10.1002/jps.10254>
- Preechapornkul, P., Imwong, M., Chotivanich, K., Pongtavornpinyo, W., Dondorp, A. M., Day, N. P. J., ... Pukrittayakamee, S. (2009). *Plasmodium falciparum* *pfmdr1* amplification, mefloquine resistance, and parasite fitness. *Antimicrobial Agents and Chemotherapy*, 53(4), 1509–15. <https://doi.org/10.1128/AAC.00241-08>
- Prommana, P., Uthapibull, C., Wongsombat, C., Kamchonwongpaisan, S., Yuthavong, Y., Knuepfer, E., ... Shaw, P. J. (2013). Inducible knockdown of *Plasmodium* gene expression using the glmS ribozyme. *PLoS One*, 8(8), e73783. <https://doi.org/10.1371/journal.pone.0073783>

- Raina, H., Zacharia, J., Li, M., & Wier, W. G. (2009). Activation by Ca<sup>2+</sup>/calmodulin of an exogenous myosin light chain kinase in mouse arteries. *The Journal of Physiology*, 587(Pt 11), 2599–612. <https://doi.org/10.1113/jphysiol.2008.165258>
- Ramamoorthy, S., Shippenberg, T. S., & Jayanthi, L. D. (2011). Regulation of monoamine transporters: Role of transporter phosphorylation. *Pharmacology & Therapeutics*, 129(2), 220–38. <https://doi.org/10.1016/j.pharmthera.2010.09.009>
- Rathnapala, U. L., Goodman, C. D., & McFadden, G. I. (2017). A novel genetic technique in *Plasmodium berghei* allows liver stage analysis of genes required for mosquito stage development and demonstrates that de novo heme synthesis is essential for liver stage development in the malaria parasite. *PLoS Pathogens*, 13(6), 1–18. <https://doi.org/10.1371/journal.ppat.1006396>
- Rathod, P. K., Mcerlean, T., & Lee, P.-C. (1997). Variations in frequencies of drug resistance in *Plasmodium falciparum*. *Microbiology*, 94, 9389–9393. Retrieved from <https://www.ncbi.nlm.nih.gov/pmc/articles/PMC23200/>
- Reed, M. B., Saliba, K. J., Caruana, S. R., Kirk, K., & Cowman, A. F. (2000). Pgh1 modulates sensitivity and resistance to multiple antimalarials in *Plasmodium falciparum*. *Nature*, 403(6772), 906–909. <https://doi.org/10.1038/35002615>
- Reilly, H. B., Wang, H., Steuter, J. A., Marx, A. M., & Ferdig, M. T. (2007). Quantitative dissection of clone-specific growth rates in cultured malaria parasites. *International Journal for Parasitology*, 37(14), 1599–1607. <https://doi.org/10.1016/j.ijpara.2007.05.003>
- Reiter, K., Mukhopadhyay, D., Zhang, H., Boucher, L. E., Kumar, N., Bosch, J., & Matunis, M. J. (2013). Identification of biochemically distinct properties of the small ubiquitin-related modifier (SUMO) conjugation pathway in *Plasmodium falciparum*. *The Journal of Biological Chemistry*, 288(39), 27724–36. <https://doi.org/10.1074/jbc.M113.498410>
- Ridley, R. G. (1998). Malaria : Dissecting chloroquine resistance. *Current Biology*, 8(10), 346–349. Retrieved from <https://www.sciencedirect.com/science/article/pii/S0960982298702180>
- Robbins, J. A., Absalon, S., Streva, V. A., & Dvorin, J. D. (2017). The malaria parasite cyclin H homolog PfCyc1 is required for efficient cytokinesis in blood-stage *Plasmodium falciparum*. *mBio*, 8(3). <https://doi.org/10.1128/mBio.00605-17>
- Rocamora, F., Zhu, L., Liong, K. Y., Dondorp, A., Miotto, O., Mok, S., & Bozdech, Z. (2018). Oxidative stress and protein damage responses mediate artemisinin resistance in malaria parasites. *PLoS Pathogens*, 14(3), e1006930. Retrieved from <https://www.ncbi.nlm.nih.gov/pmc/articles/PMC5868857/>
- Roques, M., Wall, R. J., Douglass, A. P., Ramaprasad, A., Ferguson, D. J. P., Kaindama, M. L., ... Tewari, R. (2015). *Plasmodium* P-type cyclin CYC3 modulates endomitotic growth during oocyst development in mosquitoes. *PLoS Pathogens*, 11(11), e1005273. <https://doi.org/10.1371/journal.ppat.1005273>
- Roth, A., Nahvi, A., Lee, M., Jona, I., & Breaker, R. R. (2006). Characteristics of the glmS ribozyme suggest only structural roles for divalent metal ions. *RNA*, 12(4), 607–19. <https://doi.org/10.1261/rna.2266506>
- Rovira-Graells, N., Gupta, A. P., Planet, E., Crowley, V. M., Mok, S., Ribas de Pouplana, L., ... Cortés, A. (2012). Transcriptional variation in the malaria parasite *Plasmodium falciparum*. *Genome Research*, 22(5), 925–38. <https://doi.org/10.1101/gr.129692.111>

- Sadowski, M., & Sarcevic, B. (2010). Mechanisms of mono- and poly-ubiquitination: Ubiquitination specificity depends on compatibility between the E2 catalytic core and amino acid residues proximal to the lysine. *Cell Division*, 5(1), 19. <https://doi.org/10.1186/1747-1028-5-19>
- Saifi, A. (2014). Antimalarial drugs: Mode of action and status of resistance. *African Journal of Pharmacy and Pharmacology*, 7(5), 148–156. <https://doi.org/10.5897/ajppx12.015>
- Sanchez, C. P., Dave, A., Stein, W. D., & Lanzer, M. (2010). Transporters as mediators of drug resistance in *Plasmodium falciparum*. *International Journal for Parasitology*, 40(10), 1109–18. <https://doi.org/10.1016/j.ijpara.2010.04.001>
- Sanchez, C. P., Liu, C. H., Mayer, S., Nurhasanah, A., Cyrklaff, M., Mu, J., ... Lanzer, M. (2014). A HECT ubiquitin-protein ligase as a novel candidate gene for altered quinine and quinidine responses in *Plasmodium falciparum*. *PLoS Genetics*, 10(5), 15–24. <https://doi.org/10.1371/journal.pgen.1004382>
- Saridaki, T., Sanchez, C. P., Pfahler, J., & Lanzer, M. (2008). A conditional export system provides new insights into protein export in *Plasmodium falciparum*-infected erythrocytes. *Cellular Microbiology*, 10(12), 2483–2495. <https://doi.org/10.1111/j.1462-5822.2008.01223.x>
- Schneider, K. A., & Escalante, A. A. (2013). Fitness components and natural selection: why are there different patterns on the emergence of drug resistance in *Plasmodium falciparum* and *Plasmodium vivax*? *Malaria Journal*, 12, 15. <https://doi.org/10.1186/1475-2875-12-15>
- Schoenberg, D. R. (2007). The end defines the means in bacterial mRNA decay: How the 5' phosphorylation state controls bacterial mRNA decay. *Nature Chemical Biology*, 3(9), 535–6. <https://doi.org/10.1038/nchembio0907-535>
- Shahinas, D., Folefoc, A., Taldone, T., Chiosis, G., Crandall, I., & Pillai, D. R. (2013). A purine analog synergizes with chloroquine (CQ) by targeting *Plasmodium falciparum* Hsp90 (PfHsp90). *PLoS ONE*, 8(9). <https://doi.org/10.1371/journal.pone.0075446>
- Sharma, D., Lather, M., Dykes, C. L., Dang, A. S., Adak, T., & Singh, O. P. (2016). Disagreement in genotyping results of drug resistance alleles of the *Plasmodium falciparum* dihydrofolate reductase (Pfdhfr) gene by allele-specific PCR (ASPCR) assays and Sanger sequencing. *Parasitology Research*, 115(1), 323–328. <https://doi.org/10.1007/s00436-015-4750-2>
- Sharp, J. S., & Bechhofer, D. H. (2003). Effect of translational signals on mRNA decay in *Bacillus subtilis*. *Journal of Bacteriology*, 185(18), 5372–9. <https://doi.org/10.1128/JB.185.18.5372-5379.2003>
- Sherling, E. S., Knuepfer, E., Brzostowski, J. A., Miller, L. H., Blackman, M. J., & Ooij, C. van. (2017). The *Plasmodium falciparum* rhoptry protein RhopH3 plays essential roles in host cell invasion and nutrient uptake. *eLife*, 6. <https://doi.org/10.7554/eLife.23239>
- Sidhu, A. B. S., Valderramos, S. G., & Fidock, D. A. (2005). *pfmdr1* mutations contribute to quinine resistance and enhance mefloquine and artemisinin sensitivity in *Plasmodium falciparum*. *Molecular Microbiology*, 57(4), 913–926. <https://doi.org/10.1111/j.1365-2958.2005.04729.x>
- Silva-Neto, M. A. C., Atella, G. C., & Shahabuddin, M. (2002). Inhibition of Ca<sup>2+</sup>/calmodulin-dependent protein kinase blocks morphological differentiation of *Plasmodium gallinaceum* zygotes to ookinetes. *The Journal of Biological Chemistry*, 277(16), 14085–91. <https://doi.org/10.1074/jbc.M107903200>



- Skinner-Adams, T. S., Lawrie, P. M., Hawthorne, P. L., Gardiner, D. L., & Trenholme, K. R. (2003). Comparison of *Plasmodium falciparum* transfection methods. *Malaria Journal*, 2, 1–4. Retrieved from <https://www.ncbi.nlm.nih.gov/pmc/articles/PMC166142/>
- Smilkstein, M., Sriwilaijaroen, N., Kelly, J. X., Wilairat, P., & Riscoe, M. (2004). Simple and inexpensive fluorescence-based technique for high-throughput antimalarial drug screening. *Antimicrobial Agents and Chemotherapy*, 48(5), 1803–6. <https://doi.org/10.1128/AAC.48.5.1803-1806.2004>
- Solyakov, L., Halbert, J., Alam, M. M., Semblat, J.-P., Dorin-Semblat, D., Reininger, L., ... Doerig, C. (2011). Global kinomic and phospho-proteomic analyses of the human malaria parasite *Plasmodium falciparum*. *Nature Communications*, 2(1), 565. <https://doi.org/10.1038/ncomms1558>
- Song, J., Wang, H., Wang, J., Leier, A., Marquez-Lago, T., Yang, B., ... Daly, R. J. (2017). PhosphoPredict: A bioinformatics tool for prediction of human kinase-specific phosphorylation substrates and sites by integrating heterogeneous feature selection. *Scientific Reports*, 7(1), 6862. <https://doi.org/10.1038/s41598-017-07199-4>
- Song, M., Hakala, K., Weintraub, S. T., & Shio, Y. (2011). Quantitative proteomic identification of the BRCA1 ubiquitination substrates. *Journal of Proteome Research*, 10(11), 5191–8. <https://doi.org/10.1021/pr200662b>
- Stolarczyk, E. I., Reiling, C. J., & Paumi, C. M. (2011). Regulation of ABC transporter function via phosphorylation by protein kinases. *Current Pharmaceutical Biotechnology*, 12(4), 621–35. Retrieved from <http://www.ncbi.nlm.nih.gov/pubmed/21118091>
- Suryadinata, R., Roesley, S. N. A., Yang, G., & Sarčević, B. (2014). Mechanisms of generating polyubiquitin chains of different topology. *Cells*, 3(3), 674–89. <https://doi.org/10.3390/cells3030674>
- Syin, C., Parzy, D., Traincard, F., Boccaccio, I., Joshi, M. B., Lin, D. T., ... Langsley, G. (2001). The H89 cAMP-dependent protein kinase inhibitor blocks *Plasmodium falciparum* development in infected erythrocytes. *European Journal of Biochemistry*, 268(18), 4842–9. Retrieved from <https://www.semanticscholar.org/paper/The-H89-cAMP-dependent-protein-kinase-inhibitor-in-Syin-Parzy/ba32d559e3e9b86967d38b7a500c7fbec8777b12>
- Takala-Harrison, S., Clark, T. G., Jacob, C. G., Cummings, M. P., Miotto, O., Dondorp, A. M., ... Plowe, C. V. (2013). Genetic loci associated with delayed clearance of *Plasmodium falciparum* following artemisinin treatment in Southeast Asia. *Proceedings of the National Academy of Sciences of the United States of America*, 110(1), 240–245. <https://doi.org/10.1073/pnas.1211205110>
- Tewari, R., Bailes, E., Bunting, K. A., & Coates, J. C. (2010). Armadillo-repeat protein functions: Questions for little creatures. *Trends in Cell Biology*, 20(8), 470–481. <https://doi.org/10.1016/j.tcb.2010.05.003>
- Thaithong, S., Suebsaeng, L., Rooney, W., & Beale, G. H. (1988). Evidence of increased chloroquine sensitivity in Thai isolates of *Plasmodium falciparum*. *Transactions of the Royal Society of Tropical Medicine and Hygiene*, 82(1), 37–8. Retrieved from <http://www.ncbi.nlm.nih.gov/pubmed/3051547>
- Thériault, C., & Richard, D. (2017). Characterization of a putative *Plasmodium falciparum* SAC1 phosphoinositide-phosphatase homologue potentially required for survival during the asexual erythrocytic stages. *Scientific Reports*, 7(1), 12710. <https://doi.org/10.1038/s41598-017-12762-0>

- Tizifa, T. A., Kabaghe, A. N., McCann, R. S., van den Berg, H., Van Vugt, M., & Phiri, K. S. (2018). Prevention efforts for malaria. *Current Tropical Medicine Reports*, 5(1), 41–50. <https://doi.org/10.1007/s40475-018-0133-y>
- Totland, M. Z., Bergsland, C. H., Fykerud, T. A., Knudsen, L. M., Rasmussen, N. L., Eide, P. W., ... Leithe, E. (2017). The E3 ubiquitin ligase NEDD4 induces endocytosis and lysosomal sorting of connexin 43 to promote loss of gap junctions. *Journal of Cell Science*, 130(17), 2867–2882. <https://doi.org/10.1242/JCS.202408>
- Trager, W., & Jensen, J. B. (1976). Human malaria parasites in continuous culture. *Science*, 193(4254), 673–5. Retrieved from <http://www.ncbi.nlm.nih.gov/pubmed/781840>
- Travassos, M., & Laufer, M. K. (2016). Antimalarial Drugs: an Overview. *UpToDate*. Retrieved April 24, 2019, from <https://pl.scribd.com/document/331138680/Antimalarial-Drugs-an-Overview-UpToDate>
- Traweger, A., Fang, D., Liu, Y., Stelzhammer, W., Krizbai, A., Bauer, H., & Bauer, H. (2002). The tight junction-specific protein occludin is a functional target of the E3 ubiquitin-protein ligase itch. *The Journal of Biological Chemistry*, 277(12), 10201–10208. <https://doi.org/10.1074/jbc.M111384200>
- Vaid, A., & Sharma, P. (2006). PfPKB, a protein kinase B-like enzyme from *Plasmodium falciparum*: II. Identification of calcium/calmodulin as its upstream activator and dissection of a novel signaling pathway. *The Journal of Biological Chemistry*, 281(37), 27126–33. <https://doi.org/10.1074/jbc.M601914200>
- Vaid, A., Thomas, D. C., & Sharma, P. (2008). Role of Ca<sup>2+</sup>/calmodulin-PfPKB signaling pathway in erythrocyte invasion by *Plasmodium falciparum*. *The Journal of Biological Chemistry*, 283(9), 5589–97. <https://doi.org/10.1074/jbc.M708465200>
- Valderramos, S. G., Valderramos, Juan-CarlosMusset, L., Purcell, L. A., Mercereau-Puijalon, O., Legrand, E., & Fidock, D. A. (2010). Identification of a mutant PfCRT-mediated chloroquine tolerance phenotype in *Plasmodium falciparum*. *PLoS Pathogens*, 6(5), e1000887. <https://doi.org/10.1371/journal.ppat.1000887>
- van Biljon, R., Niemand, J., van Wyk, R., Clark, K., Verlinden, B., Abrie, C., ... Birkholtz, L.-M. (2018). Inducing controlled cell cycle arrest and re-entry during asexual proliferation of *Plasmodium falciparum* malaria parasites. *Scientific Reports*, 8(1), 16581. <https://doi.org/10.1038/s41598-018-34964-w>
- Veiga, M. I., Dhingra, S. K., Henrich, P. P., Straimer, J., Gnädig, N., Uhlemann, A.-C., ... Fidock, D. A. (2016). Globally prevalent PfMDR1 mutations modulate *Plasmodium falciparum* susceptibility to artemisinin-based combination therapies. *Nature Communications*, 7, 11553. <https://doi.org/10.1038/ncomms11553>
- Vial, H. J., Eldin, P., Tielens, A. G. M., & Van Hellemond, J. J. (2003). Phospholipids in parasitic protozoa. *Molecular and Biochemical Parasitology*, 126(2), 143–154. [https://doi.org/10.1016/S0166-6851\(02\)00281-5](https://doi.org/10.1016/S0166-6851(02)00281-5)
- Visser, B. J., Wieten, R. W., Nagel, I. M., & Grobusch, M. P. (2013). Serum lipids and lipoproteins in malaria--a systematic review and meta-analysis. *Malaria Journal*, 12, 442. <https://doi.org/10.1186/1475-2875-12-442>
- Voss, T. S., Bozdech, Z., & Bártfai, R. (2014). Epigenetic memory takes center stage in the survival strategy of malaria parasites. *Current Opinion in Microbiology*, 20, 88–95.

- Wagner, S. A., Beli, P., Weinert, B. T., Nielsen, M. L., Cox, J., Mann, M., & Choudhary, C. (2011). A proteome-wide, quantitative survey of in vivo ubiquitylation sites reveals widespread regulatory roles. *Molecular & Cellular Proteomics: MCP*, 10(10), M111.013284. <https://doi.org/10.1074/mcp.M111.013284>
- Walliker, D. (2005). Fitness of drug-resistant malaria parasites. *Acta Tropica*, 94, 5–6. <https://doi.org/10.1016/j.actatropica.2005.04.005>
- Walliker, D., Quakyi, I. A., Wellem, T. E., McCutchan, T. F., Szarfman, A., London, W. T., ... Carter, R. (1987). Genetic analysis of the human malaria parasite *Plasmodium falciparum*. *Science*, 236(4809), 1661–6. Retrieved from <http://www.ncbi.nlm.nih.gov/pubmed/3299700>
- Wang, F., Krai, P., Deu, E., Bibb, B., Lauritzen, C., Pedersen, J., ... Klemba, M. (2011). Biochemical characterization of *Plasmodium falciparum* dipeptidyl aminopeptidase 1. *Molecular and Biochemical Parasitology*, 175(1), 10–20. <https://doi.org/10.1016/J.MOLBIOPARA.2010.08.004>
- Wang, G., Gao, Y., Li, L., Jin, G., Cai, Z., Chao, J.-I., & Lin, H.-K. (2012). K63-Linked ubiquitination in kinase activation and cancer. *Frontiers in Oncology*, 2. <https://doi.org/10.3389/fonc.2012.00005>
- Wang, L., Delahunty, C., Fritz-Wolf, K., Rahlfs, S., Helena Prieto, J., Yates, J. R., & Becker, K. (2015). Characterization of the 26S proteasome network in *Plasmodium falciparum*. *Scientific Reports*, 5(1), 17818. <https://doi.org/10.1038/srep17818>
- Wang, L., Delahunty, C., Prieto, J. H., Rahlfs, S., Jortzik, E., Yates, J. R., & Becker, K. (2014). Protein S-nitrosylation in *Plasmodium falciparum*. *Antioxidants & Redox Signaling*, 20(18), 2923–2935. <https://doi.org/10.1089/ars.2013.5553>
- Wang, Y., & Oram, J. F. (2007). Unsaturated fatty acids phosphorylate and destabilize ABCA1 through a protein kinase C  $\delta$  pathway. *Journal of Lipid Research*, 48(5), 1062–1068. <https://doi.org/10.1194/jlr.m600437-jlr200>
- Warrier, A., & Hjelmstad, G. O. (2007). Protein kinase inhibitors reduce GABA but not glutamate release in the nucleus accumbens. *Neuropharmacology*, 53(8), 925–9. <https://doi.org/10.1016/j.neuropharm.2007.09.004>
- Wein, S., Ghezal, S., Buré, C., Maynadier, M., Périgaud, C., Vial, H. J., ... Cerdan, R. (2018). Contribution of the precursors and interplay of the pathways in the phospholipid metabolism of the malaria parasite. *Journal of Lipid Research*, 59(8), 1461–1471. <https://doi.org/10.1194/jlr.M085589>
- Wenzel, D. M., & Klevit, R. E. (2012). Following Ariadne's thread : a new perspective on RBR ubiquitin ligases. *BMC Biology*, 10, 24. Retrieved from <https://www.ncbi.nlm.nih.gov/pmc/articles/PMC3305615/>
- Wezena, C. A., Alisch, R., Golzmann, A., Liedgens, L., Staudacher, V., Pradel, G., & Deponte, M. (2018). The cytosolic glyoxalases of *Plasmodium falciparum* are dispensable during asexual blood-stage development. *Microbial Cell*, 5(1), 32–41. <https://doi.org/10.15698/mic2018.01.608>
- White, N. J. (2004). Antimalarial drug resistance. *Journal of Clinical Investigation*, 113(8). <https://doi.org/10.1172/JCI200421682.1084>
- White, N. J., Pukrittayakamee, S., Hien, T. T., Faiz, M. A., Mokuolu, O. A., & Dondorp, A. M. (2014). Malaria. *The Lancet*, 383(9918), 723–735. [https://doi.org/10.1016/S0140-6736\(13\)60024-0](https://doi.org/10.1016/S0140-6736(13)60024-0)

- WHO. (2017). International travel and health: Malaria. *World Health Organization*. Retrieved from <https://www.who.int/ith/en/>
- WHO. (2018a). Overview of malaria treatment. *WHO*. Retrieved from <https://www.who.int/malaria/areas/treatment/overview/en/>
- WHO. (2018b). World malaria report 2018. *WHO*. Retrieved from <https://www.who.int/malaria/publications/world-malaria-report-2018/en/>
- Wilson, D. W., Langer, C., Goodman, C. D., McFadden, G. I., & Beeson, J. G. (2013). Defining the timing of action of antimalarial drugs against *Plasmodium falciparum*. *Antimicrobial Agents and Chemotherapy*, 57(3), 1455–1467. <https://doi.org/10.1128/AAC.01881-12>
- Witkowski, B., Berry, A., & Benoit-Vical, F. (2009). Resistance to antimalarial compounds: methods and applications. *Drug Resistance Updates : Reviews and Commentaries in Antimicrobial and Anticancer Chemotherapy*, 12(1–2), 42–50. <https://doi.org/10.1016/j.drug.2009.01.001>
- Witkowski, B., Lelièvre, J., Barragán, M. J. L., Laurent, V., Su, X., Berry, A., & Benoit-Vical, F. (2010). Increased tolerance to artemisinin in *Plasmodium falciparum* is mediated by a quiescence mechanism. *Antimicrobial Agents and Chemotherapy*, 54(5), 1872–7. <https://doi.org/10.1128/AAC.01636-09>
- Wu, Y., Sifri, C. D., Lei, H. H., Su, X. Z., & Wellems, T. E. (1995). Transfection of *Plasmodium falciparum* within human red blood cells. *Proceedings of the National Academy of Sciences of the United States of America*, 92(4), 973–7. Retrieved from <http://www.ncbi.nlm.nih.gov/pubmed/7862676>
- Wunderlich, F., Fiebig, S., Vial, H., & Kleinig, H. (1991). Distinct lipid compositions of parasite and host cell plasma membranes from *Plasmodium chabaudi*-infected erythrocytes. *Molecular and Biochemical Parasitology*, 44(2), 271–277. [https://doi.org/10.1016/0166-6851\(91\)90013-V](https://doi.org/10.1016/0166-6851(91)90013-V)
- Xie, Y., Xu, K., Linn, D. E., Yang, X., Guo, Z., Shimelis, H., ... Qiu, Y. (2008). The 44-kDa Pim-1 kinase phosphorylates BCRP/ABCG2 and thereby promotes its multimerization and drug-resistant activity in human prostate cancer cells. *The Journal of Biological Chemistry*, 283(6), 3349–56. <https://doi.org/10.1074/jbc.M707773200>
- Xiong, Y., Wang, C., Shi, L., Wang, L., Zhou, Z., Chen, D., ... Guo, H. (2017). Myosin Light Chain Kinase: A potential target for treatment of inflammatory diseases. *Frontiers in Pharmacology*, 8, 292. <https://doi.org/10.3389/fphar.2017.00292>
- Yakubu, R. R., Weiss, L. M., & Silmon de Monerri, N. C. (2018). Post-translational modifications as key regulators of apicomplexan biology: insights from proteome-wide studies. *Molecular Microbiology*, 107(1), 1–23. <https://doi.org/10.1111/mmi.13867>
- Ye, Y. (2006). Diverse functions with a common regulator: Ubiquitin takes command of an AAA ATPase. *Journal of Structural Biology*, 156(1), 29–40. <https://doi.org/10.1016/J.JSB.2006.01.005>
- Zhang, J., Krugliak, M., & Ginsburg, H. (1999). The fate of ferriprotophyrin IX in malaria infected erythrocytes in conjunction with the mode of action of antimalarial drugs. *Molecular and Biochemical Parasitology*, 99(1), 129–141. [https://doi.org/10.1016/S0166-6851\(99\)00008-0](https://doi.org/10.1016/S0166-6851(99)00008-0)
- Zhang, M., Wang, C., Otto, T. D., Oberstaller, J., Liao, X., Adapa, S. R., ... Adams, J. H. (2018). Uncovering the essential genes of the human malaria parasite *Plasmodium falciparum* by saturation mutagenesis. *Science*, 360(6388), eaap7847. <https://doi.org/10.1126/science.aap7847>

- Zhou, H., Zheng, C., Su, J., Chen, B., Fu, Y., Xie, Y., ... He, J. (2016). Characterization of a natural triple-tandem c-di-GMP riboswitch and application of the riboswitch-based dual-fluorescence reporter. *Scientific Reports*, 6, 20871. <https://doi.org/10.1038/srep20871>
- Zidovetzki, R., Sherman, I. W. ., & O'Brien, L. (1993). Inhibition of *Plasmodium falciparum* phospholipase A 2 by chloroquine, quinine, and arteether. *The American Society of Parasitologist*, 79(4), 565–570. Retrieved from <https://www.ncbi.nlm.nih.gov/pubmed/8331477>
- Zou, L., Wang, M., Shen, Y., Liao, J., Li, A., & Wang, M. (2013). PKIS: computational identification of protein kinases for experimentally discovered protein phosphorylation sites. *BMC Bioinformatics*, 14, 247. <https://doi.org/10.1186/1471-2105-14-247>



# Appendix I: Supplementary figures

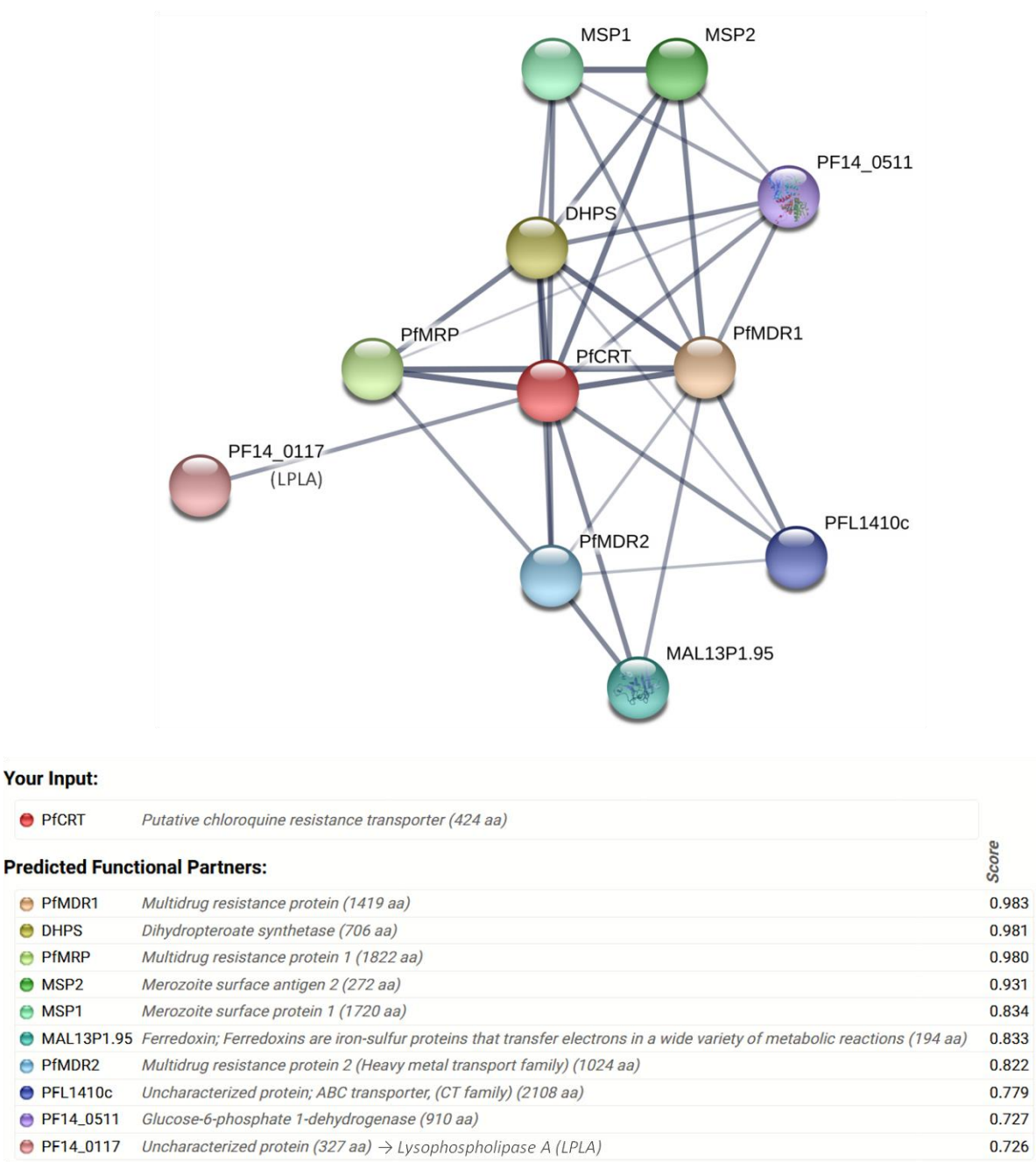
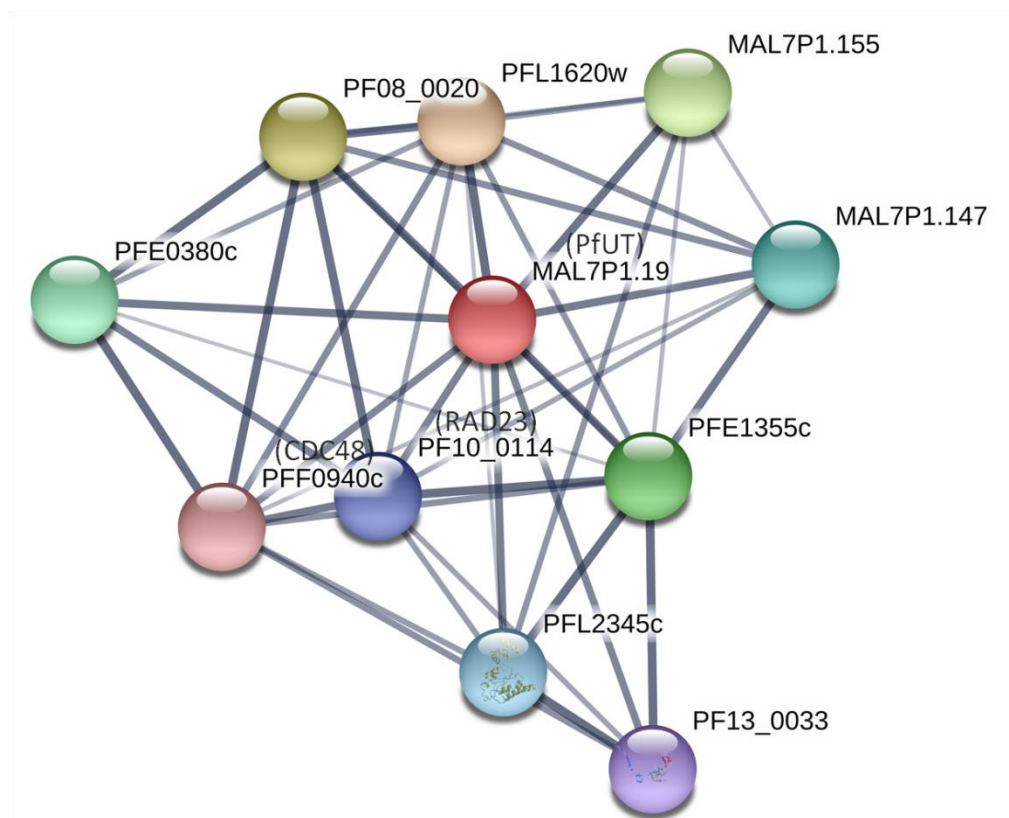


**Figure I.1. STRING protein-protein interaction network depicted for PfCRT.** Colourful nodes represent interacting partners of PfCRT (central, red) in *P. falciparum*. Filled nodes indicate proteins for which 3D structure is known or predicted. Line thickness indicates the strength of data support. Adapted from [www.string-db.org](http://www.string-db.org).



#### Your Input:

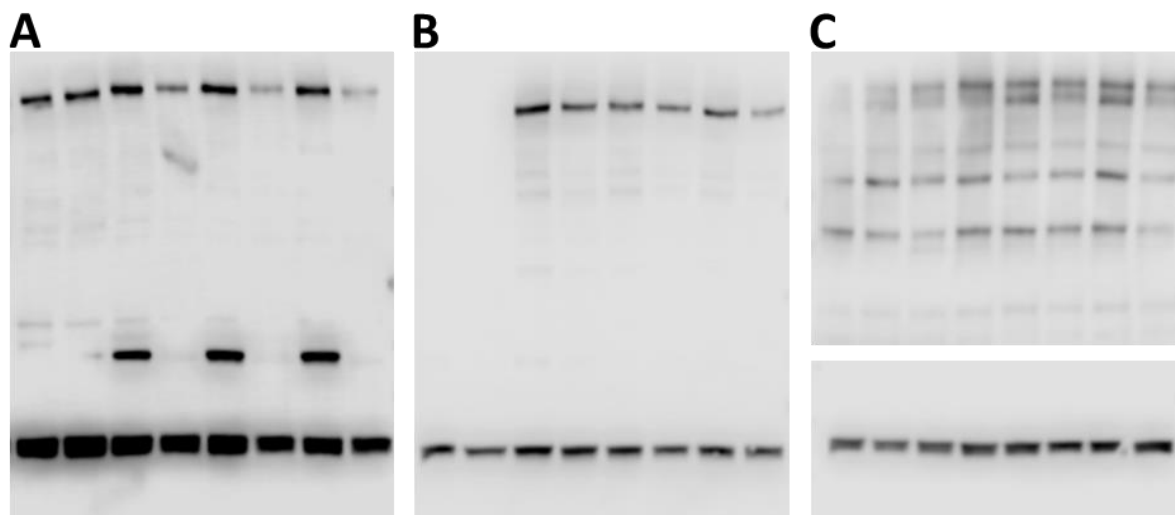
● MAL7P1.19 Uncharacterized protein; Ubiquitin transferase, putative (3893 aa) → PfUT

#### Predicted Functional Partners:

|   | Score |
|---|-------|
| ● PFL1620w Asparagine/aspartate rich protein, putative (5439 aa)  | 0.999 |
| ● PF08_0020 Uncharacterized protein; Ubiquitination-mediated degradation component, putative (1326 aa)                      | 0.972 |
| ● MAL7P1.155 Uncharacterized protein; Zinc finger, C3HC4 type, putative (2162 aa)   | 0.950 |
| ● PFE1355c Uncharacterized protein; Ubiquitin carboxyl-terminal hydrolase; Belongs to the peptidase C19 family (605 aa)     | 0.927 |
| ● PFE0380c Nuclear pore associated protein (NLP4), putative (531 aa)  | 0.919 |
| ● MAL7P1.147 Uncharacterized protein; Ubiquitin carboxyl-terminal hydrolase; Belongs to the peptidase C19 family (3183 aa)  | 0.903 |
| ● PFL2345c 26S protease regulatory subunit 8; Tat-binding protein homolog; Belongs to the AAA ATPase family (435 aa)        | 0.886 |
| ● PF10_0114 DNA repair protein RAD23, putative (389 aa)   | 0.856 |
| ● PF13_0033 Uncharacterized protein; 26S proteasome regulatory subunit, putative; Belongs to the AAA ATPase family (393 aa) | 0.846 |
| ● PFF0940c Cell division cycle protein 48 homologue, putative (828 aa)  | 0.835 |

**Figure I.2. STRING protein-protein interaction network depicted for PfUT.** Colourful nodes represent interacting partners of PfUT (central, red) in *P. falciparum*. Filled nodes indicate proteins for which 3D structure is known or predicted. Line thickness indicates the strength of data support. Adapted from [www.string-db.org](http://www.string-db.org).







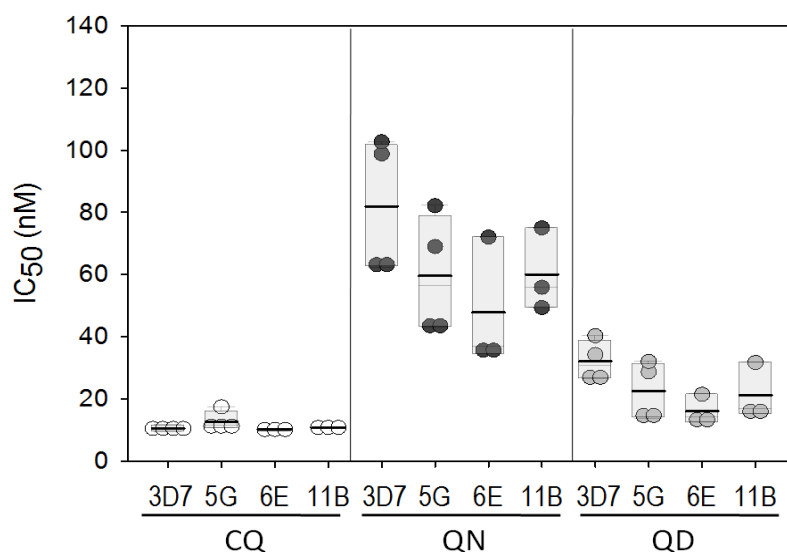





**Figure I.3. Western blot analysis of PfUT-HA-glms.** A full, uncropped view of western blot membrane fragments depicted in Figure 3.11.A (chapter 3.2.1.3). **A.** Top bands represent labelling with N-terminal anti-PfUT antibody. Bottom bands indicate staining with anti- $\alpha$ -tubulin. **B.** Top bands represent labelling with anti-HA antibody. Bottom bands indicate staining with anti- $\alpha$ -tubulin. **C.** Top bands represent labelling with C-terminal anti-PfUT antibody. Bottom bands indicate staining with anti- $\alpha$ -tubulin.



**Figure I.4. Growth inhibition assays of 3D7 wild type and PfUT-HA-glms parasites in the presence of 2.5 mM GlcN.** Half-maximal inhibitory concentrations (IC<sub>50</sub>) were determined for chloroquine (CQ, control drug), quinine (QN) and quinidine (QD, stereoisomer of QN). Each symbol represents an independent biological replicate. A thick black line indicates the mean value of each data set in a box plot analysis. The differences between the data sets consisting of 3-4 independent measurements for each clone were not significant according to One Way ANOVA Holm-Sidak.

| Attempted modification  | Fusion protein   | Molecular weight | Successful? | Method      |
|---|------------------|------------------|-------------|-------------|
|  | HA               | 3 kDa            | ✓           | CRISPR-Cas9 |
|  | HA               | 3 kDa            | ✗           | CRISPR-Cas9 |
|  | BirA-myc         | 36 kDa           | ✗           | CRISPR-Cas9 |
|  | BirA-myc         | 36 kDa           | ✗           | CRISPR-Cas9 |
|  | APEX2            | 27 kDa           | ✗           | SLI         |
|  | allelic exchange | -                | ✗           | CRISPR-Cas9 |
|  | disruption       | -                | ✗           | SLI-TGD     |

\* graphical representation does not reflect the real distance in the genome

**Figure I.5. Modifications attempted in PfUT.** HA-hemagglutinin tag; glmS ribo – glmS ribozyme; HECT\* - HECT catalytic domain with replacement of cysteine active site by a serine residue; BirA – biotin ligase; myc – myc tag; APEX2 - ascorbate peroxidase; AIEx – allelic exchange of conserved polymorphic residues in resistant PfUT by their sensitive alleles; GFP – green fluorescent protein tag; Neo-R – neomycin resistance gene; \* - stop codon.

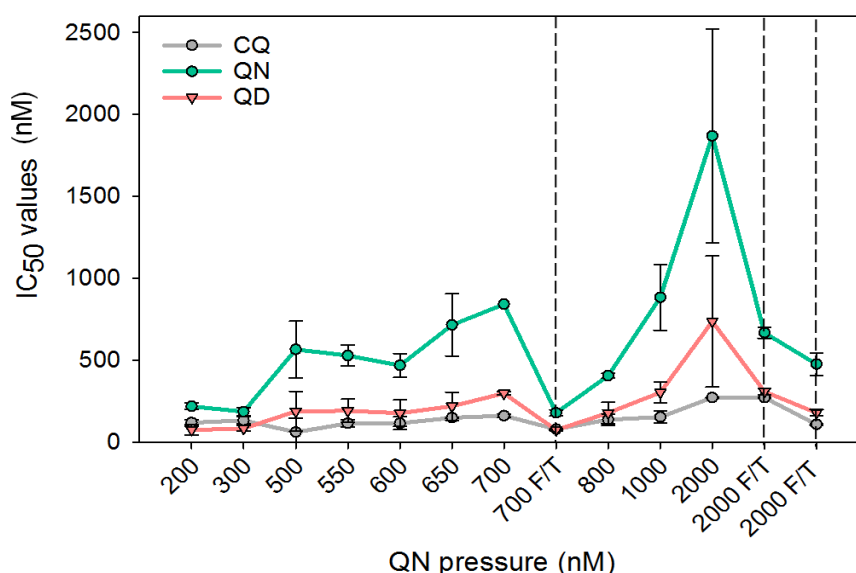


**Figure I.6. Effect of the stepwise increase of quinine pressure on drug susceptibility of *P. falciparum* Dd2 strain.** Above graph displays results of a representative culture flask (out of the initial pool of 8 that were cultivated in parallel), showing the strongest response to the increasing drug pressure over time. Susceptibility of parasites was determined by measuring IC<sub>50</sub> values for quinine (QN), quinidine (QD), along with chloroquine (CQ) as a control. Each symbol represents a mean ± SD of 2-5 IC<sub>50</sub>

determinations. Dashed lines signify the measurements conducted within a week after parasites' freezing and thawing (F/T). Initially, with the stepwise increase of QN concentrations, similar increases in  $IC_{50}$  values for both QN and QD have been observed, indicating that the parasites are adapting to the applied drug pressure. Parasites freezing and thawing (e.g. after culture contamination) led to a decrease in  $IC_{50}$  values, indicating that previously observed changes do not arise from adaptive mutations but rather some reversible epigenetic mechanisms, which allow parasites to acquire and revert from drug resistant phenotypes.

# Appendix II: Plasmid maps

## CRISPR-Cas9 plasmids

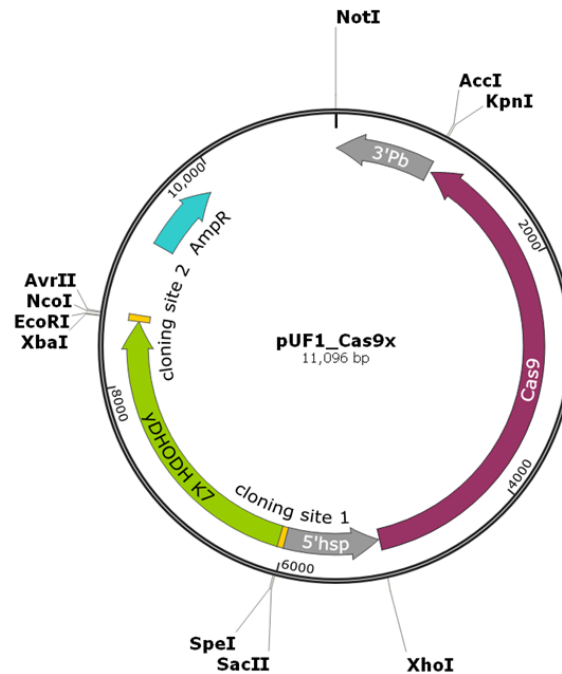


**Figure II.1. pUF1-Cas9 encoding the Cas9 endonuclease.** The sequence of Cas9 is flanked by nuclear localization signals (NLS) and its expression is regulated by the promoter region of heat shock protein 86 (5' hsp) and 3'UTR region of the *P. berghei* dihydrofolate reductase (3' Pb dhfr). Upon transfection the plasmid is selected using yeast dihydroorotate dehydrogenase marker (*ydhodh*), conferring resistance to DSM1. The plasmid was kindly provided by Dr. José Juan Lopez Rubio (Ghorbal et al., 2014).

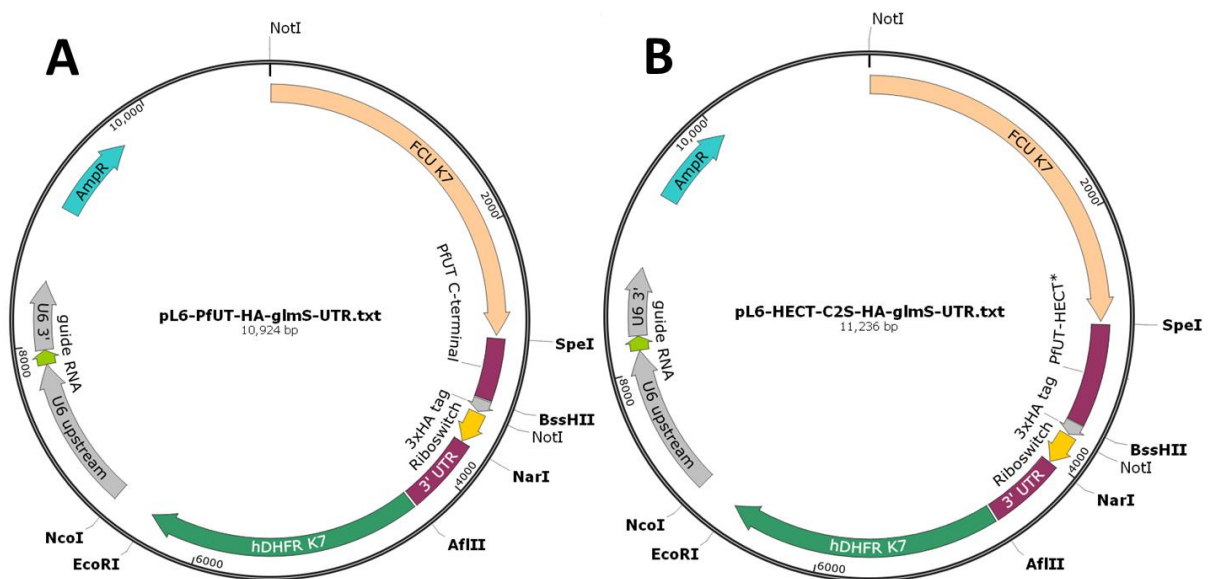


**Figure II.2. pL6-HA-glmS-based constructs for PfUT downregulation.** The plasmid contains the sequences of triple hemagglutinin (3xHA tag) and glmS ribozyme integrated into the backbone. Left and right homology regions of pL6-PfUT-HA-glmS-UTR (A) were amplified with primers 1-2 and 3-4,

cloned into the vector using enzymes *SpeI*-*BssHII* and *NarI*-*AflIII*, respectively. **pL6-HECT-C2S-HA-glmS-UTR (B)** was generated by replacing the left homology region in pL6-PfUT-HA-glmS-UTR with a DNA fragment amplified using primers 12-13. Expression of guide RNA is regulated by the promoter and the 3'UTR region of the *P. falciparum* U6 small nuclear RNA polymerase III (5' U6). The original pL6 vector was digested with the enzyme *BtgZI* and the guide RNA 1 (primers 5 and 6, chapter 2.1.5.6) was cloned into the pL6 vector using the *In Fusion* cloning technology. The plasmid is selected using human dihydrofolate reductase marker (hDHFR), whereas the negative selection is carried out by means of bifunctional yeast cytosine deaminase and uridyl phosphorybosyl transferase (FCU). The original pL6 plasmid was kindly provided by Dr. José Juan Lopez Rubio (Ghorbal et al., 2014).

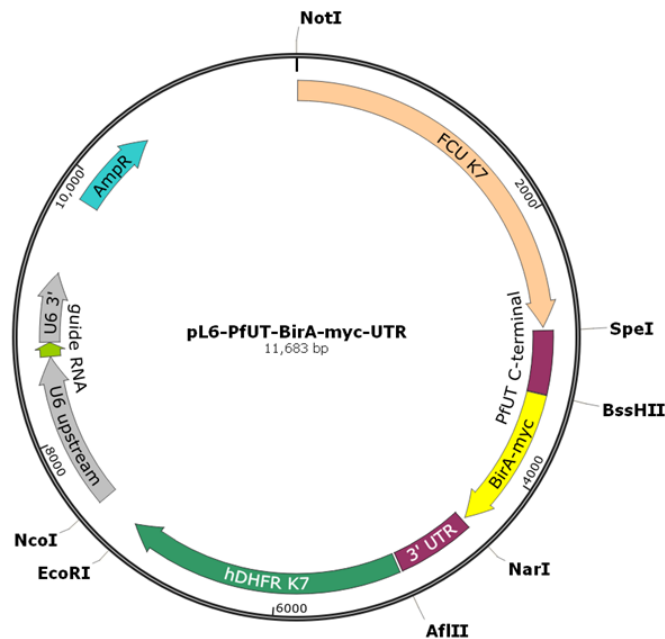


**Figure II.3. pL6-PfUT-BirA-myc-UTR.** The construct was generated by replacing the HA-glmS sequence from the pL6-PfUT-HA-glmS-UTR with a sequence encoding a biotin ligase (BirA) fused to triple Myc-tag (primers 15-16) using enzymes *BssHII* and *NarI*.

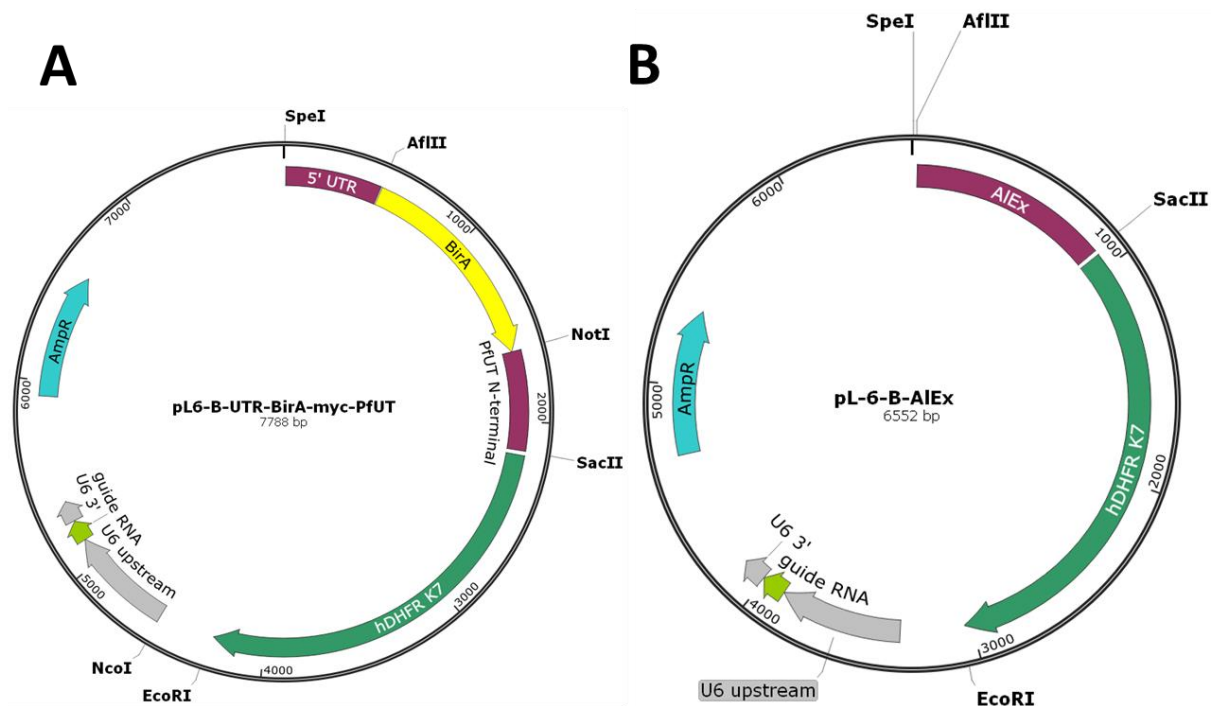


**Figure II.4. pL6-B-based plasmids for N-terminal BirA fusion (A) and allelic exchange (B).** The pL6-B is a modified version of pL6 in which FCU K7 cassette is removed and a U6 cassette is shortened. **A. pL6-B-UTR-BirA-myc-PfUT.** A sequence of BirA-myc was amplified using primers 33 and 34, and cloned into the pL6-B using enzymes AflII and NotI. Left and right homology regions of **pL6-PfUT-HA-glmS-UTR (A)** were amplified with primers 29-30 and 31-32, cloned into the vector using enzymes SpeI-AflII and NotI-SacII, respectively. The guide RNA 4 was amplified using primers 35 and 36. **B. pL6-B-AIEx** was generated by cloning of the PfUT allelic exchange fragment (AIEx), aiming to replace the resistant alleles by sensitive ones using enzymes AflII and SacII. The AIEx mutagenesis was carried out using primers 21-24. The guide RNA 3 was amplified using primers 25 and 26. The pL6-B plasmid was kindly provided by Dr. José Juan Lopez Rubio (Ghorbal et al., 2014), designed jointly with Marcus Lee (Sanger Institute).

## SLI plasmids

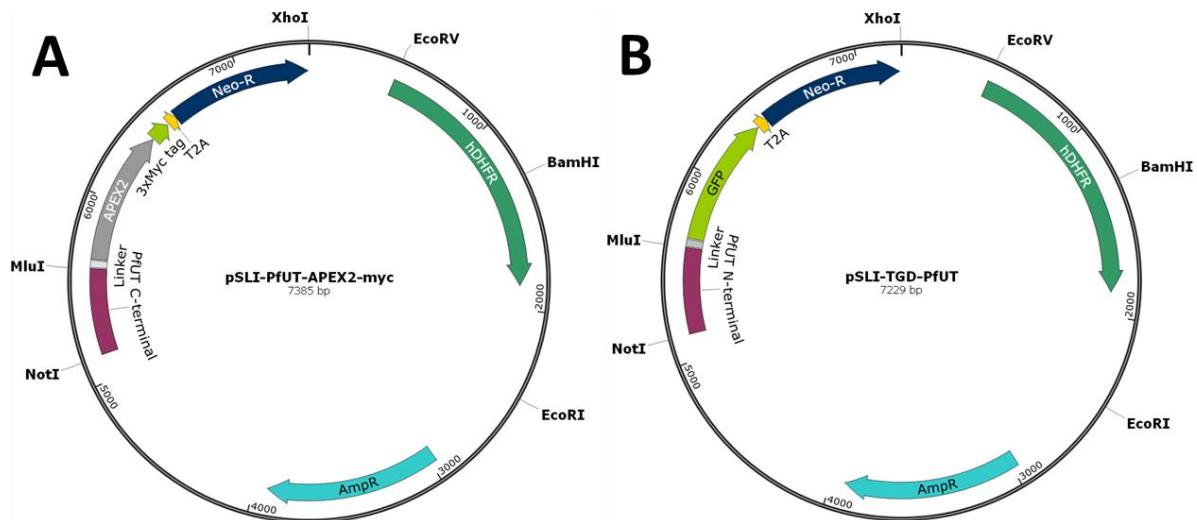


**Figure II.5. pSLI plasmids for BioID (A) and gene disruption (B).** The PfUT homology region (HR) in **pSLI-PfUT-APEX2 (A)** was amplified with primers and cloned using enzymes NotI and MluI. An ascorbate peroxidase (APEX2) fused to triple Myc (3xMyc tag) is separated from the HR with a linker. The N-terminal PfUT fragment in **pSLI-TGD-PfUT (B)** was amplified using primers 17 and 18 and cloned to the vector using enzymes NotI and MluI. Selection of pSLI construct is carried out using human dihydrofolate reductase marker (hDHFR), conferring resistance to WR99210. The parasites which integrated the plasmid (“integrants”) are selected with the neomycin phosphotransferase resistance marker (Neo-R), conferring resistance to G418. The Neo-R is separated from the fusion protein (APEX2 or GFP) with a T2A skip peptide. The pSLI-APEX2 plasmid was kindly provided by Dr. Markus Ganter. The pSLI-TGD plasmid was kindly provided by Dr. Tobias Spielmann (Birnbaum et al., 2017).

# Appendix III: DNA sequences

## III.1. Homology regions

The homology regions used during cloning of the transfection vectors are indicated below. The coding sequence and introns are indicated in capital and small letters, respectively. The sequences recognized by primers used for amplification (chapter 2.1.5.6) are underlined.

- DNA fragments of PfUT used in constructs for glmS ribozyme-based conditional knockdown and BirA C-terminal fusion (CRISPR-Cas9 system):

### Left homology region: C-terminal PfUT (primers 1 and 2)

TTAATGAAAGTTGTTAAGAAGGAGGACAATAATGATTTACCAAGTGTGATGACTTGTACAAATTATTTAAAAATA  
CCAGATTATAAAAAATAAGAAAACTAAGGAACAGATTAATTTATGCCATTAATGAAGGtatatatataatatat  
ataatatatatataatatatatatatgtatatatatatttataaaaaaaaaaagaaaaaaaaaattaagtgaagag  
taaaaaaaaaatttttttttttttttttttttaaatagtgcatataatatacatatatataataatatgtttat  
gtatacttatattattatatgccccttttacgtaaatatatattaatacggctattttattatatatatatgtatat  
atgtatatattttatttataagcacacatacatatatatatatatattttattattattttcttcttaggCC  
AAAAGAATTTTTCCTTTCTG

The shield mutations are indicated with grey distinctions.

### Right homology region: 3' UTR (primers 3 and 4)

TTTTTGTTCGACCCGATGTATTATAATTTTTTTTTTTTAACTCATAAAATATAAACCTTGAGACTTTAATCAG  
GTATTATAATATTAATAATGAGAGATTCCCCAAATGTTAAAAAGGAAAAATTTATACATATAAATATATATAT  
ATATATATATGATTTTCCTTATTTTACGCATAGTTCAAAAAAAAAAAAAAAAAATATATATATATAATATATATAT  
ATTTAAATATTAGTCTTGTGTATTTTATAATGTGTGTATATAATATATTATATATTTTCTTATGTGTATTATTT  
ATTATTATTATTTATTTTCTTTCATGCAATAAATATATGAATATATTTTATTATTTTTTTTTTTTTTTTATAT  
ATATTACTTACAAACATTGTGTATATATGGAATAATAGGAAATACAAAATTGTGTTATTATGTTACTTTTAAAA  
GAAATAATATACACACATATATAAAATAAATATATAATATAATATAATATACATATATATATATATATATATA  
TATATATTAATATATATGTGTATATATTATATATGTCAAGGACATATACATTAAAGA

- DNA fragments of PfUT used in construct for active cysteine to serine replacement in PfUT's HECT catalytic domain (CRISPR-Cas9 system):

### Left homology region: C-terminal PfUT (primers 11 and 2)

agATATACGAACGATTCAATTACTTTTATTACATTAATTGAAATACTTTCCGAATTTAATAAGGAAGAGAGAAAA  
CAATTTGTAAATTTTGTACGGGAACATCTGCCCTACCTAATAATGGCTTTGCAGCATTAAAGtaataattatat  
atatatatatatatatatatatatgtgaaatgctgttttatattatatatatatatatatatatatatgtgtgtgtg  
tgtgtgtgtgtgtatgtattttattataatacttcataatattttttattattttttttattattactttttata  
attttaggCCCTTAATGAAAGTTGTTAAGAAGGAGGACAATAATGATTTACCAAGTGTGATGACTTCTACAAATT  
ATTTAAAAATACCAGATTATAAAAAATAAGAAAACTAAGGAACAGATTAATTTATGCCATTAATGAAGGtatat  
ataataatatataataatatataatatatatatatgtatatatatatttataaaaaaaaaaagaaaaaaaaaata  
taagtgaagtaaaaaaaaaatttttttttttttttttttaaatagtgcatataatatacatatatatatataat  
aatatgtttatgtatacttatattattatatgccccttttacgtaaatatatattaatacggctattttattatata  
tatatgtatatatgtatatattttatttataagcacacatacatatatatatatatattttattattatttt  
cttcttaggCCAAAGAATTTTTCCTTTCTG

A point mutation resulting in a cysteine to serine replacement (TGT → TCT) is highlighted with black distinction, whereas the shield mutations are indicated with grey distinctions.

**Right homology region: 3' UTR (primers 3 and 4)**

TTTTTGTTTGCGACCCGATGATTATAAATTTTTTTTTTTTAACTCATAAAATATAAACCTTGAGACTTTAATCAG  
GTATTATAATATTTAAATGAGAGATTCCCCCAAATGTTAAAAAGGAAAAATTTATACATATAAAATATATATATAT  
ATATATATATGATTTTCCCTTATTTTACGCATAGTTCAAAAAAAAAAAAAAAAAATATATATATATAATATATATATAT  
ATTTAAATATTAGTCTTGTGTATTTTATAATGTGTGTATATAATATATTATATATTTTCTTATGTGTATTATTT  
ATTATTATTATTTATTTTCTTTGCATGCAATAAAATATATGAATATATTTTATTATTTTTTTTTTTTTTTTTATAT  
ATATTACTTACAAACATTGTGTATATATGGAATAATAGGAAATACAAAATTTGTGTTATTATGTTTACTTTTAAAA  
GAAATAATATACACACATATATAAAAAATAAAATATATAATATAATATAATATACATATATATATATATATATATA  
TATATATTAATATATATGTGTATATATTATATATGTCAAGGACATATACATTAAAGA

- DNA fragments of PfUT used in construct for targeted gene disruption (SLI-TGD approach):

### N-terminal PfUT (primers 17 and 18)

ttaaAATGGAGATGAATCTGAAATGgtaaatataataatatatttggataatgcaatgttaagaatgtgtgaattggttatattattgtgtaatcatattatataatataatataatataatatttaattttttttattttattttttattttttttatattttttttttttttttttttttttttttttttttttttacttttttagCTAGCTGCGCTGAACGATTTTTATGAACAATTGAATTTGTCTCAGCTGACGGAGGTTTGAGCAATTCGACTTTAGAAGAATATATGAACGTGCTTATTCACGTAATAAAAAAGTCCTCACATAAGTTATAAATAGTGTTTACGGAGAAAATGAGAACAAACAACAATAATAATAATAATAAAAAAGAAGATGTGAAAAATTCCACAAACGCACAGAAAGGAAATTCTTCTGAAAGGATAAATGAGGTTGTAGGTAG

The intentionally added stop codon (TAA) required for the success of the system is highlighted with grey distinction.

- DNA fragments of PfUT used in construct for BirA N-terminal fusion (CRISPR-Cas9 system):

**Left homology region: 5' UTR** (primers 29 and 30)

TTTTGCAGTTTCATACATATATCTGTGAAAAAAAAAATGAAATAAAATAAAATAAAATAAAATATATATATATATA  
TATATATATATATATATATATATAATATAATATAGTATAATTTTATATGTTGAAGAATGAAATACAATATATTATA  
TTTCATAATAGTAATATTTTATATTTTATAACGAGAGCACACTTATTTTATATAAAATATAACAATAATATATATATAT  
ATATATATATTGATGTCATATATTTTACGTCATTTTTTTTCCATATTAAGTTTTTATTTTTTGAGAAAAGCTACATAT  
ATATAATTTAGGGCATCTCATAAAAAGAAAAATAAAAAAGGAATTAACACATAATTTGATTTTCAATATAAATTCGTGA  
AATTATATATTTCAATAAAATAGAAATATATTATATTATATATGATATATTTTATATGATATATCTTTATTTCTACAT  
CATGCTTTAAGTATAATATATATATATAAATTTTAGTTAAAGAATAA

**Right homology region: N-terminal PfUT (primers 31 and 32)**

TTGAAGAAATACCTTGCTCTTTGAA<sup>1</sup>AATTCCCAGTATTCCTATATTATTAACAGTATAAAAAATGGAGATGAATCT  
GAAATGgtaaataataataatattggataatgcaatgtttaagaatgtgtgaattgtttatattattgtgtaatca  
tattatataatatatatatatatatattttaatttttttttattttattttttttatttttttatatttttttt  
ttttttttttttttttttttttttttttttacttttttagCTAGCTGCGCTGAACGATTTTTTATGAACAATTGAA  
TTTGTGCTGAGCTGACGGAGGTTTGAGCAATTCGACTTTAGAGAATATATGAACGTGCTTATTCACGTAATAAAAAAG  
TCCTCACATAAGTTATAATAGTGTTTACGGAAGAAATGAGAACAAACAACAATAATAATAATAATAAAAAAGAA  
GAATGTGAAAAATTCCACAAACGACAAGAAAGGAAATTCTTCTGAAAGGATAAATGAGGTTGTAGGTAGT

The shield mutations are indicated with grey distinctions.



- DNA fragments of PfUT used in constructs for APEX2 C-terminal fusion (SLI system):

#### C-terminal PfUT (primers 38 and 39)

TAATGAAAGTTGTTAAGAAGGAGGACAATAATGATTTACCAAGTGTGATGACTTGTACAAATTATTTAAAAATAC  
CAGATTATAAAAAATAAAGAAAAACTAAGGAACAGATTAATTTATGCCATTAATGAAGgtatatatatataatatata  
 taatatatatataatatatatatatatgtatatatatattataaaaaaaaaaagaaaaaaaaaaaaattaagtgaaggt  
 aaaaaaaaaaatttttttttttttttttttaaatagtgcattaatatatacatatatatatataataatatgtttatg  
 tatacttatattattatatatgcccttttacgtaaatatatattaatacggctattttattatatatatatgtatata  
 tgtatatattttatttataagcacacatacatatatatatatatattttatttattattattttcttcttagGCCA  
AAAGAACTTTTCACTTTCT

- DNA fragments of PfUT used in construct for allelic exchange replacing PfUT resistant alleles by conserved ones (CRISPR-Cas9 system):

#### Central part of PfUT (primers 21-24)

TCTAAATACTATACGCAAGATATGATAATTAAAGAGAAGAATAAAATGGATGTTTTGGAATTATTAAAAAGTATT  
GATAGAAATATTCGTTTATATATATTTTTATATGCTTTATTATTTGTTAATAATAAAAGAAAAGAGATATGGTA  
 CATGGTTTATTTTTGAATAGTATAAAAAGGATATATAAAATATTTTCAGAAAATATGTTAGGAGAAAAAATATA  
 GAAGATATTAATAGTAATGATATTATGCATATAAAATCATTAGTTGTAAAAATATTTGATTCATATCATTATTAT  
 TTAATAATTAATAATTTATCATTTTAAAAGTTGTTATGAACCTTATAAAAAATAATCAAGGAATGTTTAAATATTTAT  
 GATCACTTTTCTATATATTTTTTCAAAGATAATTTTTCAAATAAGAATAATACGAAAAGGGTATGTCCTAATAAA  
 TATTATGATTATATAAACCGTGAATGACCCGAAAGGTAAAGGTGATGGTGAATGTGATCGTGAGGTGAAGGTGAA  
 GATGACGATGAAGATGATGATGATAATAATAATAATAAAGGACGATGGGAATGGAAAAAGAAAAAGAAAGAG  
 AGAGAGAGAGAAAAAATGAATTATTTTATGAATGGAAAAAGGAATATGATGAATTTCCATCATTAAGA  
 CAAGATTTTTCATATAATGTATATTCGAGGAATAGAAAATCTAGCGAGCTATCAAAAAATAGCAAGCCAAAAAG  
 AAGAAGGACAATAAAAAATGTTTCATGTGGTAGTTCTCCAATATGGATAGTATAATAATAATGAAATAATAAAA  
AATACGAATGAAAATAAGAACAATTGTGATTATAATATTAAGGAGGATGATGAATCTGGTAGT

Conserved polymorphic residues characteristic for sensitive variant of PfUT are highlighted with black distinction, whereas the shield mutations are indicated with grey distinctions.

Alignment of a respective fragment of pL6-PfUT-HA-glmS-UTR plasmid (Sequence\_2) with the DNA sequencing results of PfUT-HA-glmS parasite transgenic line (Sequence\_1), shown for the representative clone:

| Seq_1 | 1    | -----c-at-GgCCCcTtTcgcGgGagCTaG-gTTTAaTGAAa                                | 36   |
|-------|------|--|------|
| Seq_2 | 2821 | ATGGAATACTAAATATATATATCCAATGGCCCCCTTccgcggggaggACTAGT <b>TTAATGAAA</b>     | 2880 |
| Seq_1 | 37   | GTTGttAaGAAGGaggaCAATAATGATTTAccaagtGTGATGActtgTACAAATTATTTA               | 96   |
| Seq_2 | 2881 | <b>GTTGTTAAGAAGGAGGACAATAATGATTTACCAAGTGTGATGACTTGTACAAATTATTTA</b>        | 2940 |
| Seq_1 | 97   | AAAATACCAGATTATAAAAAATAAGAAAAAACTAAGGAACAGATTAATTTATGCCATTAAT              | 156  |
| Seq_2 | 2941 | <b>AAAATACCAGATTATAAAAAATAAGAAAAAACTAAGGAACAGATTAATTTATGCCATTAAT</b>       | 3000 |
| Seq_1 | 157  | GAAGGTATATATATAATATATATAATATATATATAATATATATATATATGTATATATATTTA             | 216  |
| Seq_2 | 3001 | <b>GAAGGtatatatataatatatatataatatatatataatatgtatatatatatta</b>             | 3060 |
| Seq_1 | 217  | TAAAAAAAAAaGAAAAAAAAAAaTTAAGTGAAGTAAAAAAAAAaTTTTTTTTTTTTT                  | 276  |
| Seq_2 | 3061 | <b>taaaaaaaaaagaaaaaaaaaaaattaagtgaagtaaaaaaaaaaattttttttttt</b>           | 3120 |
| Seq_1 | 277  | TTTTTTAAATAGTGCATTAATATATACATATATATATAATAATATGTTTATGTATACTTA               | 606  |
| Seq_2 | 3121 | <b>ttttttaaatagtgcatatatatacatatatataataatatgtttatgtatactta</b>            | 3180 |
| Seq_1 | 337  | TATTATTATATGCCCTTTTACGTAAATATATATTAATACGGCTATTTATTATATATATAT               | 546  |
| Seq_2 | 3181 | <b>tattattatatgcccttttacgtaaatatattaatacggctattttattatatatat</b>           | 3240 |
| Seq_1 | 397  | GTATATATGTATATATTTATTTATAAGCACACATACATACATATATATATATATTTATTT               | 486  |
| Seq_2 | 3241 | <b>gtatatatgtatatattttatttataagcacacatacatatatatatatatattttattt</b>        | 3300 |
| Seq_1 | 457  | ATTATTATTTCTTCTTAGGCCAAAAGAATTTTCCCTTTCTGGCGGCCAGGCGGTGGAT                 | 426  |
| Seq_2 | 3301 | <b>attattattttcttcttaggCCAAAAGAATTTTCCCTTTCTG<b>GcGCGC</b>CagggcgtggaT</b> | 3360 |
| Seq_1 | 517  | ACCCTTACGATGTGCCTGATTACGCGTATCCCTATGACGTACCAGACTATGCGTACCCTT               | 366  |
| Seq_2 | 3361 | ACCCTTACGATGTGCCTGATTACGCGTAtCCcTAtGAcGTaCCaGAcTAtGCaTACCcT                | 3420 |
| Seq_1 | 577  | ATGACGTTCCGGATTATGCTCACGGGTGTAAGCGGCCGCGGTCTTGTTCCTATTTTCTC                | 306  |
| Seq_2 | 3421 | AtGAcGTtCCgGATTAtGCtcacggggtgTAAGCGGCCG <b>GGTCTTGTTCTTATTTTCTC</b>        | 3480 |
| Seq_1 | 637  | AATAGGAAAAGAAGACGGGATTATTGCTTTACCTATAATTATAGCGCCCGAACTAAGCGC               | 246  |
| Seq_2 | 3481 | <b>AATAGGAAAAGAAGACGGGATTATTGCTTTACCTATAATTATAGCGCCCGAACTAAGCGC</b>        | 3540 |
| Seq_1 | 697  | CCGGAAAAAGGCTTAGTTGACGAGGATGGAGGTTATCGAATTTTCGGCGGATGCCTCCCG               | 186  |
| Seq_2 | 3541 | <b>CCGGAAAAAGGCTTAGTTGACGAGGATGGAGGTTATCGAATTTTCGGCGGATGCCTCCCG</b>        | 3600 |

|       |      |   |      |
|-------|------|---|------|
| Seq_1 | 757  | GCTGAGTGTGCAGATCACAGCCGTAAGGATTTCTTCAAACCAAGGGGGTGACTCCTTGAA  | 126  |
| Seq_2 | 3601 | GCTGAGTGTGCAGATCACAGCCGTAAGGATTTCTTCAAACCAAGGGGGTGACTCCTTGAA  | 3660 |
| Seq_1 | 817  | CAAAGAGAAATCACATGATCTTCCAAAAACATGTAGGAGGGGACGGCGCCTTTTTGT     | 66   |
| Seq_2 | 3661 | CAAAGAGAAATCACATGATCTTCCAAAAACATGTAGGAGGGGACggcgcdTTTTGT      | 3720 |
| Seq_1 | 877  | TGCGACCCGATGTATTATAATTTTTTTTTTTAACTCATAAAATATAAACCTTGAGACTT   | 595  |
| Seq_2 | 3720 | TGCGACCCGATGTATTATAATTTTTTTTTTTAACTCATAAAATATAAACCTTGAGACTT   | 3779 |
| Seq_1 | 937  | TAATCAGGTATTATAATATTTAAATGAGAGATTCCTCAAATGTTAAAAAGGAAAAATTT   | 535  |
| Seq_2 | 3780 | TAATCAGGTATTATAATATTTAAATGAGAGATTCCTCAAATGTTAAAAAGGAAAAATTT   | 3839 |
| Seq_1 | 996  | ATACATATAAATATATATATATATATATATATATATATATATATTTTCTTATTTTACGCA  | 475  |
| Seq_2 | 3840 | ATACATATAAATATATATATATATATATATATATATG-----ATTTTCTTATTTTACGCA  | 3891 |
| Seq_1 | 1056 | TAGTTCAAAAAAAAAAAAAAAAAATATATATATAATATATATATATATATTTAAAT      | 415  |
| Seq_2 | 3892 | TAGTTCAAAAAAAAAAAAAAAA--TATATATATAATATATATATATAT----TTAAAT    | 3945 |
| Seq_1 | 1116 | ATTAGTCTGTGTATTTTATAATGTGTATATAATATATTATATATTTTCTTATGTGTA     | 355  |
| Seq_2 | 3946 | ATTAGTCTGTGTATTTTATAATGTGTATATAATATATTATATATTTTCTTATGTGTA     | 4005 |
| Seq_1 | 1176 | TTATTTATTATTATTATTTATTTTCTTGCATGCAATAAATATATGAATATATTTTATT    | 295  |
| Seq_2 | 4006 | TTATTTATTATTATTATTTATTTTCTTGCATGCAATAAATATATGAATATATTTTATT    | 4065 |
| Seq_1 | 1236 | ATTTTTTTTTTTTTTTT-ATATATATTACTTACAAACATTGTGTATATATGGAATAATAGG | 236  |
| Seq_2 | 4066 | ATTTTTTTTTTTTTTTTATATATATTACTTACAAACATTGTGTATATATGGAATAATAGG  | 4125 |
| Seq_1 | 1296 | AAATACAAAATTGTGTTATTATGTTTACTTATAAAAGAAATAATATACACACATATATAA  | 176  |
| Seq_2 | 4126 | AAATACAAAATTGTGTTATTATGTTTACTTTTAAAGAAATAATATACACACATATATAA   | 4185 |
| Seq_1 | 1356 | AAATAAAATATATAATATAATATACATA---ATATATATATATATATATATATAT--T    | 121  |
| Seq_2 | 4186 | AAATAAAATATATAATATAATATA-ATATACATATATATATATATATATATATATATT    | 4244 |
| Seq_1 | 1416 | AATATATATGTGTATATATTATATATGTCAAGGACATATACATTAAAGACTTAAGCATtt  | 61   |
| Seq_2 | 4245 | AATATATATGTGTATATATTATATATGTCAAGGACATATACATTAAAGACttaag-----  | 4299 |